UNIVERSITY OF SOUTHAMPTON

FACULTY OF ENGINEERING AND THE ENVIRONMENT

An anatomical and surface electromyography study of the fatigue characteristics of Longissimus Thoracis pars Thoracis, Iliocostalis Lumborum pars Thoracis and Lumbar Multifidus.

by

RICHARD COLLIER

Thesis for the degree of Doctor of Philosophy

2014

UNIVERSITY OF SOUTHAMPTON

ABSTRACT

FACULTY OF ENGINEERING AND THE ENVIRONMENT

Thesis submitted for the degree of Doctor of Philosophy

This study investigated the myoelectric effects of muscle fatigue in Longissimus Thoracis, Iliocostalis Lumborum pars Thoracis and lumbar Multifidus during standardised muscle fatigue tests and in a marine environment. These muscles contribute significantly to the extensor moment of the lumbar spine and are an important postural stabiliser. Fatigue of these muscles is considered to contribute to the aetiology of low back pain; rehabilitation approaches that improve muscle endurance capacity would benefit from a better understanding of how these muscles fatigue

A feasibility study methodology was developed and a case series study undertaken to establish the utility of standardised fatigue testing before and after a marine high-speed transit that is considered to cause muscle fatigue. Surface EMG data were collected in combination with heart rate and motion data of the vessel and study participants. Standardised fatigue testing was utilised before and after the task to determine the sensitivity of the test; the test was not shown to have clinical utility in this case.

Methodology was developed, using high-density surface electromyography (sEMG) and high-density surface electrodes, in order to analyse data from multiple locations over each muscle of interest. Software was developed that enabled specific channels and segments of data to be analysed.

A post-mortem anatomical study, in an older population, was completed and this provided position and angle data from bony landmarks for the accurate positioning of high-density surface electrodes and subsequent interpretation of high-density sEMG signal data.

A pilot validation study, utilising magnetic resonance images (MRI), compared results of the anatomical study with a MRI series from an older population and a further series in a younger population. The results of these studies partly concur, add to previous study results and provide data on sEMG electrode placement that will aid further sEMG studies.

Contents

Definitions and abbreviations

In the interests of brevity, throughout this thesis, the following abbreviations and acronyms will be used within the text. Definitions are given where it is thought this is necessary.

ILpT or Iliocostalis – Iliocostalis Lumborum pars Thoracis

LM or Multifidus – Lumbar Multifidus

LTpT or Longissimus – Longissimus Thoracis pars Thoracis

A/D – Analogue to digital

ADP – Adenosine diphosphate

AP – Action potential

ATP – Adenosine triphosphate

CGM – Central governor model

CLAS – Centre for learning anatomical sciences

CNS – Central nervous system

CV – Conduction velocity

EAV – Exposure action value; The EU the Physical Agents Directive (Directive 2002/44/EC 2002) sets an action limit for VDV (See below) of 9.1 m/s^2.

ECG – Electrocardiogram

ELV – Exposure limit value; The EU the Physical Agents Directive (Directive 2002/44/EC 2002) sets an exposure limit for VDV (See below) of 21.0 m/s^2

EMG – Electromyography

EOP – External occipital protuberance

EPSRC – Engineering and physical sciences research council

ES – Erector Spinae

FFT – Fast Fourier transform – a fast Fourier transform is a mathematical method to decompose a sequence of events (in this thesis an analogue sEMG signal) into components of different frequencies so that the frequency distribution can be calculated and median

values obtained.

GPS – Global positioning satellite

GUI – Graphical user interface

IED – Inter-electrode distance

ILpT – Iliocostalis Lumborum pars Thoracis

ISVR – Institute of sound and vibration research

IV – Intervertebral

L3 L4 L5 – Third, fourth, fifth lumbar vertebrae levels

L2/3 – Lumbar spinal segment at second and third spinal level.

L4/5 – Lumbar spinal segment at fourth and fifth spinal level.

LBP – Low back pain

LCG – Longitudinal centre of gravity

LOA – Limit/s of agreement

MDF – Median frequency. The median frequency is the value that divides the power spectrum into two regions of equal parts. The MDF is calculated as part of the FFT (See below).

MRI – Magnetic resonance imaging

MU – Motor unit

MUAP – Motor unit action potential

MVC – Maximum voluntary contraction

N – Newton

PACs – Picture archiving and communications system

PM – Psoas Major

PSD – Power spectral density. This describes the variance of how the data are distributed over the frequency components into which it has been decomposed. This distribution is achieved with a Fast Fourier Transform of the signal of interest.

PSIS – Posterior Inferior Iliac Spines

RF – Radio frequency

RIB/S – Rigid inflatable boat/s

rms – Root mean squared. Also known as the quadratic mean; it is the square root of the arithmetic mean of the squares of the original values.

RNLI – Royal national lifeboat institute

RPE – Rating of perceived exertion

SD – Standard deviation

sEMG – Surface electromyography

SENIAM – Surface electromyography for the non-invasive assessment of muscles

T10 – Thoracis 10th vertebral level

T11 – Thoracis 11th vertebral level

UOS – University of Southampton

VAS – Visual analogue scale

VDV – Vibration dose value; the VDV is calculated as a weighted mean from the magnitude, frequency and direction of vibration in the x, y and z axis of the individual being exposed. The value is calculated according to various national standards e.g. BSI 6841 1987 and EU the Physical Agents Directive (Directive 2002/44/EC 2002). 'Comfort' values have been set and action/exposure values, at which action must be taken to protect workers, see EAV & ELV. These values are frequently exceeded in a marine environment.

WBV – Whole body vibration; is defined as the transmission and absorption of vibration energy normally through the feet (when standing) or through a seat. Particular frequencies of vibration are considered more likely to cause discomfort or harm to the human body (See VDV).

1. Foreword to thesis

This study was conceived as a consequence of collaboration between the University of Southampton's (UOS) Ship Science department and the Institute of Sound and Vibration Research (ISVR), the University of Chichester's Sport's Science department, the Royal National Lifeboat Institute (RNLI) and the author. A Memorandum of Understanding exists between the University of Southampton and the RNLI that facilitated collaboration; initial work was undertaken with the RNLI to determine to what extent spinal pain and injury were affecting the lifeboat crew members. These initial discussions and subsequent work were the catalyst for this thesis.

A study, supported by a grant from the Engineering and Physical Sciences Council (EPSRC), was investigating the effects on human performance of high-speed boat journeys in small fast rigid inflatable boats (RIBS) that typically operate in inshore waters (known as 'high-speed transits'). Of particular concern to the RNLI were the high numbers of anecdotal reported incidents of muscle fatigue and the high number of anecdotal reports of injuries occurring to crew members and in particular reports of low back pain and injury during or following high-speed transits. There is widespread concern within the marine industry that exposure to high levels of random and shock vibration and the harsh marine environment in which the RNLI crews and other mariners operate are linked to subsequent fatigue and injury (Cripps, Cain, Philips, Rees, & Richards 2008; Goldfinch 2012; Myers, Dobbins, King, Hall, Ayling, Holmes, Gunston, & Dyson 2011).

The RNLI has 4,500 crew members based around the shores of the UK. Many are not employed or involved in the marine industry; in fact, 80% of crews on joining the RNLI, as a volunteer, are going to sea for the first time. The RNLI is a voluntary organisation that relies on donations from the public; it does not include fitness screening as part of its recruitment or crew retention process, nevertheless it has a duty of care to its volunteers and this responsibility motivated later aspects of this study.

Ship Science at the University of Southampton had initiated a number of studies that were investigating the potential for mitigating the effects of

random and shock vibration through vessel design. The University of Chichester had undertaken a study that investigated whether non-specific pre- and post-transit tests of fitness could quantify the level of fatigue resulting from a high-speed transit. This study had not resulted in definitive conclusions (Myers et al. 2011).

The close academic links between Health Sciences, with its focus on human performance, ISVR with its signal processing and control systems expertise and the School of Medicine's Centre for Learning Anatomical Studies (CLAS) provided an opportunity to initiate a study to seek a better understanding of how fatigue of specific muscles could be measured.

The author's aim, as a physiotherapist with experience treating individuals with low back pain (LBP) and as an academic teaching on all aspects of LBP, was to discover more about the evaluation of spinal muscle fatigue and its possible relationship to LBP. This thesis will describe the journey taken in pursuit of this aim.

The thesis builds on an understanding of how fatigue of muscles that stabilise the lumbar region could be investigated during standardised fatiguing tasks and during an occupational expose to a fatiguing activity. A feasibility study is presented that gives details of how spinal muscle fatigue could be measured in an occupational environment and recommendations made for further research.

A literature review is presented that relates to the main study. A link is made between the use of standardised fatigue testing in a real world situation and the discoveries that underpinned this. The development of a methodology for investigating muscle fatigue using high-density surface electromyography is given, a post-mortem anatomy study that investigated position and angles of muscles in relation to known bony landmarks, a pilot validation studying using magnetic resonance imaging are reported.

1.1 Outline of study

The overall aim of this study was to undertake research that adds to the understanding of how fatigue testing of the following muscles, which contribute to the extensor mechanism of the lumbar spine, can be undertaken;

Iliocostalis Lumborum pars Thoracis (ILpT/Iliocostalis)

Lumbar Multifidus (LM/Multifidus)

Longissimus Thoracis pars thoracic (LTpT/Longissimus)

In the interests of brevity, following the section where structural anatomy is described, the acronyms and abbreviations above will be used for the muscles of interest in this study. The full anatomical names will be used in cases where other muscles are referred to or where this improves clarity.

1.2 Purpose and method to investigate the utility of standardised fatigue testing

A single participant feasibility case study was undertaken, in a marine environment, to establish if spinal muscle surface electromyography (sEMG) could be recorded. This study also collected and correlated other measures of human physiology, movement and boat motion during a high-speed transit and evaluated the utility of a standardised fatigue test pre- and post-high-speed transits.

A methodology was developed to investigate the sEMG characteristics of the spinal muscles using high-density sEMG during standard fatigue testing. Specifically, root mean square (rms) and median frequencies (MDF) were calculated from the sEMG signal collected.

Electrode placements for this novel investigation were not known. Detailed description of muscles, their fibre position and angular orientation were not available in sufficient depth to be able to determine with accuracy where high-density sEMG electrodes should be positioned based on surface anatomical features.

This study initially utilised electrode placements based on published anatomical data for sEMG studies in order to obtain a better understanding of the characteristics and patterns of muscle fatigue. An experimental approach developed novel data manipulation and analysis techniques but was limited by the lack of anatomical knowledge applicable to high-density electrode placement. This lack of knowledge was the motivation for a detailed study of spinal muscle anatomy.

A post-mortem anatomical study that detailed the position and the angle of muscles of interest muscle was undertaken. A method comparison analysis of different ways to measure muscle angles was completed. However, studying the anatomy of elderly individuals limits the generalisability of results and a validation of the anatomy results was undertaken.

A magnetic resonance imaging (MRI) study described and validated the location of relevant lumbar and thoracic spine musculature in the same age group as the anatomical study and in a younger population in order to inform future sEMG studies that incorporate sEMG and standardised fatigue testing.

Individuals with low back pain will benefit from this work; it has the potential to inform a better understanding of the mechanism by which stabilising muscles of the lumbar region function. The study provided baseline data for future intervention studies and described testing that could be modified for other real world environments.

2. Introduction

This section will be divided into sections to describe the known anatomy of the relevant spinal regions and muscles of interest in this study; the following sections will describe biomechanics of the spine and the neural control of movement. A critical review of models of fatigue and the relevance to low back pain, measurement approaches of fatigue and the use of electromyography in the analysis of fatigue will complete the section.

2.1 Anatomy of the lumbar spine

The human spine is a remarkable structure. It is capable of resisting compressive, tensile, torsion and shear forces; protecting the integrity of neural tissue while enabling mobility and contributing to normal human functioning. Additionally, the axial skeleton (the spine, ribs, sternum and skull), provide support for and protection of many organs essential for life (Adams, Bogduck, Burton, & Dolan 2006).

The human spine achieves stability and mobility through an interlocking set of components that consist of vertebrae, intervertebral discs, ligaments and zygapophysial joints and further supported and protected by fascia and muscles; these components make up the vertebral column. Mobility of the spine and the ability to gain and maintain postures is achieved by joints and muscles that either originate in the lumbar spine or act on the lumbar spine, under the control of the central nervous system. The control of movement is a complex process that involves afferent and efferent neural processes.

The lumbar spine is that portion of the vertebral column between the thorax cranially and the sacrum caudally. It is normally made up of five vertebrae that once surrounded by the supporting muscles and fascia make up the lumbar spine. This section of the vertebral column is prone to disorders that cause impairment in function due to lack of postural control, instability and loss of protection to components of the central and peripheral nervous system. Pain and disability often result due to pathological and degenerative processes of this region.

2.1.1 Spinal column

The spinal column consists of seven cervical, twelve thoracic and five lumbar vertebrae that are linked in the upper cervical region to the occipital bone of the skull and caudally to the fused vertebrae of the sacrum. Each vertebra (with the exception of the atlanto-occipital and the atlanto-axial levels) articulates with its rostral and caudal neighbour through inter-body joints that consist of vertebral bodies, intervertebral discs and a pair of posteriorly located zygapophysial joints between each segment.

The thoracic spine additionally articulates with the ribs at the costovertebral and costotransverse joints. In functional term, these additional joints reduce the segmental mobility of the thoracic region compared to the cervical spine.

Each segment of the spine is additionally supported with ligamentous structures, muscles that act segmentally and globally (Figure 1) and facia. Further details of structures relevant to this thesis will be expanded on in subsequent sections.

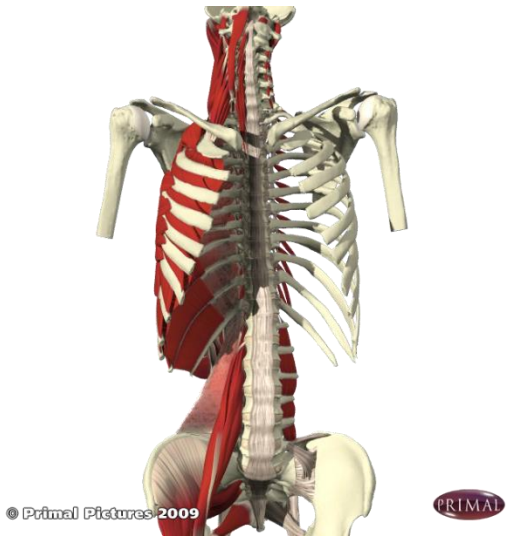

Figure 1. Muscles and ligaments supporting the spine.

2.1.2 Spinal curves

The stability of the spine is partly achieved by the cervical and lumbar lordosis, and the thoracic and sacral kyphosis. The function of these antero-posterior curves is thought to add stability to the region provided that this is complemented by the additional support from the posterior elements (the

pedicle, laminae, spinous processes and zygapophysial joints) (Adams et al. 2006). The thoracic and sacral curves are termed ‘primary’ and develop in the early developing embryo while the lumbar and cervical lordotic curves (termed secondary) develop later on in embryonic life. The secondary curves become accentuated during infancy as an upright posture is adopted.

Figure 2. Normal spinal curves, lateral view.

2.1.3 Muscles of the lumbar spine

2.1.3.1 Anatomical features of the muscles of the lumbar region

The following descriptions of muscles of the spinal region provide an overview before a more detailed description is given of the muscles that were investigated in this study. Detailed descriptions of all muscles of the spine and the thoraco-lumbar fascia are provided elsewhere (Bogduk and Twomey 1987; Bogduk and Macintosh 1984).

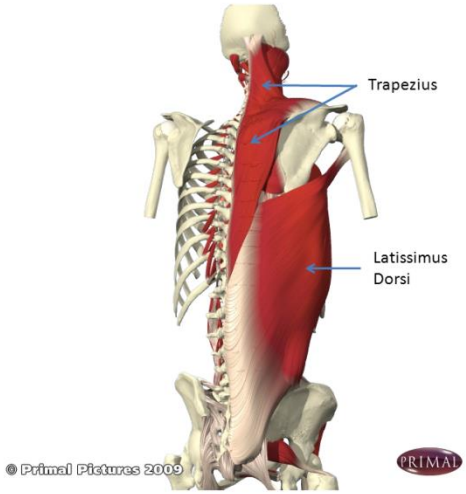

Figure 3. Latissimus Dorsi and Trapezius.

Figure 3 illustrates the arrangement of the superficial posterior muscles, arising and acting on the spine. Latissimus Dorsi can be seen as a large muscle arising from the sheet of thoracolumbar fascia and then passing upwards, outwards and laterally to attach to the floor of the intertubercular sulcus of the humerus.

The large superficial Trapezius muscle can be seen arising from the superior nuchal line of the occipital bone, from the Ligamentum Nuchae and the tips of the spinous processes in the cervical and thoracic regions from the and attaching to the posterior border of the clavicle, the spine of the scapular and the acromion.

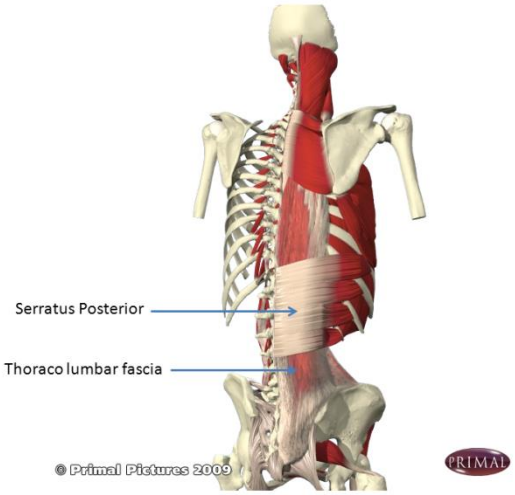

Figure 4. Thoracolumbar fascia and Serratus Posterior.

Figure 4 Illustrates Serratus Posterior and its position superficial to the thoracolumbar fascia that in turn covers the Erector Spinae group.

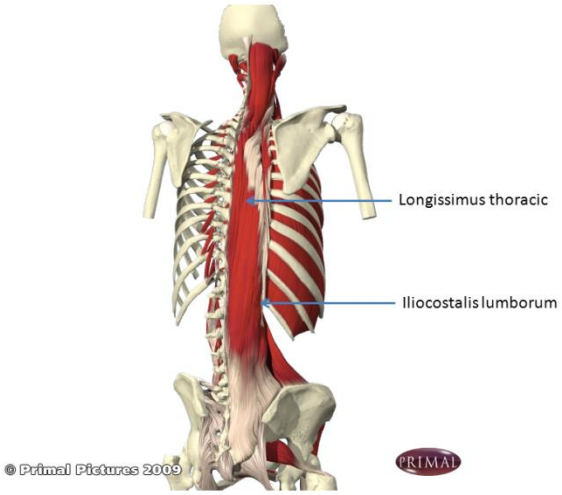

Figure 5. Erector Spinae group of muscles.

Figure 5 illustrates the Erector Spinae that consists of Longissimus (labelled Longissimus Thoracic in Figure 5) and Iliocostalis (Iliocostalis Lumborum in Figure 5); these muscles form part of a large continuation of Erector Spinae. They have a distal attachment in the lumbar region from the Erector Spinae aponeurosis through which the muscle group exerts much of its force.

Deep to Longissimus and Iliocostalis are the muscles that make up the remainder of the Erector Spinae group. This group consists of Multifidus (Figure 6), Longissimus Thoracis pars Lumborum and Iliocostalis Lumborum pars Lumborum.

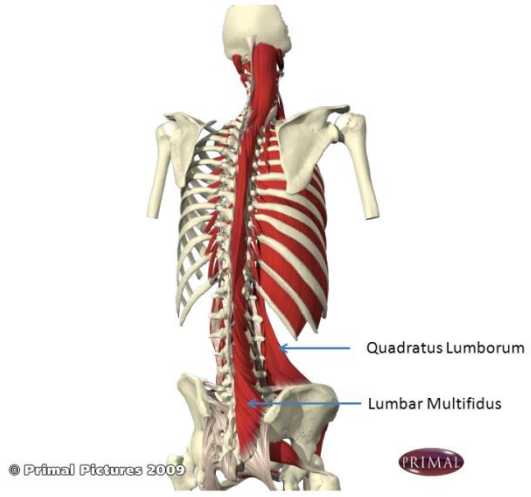

Figure 6. Multifidus and Quadrates Lumborum.

Figure 6 illustrates the general arrangement of Multifidus, the most medial muscle group, fascicles of this muscle are evident at all levels of the spine from C2 to the sacrum.

Attaching to the iliac crest and running upwards and medially, Quadrates Lumborum can be seen attaching to the twelfth rib. The small Levatores Costarum Longi are four small muscles situated between T7 and T10; these muscle groups are not shown, they function as segmental stabilisers.

2.1.3.2 Anatomy of the muscles of the lumbar region

Muscles that act on the lumbar spine can be divided into groups on the basis of their function (Bogduk & Twomey 1987; McGill 2002). Psoas Major and Psoas Minor cover the anterior aspect of the lumbar vertebral column. These muscles act primarily as hip flexors but can act as a weak flexor of the lower lumbar spine. The role of Intertransversarii Laterales and Medialis, and Rotatores have not been determined experimentally but they may have a role in proprioception and therefore act as length transducers (Bogduk 2005; McGill 2002) and would act as muscle spindles do in providing afferent input into the central nervous system as part of the mechanism that controls movement.

Quadrates Lumborum attaches to the transverse processes of the lumbar spine and covers the transverse processes laterally from L1 to L4. This muscle is orientated in such a way that it acts as an extensor and stabiliser of the lumbar spine.

The posterior muscles of the lumbar region are often collectively referred to as the Erector Spinae group (Kapandji 2008). This group consists of Multifidus, Longissimus and Iliocostalis – the present study is concerned with this group of muscles, see Section 2.1.3.3 and 2.1.5. Those of the thoracic region interconnect with the lumbar spinal muscles and contribute to the mechanical control and support of the lumbar spine.

Within the context of the biomechanics of lumbar spine control and movement, the role of the muscles that act on the hip joint such as Gluteus Maximus, Biceps Femoris, Semimembranosus and Semitendinosus are not being considered although their role in contributing to the general stability of the lumbar spinal region is not denied.

The posterior muscles of the lumbar region can be further divided according to their morphology and function (Bogduk & Twomey 1987) into the following three groups;

1. Short intersegmental muscles – Interspinalis and Intertransversarii, these are not visible in Figure 5.
2. Short polysegmental muscles, these attach to the lumbar vertebrae – Multifidus and the lumbar components of Longissimus Thoracis and Iliocostalis Lumborum.
3. Long polysegmental muscles – thoracic components of Longissimus Thoracis and Iliocostalis Lumborum. These generally do not attach to lumbar vertebrae but cross the lumbar region and attach to the ilium and sacrum.

2.1.3.3 Description of the extensor muscles of the lumbar region

Traditional anatomical texts do not always give comprehensive detail of muscles of the lumbar region or of their orientation. Some texts refer to the extensor muscles of the lumbar region generically as the 'Erector Spinae' group, while others use a naming convention that is inconsistent with standard texts. In Kapandji's text (Kapandji 2008) the Multifidus group is not mentioned. In others, the Multifidus group is described separately from the Longissimus Lumborum and the Iliocostalis Thoracis, which are grouped together as the Erector Spinae group (Gray 2009).

The general arrangement of the muscles of the lumbar region is complex with many layers and with a lack of clarity regarding fibre direction. The general consensus is that the muscles, within the thoracic and lumbar regions, midline outwards described from the posterior aspect are; Interspinalis, Multifidus, Longissimus Thoracis and Iliocostalis Lumborum (Bogduk 1980). Both the Longissimus Thoracis and the Iliocostalis Lumborum muscle groups have a lumbar and a thoracic component; known respectively as Longissimus Thoracis pars Lumborum and Longissimus Thoracis pars Thoracis and Iliocostalis Lumborum pars Lumborum and Iliocostalis Lumborum pars Thoracis. The thoracic components of each muscle have their respective rostral attachments in the thoracic region and the lumbar parts in the lumbar (Bogduk & Twomey 1987; Bogduk 1980).

The Longissimus Thoracis pars Thoracis has long tendinous attachments into the erector spinal aponeurosis, this covers the deeper components of the Erector Spinae group and it is reported that this muscle group contributes significantly to the total extensor moment at the upper lumbar levels (McGill, Patt, & Norman 1988). The erector spinal aponeurosis effectively acts as the tendinous attachment for the Longissimus Thoracis pars Thoracis and the Iliocostalis to the ilium, sacrum and the lumbar and sacral spinous processes.

A point of contention in the literature is whether the fascicles of Iliocostalis have direct attachment to the ilium or additionally attach via the Erector Spinae aponeurosis. In a study that used data from the Visible Human Anatomy (Ackerman, Spitzer, Scherzinger, & Whitlock 1995) it was concluded that a large number of the fibres of the lumbar part of Erector Spinae attached to the Erector Spinae aponeurosis (Daggfeldt, Huang, & Thorstensson 2000). In another study a clear distinction between the morphology and the functionality of the two parts of the lumbar Erector Spinae are claimed (Bogduk 1980). From a biomechanical perspective, the argument that the two components of the lumbar Erector Spinae are separate and act independently on the lumbar spine is an important distinction in this thesis, as the two muscle groups are being examined as if they operate independently on the lumbar spine while producing similar movements. In cases of a fatiguing activity, it could be the case that the two components could act in concert to maintain position, or force, more effectively if they were functionally interdependent. In the case of the Visible Human Anatomy project, there were two subjects, one male and

one female whose anatomy was considered to be representative (Ackerman 1998; Spitzer, Ackerman, Scherzinger, & Whitlock 1996). However, while fibres between the Erector Spinae aponeurosis and the lumbar part of Erector Spinae were identified, no biomechanical study has concluded that the lumbar and thoracic muscles are biomechanically dependent.

2.1.3.4 Muscle histology

The muscle groups of the lumbar and thoracic spine are morphologically distinct, with muscle fibre type analysis revealing that overall the thoracic components is made up of 75% slow twitch fibres while the lumbar spine muscles contains an even mix of fibre types (Sirca and Kostevc 1985). These proportions are consistent with the function of the maintenance of posture. Another study reported that the Longissimus is made up of 70% slow twitch fibres (Type I) while Iliocostalis and Multifidus have 55% slow twitch (Type I) (Jorgensen, Nicholaisen, & Kato 1993) although in this study the fast twitch sub type was not specified. Fast twitch Type IIa muscle fibres made up 20% of Multifidus, Iliocostalis and Longissimus and fast twitch Type IIb, 25% of Multifidus and only 11% of Longissimus (Jorgensen, Nicholaisen, & Kato 1993). From a functional perspective, the relatively low proportion of fast twitch Type IIb (very fast, low fatigue resistant, glycolytic fibres) and the high percentage slow twitch (aerobic) fatigue resistant fibres is consistent with the fatigue resistance and relatively high endurance capabilities of the spinal muscles (Jorgensen, Nicholaisen, & Kato 1993). The differences that exist in the relative proportions may have a bearing on functional biomechanics.

2.1.3.5 Strength of spinal muscles

The absolute maximum strength of the muscles of the back as a whole in an the upright position has been calculated at around 4000N (McNeill, Warwick, Andersson, & Schultz 1980). The same study calculated that this force converts to an extensor moment of 200Nm, acting on the spinous process and pedicles, for an average male over 30 years old and is some 40% lower for an average female. For over 30 year olds, the power reduces between 10 – 30%. In easy standing, the force is calculated to be some 2–5%; sitting involves 3 – 15% and manual handing of heavy loads between 75–100% of maximum strength.

In one study, it was calculated that the thoracic fibres of the Erector Spinae group contribute 50% of the total extensor moment exerted on L4 and L5 and that Multifidus contributes 20%, the remainder of the force is exerted by the lumbar fibres of Erector Spinae (Bogduk, Macintosh, & Pearcy 1992). If this is the case then the accurate positioning of the electrodes for any EMG study will be important so that the muscles contributing to the extensor moment are identified, recorded from and appropriate conclusions reached.

2.1.3.6 Muscles of interest in this study

The following section will provide detailed description of muscles of interest in this thesis. Figure 7 shows, in transverse section, the lumbar region, Multifidus and the lumbar components of Longissimus and Iliocostalis and thoracic components of Longissimus and Iliocostalis Lumborum. In this study, sEMG signals acquisition is targeted at the polysegmental muscles of both the lumbar and thoracic region.

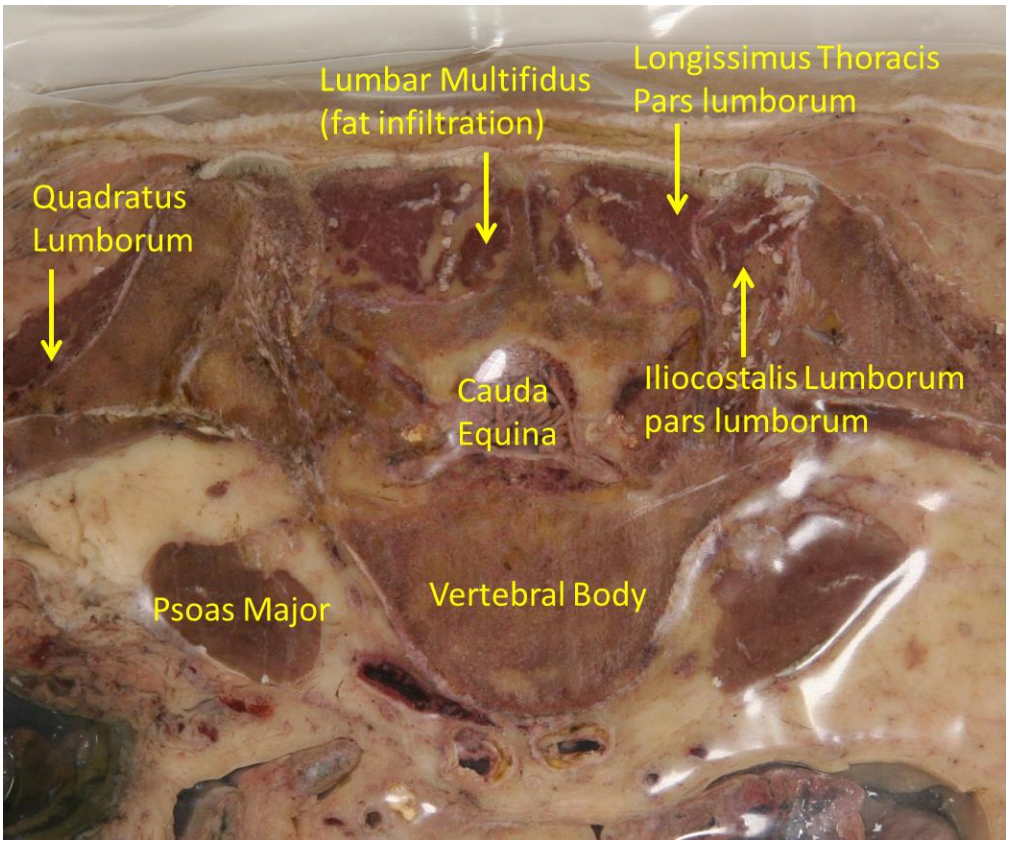

Figure 7. Transverse section through lumbo-sacral region.

In transverse section (Figure 7) the posterior arrangement of the Erector Spinae group can be seen. From midline laterally, lumbar Multifidus, Longissimus

Thoracis pars Lumborum and Iliocostalis Lumborum pars Lumborum can be identified. Lateral to the intervertebral disc (IV disc) the two columns of psoas major (PM) can also be seen in transverse section.

2.1.3.6.1 Lumbar Multifidus

This muscle is the largest and most medial of the lumbar spine muscles. It consists of a repeating set of symmetrical fascicles (Figure 8) which arise from the lamina and spinous processes of the lumbar spine vertebrae and attached to mammillary processes of levels two segments caudally and to the sacrum above S1 foramen. Fibres are arranged as five large overlapping fascicles, one from each vertebra from a common spinous process tendon which diverts caudally to attach onto mammillary process, ilium and sacrum (Figure 9) where Multifidus can be seen in relation to other deep muscle of the lumbar region.

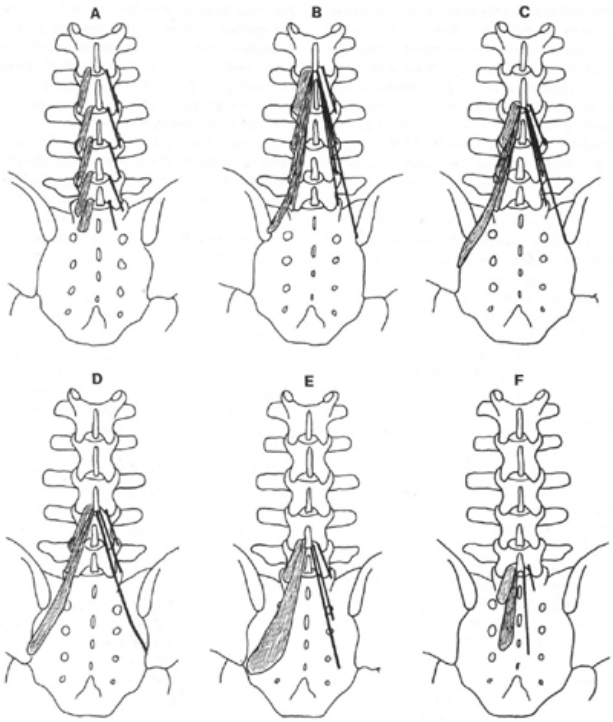

Figure 8. Fascicles of Multifidus (Bogduk 2005).
Reproduced with permission from Clinical Anatomy of the Lumbar Spine and Sacrum. Published by Elsevier (2005)

The innervation of Multifidus is from the medial branch of the posterior primary ramus that emerges from the vertebrae below the rostral attachment,

the nerve therefore innervates the fascicles that act on the segment from which the nerve arises. The principle action of Multifidus is primary as a segmental sagittal rotator acting through the spinous process.

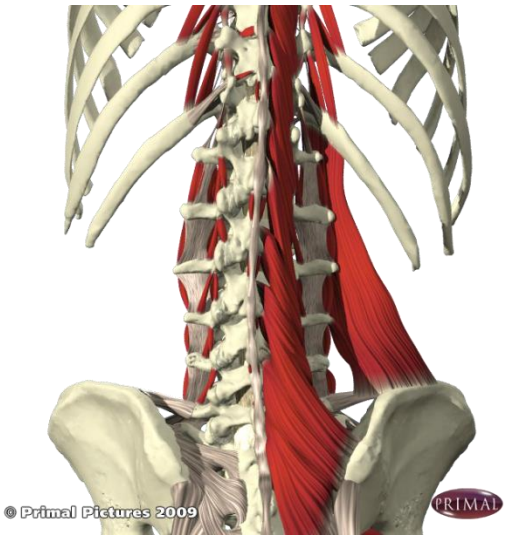

Figure 9. Multifidus in situ.

2.1.3.6.2 Erector Spinae

Multifidus is bounded on its lateral aspect by the Erector Spinae muscle group. This group forms the prominent dorsolateral contour of the back muscles and consists of two muscles; Longissimus Thoracis and Iliocostalis Lumborum. These two muscles each have two parts;

Longissimus Thoracis pars Lumborum
Iliocostalis Lumborum pars Lumborum
Longissimus Thoracis pars Thoracis
Iliocostalis Lumborum pars Thoracis

Only the Longissimus Thoracis pars Thoracis and the Iliocostalis Lumborum pars Thoracis will be described in detail.

2.1.3.6.3 Longissimus Thoracis pars Thoracis

This muscle is formed from 11 – 12 pairs of small fascicles that arise from ribs and transverse processes of the thoracic region. Each fascicle has two tendons; a medial tendon that arise from the transverse process and a

lateral tendon from the rib. These fascicles join to form a caudal tendon that becomes the Erector Spinae aponeurosis (ESA). The innervation is segmental and originates from the medial branch of the posterior primary ramus.

Each fascicle acts on the thoracic vertebrae and ribs to which it is attached and its action is thought to be as a segmental stabiliser. Through the ESA these fascicles also act to increase lumbar lordosis and so contribute to the extensor moment.

2.1.3.6.4 Iliocostalis Lumborum pars Thoracis

This muscle is formed from fascicles from lower 7 or 8 ribs, its distal component is attached to the ESA that inserts into ilium and sacrum. The innervation is segmental and is from the medial branch of the posterior primary ramus. Each fascicle acts as a segmental stabiliser of the rib and through the ESA acts to increase lumbar lordosis and so contribute to the extensor moment.

2.1.3.7 Muscle fibre orientation

In a study, designed to describe fibre direction for the purposes of informing sEMG studies (De Foa, Forrest, & Biedermann 1989), six male embalmed cadavers were dissected and the orientation and direction of Longissimus Thoracis pars Thoracis, Iliocostalis and Multifidus were described in the frontal plane. Direct measurements of fibre direction proved impractical due to reported distortion of flaccid muscle. Estimations were therefore made of the angles from photographs taken at right angles to the dorsal surface of the body. Results revealed that considerable variation existed between individuals but that a general estimation could be made of fibre direction from easily discernible surface markings. The findings of this study were that the angles of muscles, with respect to the mid-line of the body, were;

Iliocostalis Lumborum pars Thoracis *13˚ (SD = 2.11˚)*

Multifidus *15.1˚ (SD = 1.43˚)*

Longissimus Thoracis pars Thoracis 0.8˚ *(SD = 7.67˚)*

In a follow up study to De Foa's et al. (1989), Biedermann et al. (1991) looked at differences between male and female muscle fibre orientation by examining lumbar spine muscles from seven embalmed female cadavers (Biedermann, DeFoa, & Forrest 1991). In this study, which was informed by the previous study of De Foa et al. (1989), it was found that the angles of muscle orientation were in agreement with original study but with additional female data on muscle angles with respect to the mid-line of the body;

Iliocostalis Lumborum pars Thoracis;

Male *13˚ (SD = 2.11˚), female* 12.9°, *(SD=1.2˚)*

Multifidus

Male; *15.1˚ (SD = 1.43˚), female* 23.5°, (*SD*=4.5˚)

These two studies used relatively small number of cadavers and employed photographic evidence on which to base calculations. The preparation of the cadavers during the embalming process is not described; this process could have affected the fibre orientation during the embalming process.

In a study, (n = 52) that investigated normal participants, the difference that age made to muscle fibre angle found that the angle of the lumbar spine extensors at the L3 level decreased in the older population (n = 26, M age = 72.1, *SD* = 5.9) compared to the younger population (n = 26, M age = 26, *SD* 5.2) (Singh, Bailey, & Lee 2011). No details are given in this paper of which muscle was investigated but it is assumed to be Longissimus pars Lumborum from the methodology. This study used ultrasonography to measure muscle fibre angle in the sagittal plane; the results of this study indicate that a reduction in fibre angle occurs with age. Results indicate that the mean angle of the extensor muscle reduced from 12.1° (*SD* 2.3°) to 10.1° (*SD* 1.4°) in the older population. These results were compared to a cadaveric study that found the angles of pennation of Longissimus Thoracis and Iliocostalis Lumborum were 12.6° (*SD* 5.8°) and 13.8° (*SD* 4.5°) respectively (Delp, Suryanarayanan, Murray, Uhlir, & Triolo 2001). However, the comparison by the authors maybe inappropriate, as angles of pennation is the angle that muscle fibres make in relation to their tendon and not the angle in relation to the cardinal planes of the body.

2.1.4 Biomechanics of the spinal stabilisation system model

The biomechanics of the spine has been described in detail elsewhere (Bogduk & Twomey 1987; Bogduk 1980; Bogduk & Macintosh 1984; Bogduk, Macintosh, & Pearcy 1992; Macintosh and Bogduk 1991). The mechanism for maintenance of an upright bi-pedal posture is complex and requires contributions from many structures. The interconnecting roles that the muscles of the spine, the central nervous system and the passive structures of the spine are best illustrated by the model proposed by Panjabi (Panjabi 1992a; Panjabi 1992b) in which the interrelationships between three systems are described; failure of any part of this system results in spinal instability (Figure 10). Each component part is dependent on the others for normal function.

The components of the spinal stabilisation system are:

1. Passive sub-system – the vertebrae, intervertebral discs and ligaments
2. Active sub-system – the muscles and tendons that act on the vertebral column
3. Neural sub-system – the central nervous system control and feedback mechanisms

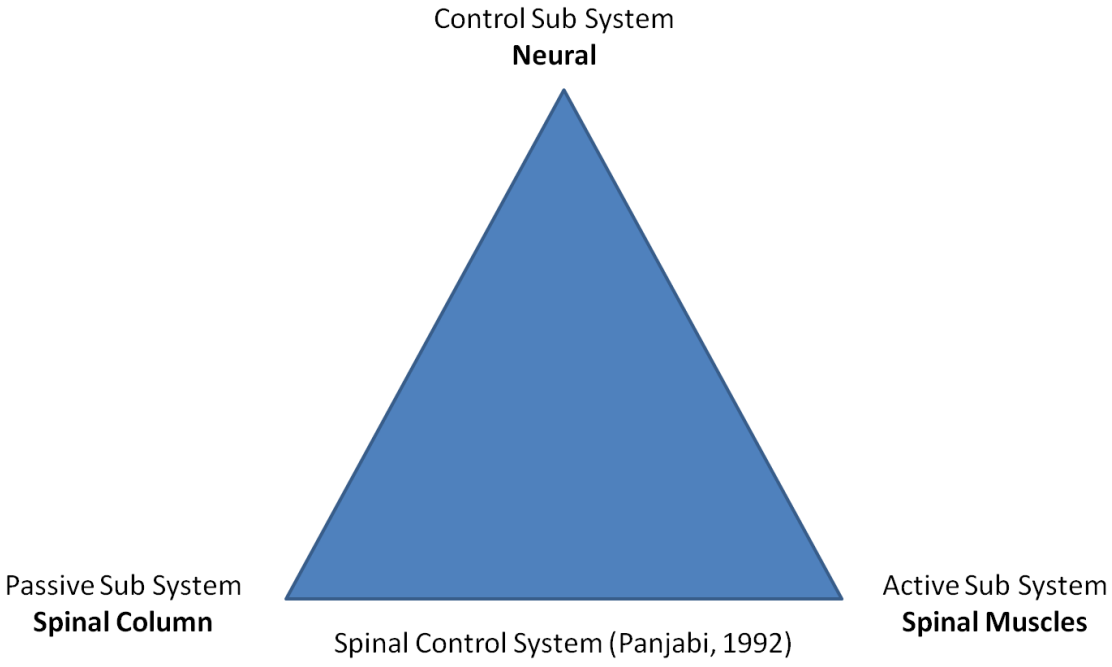

Figure 10. Spinal stability model.

The spinal stability model of Panjabi (1992) illustrates the three components that are required for spinal control. Panjabi (1992) argued that failure in any part of the spinal stabilisation system could result in spinal instability and the following possibilities might then occur;

1. Compensation from one of the other sub-systems.
2. Long-term adaptation in one or both of the other sub-systems.
3. Injury to any component of the spinal stabilisation system can lead to pain and/or dysfunction.

In the context of this thesis, either long- or short-term fatigue mechanisms that modulate the motor output of the central nervous system (CNS) or subsequent instability that results from failure of any component of the spinal stabilisation system has the potential to cause pain and/or dysfunction. In particular, the stabilising role of the spinal extensor muscles is a significant component.

2.1.5 Extensor mechanism

It has been calculated that the spine, unsupported by muscles, will buckle under a load as low as 88 Newton (N), however, in vivo the compressive forces acting on the lumbar spine often exceed 2,600 N as demonstrated using intra-discal pressure measures and through calculations from biomechanical models of lifting (Nachemson 1966). Panjabi's model proposes that each component of the spinal control system contributes to maintaining the stability of the spine. In the neutral position the role of the muscles is to provide the appropriate level of stability through the force that they generate in addition to their inherent mechanical stiffness (Bergmark 1989). It has been calculated that the lumbar spine is inherently unstable; the passive sub-system made up from the joints and ligaments have virtually no stabilising influence around the neutral position of the spine. The significance of the active sub-system, the spinal muscles, is that it provides the stability and stiffness to resist the high forces frequently required to maintain position and perform activities of normal daily living.

2.1.6 Neural control of movement

This section will outline briefly how the CNS controls movement of the spine including the control of posture and core stability.

2.1.6.1 Posture control

The work of many (Deliagina, Beloozerova, Zelenin, & Orlovsky 2008; Deliagina, Orlovsky, Zelenin, & Beloozerova 2006; Gandevia 2001) provide evidence that both supraspinal and spinal level motor control are responsible for the maintenance of body orientation in space and how the body responds to gravitational forces. Efficient control of spinal posture and movement is required for activities of normal everyday living including activities that involve head, trunk and limbs (Hodges 2003; Hodges, Gurfinkel, Brumagne, Smith, & Cordo 2002; Hodges and Richardson 1997; Moseley, Hodges, & Gandevia 2002).

There are two main modes of postural control; a feedback or reflex control system and an anticipatory control system (Deliagina et al. 2008) . The feedback or reflex system responds to external perturbations that destabilise posture and this mechanism results in correction of posture (Deliagina and Orlovsky 2002). The anticipatory control system responds in advance of voluntary activities, such as limb or head movements which would destabilise the body, by appropriate changes in postural control (Hodges & Richardson 1997). Both these mechanisms require complex integrated feedback and feed-forward control systems (Carpenter 2003; Grillner, Wallen, Saitoh, Kozlov, & Robertson 2008; Jordan, Liu, Hedlund, Akay, & Pearson 2008) that involve both supraspinal and spinal mechanisms.

It is thought that the control of posture may be affected at a supraspinal level in individuals with low back pain where reorganisation of the motor cortex may occur (Tsao, Galea, & Hodges 2008; Tsao, Galea, & Hodges 2009). Therefore an appreciation of motor control of posture and voluntary movement of the spine is necessary for a full appreciation of how low back pain could affect motor output.

2.1.6.2 Voluntary motor control

The complexity of the human nervous system and in particular the difficulties in understanding motor control make this area of neurosciences a challenging area to research (Enoka and Fuglevand 2001; Jordan et al. 2008). However, a number of postural control models have been proposed, including ballistic control systems , parametric adjusted feedback and feed-forward control and those using internal feedback with efference copy and virtual models (Carpenter 2003). All models incorporate complex interactions between afferent and efferent information and complex processing within components of the CNS and spinal cord that result in synaptic output. Whatever the model, the CNS produces synaptic output that is coded to produce specific and purposeful movement (Enoka and Stuart 1992; Farina and Negro 2012; Farina, Negro, Gazzoni, & Enoka 2008).

There is also a model of motor control also involves a central governor that regulates motor output and thus the force produced by muscle contraction. This central governor mechanism functions to maintain homeostasis through the conscious and unconscious perception of fatigue (Cohen, Goel, Frank, & Gibson 1994; Lambert, St Clair, & Noakes 2005; Noakes, St Clair, & Lambert 2005; St Clair, Baden, Lambert, Lambert, Harley, Hampson, Russell, & Noakes 2003; St Clair and Noakes 2004) (See Section 2.2.5).

Supraspinal output utilise descending pathways such as the corticospinal, tectospinal and rubrospinal tracts (Carpenter 2003) and the spinal cord utilises inter-neuronal pathways to project onto alpha motor neurones in the ventral horn of the spinal cord. This convergence of output from the CNS onto the alpha motor neurones is referred to as the final common pathway as all motor output from the CNS synapses on these neurones.

At the alpha motor neurones the action potentials innervating the muscle constitute the neural drive; this drive is the neural code and contains all information required for the motor task. Neural signals are modulated by the CNS to produce muscle forces and combinations of force that ultimately produce purposeful movement (Farina & Negro 2012).

Each alpha motor neurone has connections to an axon that may branch multiple times and innervate a considerable number of muscle fibres – this forms what is known as the motor unit. The motor unit is defined as the cell

body and dendrites of a motor neuron, the multiple branches of the axon, and the muscle fibres that it innervates (Enoka and Duchateau 2008; Enoka & Stuart 1992). Each motor unit may innervate hundreds or thousands of individual muscle fibres (typically an average of 338 muscle fibres in each motor unit (Enoka & Fuglevand 2001); this variation can be utilised by the CNS as part of a strategy to control movement. Furthermore, the innervation of type II muscle fibres is significantly less that the type I which, in the case of the first dorsal interosseous muscle, are innervated by 84% of the motor neurone pool despite 50% of the fibre types being type II fibres (Enoka & Fuglevand 2001); this enables additional modulation of motor control.

Muscle force is modulated by the number and type of motor units recruited, and also by the motor unit discharge rate and discharge pattern. Given that there is a direct relationship between the discharges in the axon and the action potentials generated in the innervated muscle, then recording the action potentials from muscle fibres gives an insight into the neural code generated by the CNS. This insight can be achieved with sEMG systems and intramuscular EMG but with some caution as neither gives a complete picture of the entire neural coding necessary to understand fully the control of movement (Farina, Gazzoni, & Merletti 2003b; Merletti, Farina, & Gazzoni 2003). Multi-channel sEMG systems, that utilise numerous EMG sensors, are capable of recording from up to 83% of motor units (Farina et al. 2008), this provides a better insight into neural code.

CNS Motor control is achieved through the complex interplay of motor unit activation across a wide range of muscle groups using time, amplitude and frequency modulation (Negro and Farina 2012) and under the control of a central governor that maintains homeostasis (Noakes 2011b).

2.1.6.3 Global and local stabilisation

In the view of some (Bergmark 1989; Hides, Wilson, Stanton, McMahon, Keto, McMahon, Bryant, & Richardson 2006; Hides, Jull, & Richardson 2001; Hides, Richardson, & Jull 1996; Hodges & Richardson 1997; Ng, Richardson, Parnianpour, & Kippers 2002), the spinal muscles operate as two separate groups; one to provide global and the other local (segmental) stabilisation of the lumbar spine (Table 1 and Table 2). Details of individual muscle function

are given elsewhere (Bogduk & Twomey 1987; Bogduk 1980; Bogduk & Macintosh 1984; Bogduk, Macintosh, & Pearcy 1992; Macintosh and Bogduk 1987; Macintosh & Bogduk 1991).

The following table (Table 1) groups muscles according to function based on biomechanical principles extrapolated from anatomical studies (Bogduk & Twomey 1987; Bogduk 1980; Bogduk & Macintosh 1984; Bogduk, Macintosh, & Pearcy 1992; Macintosh & Bogduk 1987; Macintosh & Bogduk 1991).

Table 1. Categorisation of lumbar spinal muscles.

Local Stabiliser	Global Stabilisers
Intertransversarii Interspinales Multifidus Longissimus Thoracis pars Lumborum Iliocostalis Lumborum pars Lumborum Quadratus Lumborum medial fibres Transversus abdominis Obliquus internus abdominus (fibres that insert into thoracolumbar fascia)	Longissimus Thoracis pars Thoracis Iliocostalis Lumborum pars Thoracis Quadratus Lumborum lateral fibres Rectus abdominus Obliquus externus abdominus Obliquus internus abdominus

Categorisation of lumbar spinal muscles based on function (Bergmark 1989)

This particular characterisation of muscles into two functional groups has been broadly adopted within the literature and its basis is accepted for this thesis although the role of Intertransversarii and Interspinalis is challenged by some (Table 2) (Bogduk 2005; Bogduk 1983; Bogduk, Wilson, & Tynan 1982) who assert that these muscles mainly act as proprioceptors.

Table 2. Categorisation of lumbar spinal muscles based on Bogduk (2005).

Proprioception	Local Stabiliser	Global Stabilisers
Intertransversarii Interspinales	Multifidus Longissimus Thoracis pars Lumborum Iliocostalis Lumborum pars Lumborum Quadratus Lumborum medial fibres Transversus abdominis Obliquus internus abdominus (fibres that insert into thoracolumbar fascia)	Longissimus Thoracis pars Thoracis Iliocostalis Lumborum pars Thoracis Quadratus Lumborum lateral fibres Rectus abdominus Obliquus externus abdominus Obliquus internus abdominus

Categorisation of lumbar spinal muscles based on Bogduk (Bogduk 2005; Bogduk 1983; Bogduk, Wilson, & Tynan 1982).

Muscles that were studied in this thesis were;

Lumbar Multifidus– a local lumbar spine stabiliser

Longissimus Thoracis pars Thoracis – a global lumbar spine stabiliser

Iliocostalis – a global lumbar spine stabiliser

2.1.6.4 Muscle innervation

Muscles that stabilise the spine are innervated by the dorsal rami of the spinal nerves. Each dorsal ramus is a tiny branch from the spinal nerve that passes posteriorly into the posterior compartment of the spine. Each branch divides into lateral, intermediate and medial branches. The innervation is illustrated (Table 3); each dorsal ramus at a particular vertebral level only innervates muscles that act on that segment.

Table 3. Innervation by dorsal rami.

Medial branch	Intermediate branch (variable)	Lateral branch (not present at L5)	Dorsal rami from L1, L and L3 (Superior clunial nerve)
Multifidus Interspinalis Intertransversarii lateralis and medialis Zygapophysial joints above and below segmental level.	Longissimus Lumborum pars Lumborum Longissimus Lumborum pars Thoracis	Iliocostalis Lumborum pars Lumborum Iliocostalis Lumborum pars Thoracis	Cutaneous branch to upper and lateral buttock region.

Innervation by dorsal rami (Bogduk 2005; Bogduk 1983).

Based on anatomical evidence, control of stability at a segmental and at a global level is possible. Muscles acting on each vertebral segment can be driven by neural code to each segment and also to different fascicles of each muscle. This evidence is further supported by a study that has demonstrated that the lumbar Multifidus and the lumbar Erector Spinae (Tsao, Danneels, & Hodges 2011) have separate motor cortical regions which are therefore responsible for the activation of the deep and superficial fascicles of the lumbar Multifidus and the lumbar Erector Spinae muscles. It is assumed in this thesis that the lumbar Erector Spinae muscle is Longissimus Thoracis pars Lumborum which is situated laterally to Multifidus and which, is a segmental stabiliser (Bogduk 2005).

2.1.6.5 Segmental stability and clinical instability

Spinal stability is a term that has been defined by Panjabi (1992a, 1992b) and is described in section 2.1.4. Panjabi hypothesises that segmental stability is a function of the contribution made by the local and global of the spine stabilisers (the active sub-system) that provide dynamic stiffness to the spinal segments.

Panjabi's spinal stability model encompasses the concept of a 'neutral zone' (Panjabi 1992a; Panjabi 1992b). The neutral zone is defined as the movement

region of each spinal segment where the restraining passive sub-system (the soft tissue and bony restraints) provide minimal internal resistance to physiological movements. At the limit of physiological motion, the passive restraints limit the range of motion. Failure of any component of the passive sub-system to limit the range can result in an increase in the neutral zone range that contributes to instability of the spinal segment. The active and neural sub-systems contribute to the control of the neutral zone and play an important role in providing dynamic control over the neutral zone; however, when this range is increased or the active sub-systems fail to provide sufficient control then clinical instability could result.

Panjabi (1992) defined clinical instability as…

"A significant decrease in the capacity of the stabilizing system of the spine to maintaining the intervertebral neutral zone within physiological limits which results in pain and disability" (Panjabi 1992b).

Panjabi also postulated the concept of decreasing muscle 'stiffness' of the spine that results from failure of the passive subsystem, muscle fatigue and motor control deficiencies.

2.1.6.6 Core stability and mechanical support

The mechanical support for the spine derived from muscle endurance and muscle strength (force) is different. For the spine to be stable in any given position, muscles need to be able to generate sufficient force over a sufficient period of time to enable normal activities of daily living. The spinal extensor muscles are particularly important in maintaining appropriate postures (Morris, Lucas, & Bresler 1961), although since the conclusions were drawn from early work, more recent studies have challenged the validity of modelling based on EMG studies compared to direct measurement (Arjmand, Gagnon, Plamondon, Shirazi-Adl, & Lariviere 2009) where EMG-based modelling can overestimate the spinal loading forces.

'Core Stability' training has become a popular method for addressing both the presumed lack of ability to generate muscle force and lack of endurance as well as poor motor coordination in patients with LBP. This specific method is not without its critics (Lederman 2010) who challenge the validity of the

approach; others such as Hodges (Hodges 2003) view 'core stability' training as an evolving process which focuses on motor control and muscle capacity. The alternative 'aerobic capacity' approach to retraining and regaining motor control and muscle capacity is supported by a number of studies and recommendations that focus on the importance of exercise in the reduction of recurrences of low back pain (LBP) although the specificity of exercise is frequently ignored in the literature (Choi, Verbeek, Tam, & Jiang 2010).

2.2 Fatigue

2.2.1 Definitions

Traditional models of fatigue have tended to focus on fatiguing mechanisms that occur within muscle (models of peripheral fatigue) that were initially proposed in 1924 (Hill 1924) and informed by the work of Fletcher and Hopkins (Fletcher 1907) which implicated lactic acid as the causal factor in fatigue. Prior to this, Angelo Mosso in the late 1800s identified in his seminal paper that fatigue probably occurred both within the central nervous system and within the muscle (Di Giulio, Daniele, & Tipton 2006; Mosso 1915) and that these two mechanisms, which cause degradation in performance, are interdependent; it will be shown that this view now dominates current thinking. Fatigue occurs as one or more of the physiological processes that enable the contractile proteins within a muscle to generate force are impaired (Enoka & Duchateau 2008).

The term 'fatigue' has defied accurate definition. To the lay person the term 'fatigue' has quite a different meaning to that of physiologists and clinicians. It is common to 'experience' what is describe as 'exhaustion', 'fatigue', 'tiredness' and 'lack of motivation' that limits work or task performance. Activities cease because they are 'too hard' or 'given up' as an object becomes 'too heavy' or the task 'too difficult'. Often, performance degradation occurs, as an individual 'tires'; an activity that is normally skilfully performed becomes clumsy and inefficient. This subjective feeling of 'fatigue' or 'sense of effort' is quite different to the unconscious physiological processes that occur and which actually cause the diminution in force output and the associated performance degradation. This distinction is important and will be discussed in further detail in the section on the measurement of fatigue (Section 2.4).

It is tempting to assume that within the scientific community, the term 'fatigue' has an accurate definition; this is not the case (Enoka & Duchateau 2008; Gandevia 2001). When applied to exercise, fatigue can be defined as 'failure to maintain the required or expected force' (Edwards 1981), or 'failure to continue working at a given exercise intensity' (Booth and Thomason 1991). These two views of fatigue imply that when the 'point of fatigue' is reached there is a sudden inability to continue with the exercise or task. This is not the case, but it does lead to the further implication that muscles and the central nervous system only show evidence of fatigue at the 'point of failure' or at 'exhaustion'. It will be seen that measurements of myoelectric manifestations of fatigue are evident as soon as a task begins; furthermore, force output begins to fall early in exercise along with task performance (Gandevia 2001) although this may often be a qualitative change in performance rather than a task failure.

A more appropriate definition of fatigue is 'any exercise induced reduction in the ability to exert muscle force or power, regardless of whether or not the task can be sustained' (Bigland-Ritchie and Woods 1984). This definition was further refined at a National Heart, Lung and Blood Institute workshop on respiratory medicine, to 'A loss in the capacity for developing force and/or velocity of a muscle, resulting from muscle activity under load and which is reversible by rest' (NHLBI 1990). This last definition introduced the important qualification that fatigue is reversible by rest; this implies that the mechanisms that cause task failure result from physiological processes that are reversible. This definition also focuses on the performance of the task, which can then be applicable to any human task performance and not just exercise. Gandevia (2001) defined fatigue as an 'exercise induced reduction in maximum voluntary muscle force'. This use of the term 'maximum' has an important consideration when designing testing procedures if this definition is used, as many testing procedures do not use maximum force; the use of this definition may also be inappropriate when endurance fatiguing protocols are used.

Therefore, during any physical activity the inability to maintain the required force or output, which was there at the beginning of the activity, is dependent on both peripheral and central mechanisms. In this thesis, the definitions

based on Gandevia (2001) are used (Table 4) and their use discussed in the following section that relates to models of fatigue.

Table 4. Definitions of terms related to fatigue (Gandevia, 2001).

Muscle fatigue	Any exercise induced reduction in the ability of the muscle to generate force or power; it has peripheral and central causes – rest reverses it.
Peripheral fatigue	Fatigue produced by changes at, or distal to, the neuromuscular junction.
Central Fatigue	A progressive reduction in voluntary activation of muscle during exercise.
Supraspinal fatigue	Fatigue produced by failure to generate output from the motor cortex; a subset of central fatigue.
Task failure	Cessation of a bout of exercise. This may be accompanied by peripheral fatigue, central fatigue, or both.
Sense of effort	A subjective sensation of effort involved in a task

2.2.2 Model of peripheral fatigue

Peripheral fatigue is usually defined as the mechanism that occurs distal to the point of motor nerve stimulation i.e. any peripheral synapse at the neuromuscular junction and includes any of the processes occurring within the muscle cells that degrades performance. This includes failure of a sufficient rate of energy substrate availability for the process of excitation-contraction coupling in muscle contraction. This may result in failure of the action potential to propagate across the surface membrane and the t-tubular system of the muscle fibre, failure of the coupling mechanism between action potential and the release of calcium or failure of calcium regulation in the muscle cell (Jones 1996).

A reduction in available rate at which adenosine triphosphate (ATP) can be supplied to the exercising muscle is often quoted as a cause of fatigue and loss of performance (Fletcher 1907; Hill 1924; Noakes 2000). The belief is that during high intensity exercise, fatigue occurs whenever the rate of ATP need exceeds that which the oxidative processes within the muscle can provide; at this point a shift to less sustainable anaerobic ATP production occurs to

supplement the rapidly dwindling rate at which ATP can be provided. Fatigue occurs as a result of the failure to maintain the required rate of ATP supply to the exercising muscle and a reduction in force or performance results. In high intensity exercise this results in a failure to continue with the task or the task performance has to continue but at a lower intensity which is determined by the rate at which ATP can be supplied.

Models of fatigue that are predicated on peripheral mechanisms are often referred to as 'catastrophe' models (Noakes, St Clair, & Lambert 2004; Noakes, St Clair, & Lambert 2005). If it was the case that the mechanism of fatigue resulted in an exercising muscle becoming depleted of ATP, then muscle rigor is hypothesised as ATP is required for the excitation-contraction uncoupling process. As rigor is not seen or described in the literature, then the rates of ATP production must be matched, even during maximum exercise, with uptake. It would appear that muscle concentrations of ATP are as homoeostatically regulated during exercise as they are under resting conditions. The physiological processes by which the synthesis of ATP within the mitochondria is coupled to the breakdown of carbohydrates and fats to provide ATP and the oxidative phosphorylation of adenosine diphosphate (ADP) into ATP prevents such catastrophic depletion of substrate. Thus, such catastrophe models are dismissed as too simplistic and likely to be inaccurate; if true, this model would imply that all muscles could act independently of one another and would continue independently contracting until stressed beyond capacity and rigor would develop. As neither rigor is seen, nor are there physiological markers that would indicate that ATP levels drop significantly during fatiguing exercise other models to explain the phenomena of fatigue have emerged (Noakes and St Clair 2004).

2.2.3 Muscular wisdom model of fatigue

The 'Muscle Wisdom' model proposes that the motor neuron firing rates reduce to match the capacity of the muscle to contract (Jones 1981; Marsden, Meadows, & Merton 1983). In this model, the output of a motor unit is controlled locally by a mechanism that is driven by feedback from the muscle itself. Modulation at the motor neuron pool would occur as metabolites accumulated within the muscle, ATP reserves become depleted or some other

event that affected the capacity of the muscle to contract such as injury or failure in the excitation-contraction coupling.

The likely effects on muscle, because of local muscle receptor sensitivity, are outlined in Figure 11, in particular, the type III and IV afferent fibres from receptors within the muscle which may act as metaboloreceptors or chemoreceptors in addition to the group Ia/II from muscle spindles and Ib from the Golgi tendon organ. While these data are taken from cat studies, it is proposed that the muscle afferents in the human act similarly (Gandevia 2001). As certain physiological processes develop within the muscle cell, it has been shown that the type III and IV afferents cause a decline in motor neuron firing rates (Garland, Garner, & McComas 1988) and these findings have formed the basis of the muscular wisdom theory.

Metabolic changes that do occur within an exercising muscle and which have been associated with the muscular wisdom theory are lactic acid accumulation, a decrease in pH and proton accumulation, ATP and creatine phosphate depletion, increases in ADP and other inorganic phosphates, changes in skeletal muscle Na^+/K^+ ATPase pump and changes within the sarcolemma, t-tubular system and sarcoplasmic reticulum (Jones 1996). The model suggests each of these could act via afferent feedback to inhibit motor neuron firing and thus produce the effects of fatigue. This could be evident by a reduction in force, endurance or the elecromyographic changes that are associated with fatigue.

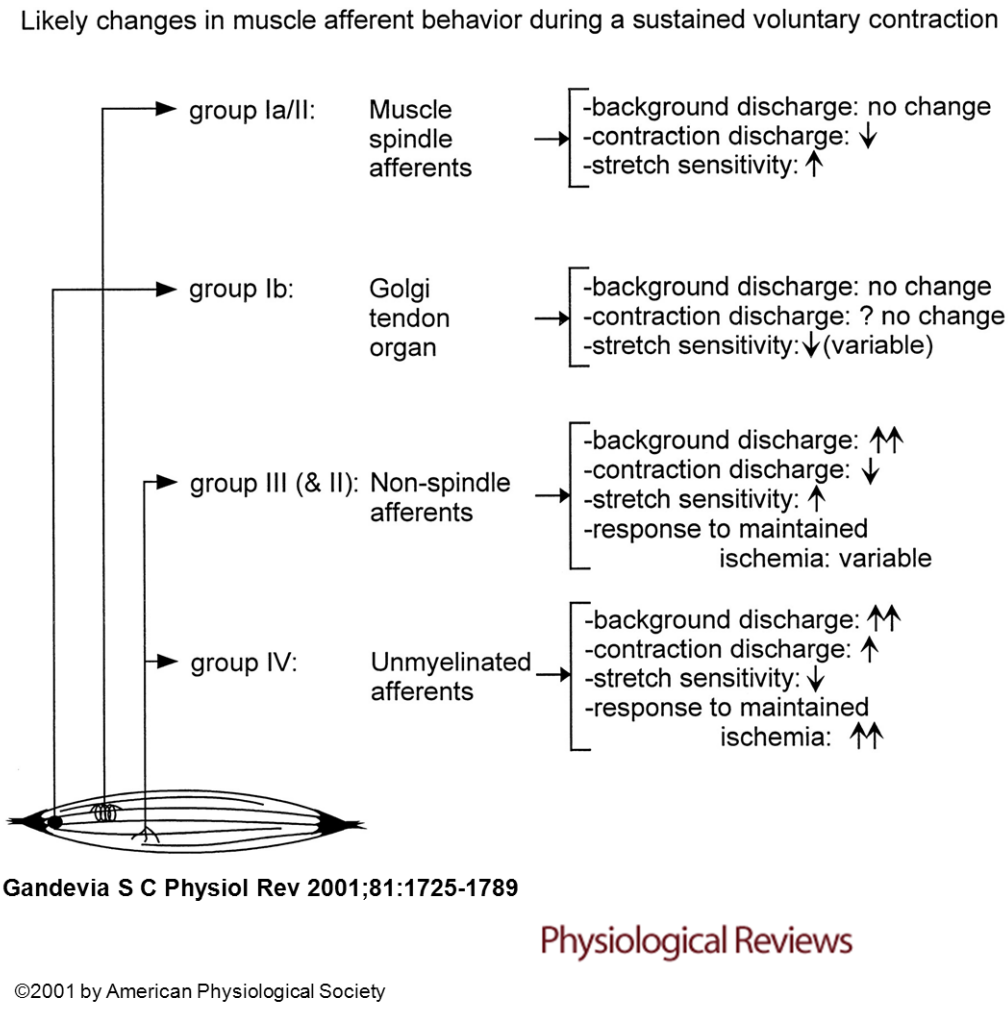

Figure 11. Likely effects of muscle fatigue on the input from different classes of muscle receptor.

Data are shown in Figure 11 for background discharge rate, responses to a muscle contraction, responses to muscle stretch and responses to muscle ischemia maintained after a contraction.

Both the muscle wisdom model and models of peripheral fatigue are described as linear dynamic systems and such models predict that fatigue is an end point in which changes occur in direct response to input variables which define the limits of the system. Such models predict that activity would continue to an end point driven by the maximum capacity of the metabolic and physiological processes. These models have proved to be too simplistic and have resulted in more complex models being proposed that more fully predict and explain fatigue (Noakes 2000) (Section 2.2.5).

2.2.4 Central fatigue model

A version of peripheral fatigue known as central fatigue (Dalsgaard and Secher 2007; Meeusen, Watson, Hasegawa, Roelands, & Piacentini 2006) is also described as a 'catastrophe' model as the central nervous system changes are reactions to changes in the periphery and therefore cannot be controlled nor predicted. The nervous system in this model acts as a linear dynamic control system; central drive to the motor neuron pool would diminish as a consequence of feedback from the periphery until exhaustion results (Swart, Lamberts, Lambert, St Clair, Lambert, Skowno, & Noakes 2009).

Illustrated in Figure 12 is an interpretation of central fatigue model from Gandevia (2001) that illustrates how such a linear dynamic control system might operate. There is some complexity in this model but it can be seen that this model is reactive to changes in the periphery and is essentially a catastrophe model in which the local control mechanisms can override the homeostatic role of the CNS. If any peripheral control system could override the central control of the nervous system then, in theory, such a mechanism could deplete the local and ultimately, the global reserves of energy leaving the organism vulnerable if a critical life or death situation occurred. In nature and in terms of the evolutionary process, this could endanger the individual or the species, which would be vulnerable to predation.

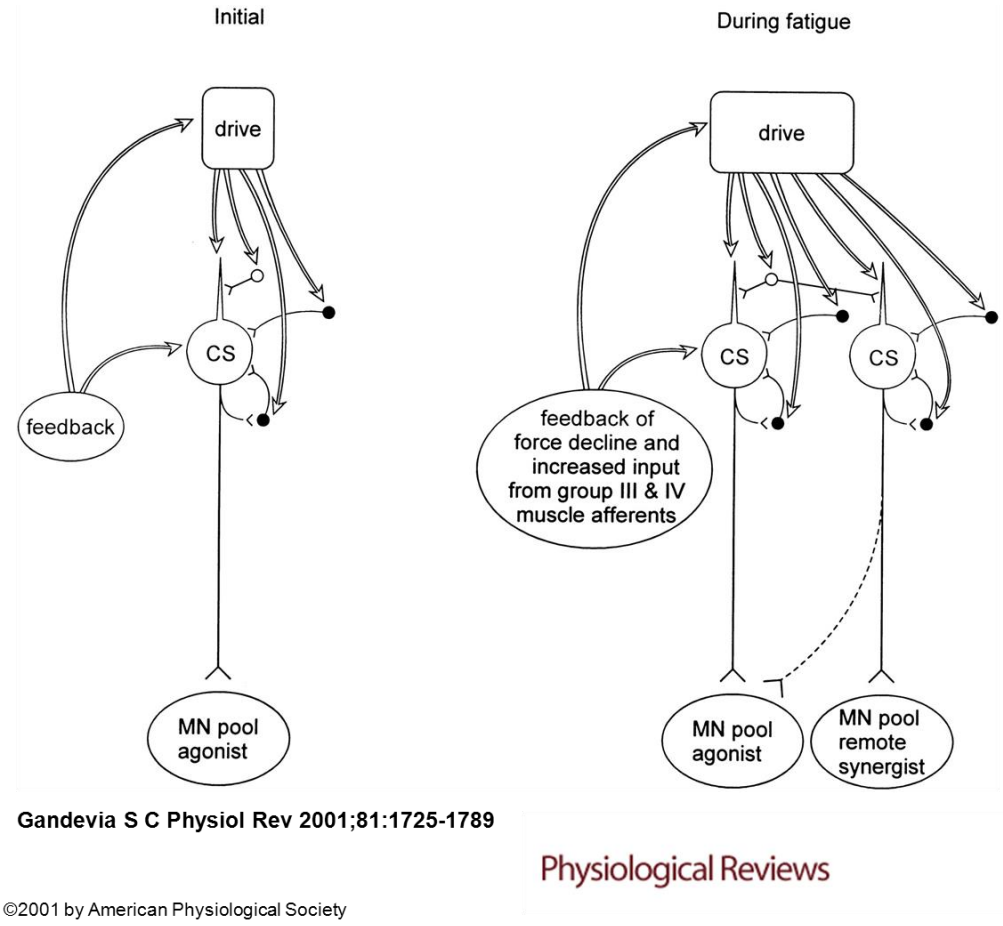

Figure 12. Possible changes at a motor cortical level resulting from muscle fatigue.

Figure 12 illustrates the possible changes at a motor cortical level with muscle fatigue. Simplified schema for reflex input and 'supra' motor cortical input to a corticospinal cell (CS) under control conditions (left) and during fatigue (right). Solid cells are inhibitory, and open ones are excitatory. During fatigue there is increased drive to corticospinal cells and more are 'recruited.'

2.2.5 Central governor model of fatigue

This model of fatigue has gained popularity particularly within the sports medicine community (Okano, Fontes, Montenegro, Farinatti, Cyrino, Li, Bikson, & Noakes 2013); it is an integrated approach with a comprehensive ability to explain how multiple peripheral physiological systems interact with the central nervous system. The central governor model (CGM) of fatigue is an example of a non-linear complex integrative control system in which all physiological

systems interact continuously in a deterministic manner (Lambert, St Clair, & Noakes 2005; St Clair & Noakes 2004; Swart et al. 2009). While this integrative model is popular, it does not receive universal support. Some dismiss the model and support either more peripheral models of fatigue (Shephard 2009; Weir, Beck, Cramer, & Housh 2006) or a model based on the notion that there is no global mechanism responsible for fatigue but that there is specificity with regard to the mechanisms that cause reductions in power and that these are task specific (Enoka & Duchateau 2008). The debate continues with robust evidence based and experimental defences of the CGM of fatigue (Noakes 2011a; Noakes 2011b).

In this thesis it will be assumed that the CGM of fatigue is the dominant model and that other models are essentially based on and subservient to this model.

The CGM is not a catastrophe model but a model in which the CNS functions to maintain homeostasis of all physiological systems by modulating the output to the motor neurone pool (Noakes 2012; Ulmer 1996). The CNS uses changes in the peripheral physiological systems as afferent signals to modulate control processes in a dynamic, non-linear, integrative way. The CGM does not deny the importance of substrate depletion and other physiological processes that peripheral models of fatigue state cause fatigue; in the CGM, changes in all physiological processes are integrated into a model that allows the CNS to plan, pace and execute motor output as efficiently as possible. Motor output relies on feed-forward as well as complex feedback mechanisms and in a complex non-linear control system, there will be evidence that the system is subject to 'gain'. With physiological systems that cannot return to baseline immediately following perturbation and a system that needs to fully integrate all physiological systems there will inevitably be fluctuations; this is a feature of integrative physiological systems and commonly seen. Furthermore, the CGM has the capacity to reconcile the competing issue of the sense of effort perceived during a fatiguing task and the measurable objective outputs that are used to indicate that the system is fatiguing, often, these subjective and objective measures are not associated. This model is consistent with Mosso's original notion that both the CNS and muscles alter function during activity and that the sense of 'fatigue' is largely an emotion (Mosso 1915).

The CGM is also capable of explaining phenomena such as pacing that occurs during exercise, training and how factors such as heat, state of fitness, injury,

prior experiences, psychological distress and emergency situations can be factored in to ensure that whatever motor output is required is optimised for that given situation. Only in extreme and often pathological or life threatening situations does the CGM allow exhaustion to occur.

The significance of the CGM is that it predicts that as the central drive to the motor neuron pool is under central not peripheral control then any measurements taken that result from the motor neuron pool output, such as EMG, are modulated centrally. The implication being that such measures are likely not to be true measures of any fatigue mechanism that is operating only within the muscle as has been previously assumed. This has profound implications when comparisons or assumptions are based only on measures taken from the periphery.

In relation to low back pain, the role of fatigue will be addressed in the following sections.

2.3 Low back pain

2.3.1 Definitions

Low back pain is commonly defined as pain or discomfort perceived to be in the area bounded by the bottom of the rib cage and the buttock creases. Non-specific low back pain may also be felt in the posterior aspect of the upper legs but not below the knee (Savigny, Kuntze, Watson, & Underwood 2009).

In the context of this thesis, LBP is defined as a symptom which is non-acute i.e. greater than six weeks since initial onset. Excluded are cases with neurological symptoms, symptoms below the knee and symptoms of less than six weeks since initial onset. Non-specific LBP is also often described as persistent or recurrent low back pain that has lasted for more than six weeks, but for less than 12 months. Excluded from this definition is LBP where malignancy, infection, fracture, ankylosing spondylitis or other inflammatory disorders, radicular pain resulting from nerve root compression or cauda equina compression are the causal factor (Savigny, Watson, & Underwood 2009). In this thesis, the term LBP refers to non-specific LBP and excludes all acute causes and the conditions specified and defined above.

2.3.2 Introduction: non-specific low back pain

Non-specific LBP is endemic; it is a commonly reported symptom in all cultures and ethnic groups but increasingly associated with post-industrial society. It is often reported that between 70% - 80% of the population in industrialised countries will have at least one major episode of LBP during their lifetime requiring some form of intervention, time off work or limitations in other activities (Bevan, Passmore, & Mahon 2009; Bigos, McKee, Holland, Holland, & Hildebrandt 2001; Ehrlich 2003; Svensson, Andersson, Johansson, Wilhelmsson, & Vedin 1988; Webb, Brammah, Lunt, Urwin, Allison, & Symmons 2003; Woolf and Pfleger 2003). The year prevalence of LBP is in the order of 20% - 50% and those affected by LBP often experience an episode at least once a year. The causes of LBP remain elusive; in only 10% - 20% of cases is a clearly identified cause evident (Leclere, Beaulieu, Bordage, Sindon, & Couillard 1990; Webb et al. 2003). All other LBP is commonly referred to as non-specific LBP and typically includes LBP where serious pathology and/or neurological involvement have been excluded.

In industrialised countries, non-specific LBP in the adult population who are 45 years or less is the most common cause of disability. In adults aged 45 to 65, disability due to LBP is second only to arthritis (Frank, Brooker, DeMaio, Kerr, Maetzel, Shannon, Sullivan, Norman, & Wells 1996; Frank, Kerr, Brooker, DeMaio, Maetzel, Shannon, Sullivan, Norman, & Wells 1996). Data from the United Kingdom Office of National Statistics Omnibus Surveys show no reduction between 1996 and 1998 in the UK prevalence of LBP (Omnibus Survey 1998). In the UK, 17.3 million people, over one third of the adult population, are affected. In any given year, around 3.5 million people experience back pain for the first time and for 3.1 million people their pain lasts throughout the year and some consider the problem to be of epidemic proportions (Waddell, Feder, & Lewis 1997). Despite claims that most acute episodes of LBP resolve quickly without treatment, the condition often lasts more than three months to become a chronic problem (Waddell, Feder, & Lewis 1997). Treatment regimens are often palliative with some questioning the value of most interventions (Bogduk 2004). With regard to exercise, there is moderate quality research evidence reported in the literature that post-treatment exercise programmes can prevent recurrences of back pain but there is conflicting evidence for exercise as part of treatment (Choi et al. 2010). The

general advice is to stay active during acute episodes of LBP, while in chronic LBP there is evidence that advice to stay active with the addition of specific advice, exercise and functional activities to promote active self-management has been shown to be effective in speeding resolution and avoiding chronicity (Liddle, Baxter, & Gracey 2004; Liddle, Gracey, & Baxter 2007).

The traditional view that LBP is a series of clinically independent events has changed (Dunn 2010; Dunn and Croft 2004; Webb et al. 2003) to a model that encompasses aspects of a bio-psychosocial model and a 'life course' approach to the risks, onset and disease progression. This is based not just on biological causes but also on behavioural, psychological and social factors. The current view is that LBP is a symptom that affects most if not all of the population at some point in their lives but with levels of impairment, disability and chronicity that differs significantly between individuals. It is a major public health problem with significant economic impact. In the UK, it is estimated that 4% of the general population are currently on sick leave from work due to LBP (Webb et al. 2003) with up to 2.6 million people each year seeking advice from their GP due to LBP (Arthritis Research Campaign. 2002)

2.3.3 Natural history of low back pain

A number of systematic reviews that have reported on the natural history, prevalence and incidence of LBP and population studies suggest that initially the condition is self-limiting and that there is rapid improvement within the first three months after onset. Following this, the rate is less rapid. At six months post onset, 16% of patients remain off work and at 12 months, 62% still have pain (Hestbaek, Leboeuf-Yde, Engberg, Lauritzen, Bruun, & Manniche 2003). Other authors report that 90% of patients with LBP will recover in a month (Papageorgiou, Croft, Ferry, Jayson, & Silman 1995). This apparent contradiction maybe due to the definition of 'recovery'; for example, using Waddell's definition of 'return to work', 80% - 90% of episodes of LBP will have 'recovered' within six weeks as in many cases people return to work despite persisting symptoms (Waddell and Burton 2005), whereas no claim was made that there had been a resolution of LBP .

It is concluded that LBP should not be considered as temporary, but a condition that is rarely self-limiting and often presents with episodic periods of pain and that remissions when they occur, are temporary (Hestbaek et al. 2003). Chronicity is common and characterised by episodes of exacerbation and remission.

2.3.4 Prevalence

There are various estimates of the prevalence of the problem of LBP. An often quoted figure is the life time prevalence of 80% i.e. four out of every five of the population in industrialised countries will have a significant episode of LBP at some point in their life requiring some form of intervention or time off work or other activity (Deyo and Tsui-Wu 1987). In one study in the UK, the one-month point prevalence was estimated to be between 35% and 37%, with peak prevalence in those aged 45 to 59 years old. The lifetime prevalence is estimated to be in the region of 49% – 84%, the higher figure being the figure quoted most frequently in the literature. In a systematic review of the data from 1966 – 1998 the point prevalence was given as 33%, the year prevalence as 65% and the lifetime prevalence as 84% (Walker 2000). A study carried out in the USA estimated that the cumulative lifetime prevalence of back pain was around 14% (Deyo & Tsui-Wu 1987). There is not convincing evidence that age effects prevalence (Airaksinen, Brox, Cedraschi, Hildebrandt, Klaber-Moffett, Kovacs, Mannion, Reis, Staal, Ursin, & Zanoli 2006; Svensson et al. 1988). Others estimated the annual prevalence of back pain lasting at least two weeks to be around 10% (Liddle, Baxter, & Gracey 2004; Liddle, Gracey, & Baxter 2007).

While there appears to be some variation in the underlying statistical data, in the studies referred to above, the extent of the problem is evident. There is a lifetime prevalence of between 49 – 84%; the annual prevalence is in the region of 10 – 12% and clear evidence of the economic and social burden caused by chronicity in LBP (Hestbaek, Leboeuf-Yde, & Manniche 2003).

2.3.5 Cost of low back pain

In a study of the costs of LBP in the UK, it is estimated that the direct health care costs of diagnosis and treatment of LBP to the UK health services was £1632 million in 1998. This often quoted figure hides the true cost of LBP

when compared to the £10668 million in informal care and production losses (Maniadakis and Gray 2000).

2.3.6 Management of low back pain – general recommendations

Currently, the definitive management of LBP remains unclear although there is emerging consensus based on evidence-based practice (Abbott, Franklin, & Melzack 1996; Bogduk 2004; Dagenais, Tricco, & Haldeman 2010; Koes, van, Lin, Macedo, McAuley, & Maher 2010; Lin, Haas, Maher, Machado, & van Tulder 2011a; Lin, Haas, Maher, Machado, & van Tulder 2011b). These highlight the need for those with LBP to; 'stay active', 'avoid bed rest', 'self-medicate with over-the-counter medication' and to seek 'manual therapy' (Dagenais, Tricco, & Haldeman 2010). Strategies based on a definitive pathological diagnosis have been shown to be effective where zygapophysial joint or sacroiliac joint pain has been confirmed using diagnostic blocks (Dreyfuss, Halbrook, Pauza, Joshi, McLarty, & Bogduk 2000) and there is some evidence emerging that where definitive disc disruption can be identified this too can be specifically and successfully managed in some cases. With fewer than 10% of cases being diagnosed by X-ray and MRI (Bogduk 2004), other possible causes of LBP are numerous and determining the management of LBP on this basis is problematic and as a result, strategies for rehabilitation and management have been developed which are based on symptom presentation and not definitive diagnosis (Waddell & Burton 2005).

Exercise therapy and advice have been shown to be effective in managing the symptoms of chronic LBP (Hayden, van Tulder, Malmivaara, & Koes 2005; Hayden, van Tulder, & Tomlinson 2005). Apart from medication and spinal manipulation when used to treat symptoms of LBP (Assendelft, Morton, Yu, Suttorp, & Shekelle 2004), few other approaches have been shown to be clinically effective in situations where a definitive cause has not been identified (van Tulder, Koes, & Bouter 1997). Current National Collaborating Centre for Primary Care and Royal College of General Practitioner Guidelines (Savigny, Watson, & Underwood 2009) for Non-specific LBP recommend exercise and advice on staying active. Combined physical and psychological therapies, acupuncture and pharmacological therapies are indicated where specific surgical intervention is not, although, this is beyond the scope of this thesis.

2.3.7 Pathology of low back pain – the degenerative cascade

Kirkaldy-Willis (Kirkaldy-Willis 1988) described a process of degeneration that passes from one phase to another, as a degenerative cascade (Figure 13). He emphasised the progressive nature of pathology that affects the 'three joint complex' made up of the two zygapophysial joints (often referred to as 'facet joints', Figure 13) of the adjacent vertebrae and the inter-body joint between the vertebral bodies of two adjacent vertebrae that includes the intervertebral disc. In this unifying model, Kirkaldy-Willis postulates that the degenerative processes result in a dysfunction phase, an instability phase and a phase of stabilisation. His model was one of the first to propose that LBP was a continuum and not a series of isolated painful or pathological incidents.

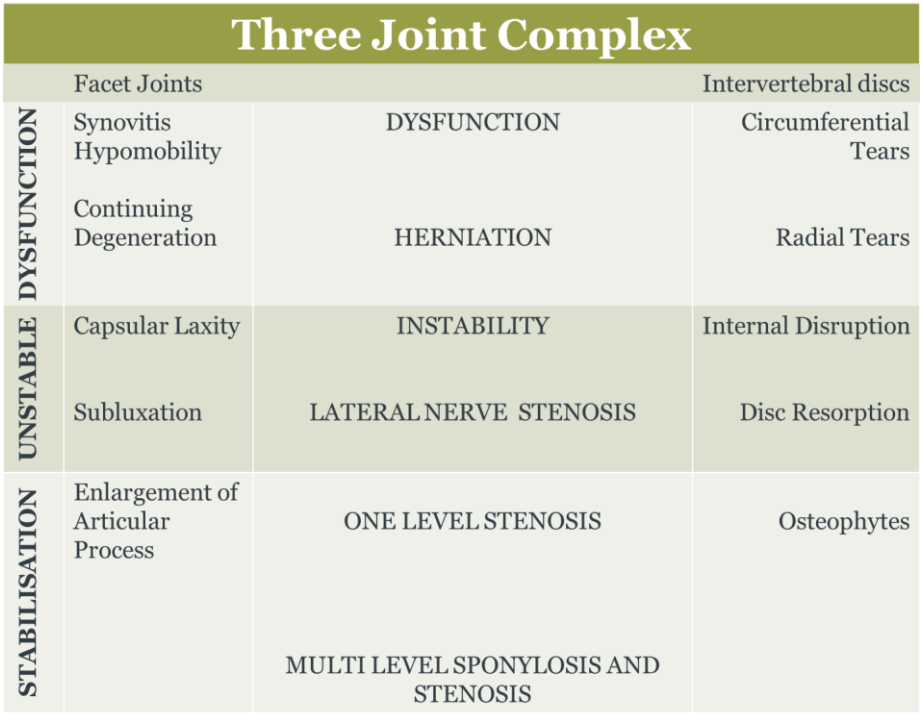

Figure 13. The degenerative cascade of Kirkaldy-Willis (1988).

Figure 13 illustrates the degenerative cascade of pathology as age progresses. It relates the pathology within the facet joints and intervertebral discs to clinical presentations such as joint 'instability'.

The degenerative cascade concept has been elaborated by numerous authors who describe the biological progress as a cascade initiated by disc degeneration (Adams and Roughley 2006; Smith, Nerurkar, Choi, Harfe, & Elliott 2011). These authors suggest that there is a distinction between age

related disc degeneration and early degenerative changes that are accelerated age-related changes. Not all age related changes result in pain, however, accelerated early disc disease frequently does. Aberrant cell mediated response to progressive structural failure occurs that further degrades the structural integrity of the intervertebral disc and this triggers the cascade process. As disc degeneration progresses the typical signs of vertebral end plate fracture, radial and circumferential fissures and herniation occur. Once the structural integrity of the intervertebral disc is lost then progressive instability at segmental levels continues to occur, this leads to accelerated changes that involve the zygapophysial joints, which also progress through phases of degeneration.

The degenerative cascade processes are consistent with patterns of LBP pain seen clinically; these are characterised by acute episodic LBP typically seen in the third decade of life to the more chronic but less severe LBP which is a characteristic of presentations seen in the fifth and sixth decades. This is consistent with a process of adaptive stabilisation in some, but which, in others, results in stenotic pathology of the spinal cord, nerve roots or cauda equina.

The model of a degenerative cascade has a focus on the degenerative processes that occur in the 'three joint complex' that can be readily demonstrated through imaging and histological techniques. The model does not seek to account for the role of the stabilising muscle of the spine nor of the role of motor control from the central nervous system. These systems are important contributors to spinal stability and this will be explained in subsequent sections.

2.3.8 Muscle physiology in low back pain

Following episodes of LBP there is a resulting decrease in muscle mass and an alteration in muscle fibre characteristics that is considered a further potential cause of chronicity (Hides, Richardson, & Jull 1996; Hides, Stokes, Saide, Jull, & Cooper 1994; O'Sullivan, Twomey, & Allison 1998). In reviews of the lumbar spinal muscle fibre type characteristics of people with LBP, it was found that the microanatomy of the lumbar spine muscles is altered (Mannion 1999a;

Mannion 1999b; Mannion, Dumas, Cooper, Espinosa, Faris, & Stevenson 1997a; Mannion, Dumas, Cooper, Espinosa, Faris, & Stevenson 1997b; Mannion, Kaser, Weber, Rhyner, Dvorak, & Muntener 2000; Mannion, Weber, Dvorak, Grob, & Muntener 1997). A significantly higher proportion of Type IIx (fast twitch) fibres develop at the expense of Type I (slow twitch) fibres. Slow twitch fibres are associated with fatigue resistance, but it is not clear if this is a result of LBP or a potential cause of LBP. A higher proportion of Type IIc fibres (an intermittent muscle fibre with both 'fast' and 'slow' twitch characteristics) occur in patients with LBP. The Type IIc fibre may be a transformational muscle fibre undergoing change as a result of LBP (Mannion 1999a). Analysis of the rms and MDF of the surface EMG and the shift in the power/frequency spectrum may highlight the myoelectric manifestations of fatigue associated with changes in muscle fibre type and subsequently any changes that may result due to endurance training that would be evident by the relative rate of shift in the MDF (See Section 2.4).

2.3.9 Muscle fatigue – general concepts

Muscles have been likened to 'motors' (Apter 1966); if this is the case then the behaviour of the muscle will depend on its intrinsic physiological and mechanical properties and in the way the nervous system provide inputs that drive the muscle and in the way that feedback from the muscle to the central nervous system modifies the characteristics of the muscle's output by modulating the output from the motor neuron pool. The following figure (Figure 14) and text provides an overview of the steps involved in voluntary force production and factors acting at the motor neuron level.

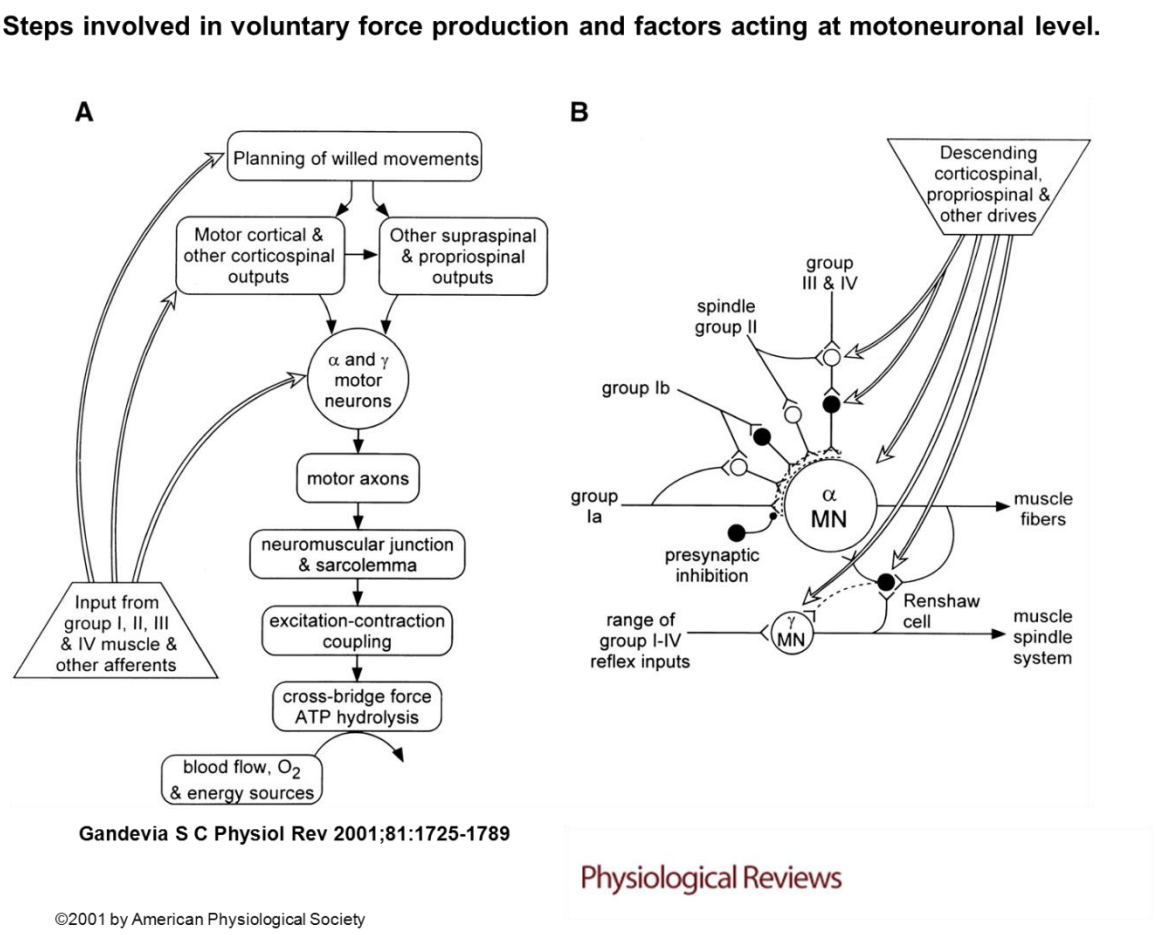

Figure 14. Motor control.

Figure 14 indicates the steps involved in voluntary force production and factors acting at motor neuronal level. A: diagrammatic representation of the 'chain' involved in voluntary contractions. A major source of feedback from the muscle is shown acting at three levels in the central nervous system. Other sources of feedback that also act at these levels are not shown. B: summary of inputs to α- and γ-motor neurons for an agonist muscle. Cells with solid circles are inhibitory. Dotted curved region at premotor neuronal terminals denotes presynaptic inhibition acting selectively on the afferent paths to motor neurons.

2.3.10 Role of fatigue in low back pain

Fatigue of the muscles of the lumbar and thoracic spine is considered a significant factor in the causality of low back pain (Deyo and Weinstein 2001; Faas, Van Eijk, Chavannes, & Gubbels 1995; Maniadakis & Gray 2000; Mannion

1999a), particularly in relation to occupational exposure to tasks that might accelerate the rate of spinal muscle fatigue. An assumption being that when local and global stabilising muscles of the spine are fatigued they generate less force and therefore have less capacity to protect the spinal components from injury or the exacerbation of underlying symptoms. This simplistic view of a local fatiguing effect only partially explains the complexity of the system of fatigue that is now considered to encompass and involve the entire nervous system (Lambert, St Clair, & Noakes 2005; Noakes 2011b).

Current models concerned with the control of movement consider that fatigue is a manifestation of a complex system interaction based around a non-linear model of control driven from the central nervous system (Lambert, St Clair, & Noakes 2005). Such a model adds a dimension of complexity to the understanding of fatigue that prevents a simplistic association between energy expenditure, the perception of fatigue and the EMG signal. This complexity will be addressed in further sections of this thesis.

Fatigue of the muscles supporting the lumbar spine has been associated with low back pain (Alaranta, Luoto, Heliovaara, & Hurri 1995; Biering-Sorensen 1984b; Holmstrom, Moritz, & Andersson 1992; Jorgensen 1997; Kujala, Taimela, Viljanen, Jutila, Viitasalo, Videman, & Battie 1996) and in some occupational groups lumbar spine muscle fatigue can significantly impact on operational performance.

Spinal muscle fatigue, as indicated by the isometric Biering-Sørensen test, was implicated over 25 years ago as a predictor of chronicity in LBP (Biering-Sorensen 1984b) and it continues to be implicated in more recent literature. This is particularly so in LBP that lasts longer than three months (Bogduk 2004) and first time LBP (Adams, Mannion, & Dolan 1999; Mannion, Connolly, Wood, & Dolan 1997). These previous studies identified outcome measures that were associated with poor endurance and the inability to complete an endurance task as evidence of spinal muscle fatigue; this logic leads to the assumption that participants in these studies would benefit from increased endurance capacity. However, few treatments strategies include exercise regimes designed specifically to address endurance. Most treatments attempt pain reduction in the acute phase followed by active rehabilitation approaches to improve strength and/or mobility. Endurance training, which is required to

improve muscle fatigue, is time consuming, requires motivation and is infrequently prescribed or undertaken.

With an ever increasingly sedentary lifestyle in industrialised countries and populations that exercise infrequently, levels of cardiovascular fitness and general endurance levels continue to reduce. With decreasing levels of activity and exercise, poorer endurance of the spinal muscles results and this reduction may further contribute to chronicity in people with LBP. Furthermore, reluctance to exercise, poor motivation and fear avoidance is often prevalent in those with chronic LBP so compounding the problem (Buer and Linton 2002; Staerkle, Mannion, Elfering, Junge, Semmer, Jacobshagen, Grob, Dvorak, & Boos 2004). Despite this, there is emerging evidence to support the use of exercise in LBP (Burton and Waddell 1998; Burton, Waddell, Tillotson, & Summerton 1999; Crossman, Mahon, Watson, Oldham, & Cooper 2004) during both the acute and the chronic phases as both a safe and an effective approach that reduces chronicity by maintaining movement, muscle strength and muscle endurance (Kankaanpaa, Taimela, Laaksonen, Hanninen, & Airaksinen 1998). The challenge is to develop effective exercise approaches that will be performed at an appropriate intensity and over a period considered effective in improving endurance capacity.

2.3.11 Role of rehabilitation in the management of low back pain

Accordingly, strategies to increase the endurance of spinal stabilising muscles would result in more consistent power output and more efficient motor patterns. This could result in fewer fatigue related injuries and less LBP within susceptible populations. Indeed, exercise strategies that increase aerobic capacity and reduce muscle fatigue are a proven method in the treatment and prevention of LBP (Biering-Sorensen 1983; Hestbaek et al. 2003; Papageorgiou et al. 1995; Waddell, Feder, & Lewis 1997). However, the evaluation of muscle fatigue is problematic and although validated testing protocols exist (Latimer, Maher, Refshauge, & Colaco 1999), these do not measure fatigue directly and thus do not lead directly to specific exercise-related treatment strategies.

2.4 Measurement of fatigue

In the following sections, a summary of the key methods to investigate the fatigue of the muscles of the lumbar region are described with particular reference to low back pain.

2.4.1 Surface electromyography

Surface Electromyography is a useful technique for measuring global and local muscle activity and measures relating to muscle fatigue can be made. Furthermore, the objectivity achieved with sEMG is thought by some to overcome problems associated with measurements where motivation, pain, pain avoidance behaviours and reporting errors can occur (Cescon, Venturi, Merletti, Bonfiglioli, & Violante 2004).

However, if measurements from specific muscles are required, it is the prevailing view that a detailed knowledge of the relationship between the underlying anatomical arrangement of muscles and the surface anatomy is necessary in order that sEMG electrodes can be orientated correctly (Farina, Pozzo, Merlo, Bottin, & Merletti 2004). The general consensus is that the orientation of the sEMG electrode array should be along the longitudinal axis of the muscle and parallel to the orientation of individual muscle fibres (Mesin, Merletti, & Rainoldi 2009). This is particularly important when repeat estimates of measures of median frequency and average rectified values are required. It follows that detailed knowledge of muscle fibre orientation and the relationship to surface anatomy is required in order to accurately place sEMG electrodes. Such anatomical detail is often absent from standard anatomical texts that frequently only provide details of muscle attachment.

Two dimensional linear array electrodes, that cover large areas could be utilised to provide global details of EMG activity. These would be particularly useful as the orientation of the lumbar muscles has yet to be precisely mapped and as the various muscle groups do not run parallel to each other. The current lack of understanding also limits interpretation from previous sEMG studies.

2.4.2 Surface EMG changes in fatigue

The global parameters of interest in studying fatigue are the MDF and rms of the signal amplitude value calculated from a sEMG signal. The rms is calculated from consecutive 1s time windows of a sEMG signals. The MDF is defined as the frequency that divides the frequency spectrum into two equal areas, the frequency is calculated from 1s non-overlapped time windows using a fast Fourier transform algorithm which is used to calculate the power/frequency spectrum.

In practice, rms values that increase concurrently as MDF values reduce are considered to be myoelectric manifestations of fatigue. Increase in force over time can occur without fatigue as can a shift to lower frequencies of the MDF fatigue plot that can occur as force decreases, but these changes are not considered manifestations of fatigue unless they occur concurrently (Luttmann, Jager, & Laurig 2000).

2.4.3 Techniques of sEMG data collecting

Various techniques exist that allow recording of the electrical field potential from muscles, the most common are;

1. Needle EMG.
2. Surface EMG using monopolar or bi-polar electrodes.
3. Multi-channel surface EMG using electrode matrices and arrays.

Needle EMG recording is an invasive technique that is limited to measurements from an area defined by the size and position of the needle. Fine wire needle EMG only records from a few muscle fibres close to the tip of the needle that makes generalisability to the whole muscle and reproducibility of the technique difficult. Needle EMG gives information on motor unit (MU) depolarisation as a time varying signal, however, it is not possible to extract information on the direction of propagation of the signal nor on muscle architecture (Zwarts and Stegeman 2003).

Surface EMG systems using either mono-polar or bipolar electrodes give more details of MU properties but have similar limitations to those of fine wire needle EMG. Indeed, it has been estimated that less than 5% of the MUs can be

discriminated in a population of MUs and that the surface action potential (AP) using few channels is not sufficient for studying single MUs. By contrast, some multi-channel systems have been reported to identify 83.8% of motor units under the same experimental conditions (Farina et al. 2008). Multi-channel sEMG systems are capable of providing details of the physical properties of the MU as the AP propagates along the muscle fibres such as position, spatial extent, innervation zones and the direction and velocity of the propagating AP (Zwarts & Stegeman 2003). However, the identification of single AP required complex signal processing and signal decomposition techniques.

2.4.4 Identification of electrode placements utilising silver bar electrode

Using conventional methods, it is not possible to have any degree of confidence over which muscles the electrodes were located and therefore from what muscles data are being collecting. In previous studies that have investigated Trapezius, Biceps Brachii, Vastus Lateralis, Abductor Minimi Digiti and Abductor Policis Longus (Falla & Farina 2008; Holobar & Zazula 2007; Holobar et al. 2009), the location of these muscles is known in relation to bony landmarks and the underlying architecture of the muscle is such that there are few other muscles in the vicinity to complicate data collection with cross talk. This was not the case in relation to the spinal muscles under investigation where the complexity of the underlying architecture is such that muscles under investigation cannot be palpated directly nor is the location of the innervation zones known in relation to bony landmarks (Tsao, Danneels, & Hodges 2011).

Techniques have been developed using an electrode array with blunt pins (Figure 15), rather than adhesive electrodes, that are used to detect innervation zones.

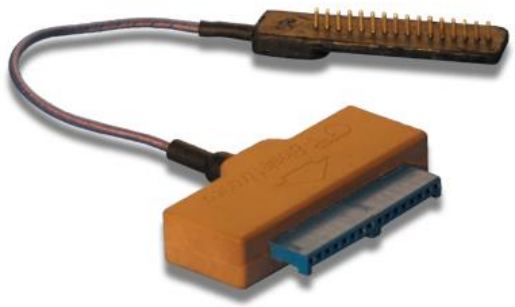

Figure 15. Silver bar electrode array.

The technique is to move the array around over the muscle, while it is contracting, until the innervation zone is visualised through a GUI. This technique is applicable for muscles innervated from nerves that originate from the anterior primary rami which therefore form plexuses and peripheral nerves that innervate the muscle at a particular zone. This has yet to be demonstrated for muscles of the spinal region that have multiple innervation zones; each segmental muscle is innervated by branches of the posterior primary rami, therefore, while innervation zones are likely to exist in each muscle at each segmental level it is not clear if they will be as clearly defined as in the peripheral muscle groups previously studied. Multifidus, for example, is a muscle with multiple fascicules and in keeping with its role as a segmental stabiliser, motor control theory would suggest that each fascicule should be able to contract independently. The muscles of the Erector Spinae group have a high density of predominantly type I (slow twitch fatigue resistant) muscle fibres (Mannion et al. 1997a) which indicates their role in fine movement and posture control at a segmental level and this is likely to be reflected in the innervation patterns.

The principles and utility of multi-channel sEMG had already been established, particularly in relation to the anal sphincter, upper fibres of trapezius, biceps brachii and deltoid (Cescon, Rebecchi, & Merletti 2007; Cescon, Sguazzi, Merletti, & Farina 2006; Farina, Kallenberg, Merletti, & Hermens 2003; Farina, Madeleine, Graven-Nielsen, Merletti, & rendt-Nielsen 2002; Farina, Merletti,

Rainoldi, Buonocore, & Casale 1999; Farina, Zennaro, Pozzo, Merletti, & Laubli 2006; Madeleine, Farina, Merletti, & rendt-Nielsen 2002; Merletti & Parker 2004; Merletti et al. 2010; Merletti et al. 2004; Merletti, Farina, & Gazzoni 2003; Merletti, Farina, & Granata 1999; Rainoldi, Galardi, Maderna, Comi, Lo, & Merletti 1999). However, few experiments had been undertaken that specifically studied the erector spine muscle group or those of interest in this study (Albert, Sleivert, Neary, & Bhambhani 2004; Dolan, Mannion, & Adams 1995; Sung, Lammers, & Danial 2009) and none that utilised high-density arrays specifically located along the alignment of the muscles of interest.

The rationale for using high-density sEMG electrode matrixes and arrays has been made in relation to studying muscles of the spine (Farina, Gazzoni, & Merletti 2003a; Farina, Merletti, & Enoka 2004) but not specifically for studying the muscles of interest in this thesis.

2.4.5 Electrode placement and anatomical arrangement of the muscles of the lumbar region

The most appropriate placement of high-density sEMG electrodes for recording from the lumbar spinal muscles has yet to be determined. An international convention guiding the position of surface EMG electrodes; the European concerted action group 'Surface Electromyography for the Non-Invasive Assessment of Muscles' (SENIAM), have made recommendations with regard to this for monopolar and bi-polar electrodes (Merletti and Hermens 2000). However, these guidelines have not been updated since publication in 2000.

Several authors have used different approaches with regard to multi-channel sEMG electrode placement for recording from the lumbar region, some recommend aligning the electrodes with the longitudinal axis of the body (Farina, Gazzoni, & Merletti 2003a; Merletti & Hermens 2000) while others advocate an alignment that follows the presumed fibre direction (Cescon et al. 2004). It seems logical to follow the orientation of the muscle fibre but this presents significant methodological problems because of the complex anatomy of the spinal musculature. In the case of spinal muscles, a method by which an operator can accurately apply sensors over appropriate muscle groups is required.

In the NEW study (Cescon et al. 2004), it was stated that electrodes were placed over Longissimus Dorsi at the level of the L3 vertebrae (presumed to be Longissimus) and Multifidus at L5 level. According to anatomical studies these placements would not have recorded the majority of EMG signals from the muscles responsible for the lumbar extensor moment, in particular they would not have incorporated the contributions of other fascicles of Multifidus arising from different spinal levels, Longissimus Thoracis pars Lumborum or Iliocostalis pars Thoracis (Figure 7).

Recently strips of array electrodes have been used which consist of 4, 8 or up to 16 electrodes in a linear array (Merletti 2008; Merletti, Holobar, & Farina 2008) (Figure 16). This arrangement allows analysis of the EMG signal which enables visualisation of the propagation of motor unit action potentials (MUAP) and the greater evaluation of parameters commonly used to calculate fatigue, in particular muscle fibre conduction velocity, with signal decomposition techniques (Farina, Gazzoni, & Merletti 2003a; Merletti, Rainoldi, & Farina 2001). These parameters include the median power spectral frequency (also known as median frequency) which is commonly used to evaluate fatigue and which has properties similar to the mean frequency (MNF) (Cescon et al. 2004).

In one study using linear arrays (Cescon et al. 2004), electrode placements followed the orientation of what was described as Longissimus Dorsi Thoracis, at the third lumbar spinal segment (L3), and the Multifidus muscle at the junction of the fourth and fifth lumbar segmental level (L4/5). However, it would appear that the electrode placements for the former were too low at the L3 level to pick up any signal from Longissimus Dorsi (Longissimus Thoracis pars Thoracis) and in fact were placed over Longissimus Lumborum (Longissimus Thoracis pars Lumborum). The angle of the electrode over Multifidus was also not specified. Furthermore, it is presumed that the rest of the Multifidus group and Iliocostalis Lumborum were not contributing to the EMG activity during the test. The fatiguing protocol that was used was based on the Biering-Sørensen test (Biering-Sorensen 1982; Mayer, Latimer, & Refshauge 2000) see section 2.4.10.

In another study (Farina, Gazzoni, & Merletti 2003a) six linear adhesive arrays, each containing eight electrodes, were applied to the lumbar region, parallel to

the spine and centred over Longissimus Thoracis at the first lumbar segment, L1, over Longissimus Lumborum at the L2 and over Multifidus at the L5 level. No attempt was made to follow the line of the presumed muscle orientation. In this study, the fatiguing protocol consisted of a series of sustained semi-flexed lumbar postures, which were difficult to evaluate against studies adopting the Biering-Sørensen test (Cescon, Gazzoni, Gobbo, Orizio, & Farina 2004)

A further study recommended a different protocol for fatiguing and different electrode placements; this study employed, six bipolar electrodes located over Longissimus Thoracis, Iliocostalis Lumborum and Multifidus at L1, L2 and L5 respectively (Oddsson and De Luca 2003). The fatiguing protocol used was based on a proportion of the participants maximum voluntary contraction (MVC) during isometric trunk extension performed in standing. Such protocols can be problematic in clinical studies due to the possible reproduction of pain during the test and its inhibition on the resultant MVC that is calculated to be lower than the real value. Maximum holding times based then on a percentage of a presumed MVC would result in an inaccurate evaluation of study results.

Other studies have used a variety of positions and test protocols (Arnall, Koumantakis, Oldham, & Cooper 2002; Elfving and Dedering 2007; Elfving, Nemeth, Arvidsson, & Lamontagne 1999). This diversity demonstrates the need for standardisation with respect to lumbar spine fatigue testing; this is critical if study results are to be comparable.

For the present study, the location of high-density sEMG electrodes were based on the anatomical details given in the papers by Biedermann and De Foa (Biedermann, DeFoa, & Forrest 1991; De Foa, Forrest, & Biedermann 1989) and informed by a concurrent anatomical study and the work of Mesin et al. (Mesin, Merletti, & Rainoldi 2009).

2.4.6 Multi-channel surface electromyography

Linear arrays and two-dimensional matrices consisting of between four and 64 electrodes were available (Figure 16). Methodologies for using multi-channel EMG have been developed particularly by Merletti (Merletti, Farina, & Granata 1999) and Farina (Farina, Fortunato, & Merletti 2000; Farina, Zagari, Gazzoni, &

Merletti 2004a); although Masuda et al. (Masuda, Miyano, & Sadoyama 1983) was one of the first to use arrays of up to 16 electrodes.

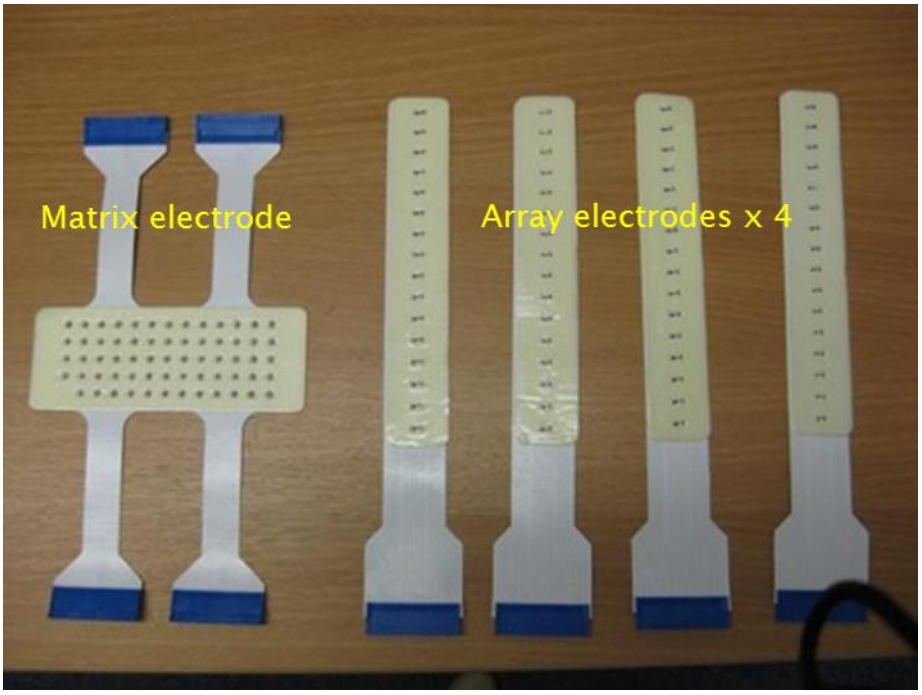

Figure 16. A 64-sensor electrode matrix and 16-electrode arrays.

Figure 16 illustrates the electrodes that have built in complex arrangements of sensors. On the left of the figure is an example of a 64- matrix and on the right are four, 16-sensor arrays. Onto each electrode is attached a double sided adhesive pad with cut-out holes that are each filled with 50 µl of electrode gel once attached to the participant.

An advantage of multi-channel sEMG, compared to monopolar or bipolar techniques that provide a one-dimensional signal, is that a grid of electrodes allows sampling over a wide area in two spatial and one temporal dimension. This enables software or hardware differential extraction techniques to analyse the EMG signal from a muscle or a group of muscles. Techniques such as single differential (Figure 17) where the differences between two signals from adjacent detection sites is made or double (or triple) differential techniques where the weighted linear summation of signals from three or four adjacent detection sites, is not possible with monopolar electrodes. The use of these techniques improves the filtering of the signal in the spatial domain (Reucher, Rau, & Silny 1987).

It is also possible to identify the properties of individual motor units such as the innervations zones and length of muscle fibres. The generation of the motor unit action potential (MUAP), as it propagates through the muscle fibre to its attachment and extinction at the tendon, can be visualised (Merletti, Farina, & Gazzoni 2003; Merletti, Holobar, & Farina 2008). Spatial filters are applied to each point which allows better resolution about the distribution of the MU electrical potential within the muscle, however, signal decomposition techniques are required to identify and classify the individual MUAP (Farina, rendt-Nielsen, Merletti, Indino, & Graven-Nielsen 2003).

Estimations of MUAP conduction velocity (CV) is possible, as array and matrix electrodes give time and spatial information which allows a three-dimensional analysis to be made of the surface EMG signal with a small standard deviation of estimate (typically in the order of 0.1 – 0.2 m/s) (Farina and Merletti 2004a; Farina and Merletti 2004b; Farina, Zagari, Gazzoni, & Merletti 2004b). This makes it a reliable method for the evaluation of CV changes that occur during muscle fatigue.

Figure 17 is a representation of the process of decomposition of multi-channel surface EMG. (a) Surface EMG was recorded from the Biceps Brachii muscle with a 13 × 5 electrode grid (corner electrodes are missing) with the columns parallel to the fibre direction. (b) Segment of 500ms duration of bipolar EMG detected by each column of the grid. The action potentials show propagation along the columns. (c) High-density action potentials for three motor units extracted from the interference signal with the decomposition algorithm described by Holobar and Zazula (Holobar and Zazula 2007). (d) Estimated discharge patterns for the three motor units (MU).

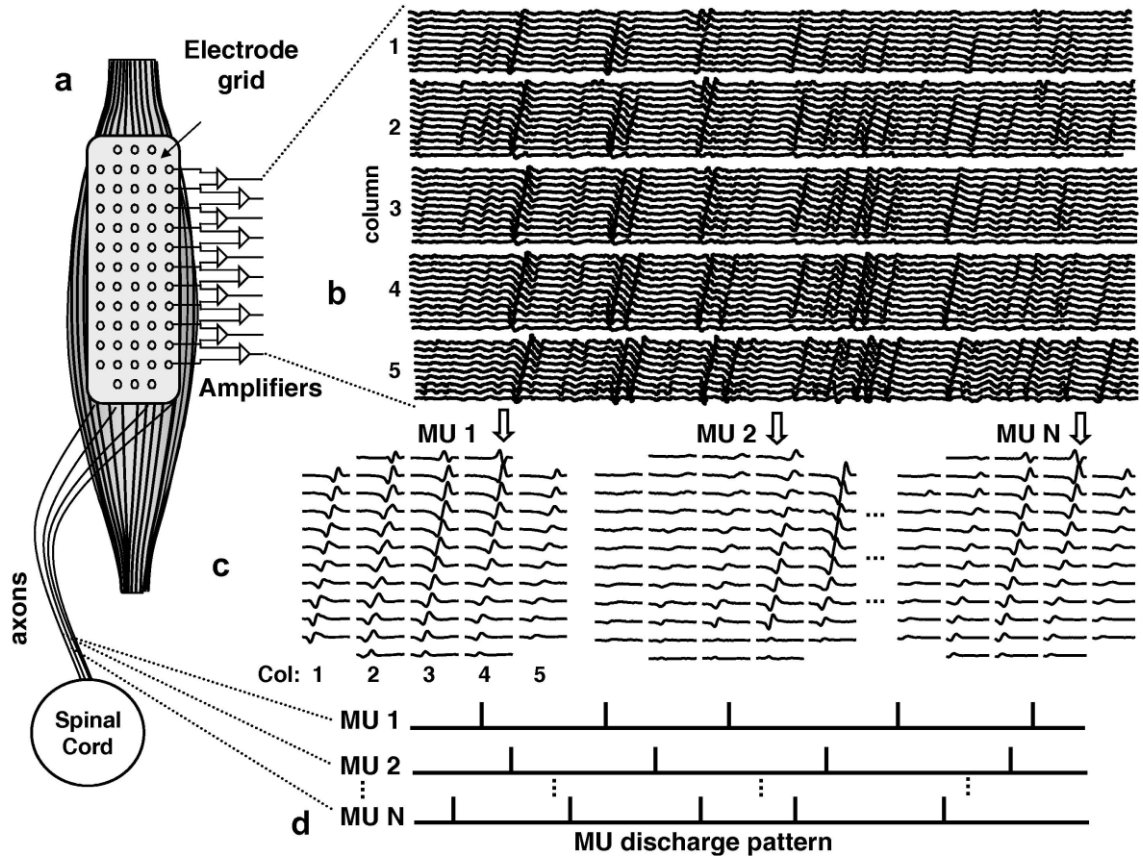

Figure 17. Matrix electrode EMG recording.

Reproduced with permission from Journal of Electromyography and Kinesiology; Analysis of motor units with high-density surface electromyography.

Some of the advantages of multi-channel systems are that information gained is now possible which was previously obtained by invasive methods. In particular, interpretation and calculation of muscle fibre conduction velocity, innervations zones and the anatomical arrangements of muscle and tendons is now possible based on analysis of the multi-channel signal. The clinical utility of multi-channel surface EMG has yet to be demonstrated although evidence is emerging of its usefulness as a research tool (Merletti, Aventaggiato, Botter, Holobar, Marateb, & Vieira 2010; Merletti, Holobar, & Farina 2008).

Using large multi-channel EMG systems results in large amounts of data; data collected from 128 channels over a period of up to 240 seconds with a sampling rate of 2048 samples/s results in data files that are often in excess

of 400Mb. The extraction methods are computationally intensive and time consuming.

2.4.7 Surface EMG recording

Data were acquired using the 128-multi-channel amplifier (LISiN Bioengineering Centre, Polytechnic of Turin, Department of Electronics). The raw data signals were amplified by the 128 multi-channel surface EMG amplifier band-pass filtered (-3-dB bandwidth, 10-750 Hz), sampled at 2,048 samples/s, and converted to digital data by the 12-bit A/D converter (Figure 18).

Software, provided with the multi-channel sEMG amplifier (OT Bioelettronica, C.so Unione Sovietica 312, 10135 – Torino, ITALY) allowed visualisation of the raw signal in real time but did not have the flexibility to view each array or matrix electrode separately. This software application (lower right Figure 18) did not provide the facility for any signal decomposition or analysis. Output was saved as a data file for later analysis.

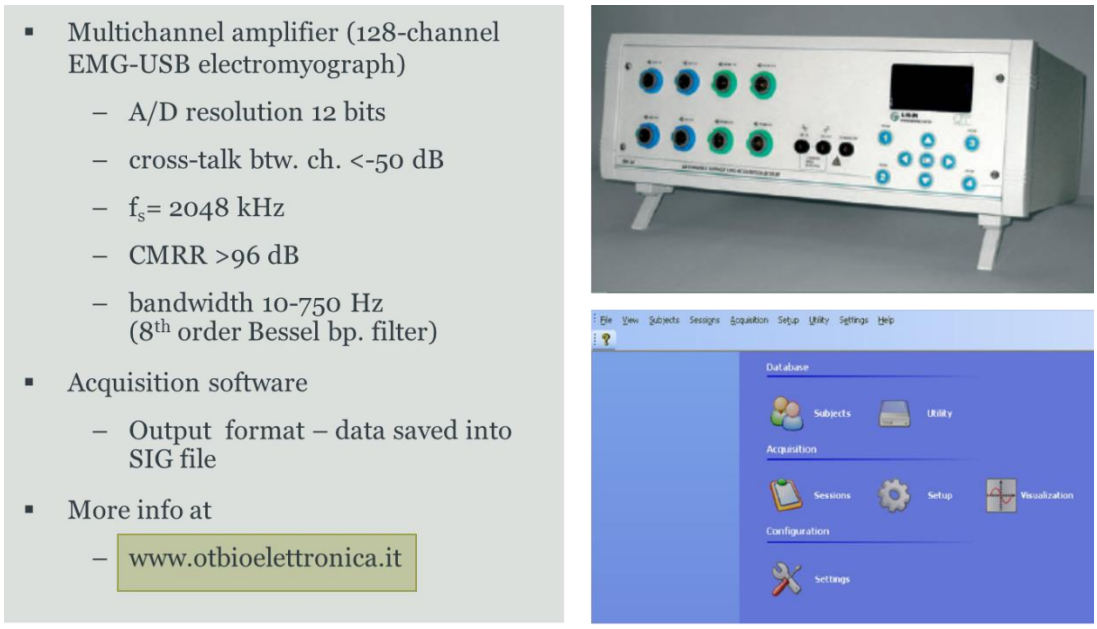

Figure 18. 128-channel sEMG amplifier and specification.

2.4.8 Testing for muscle fatigue

It is important to recognise that the term 'fatigue', which has been defined previously, can be misinterpreted when looked at from an EMG perspective. The myoelectric changes seen and described (De Luca 1984) as manifestations of 'fatigue' are not the sensation of fatigue or the 'sense of effort' often associated with a fatiguing activity. The characteristic changes seen in the EMG signal do not necessarily mean that there is a concomitant change in performance although decreases in muscle force generation and torque are usually linked closely with these changes.

The myoelectric manifestations of muscle fatigue are well documented (De Luca 1984) and occur as changes to signal amplitude, frequency and conduction velocity. During low to moderate isometric contractions, the amplitude increases during a fatiguing task mainly due to the recruitment of additional MUs but also due to an increase in firing frequency. At maximum contraction though, amplitude starts to decline, attributed to reduction in the membrane potential, conduction velocity and firing rates; although in this thesis it is the contention that frequency and amplitude modulation is controlled centrally.

Conduction velocity usually reduces during a fatiguing task; the normal conduction velocity within muscle is around 4 m/s and is normally calculated using sEMG as the weighted average of several hundred muscle fibres belonging to at least one, but more usually to more than one, MU. The microenvironment of the muscle fibre membrane undergoes progressive changes during fatiguing tasks due to the build-up of metabolic by-products of the contraction process, the reduction in circulation due to constriction of blood vessels and the high metabolic demand. There follows an accumulation of extracellular potassium particularly in the T tubules system, an accumulation of lactic acid and a lowering of the pH, all of which cause a reduction in conduction velocity of the propagating wave of depolarisation within muscle fibres (Andreassen and Arendt-Nielsen 1987; Bigland-Ritchie, Donovan, & Roussos 1981; Brody, Pollock, Roy, De Luca, & Celli 1991; Farina, rendt-Nielsen, Merletti, & Graven-Nielsen 2002). These changes in physiology

would be signalled to the CNS as part of normal afferent feedback and part of the mechanism that affects CGM output.

2.4.9 Protocols for muscle fatigue testing

A number of studies have been undertaken which establish methodologies for testing fatigue based on the assessment of the limit of endurance; typical outcome measure being 'time taken to task failure' (Adams, Mannion, & Dolan 1999; Cardozo, Goncalves, & Dolan 2011; Corin, Strutton, & McGregor 2005; Mannion and Dolan 1994). Various fatiguing protocols have been used in a laboratory situation and are designed to accelerate the onset of fatigue. Some testing procedures are tests of endurance at sub-maximal levels of muscle force; as the determination of MVC is problematic in most populations studied (Moreau, Green, Johnson, & Moreau 2001) . Neither methods test muscle strength using maximum isometric or isodynamic contractions at a controlled velocity. In practice, isometric tests against gravity or resistance are based on a percentage of MVC calculated from a MVC or calculated from the assumed weight of body components.

The following sections gives details of standard testing procedures that can be used in both clinical and laboratory situations.

2.4.10 Biering-Sørensen test

This test, to determine the endurance of the spinal extensor muscles strength, was first described by Hansen (Hansen 1964); however, following the study by Biering-Sørensen (Biering-Sorensen 1984a) the test become known as the Biering-Sørensen test and has since become a test to assess isometric spinal muscle endurance. The test as described by Biering-Sørensen measured the length of time a person could hold their unsupported upper body in a prone position; the lower part of the body is fixed to an examination couch with three belts positioned around the pelvis, knees and ankles (Figure 19). The upper edge of the iliac crests are positioned in line with the edge of the examination couch; thus the upper body is unsupported throughout the test, the assumption being that the extensor muscles of the spine contribute significantly to the maintenance of the test position although the role of the hip extensor muscles to the holding time has been challenged (Moffroid, Reid, Henry, Haugh, & Ricamato 1994; Plamondon, Trimble, Lariviere, & Desjardins

2004). Other EMG studies would support the view that the hip extensor muscles contribute significantly to holding times (Kankaanpaa, Laaksonen, Taimela, Kokko, Airaksinen, & Hanninen 1998; Moffroid et al. 1994)

Figure 19.The Biering-Sørensen test.

Figure 19 illustrates the standard set up for the Biering-Sørensen test. Straps are attached around the pelvis, knees and ankles to stabilise the lower part of the body of the participant. The participant is instructed to hold the position for as long as possible and the test is ended when the angle of the thorax drops 10° below the horizontal as measured or determined by the operator.

The outcome measure used in the original test was the holding time, measured in seconds, that the individual could maintain a horizontal position. The test was ended if the upper torso dropped below -10° from the horizontal position. The test is also terminated after 4 minutes (240 seconds) if the individual can maintain the position for this length of time although it has been suggested by some authors that the holding time be extended beyond this (Jorgensen and Nicolaisen 1986).

The predicative validity of the Biering-Sørensen makes it an appealing test to use in clinical practice. Biering-Sørensen reported that position holding times of less than 176 seconds predicted LBP in the next year while times that exceeded 198 seconds predicted absence of LBP (Biering-Sorensen 1984b). In another study (Alaranta et al. 1995) it was shown that holding times of less than 58 seconds was associated with a threefold increase in the risk of LBP. Other authors have reported a difference between male and female with females generally exhibiting longer holding times even when the differences in upper body weight is taken into account (Biering-Sorensen 1984b; Kankaanpaa et al. 1998; Mannion et al. 1997; Mannion & Dolan 1994). The study by Mannion et al. (Mannion et al. 1997a) proposes that holding times of females is related to their better adaptation to aerobic exercise due to the higher proportion of type I spinal muscle fibres.

Many studies report that holding times for those with LBP are reduced (Biering-Sorensen 1984b; Hansen 1964; Latimer et al. 1999; Simmonds, Olson, Jones, Hussein, Lee, Novy, & Radwan 1998); these findings may suggest that chronic LBP is associated with reduced isometric endurance of the spinal muscles. Most studies that have evaluated holding times in normal participants report mean holding times of 150 – 190 seconds (Mayer, Latimer, & Refshauge 2000).

The Biering-Sørensen test is the most widely used endurance test with a number of variations which results in the term 'modified Biering-Sørensen test' used to describe the variation. The following variations are commonly used;

1. Arm position – during the test the arms can be folded across the body (Muller, Strassle, & Wirth 2010) , the elbows out to the side, the hands to the ears (Mannion, Dumas, Stevenson, & Cooper 1998), forehead (Ng and Richardson 1996) back of the neck (Gibbons, Videman, & Battie 1997; Suter and Lindsay 2001) or by the side of the body (Simmonds et al. 1998).
2. Number of straps – some researchers have used from between two (Gibbons, Videman, & Battie 1997) and five straps (Tsuboi, Satou, Egawa, Izumi, & Miyazaki 1994);
3. Starting position – It is not clear from the description of the original test (Biering-Sorensen 1984a) if the participants started with the upper body inclined towards the floor at the commencement of the test or if the starting position was with the body horizontal as illustrated in Figure 19.

4. Determination of the horizontal position – in the study by Biering-Sørensen (1984a) visual estimation of the horizontal position was used. Others have used inclinometers, which the testers observe and when the horizontal angle exceeds -10°, the test is ended. Others have used visual estimation (Mannion & Dolan 1994; Mayer, Gatchel, Betancur, & Bovasso 1995) or asked the participant to maintain contact between a plumb bob hanging from a plumb line with the bob in contact with the thoracic spine (Kankaanpaa et al. 1998; Ng & Richardson 1996). In these cases, no visual feedback to the participant occurs and validity of the test is therefore questioned particularly in relation to when the test is stopped and the outcome measure of duration is measured.
5. Criteria for ending test and measuring holding time - in the original test described by Biering-Sørensen (1984a), the test was stopped when the horizontal angle of the participant's trunk exceeds -10° as determined by the tester. In other studies where visual estimation (Mannion & Dolan 1994; Mayer et al. 1995) is used, the tester ends the test and records the holding time.

In the study described in this thesis, an electrogoniometer consisting of a bi-axial wire strain gauge (model SG150B) and a torsiometer (Biometrics Ltd, Newport, Gwent) was used to measure deviation from the horizontal and lateral angles. The holding time was calculated, following the test, based on the time taken from the start of the test to the point where the horizontal angle measured by the electrogoniometer falls below -10°.

2.4.11 Ito Test

The Ito test (Ito, Shirado, Suzuki, Takahashi, Kaneda, & Strax 1996) was developed as an alternative to the Biering-Sørensen test as a means of reducing spinal loading. In this test, the participant lies prone with a support under the abdomen that is intended to reduce the lumbar lordosis. The arms are held down by the side and the lower limbs are not restrained (Figure 20). To undertake the test the participant lifts the upper body while maintaining a fully flexed cervical spine. Gluteus Maximus is contracted to stabilise the pelvis and along with the cervical flexion maximises the action of the Erector Spinae muscle. The criterion validity of this test has been demonstrated (Muller,

Strassle, & Wirth 2010). It has been shown that this test more specifically relies on the contribution from Iliocostalis and Multifidus for holding times than the Biering-Sørensen test where Semimembranosus and Multifidus mainly contributed to holding times.

Figure 20.The Ito test.

Figure 20 illustrates the standard set up for the Ito test. The participant is instructed to hold the position for as long as possible and the test is ended when the participant is no longer able to maintain the position.

The Ito test is quick to apply, does not require the fixing of the lower limbs to a couch and is better tolerated by those with LBP. There is, however, less normative data on this test, which makes it more problematic to use in clinical practice. This test has been used to assess the fatiguing effects of high-speed transits in a marine environment and EMG recordings have been made that indicate that fatigue of the Erector Spinae muscle occurs with this test. The utility of this test has also been demonstrated as being suitable for field experimentation where an assessment of spinal muscle fatigue is required (Section 3).

2.4.12 Prone lying bilateral straight leg raise (McIntosh test)

In the test, the isometric endurance of the Erector Spinae is measured by the length of time that the person, lying prone, can maintain their legs in extension and held off the couch (Figure 21).

This test is also known as the McIntosh test (McIntosh, Wilson, Affieck, & Hall 1998; Moreau et al. 2001), is less well described in the literature and is infrequently reported in the literature or used clinically.

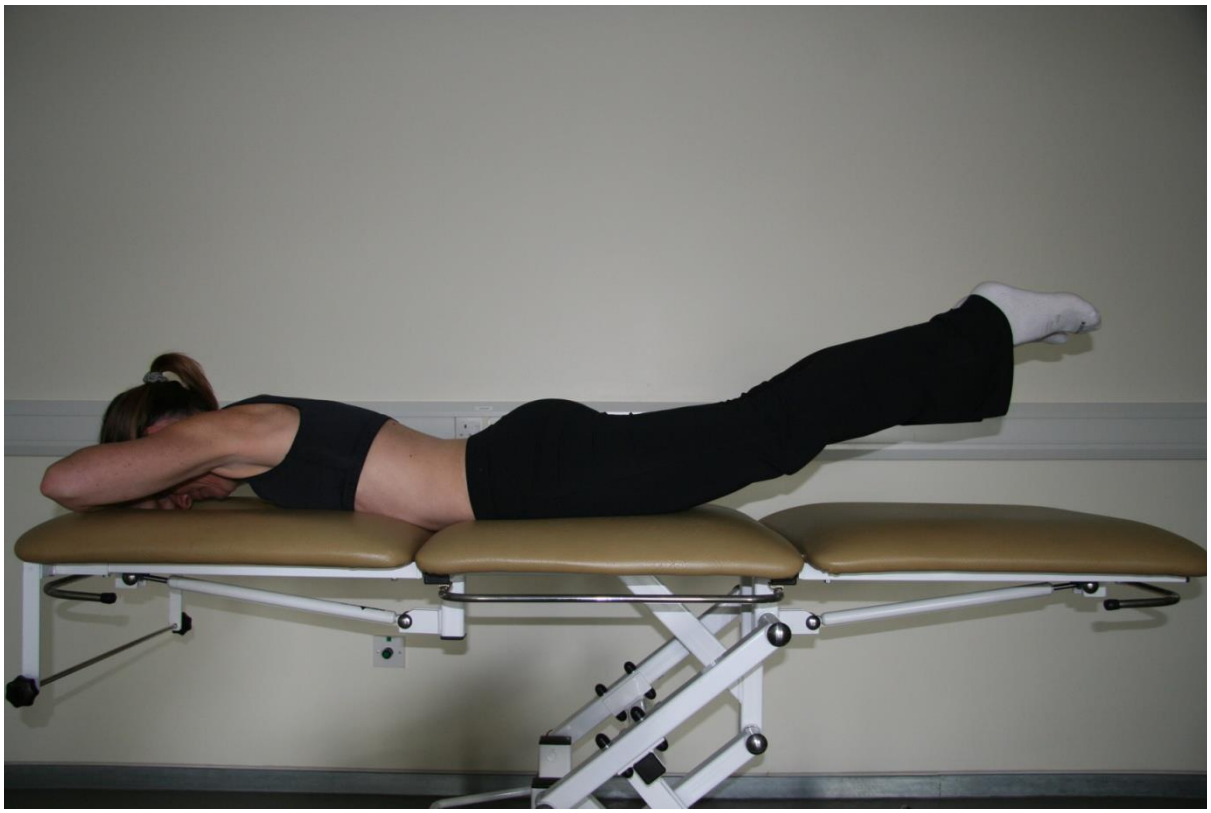

Figure 21.Prone lying bilateral straight leg test (McIntosh test).

Figure 21 illustrates the standard set up for the McIntosh test. The participant is instructed to extend the legs at the hip joint and to hold the position for as long as possible; the test is ended when the participant is no longer able to maintain the position.

2.5 Conclusion

In the context of lumbar spine muscle fatigue testing, a number of conclusions can be reached. There are established, well-researched and safe methods for

testing endurance capacity. The Biering-Sørensen test is the most commonly and most frequently used test but the number of variations of this test lead to questions regarding the validity of comparing clinical or experimental trials that use it. However, based on the original description, the test has clinical and experimental utility.

Using holding time/time to task failure, as an outcome measure, is convenient and reliable in clinical and in experimental laboratory-based situations. It has been shown to have a predictive value when evaluating future low back pain risk (Biering-Sorensen 1984a; Biering-Sorensen 1984b; Biering-Sorensen and Hilden 1984). In one study a holding time of less than 58s was associated with a threefold increase in risk of LBP than men with a holding time of more than 104s and women with a holding time of more than 110s. The test can also discriminate between those with and those without LBP (Latimer et al. 1999). However, the use of holding times as an outcome measure to demonstrate changes in fatigue resistance, resulting from training in a low back pain population, has not been demonstrated.

Incorporating sEMG analysis into the study of fatiguing muscle characteristics has been undertaken by a number of researchers and conclusions reached. To date, no research team had based electrode placements accurately on surface markings of muscles based directly on anatomical findings although multi-channel analysis has been used in an attempt to evaluate different spinal muscle group contributions. This will be addressed in Section 5, 6and 7.

However, in a real world/field-test situation, the Biering-Sørensen test may be problematic as it requires stabilising the participant on a couch. Other endurance tests such as the Ito test (Ito et al. 1996), as described above, are less frequently used and there is less normative data published; these tests may be more suited to a real world/field-test situation.

The following section describes a feasibility case study experiment to establish if usable sEMG data could be collected while undertaking an activity in a marine environment that is thought to cause spinal muscle fatigue, if sEMG changes consistent with spinal muscle fatigue can be demonstrated and if pre- and post-testing using the Ito test demonstrates any change in fatigue status.

3. Studies involving high-speed marine craft and human performance – RIB studies

3.1 Introduction

The aim of this single case feasibility study was to demonstrate if sEMG could be collected in an occupational setting and to determine if useful data could be derived from Multifidus and Upper fibres of Trapezius together with their fatiguing characteristics. The second part of this case study, additionally sought to establish the utility of the Ito test (Ito et al. 1996), a variation of the Biering-Sørensen standardised fatigue testing protocol, in a real world data collection situation.

3.2 Fatigue associated with random and shock vibration in high-speed transits

During high-speed transits, boat crews are exposed to random and shock vibration as a result of the vessel they are travelling in being subjected to perturbations caused by waves of varying sizes and the effect of wind and tide conditions.

One such occupational group are the RNLI lifeboat crews who experience high levels of random and shock vibration as part of their duties. Lifeboat crew members report, anecdotally, high levels of fatigue which they associate with a subsequent degradation in performance and link this to increasing levels of back pain. Evidence in the literature supports the notion that exposure to random and shock vibration will result in a temporary acceleration of muscle fatigue that could contribute to LBP, although the mechanism by which this occurs is not clear (Pope, Magnusson, & Wilder 1998; Pope, Wilder, & Magnusson 1998; Pope, Wilder, & Magnusson 1999). Prolonged exposure to vibration might result in more long-term changes in muscle and spinal joint physiology or pathology that might precipitate chronic LBP. A better understanding of the nature of lumbar spine muscle fatigue will add to the body of knowledge in this field of research that will have benefits to the general population.

The physiological effects of whole body vibration (WBV) are similar to that of exercise with an increase in heart rate, blood pressure and oxygen consumption. The effects of WBV, and acceleration related alternating activity, induce a tonic contraction of the spinal muscles in order to maintain any desired position, particularly when seated in an upright position or when standing (Griffin 1990). It is assumed that the effects of the muscular activity associated with maintenance of body posture and position, while continuing to work in an environment that is subjected to random and shock vibration, is the cause of fatigue. Temperature and psychological stressors will also have an impact on the perception of effort and the rate at which performance degrades and task performance failure occurs.

The range of WBV values where physiological responses are seen, begin at the lower limit of 0.7 m/s^2 rms values between 1 and 10 Hz, rising up to 30 m/s^2 rms at 100 Hz (Griffin 1998). The range of WBV that particularly affects the spine is in the 4 – 8 Hz frequency range when applied in a vertical direction. In the sitting position, internal amplification of the vertical oscillations occurs in the range of 4.5 – 5.5 Hz and further exacerbates any harmful effects (Wasserman, Wilder, Pope, Magnusson, Aleksiev, & Wasserman 1997).

Various limits have been set in order to protect workers from occupational exposure. In the EU the Physical Agents Directive (Directive 2002/44/EC 2002) sets levels of vibration based around a calculated value, the vibration dose value (VDV). This directive sets an action limit of 9.1 m/s^2 and an exposure limit of 21.0 m/s^2. In studies of exposure to WBV in a marine environment, these limits can be readily exceeded (Myers et al. 2011).

3.3 Fatigue, whole body vibration and low back pain

Laboratory studies have shown that exposure to WBV causes changes within the muscles that support and control the spine and that these changes may subsequently cause LBP (Pope, Wilder, & Magnusson 1998; Pope, Wilder, & Magnusson 1999). Studies have been conducted on occupational groups such as vehicle operators of tractors, cranes and helicopters (Bovenzi 1996; de Oliveira and Nadal 2004) where occupants of such vehicles are exposed, not only to WBV, but also to impact or random shock vibration. Fewer studies have been conducted in the marine industries that are applicable to the current study. However, it is reasonable to assume that some of the effects of WBV and

impact loading would also occur in the marine environment. A review of literature in 1998 concluded that long-term exposure to WBV does contribute to LBP; epidemiological studies have indicated that exposure to WBV does increase the prevalence of LBP, probably in a dose-related way (Lings and Leboeuf-Yde 1998; Lings and Leboeuf-Yde 2000). The review by Lings et al. (2000) concluded that research into this has ceased as the problem is on the decline; this view would not be shared in the marine industry where WBV and random shock vibration effects cannot be designed out of the problem as they can, to some extent, in the automobile and construction industries.

3.4 Low back pain: whole body vibration epidemiological studies

There is strong evidence in the literature that LBP is positively associated with exposure to WBV (Lings & Leboeuf-Yde 1998; Lings & Leboeuf-Yde 2000). Additionally, LBP is also positively associated with heavy physical work and occupational activities that involve lifting and forceful movements particularly where these activities are associated with WBV (Anderson-Putz, Bernard, Burt, Cole, Fairfield-Estill, Fin, & Grant 1997). These confounding factors can make it difficult to attribute causality to WBV; although the evidence strongly links increased exposure of WBV to an increase in LBP and accelerated degenerative changes in populations studied.

Disc and facet degeneration and ligament strain may be responsible for the potentially high rates of LBP disability in those whose jobs demand heavy physical activity. Hysteresis or creep of tissues such as ligaments and disc caused by WBV are also thought to increase the risk of LBP following such vibration exposure. Whole body vibration has been shown to reduce disc height, although most studies test participants in a seated position which itself has been shown to reduce disc height over a period of exposure (Klingenstierna and Pope 1987). Loss in disc height reduces spinal stiffness (Cholewicki and McGill 1996); this would increase vulnerability to injury in occupations or environments where forceful or jerking movements occur in awkward postures particularly if preceded by a period of fatiguing WBV (Anderson-Putz et al. 1997).

Reviews of epidemiological evidence also suggest that WBV is a risk factor in LBP (Boshuizen, Bongers, & Hulshof 1990) and highlight the possibility that WBV and degenerative changes in the spine, including the intervertebral disc, may be linked (Bovenzi and Hulshof 1999). However, not all authors describe causality and warn against the risk of drawing conclusions regarding the scope of epidemiological surveys that often cannot account for all confounding factors nor which fail to report on the whole population; in particular, women are poorly represented in many studies (Bovenzi 1996).

There are no strict limiting values for magnitudes of frequency-weighted rms vibration regarding human discomfort, although some values are given as indications of potential reaction (BSI 6841 1987; Griffin 2004). Values below 0.315 m/s^2 are considered as 'not uncomfortable', and above 2 m/s^2 as 'extremely uncomfortable' (BSI 6841 1987). In the context of this study the VDV experienced by RNLI crew members and those using RIBS is assumed to be at least that of the exposure action value set by the Physical Agents Directive (Directive 2002/44/EC 2002) and may exceed the exposure limit value.

3.5 Assessment of human performance during high-speed marine craft transits

3.5.1 Introduction

An experiment was undertaken to simultaneously measure and synchronize boat and human physiological data during a high-speed transit. Measures of interest in this study were seat motion and vibration of the vessel coupled with head motions, heart rate and the activity of specific spinal muscles. Surface EMG signals were analysed in order to describe any muscle fatigue characteristics of upper fibres of Trapezius and Multifidus and to investigate if the fatiguing characteristics of the cervical and spine lumbar muscles of the participant changed over time. It was also investigated if there was any association between muscle fatigue and exposure to shock and random vibration. Furthermore, the electrocardiogram (ECG) signals were used to analyse the effect of body vibrations on heart rate variability.

3.5.2 Aim

The aim of this feasibility study was to develop a methodology for investigating human factors specific to high-speed craft operation during high-speed transits at sea.

3.5.3 Design

An experimental single case-study design to simultaneously evaluate the effects of random and shock vibration on aspects of human physiology.

3.5.4 Hypothesis

The hypothesis was that;

> There will be a positive association between the magnitude of vibration exposure and heart rate.
> There will be an association between the magnitude of vibration exposure and myoelectric measures of fatigue.

The null hypothesis was that;

> There is no association between the magnitude of the exposure to vibration, heart rate and myoelectric measures of fatigue.

3.5.5 Method

An experiment was undertaken during a sea trial with a Rigid-hull Inflatable Boat (RIB-X Expert XT650) with the co-operation of co-investigators from the department of Ship Science, University of Southampton. A male participant participated in this study. The experiment took place off the south coast of England at The National Oceanography Centre, Southampton. The conditions of the sea were moderate (sea state 3). The trial was approximately 32 minutes long with an average boat speed of 13 m/s.

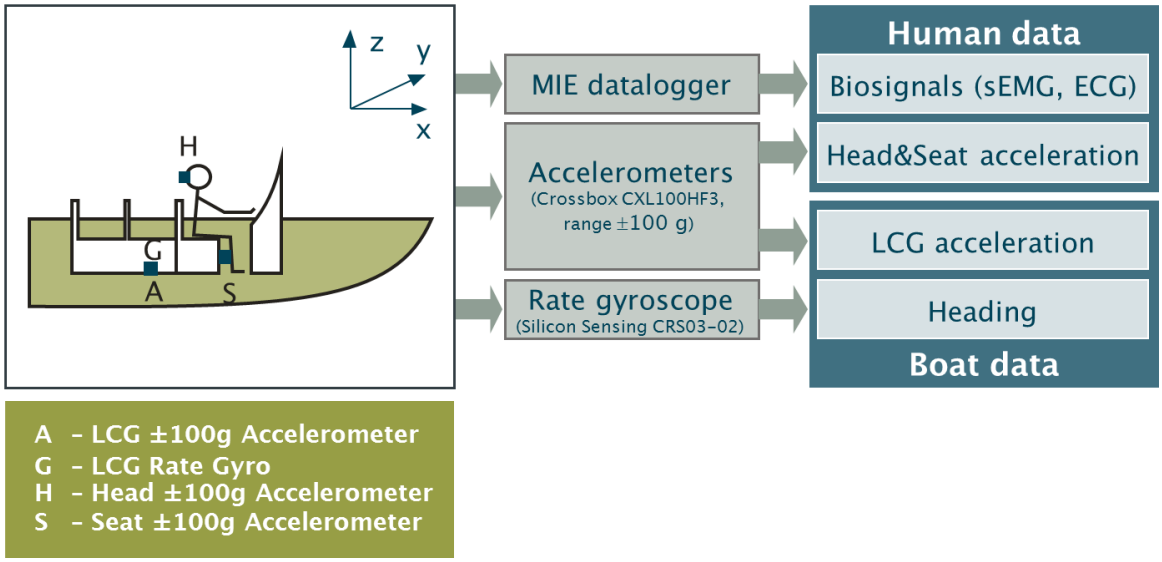

Figure 22. Experimental set-up used for collection of data during the sea trial.

A schematic representation of the experimental setup is shown in Figure 22. The data measured during the sea trial were:

1. Human WBV data – head and seat acceleration.
2. Human physiological data – the ECG and sEMG from upper fibres of Trapezius muscle and the lumbar Multifidus muscle.
3. Boat data – acceleration and heading.

3.5.6 Data acquisition and instrumentation

The locations of the tri-axial accelerometers (Crossbox CXL100HF3, range ±100 g) and the coordinate system used to collect human and boat data are illustrated in Figure 22, Figure 23 and Figure 24. The accelerometers positions (H) correspond to the passenger's head; two accelerometers were attached at the back of the helmet; one to record motion of the participant's head in three planes and an additional accelerometer to synchronise with data collection system recoding boat data. The accelerometer positioned at the front side of the seat (S). The rate gyro (G) and the 100g accelerometer (A) are located on the longitudinal centre of gravity (LCG) (Figure 22).

Measurements of boat vibration were conducted according to the method recommended by the International Organization for Standardization (ISO 2631-1 1997). The acceleration signals were acquired at a sampling frequency of 2.5 kHz using a 16-channel logger (IOTECH Logbook 300). Co-

investigators collected boat vibration data and provided this data for analysis in conjunction with physiological data collected directly from participant.

Thus, the axes of the seat and head acceleration signals were referenced to the human body such that the x-axis describes motion in the anterior-posterior axis of the body, the y-axis describes motion in the transverse axis and the z-axis describes motion in the vertical axis as in Figure 23. The relationship of axis to the cardinal planes of the body can be seen.

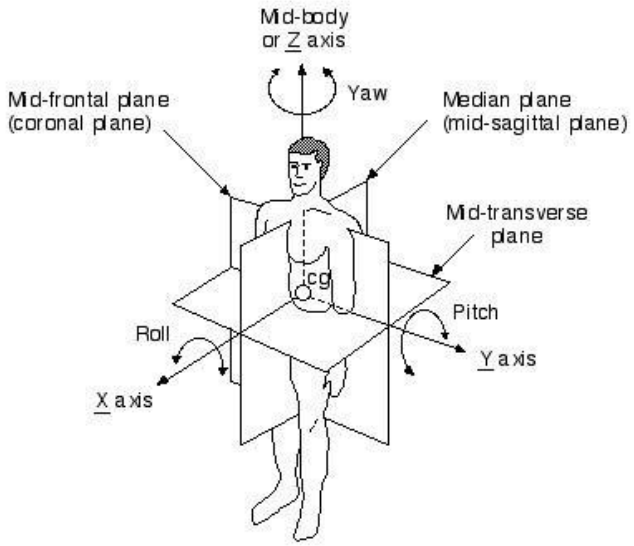

Figure 23. Axis and planes of the human body.

Figure 23 illustrates the cardinal axis and planes of the human body as they relate to the axes used in this study.

To examine responses of spinal muscles to body vibration, surface EMG signals were recorded during the trial (Figure 24). Four sEMG signals selected for this experiment were from left and right upper Trapezius, and left and right Multifidus at the level of the junction of the 4th and 5th lumbar vertebrae in accordance with SENIAM guidelines (Merletti & Hermens 2000). A differential pair of pre-gelled self-adhesive electrodes (3 cm in diameter) was positioned approximately 2.5 cm apart over each muscle of interest with an orientation parallel to the muscle fibres. A reference electrode with a built-in 1k gain preamplifier was placed at equal distance from the electrode pair. Before

attaching electrodes, the skin where the electrodes were to be placed was prepared according to SENIAM guidelines (Merletti & Hermens 2000) to reduce skin impedance. Pre-amp cables were attached to the skin with adhesive tape to reduce the potential artefacts caused by cable movements (Figure 24 and Figure 25).

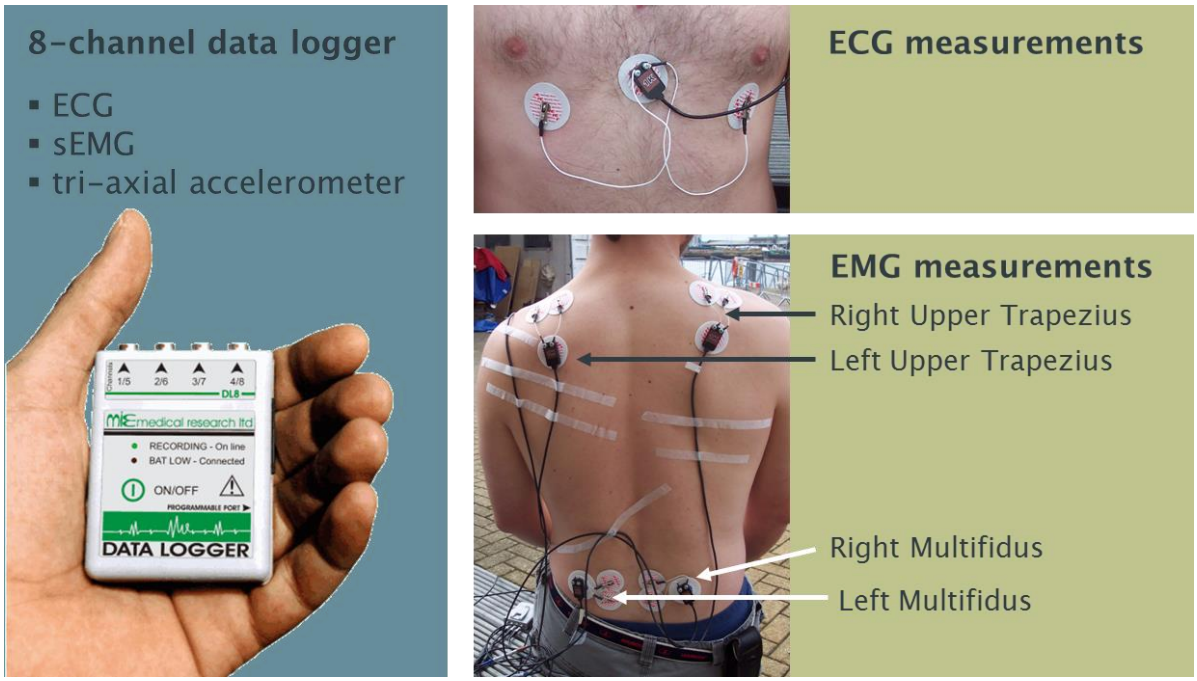

Figure 24. Data acquisition and instrumentation.

Figure 24 illustrates the 8-channel data logger (MIE Medical Research ltd) that collected ECG, EMG and head accelerometer data. The figure also shows location of the ECG and EMG electrodes attached to the participant.

Raw signals were amplified, band-pass filtered (3 dB bandwidth: 6-6000 Hz) and digitized with a sampling frequency of 1 kHz and 12-bit resolution using the 8-channel portable data logger.

To synchronize data measured with two instruments, a tri-axial accelerometer transducer (range ±25 g) was mounted on the rear of participant's helmet close to the other head accelerometer (range ±100 g) with the corresponding axes of detection aligned. The vibration signal acquired by this transducer was used in the processing stage to establish an exact match between time scales of all recorded signals. All data were stored on a memory card and converted later into a MATLAB format for processing purposes.

Figure 25. Instrumentation – position of accelerometers.

Figure 25 illustrates the position of the two accelerometers attached to the rear of the participant's helmet to record head acceleration in the x, y and z axis and to synchronise boat data.

3.5.7 Data processing

3.5.8 Whole body vibration data

The frequency-weighted seat and head accelerations were calculated using weighting filters for the horizontal x and y axes and for the vertical z-axis, according to BSI 6841 (BSI 6841 1987). These filters have high and low-pass band-limiting filters at 0.4 Hz and 100 Hz respectively and are suitable for vibration frequency range 0.5 – 80 Hz. Applying frequency-weighted filters to human vibration signals is required to correlate physical vibration measurements to human response (Griffin 1990).

The rms of the frequency-weighted acceleration was calculated for each axis for the total period during which vibration occurs to represents the average of acceleration over time. In addition, the rms magnitude of the weighted acceleration signals in the x, y and z directions was calculated and used as a measure of overall vibration.

3.5.9 Physiological data

By analysing the ECG signal, it was possible to identify potential irregularities of heart activity due to vibration exposure. The calculated instantaneous heart rate value was further compared to the rms values of the frequency-weighted seat acceleration signals calculated from the 1 s time windows prior to each heartbeat to detect for any effect of vibration/acceleration on heart rate.

The EMG variable of interest in this study was the rms value and the power spectral density. The running rms values were calculated from the consecutive 1 s time windows of the EMG signals and compared with rms values of the measured acceleration signals. Power spectral density of the EMG signal has been shown to be valuable for investigating muscle fatigue properties and motor unit behaviour (Cifrek, Medved, Tonkovic, & Ostojic 2009; Elfving et al. 1999; Farina, Gazzoni, & Merletti 2003a; Farina et al. 2004; Farina, Gazzoni, & Merletti 2003b; Mannion et al. 1997; Merletti, Biey, Biey, Prato, & Orusa 1985). Typically, power spectral density has been used to investigate the properties of muscle during sustained maximum voluntary muscle contraction, although techniques used in this study are considered appropriate for muscle contraction at lower levels during active movement (Farina, Gazzoni, & Merletti 2003a; Farina et al. 2004; Merlo, Farina, & Merletti 2003; Mesin, Merletti, & Rainoldi 2009; Muller, Strassle, & Wirth 2010). In this study, power spectral densities of the measured EMG signals were estimated and averaged using Welch's method (Welch 1967) with a fast Fourier transform (FFT) window size of 512 samples and 50% overlap.

3.5.10 Results

3.5.11 Human vibration analysis

The main vibration parameters (peak and rms values) of the frequency-weighted seat and head acceleration signals were calculated for each axis direction (Table 5).

Applying the frequency-weighting filters to the seat vibration resulted in the highest impact magnitude value of 1.54 g encountered in the lateral (*y*-axis) direction. The highest rms acceleration magnitudes of 1.005 m/s^2 occurred also in the lateral (*y*-axis) direction at the seat base. Overall frequency-weighted rms acceleration amplitude of 1.440 m/s^2 calculated for the head vibration was found to be considerably larger than the seat rms acceleration amplitude of 1.079 m/s^2 and would be considered to be 'very uncomfortable' (BSI 6841 1987).

Table 5. Vibration parameters of the frequency-weighted head and seat accelerations.

Parameter	Units	*x*-axis	*y*-axis	*z*-axis	Total
Seat Acceleration					
Peak value	[g]	**0.23**	**1.54**	**1.36**	-
	[m·s^{-2}]	**2.27**	**15.09**	**13.37**	-
rms value	[g]	**0.018**	**0.102**	**0.035**	**0.110**
	[m·s^{-2}]	**0.181**	**1.005**	**0.347**	**1.079**
Head Acceleration					
Peak value	[g]	**0.58**	**2.29**	**0.49**	-
	[m·s^{-2}]	**5.68**	**22.42**	**4.80**	-
rms value	[g]	**0.058**	**0.130**	**0.035**	**0.147**
	[m·s^{-2}]	**0.567**	**1.278**	**0.345**	**1.440**

3.5.12 EMG analysis

The frequency spectral densities of the EMG signals calculated for the successive time segments of 10 minutes duration are shown in Figure 26. The general shape of these spectral densities is in agreement with the spectral analysis of averaged EMG signal in the frequency domain during voluntary contraction (Cifrek et al. 2009; Merletti and Parker 2004). The plots of the power spectral densities from the left and right Multifidus muscles are typical of those seen as muscle fatigues during an activity – spectral content shifts to the lower frequencies – and shows a cumulative effect consistent with muscle fatigue (Merletti & Parker 2004). Similar changes are not seen in the upper fibres of Trapezius, which did not show the same fatiguing characteristics as the muscles that support the lumbar spine and lumbo-sacral region.

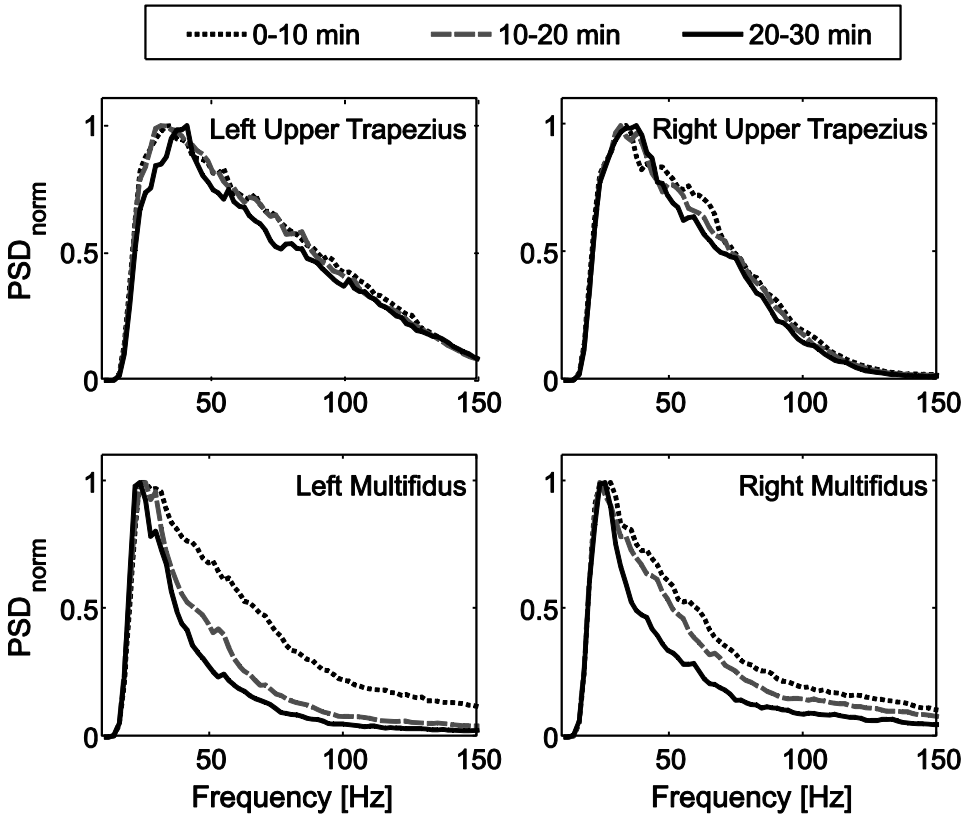

Figure 26. Frequency spectrum densities of the surface EMG signals.

Figure 26 illustrates the power spectral density (PSD) plots from 10 minutes interval plots. This demonstrates the shift in MDF that occurs from Multifidus but not from Trapezius.

3.5.13 ECG analysis

The relationship between boat and seat acceleration in the x, y and z-axis and heart rate is shown in the scatterplots (Figure 27). The cross correlation coefficients are also shown on each plot.

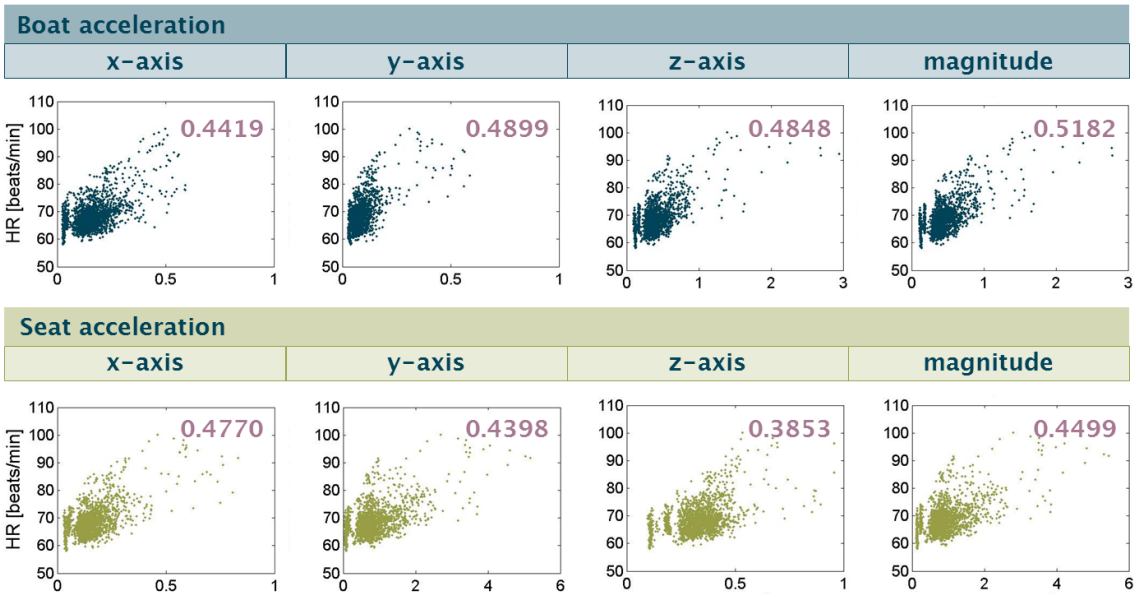

Figure 27. Scatterplots indicate relationship between boat and seat acceleration and heart rate (horizontal axis on each graph indicating magnitude of acceleration (m/s^2)).

Calculated instantaneous heart rate plotted against rms values of frequency-weighted seat acceleration magnitude is shown in Figure 28. The estimated delay between the instantaneous heart rate and seat acceleration was approximately 2 seconds and was calculated using cross correlation function.

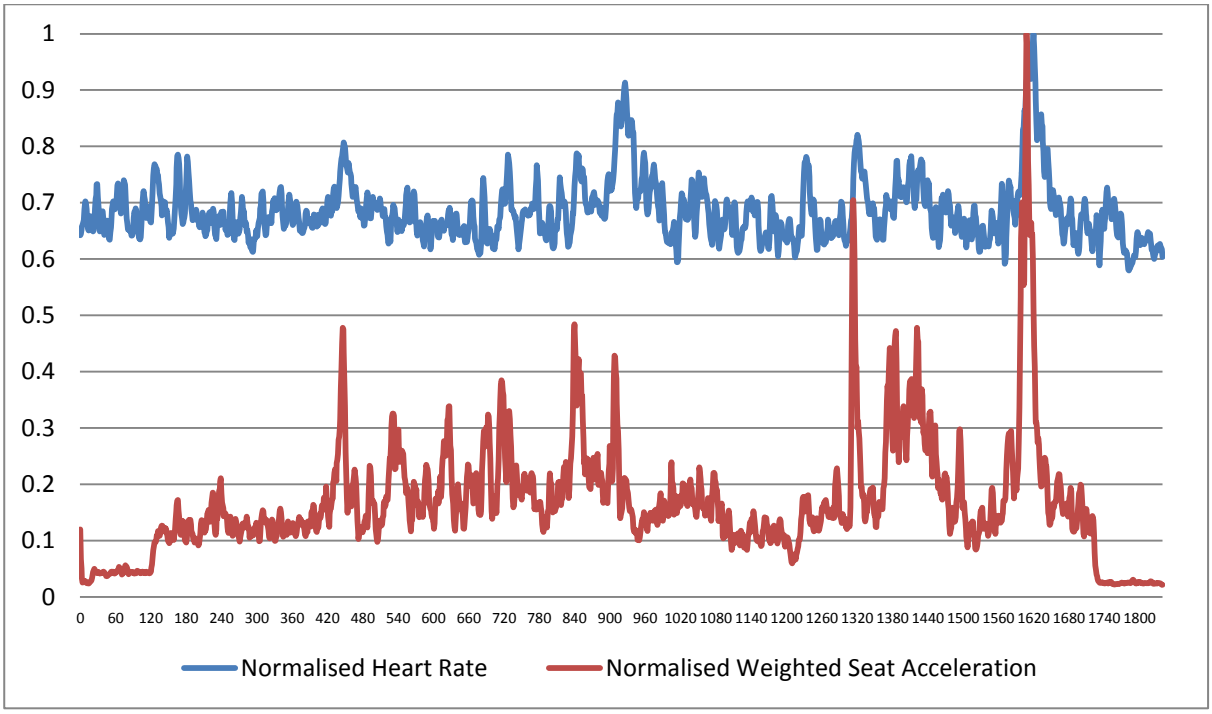

Figure 28. The frequency-weighted seat rms acceleration magnitudes (bottom) and instantaneous heart rate (HR) (top) during trial.

The results demonstrate that there were moderately significant relationships between variations in seat acceleration values and heart rate, the largest influence on the heart rate is correlated to the weighted seat vibration in the *x*-axis, $r = .48$. Correlations between other weighted and un-weighted seat acceleration and total acceleration are shown in Table 6.

Table 6. Cross-correlation coefficients (r) between the instantaneous heart rate and the un-weighted and frequency-weighted rms seat acceleration amplitudes.

Cross-Correlation coefficients (r)				
Seat acc.	*x*-axis	*y*-axis	*z*-axis	Magnitude
un-weighted	.33	.44	.37	.43
weighted	.48	.44	.39	.45

3.5.14 Discussion

The methodology presented shows the feasibility of undertaking human performance measurement during high-speed transits at sea. Boat data and human physiological data were successfully collected without significant artefacts or noise contamination. Boat data were successfully synchronised with human physiological data and tentative associations made.

The spectral EMG analysis demonstrates spectral shifts from higher to lower frequency range that is consistent with evidence of muscle fatigue during the sea transit. The preliminary results also demonstrate very high influence of body vibration on lumbar spine muscle fatigue during vibration exposure. There was no evidence of cervical spine muscles fatigue despite the head acceleration.

There was evidence that the heart rate increased in relation to seat vibration particularly in respect to the x-axis. It is assumed that the heart rate response is driven by increased sympathetic drive that occurs with the increased physiological demands associated with exercise (Rhodes and Bell 2014). Quoting the significance of the correlation coefficients is not appropriate in this single case study design.

3.5.15 Conclusion

In this single volunteer feasibility study, the hypothesis that there is an association between the magnitude of random and shock vibration exposure has been demonstrated as far as heart rate and lumbar spine muscles but not for cervical spine muscles. The methodology described is suitable for further data collection purposes in marine and possibly other occupational environments.

In the following section, an experiment is described that utilises the above methodology to determine if pre- and post-transit testing, utilising the Ito test (Ito et al. 1996) demonstrates any change.

3.6 Monitoring and assessing crew performance in high-speed marine craft: methodological considerations

3.6.1 Introduction

This study utilised the method to monitor and assess human performance specific to high-speed marine craft operation previously described in section 3.5. The high-speed craft crew's ability to efficiently perform tasks is affected by the manner in which the vessel responds to the variable sea conditions. In general, the reaction of the human body to high-speed boat motion and vibration is recognised as the main cause of fatigue during and post transits; whereas random shock represents the most likely cause of injuries during transits.

3.6.2 Aim

The feasibility study described in this section was designed and undertaken with the aim to:

Identify and evaluate measures of crew performance before, during and after a transit in a marine environment. These measures can serve to indicate increasing fatigue, decreased functional capabilities and thus possible increased risk of injury.

Assess the utility of using the Ito test, a standardised fatigue test undertaken pre- and post-high-speed transit.

3.6.3 Design

A feasibility case series study design used a previously developed methodology (See Section 3) to simultaneously evaluate the effects of random and shock vibration on aspects of human physiology with the addition of a pre and post-transit fatiguing test, the Ito test (Ito et al. 1996).

3.6.4 Hypothesis

The design tested the hypothesis that;

There will be changes in the median frequency recorded, consistent with fatigue, as a result of exposure to random and shock vibration during a high-speed boat transit.

Results from a standardised fatigue test, the Ito test, undertaken pre- and post-high-speed transit will be consistent with fatigue associated with exposure to random and shock vibration.

There will be a positive association between the magnitude of vibration exposure and an increase in heart rate.

Rating of perceived exertion will be consistent with changes in physiological parameters recorded.

The null hypothesis was that;

There will be no change in median frequency between pre- to post-transit fatigue testing.

There will be no change in the results of a standardised fatigue test, the Ito test, undertaken pre- and post-high-speed transit.

There is no association between the magnitudes of the exposure to vibration on heart rate.

Ratings of perceived exertion will not be consistent with changes in physiological parameters recorded.

3.6.5 Method

The experiment consisted of a sea trial (previously described, see section 3.5) preceded and followed by a muscle fatigue test. Physical data measured during the trials were boat acceleration and motion about the LCG, seat and head accelerations. Measurements of physiological data were ECG and surface EMG activities of four spinal muscles (upper fibres of Trapezius and Multifidus in

the lumbosacral region), performed during all phases of the experiment. Rating of perceived exertion was also collected.

A schema of the performance measurement system is depicted (Figure 29). This is identical to the experimental set up for the previous experiment (Section 3.5) with the addition of pre- and post-transit fatigue testing with the additional collection of sEMG data during both the pre- and post-test fatigue test and during the high-speed transit.

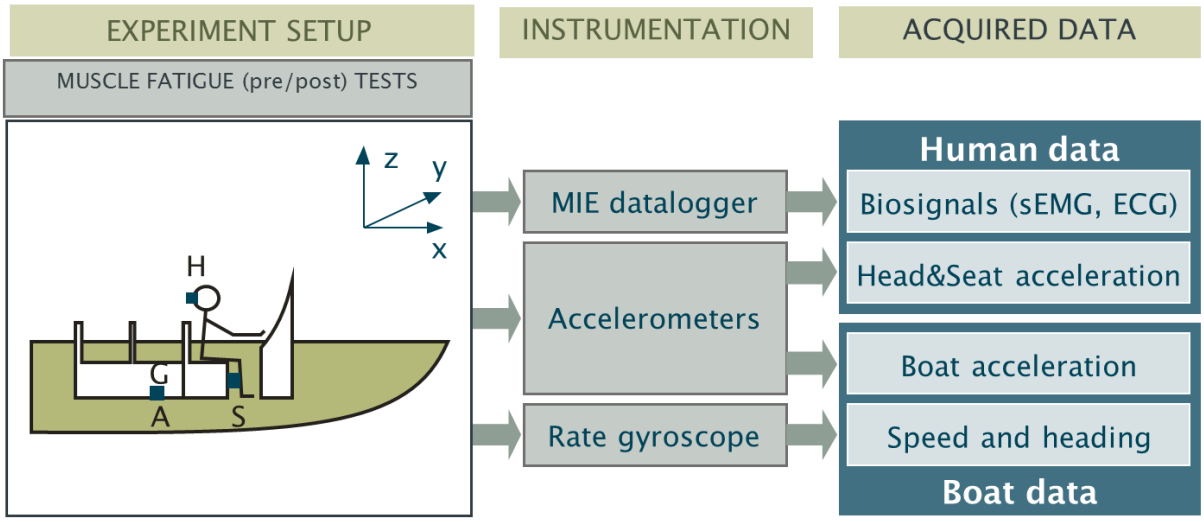

Figure 29. Performance measurement system.

In Figure 29, A, H, S and G correspond to the positions of the accelerometers placed at the boat LCG, head and seat and rate gyroscope respectively.

3.6.6 Rating of Perceived Exertion

The Borg scale is a commonly used visual analogue scale (VAS) that is used to rate perceived exertion, typically in an athletic population undertaking performance testing. The scale correlates with heart rate and uses values between 6 and 20. These values approximate to heart rate values of 60 beats per minute (beats/min), which occurs in someone completely at rest to 200 beats/min which would be an absolute maximum heart rate of a fully trained athlete of around 20 years old working at maximum intensity. The VAS is easy to apply in situations where an individual is working hard and can give an immediate response by using the scale to indicate how hard they are working. Figure 30 shows the Borg Scale and the anchor points used to help participants rate how hard they perceive that they are working.

The Borg Scale	
6	No Exertion at all
7	Extremely Light
8	
9	Very Light
10	Light
11	
12	Somewhat Hard
13	
14	
15	Hard (Heavy)
16	
17	Very Hard
18	
19	
20	Maximal Exertion

Figure 30. The Borg scale.

Figure 30 shows the basic Borg Scale (Borg G 1998) as presented to participants in a trial where rating of perceived exertion (RPE) is required.

3.6.7 Sea trials

Three sea trials were carried out with a RIB-X Expert XT650 at the south coast of England. Each trial was run with one participant sitting on the front left seat next to the helmsman. Three physically fit male participants (83±9.6 kg weight, 182±12 cm height, 28.3±3.2 age) participated in this study. The sea conditions were slight (sea state 3). The average and maximum boat speed estimated from Global Positioning Satellites (GPS) recordings for each trial are reported in Table 7 (1 knots≈0.5144 m/s).

Table 7. Boat speed during the sea trials.

Trial No.	Trial Duration	Average speed [knots]	Average speed [m/s]	Maximum speed [knots]	Maximum speed [m/s]
1	35 min 20 s	**20.84**	**10.72**	**27.58**	**14.19**
2	27 min 0 s	**25.17**	**12.95**	**37.73**	**19.41**
3	38 min 50 s	**25.58**	**13.16**	**36.54**	**18.80**

3.6.8 Muscle fatigue test

Before and after the sea trial, each participant performed a standardised isometric back extension test until fatigued (Ito et al. 1996). The participants, lying prone, were instructed to maintain the upper body above the floor as long as possible, with arms aligned with the body and the head in a neutral position looking downward (Figure 20). The test ceased when the participant was no longer able to maintain the trunk in the test position, the time for each test as well as the sEMG signals from Multifidus and the upper fibres of Trapezius, were recorded.

3.6.9 Results

In this section examples of results will be presented to illustrate examples from this case series. Vibration data for each trial are presented as this was successfully collected from both the boat and the accelerometers attached to the helmet.

Physiological data were not fully analysed from each participant as Matlab programmes needed to be written for each analysis; summary data is therefore not available. The physiological data that were analysed were chosen from the second and third trial where the VDV values were greatest as this was assumed to be most likely to result in greatest changes.

3.6.10 Boat speed and vibration

Frequency-weighted peaks and rms amplitudes of the LCG and seat accelerations calculated for each trial are reported in Table 8. For all three trials, the highest impact magnitudes occurred in the vertical direction (z-axis) at the boat's LCG and in the longitudinal (x-axis) or lateral (y-axis) directions

at the seat front. The magnitude and frequency of impacts increased significantly in the second half of each trial. Overall frequency-weighted rms seat acceleration magnitudes were found to be considerable larger than the rms magnitudes of LCG acceleration. In accordance with BS 6841 (BSI 6841 1987), vibrations with such frequency-weighted rms magnitudes are indicated as being uncomfortable.

Table 8. Vibration parameters from sea trials.

Trial	peak [g]			rms [m/s^2]			
No.	*x*-axis	*y*-axis	*z*-axis	*x*-axis	*y*-axis	*z*-axis	total
LCG acceleration (weighted)							
1	**0.119**	**0.109**	**0.866**	**0.124**	**0.083**	**0.324**	**0.357**
2	**0.148**	**0.162**	**2.165**	**0.188**	**0.103**	**0.457**	**0.505**
3	**1.740**	**0.212**	**2.292**	**0.281**	**0.191**	**0.551**	**0.647**
Seat acceleration (weighted)							
1	**0.186**	**0.708**	**0.799**	**0.119**	**0.653**	**0.248**	**0.709**
2	**0.231**	**1.538**	**1.363**	**0.181**	**1.005**	**0.347**	**1.079**
3	**0.452**	**1.359**	**1.490**	**0.200**	**1.060**	**0.352**	**1.135**

3.6.11 Vibration dose values

Partial and total VDVs calculated for all three sea trials performed in this study are listed in Table 9. The largest VDVs were reported for the third trial where a higher number of impacts were encountered, especially in the second half of the trial. It can be also seen that the total VDVs calculated at the seat (seated posture ($|S_w|$)) are larger than the total VDVs calculated at the boat's LCG (standing posture ($|A_w|$)) for all three trials. Moreover, a main contribution to the seat's total VDVs is from impacts in the lateral direction; while in the case of the boat's LCG it is predominantly the result of vertical impacts. In the second and third trial, even though the sea state was slight, the total VDVs calculated at the seat exceed the exposure action value (EAV) of 9.1 m/s$^{1.75}$ standardized for an eight-hour period within approximately 20 minutes.

Table 9.Vibration dose values derived in case of seated and standing postures.

Trial	VDV (standing posture) [m/s$^{1.75}$]				VDV (seated posture) [m/s$^{1.75}$]			
No.	*x*–axis	*y*–axis	*z*–axis	total	*x*–axis	*y*–axis	*z*–axis	total
1	**1.54**	**1.19**	**4.12**	**4.15**	**1.40**	**7.54**	**3.13**	**7.60**
2	**1.92**	**1.37**	**8.41**	**8.41**	**2.08**	**12.20**	**4.92**	**12.28**
3	**6.43**	**2.65**	**11.37**	**11.66**	**2.98**	**14.73**	**6.23**	**14.85**

The following cumulative effects of the total VDV relative to the frequency-weighted LCG and seat acceleration magnitudes during each of the trials are illustrated in Figure 31, Figure 32 & Figure 33 where the exposure action (EAV) and limit values (ELV) are marked with the horizontal fine dotted lines. The EAV is exceeded approximately 23 minutes from the beginning of the second trial and at approximately 18 minutes in the third trial. The magnitude and frequency of impacts increased significantly resulting in a rapid increase of the acceleration values.

Figure 31, Figure 32 & Figure 33 illustrate the calculated VDV_{total} that participants were exposed to during the transit; Exposure Limit Value (ELV), Exposure Action Value (EVA), Frequency weighted Boat ($|A_w|$) and Seat ($|S_w|$) acceleration values and limits are indicated.

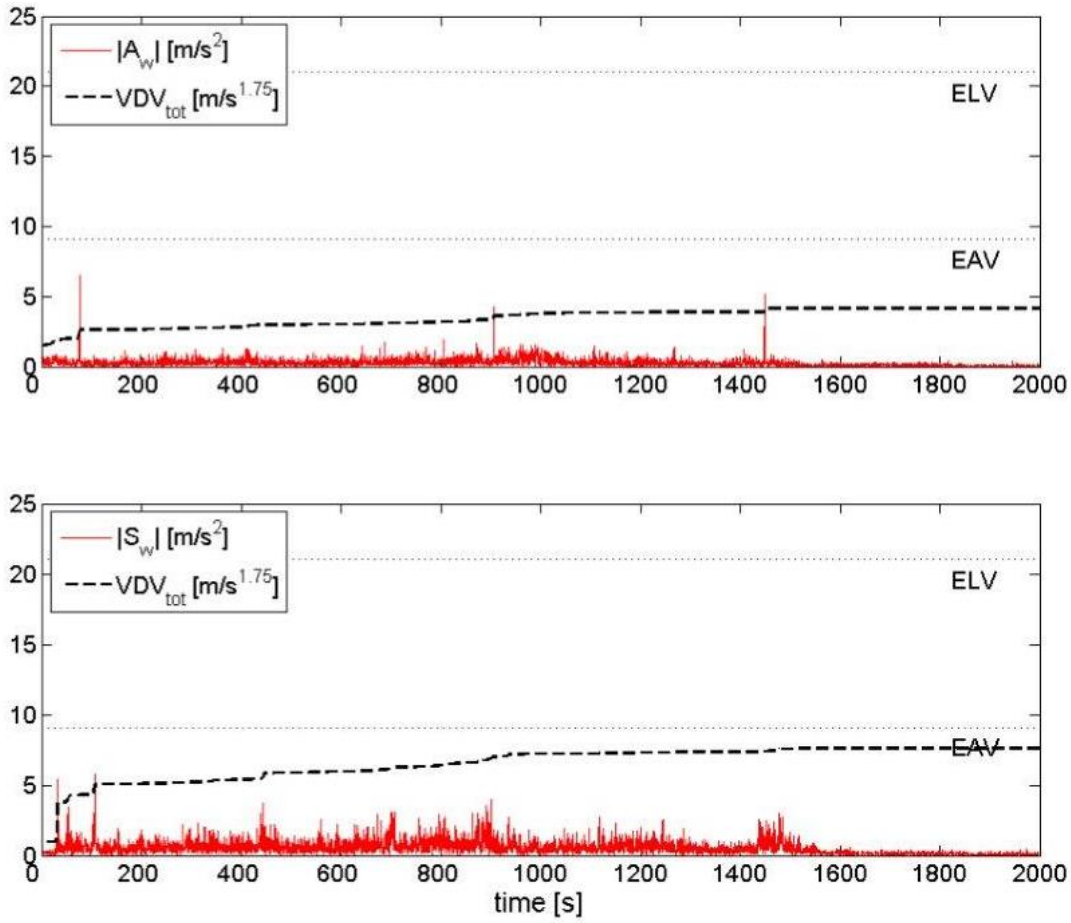

Figure 31.Frequency-weighted acceleration magnitudes and total VDV (1st trial).

In the first trial, the total calculated VDV was 4.15[$m/s^{1.75}$] & 7.60[$m/s^{1.75}$] for the standing and seated positions respectively. Neither of these values exceeded the exposure action value.

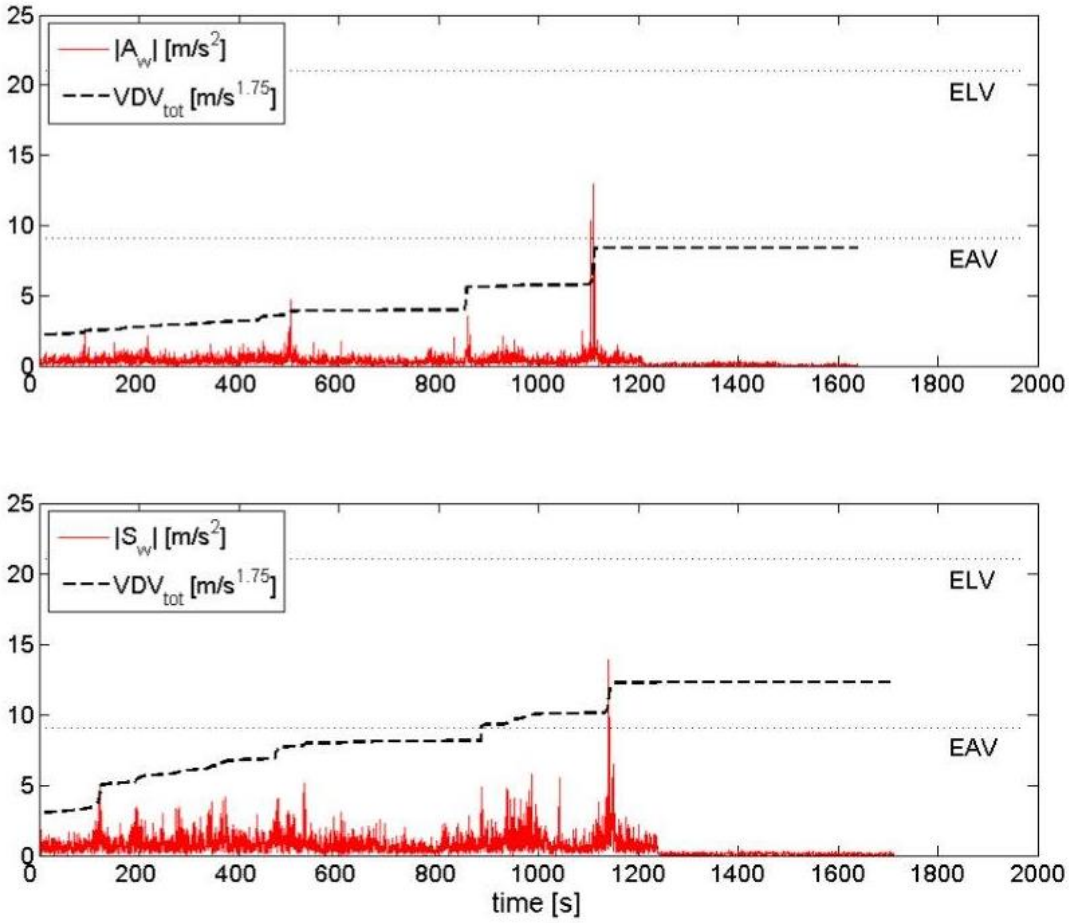

Figure 32. Frequency-weighted acceleration magnitudes and total VDV (2nd trial).

In the second trial, the total calculated VDV was 8.41[m/s$^{1.75}$] & 12.28[m/s$^{1.75}$] for the standing and seated positions respectively. In the seated position, this exceeded the calculated EAV in the seated position but not in the standing position.

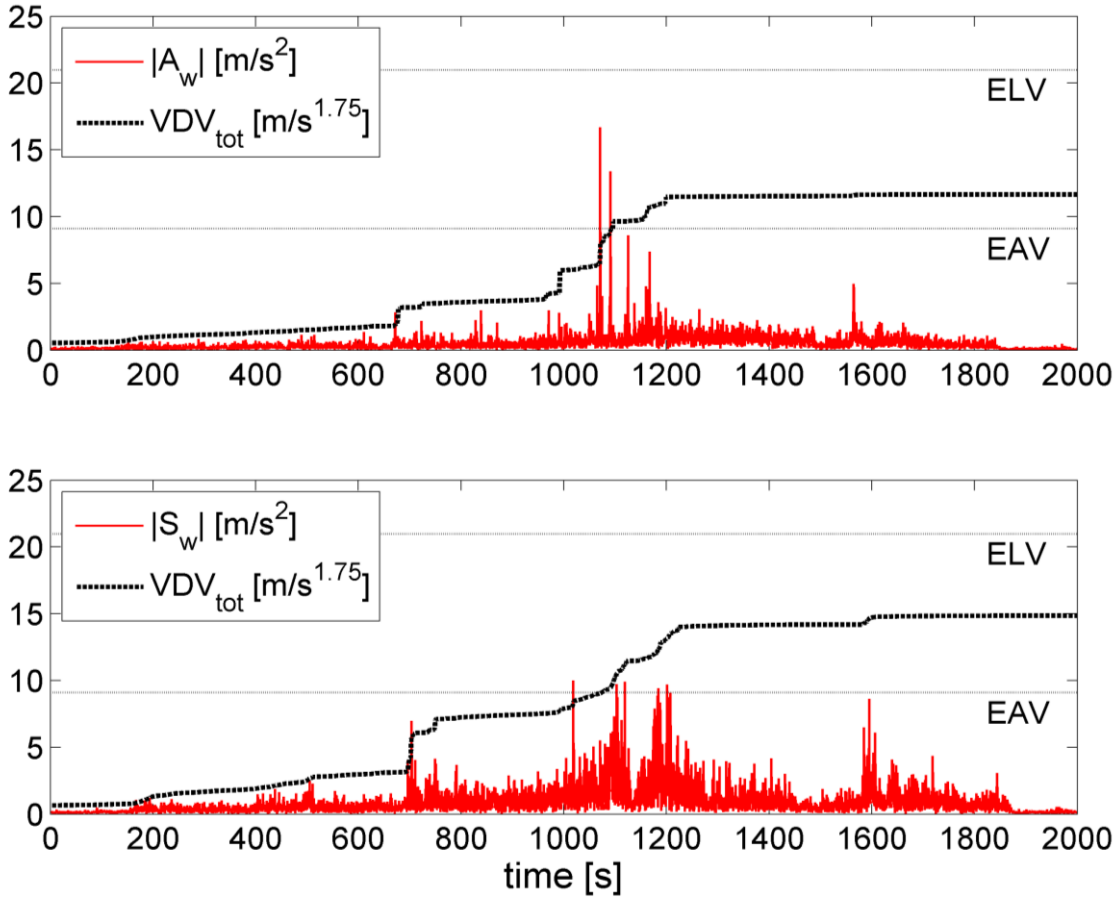

Figure 33. Frequency-weighted acceleration magnitudes and total VDV (3rd trial).

In the third trial, the total calculated VDV was 11.66[m/s$^{1.75}$] & 14.85[m/s$^{1.75}$] for the standing and seated positions respectively. In the seated position, this exceeded the calculated EAV in both the seated and the standing position.

3.6.12 Physiological data

The EMG variables considered in this study are the rms value and MDF (Cifrek et al. 2009; Merletti & Parker 2004). These parameters are calculated from the consecutive 1 s time windows of the band-pass-filtered (10-300 Hz) EMG signals.

All three trials reveal a relationship between multifidus EMG and acceleration rms values. The normalised running rms values for right and left Multifidus muscles at the level of the 4th and 5th lumbar vertebrae and seat acceleration are shown in Figure 34, Figure 35 & Figure 36. It can be seen that there is a relationship between the frequency-weighted seat acceleration (S_w) and the normalised running EMG rms amplitudes.

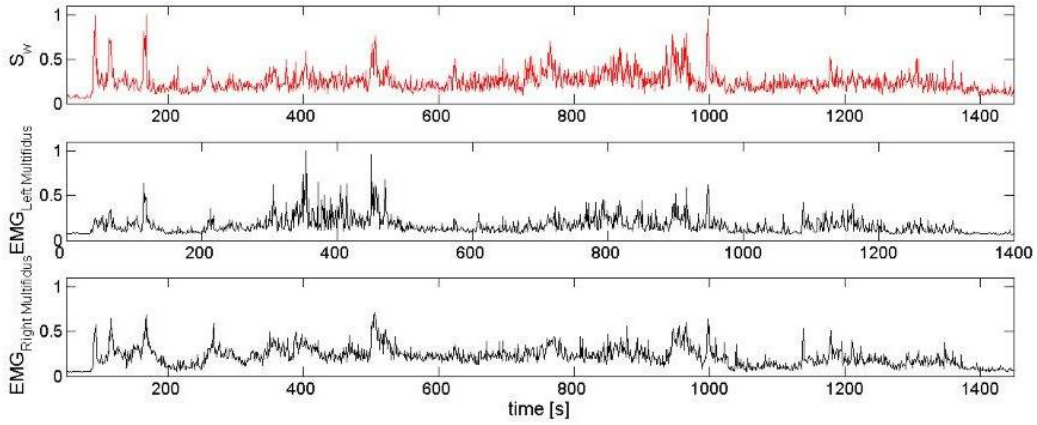

Figure 34. Frequency-weighted seat acceleration (Sw) and normalised EMG rms amplitudes of right and left Multifidus (1st trial).

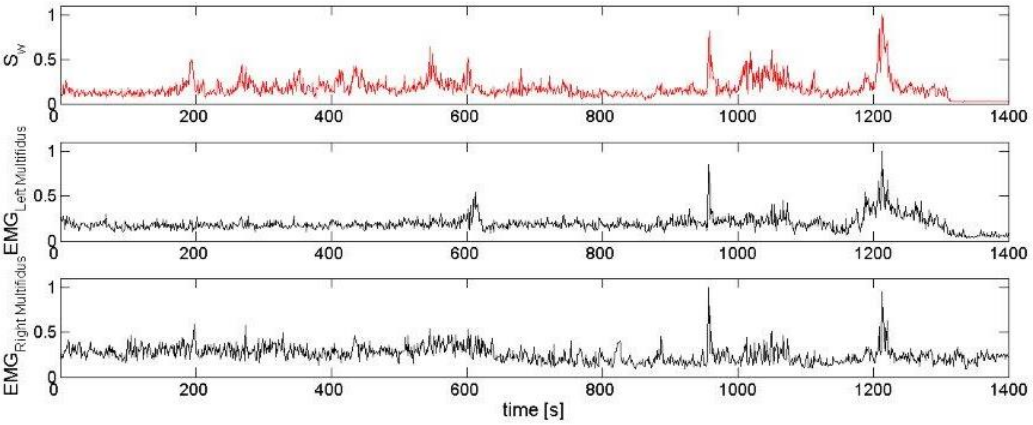

Figure 35. Frequency-weighted seat acceleration (Sw) and normalised EMG rms amplitudes of right and left Multifidus (2nd trial).

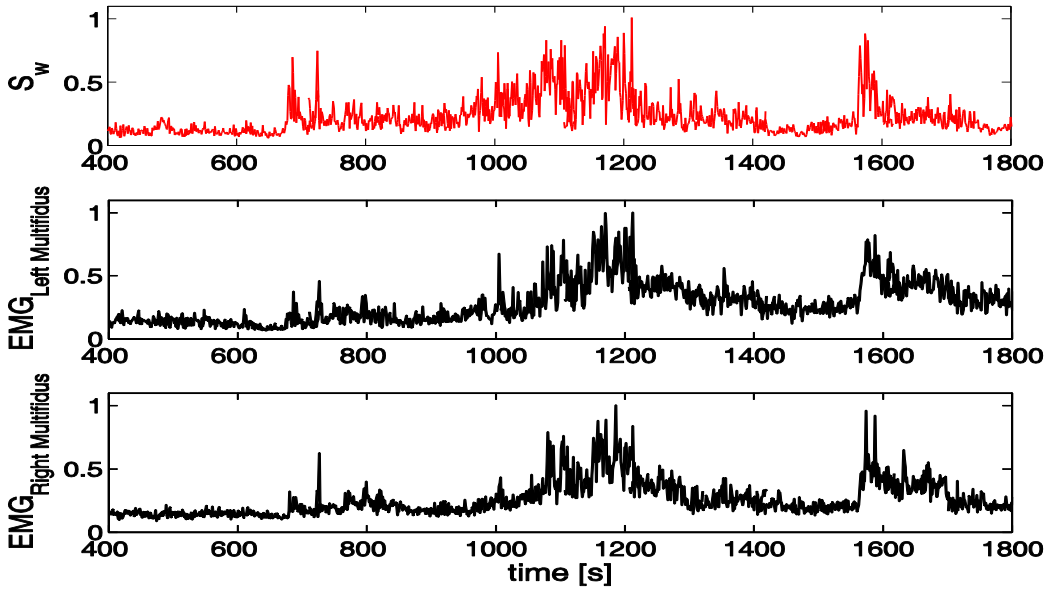

Figure 36. Frequency-weighted seat acceleration (Sw) and normalised EMG rms amplitudes of right and left Multifidus (3rd trial).

The relationship between EMG and acceleration rms values, the normalised running rms values for left and right Multifidus muscles at the level of the lumbar 4th and 5th vertebrae and seat acceleration are shown (See Figure 36). This is reported within the time interval where most impacts occurred i.e. at 400 – 1800 seconds into the trial. An increase of the EMG magnitudes caused by large impacts in seat acceleration is evident.

3.6.13 Multifidus v Trapezius fatigue during 2nd trial

For the second trial (Figure 37), fatiguing characteristics are demonstrated for the Multifidus muscle but not for the upper fibres of Trapezius. It is also evident that at the end of the trial the median frequency for the Multifidus muscles returns quickly to a pre-test level where from 1400 seconds to the end of the trial the velocity of the vessel had slowed and the sea state had reduced to flat calm.

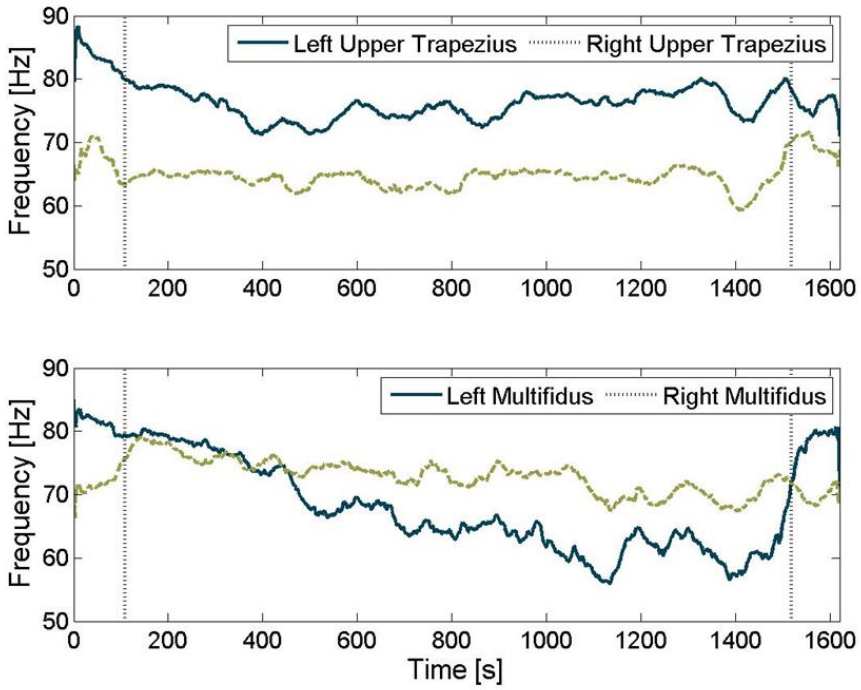

Figure 37. Median frequencies of Multifidus muscles and upper fibres of Trapezius (2nd trial).

3.6.14 Fatigue plot for Multifidus, 2nd trial

Viewing the PSD calculated from the surface EMG (Figure 38) a shift in the median frequency is evident for both right and left Multifidus group and is consistent with EMG characteristics associated with fatigue.

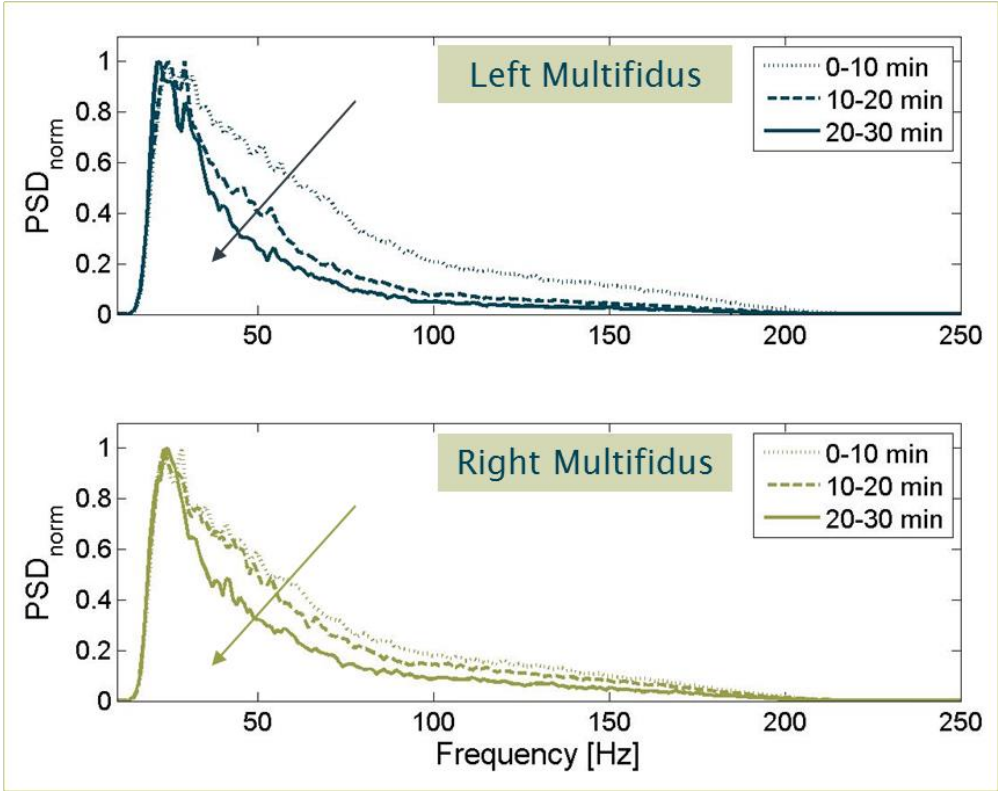

Figure 38. PSD of Multifidus calculated for 10 minute time intervals throughout the trial. Arrow indicated direction of shift in MDF (2nd trial).

3.6.15 MDF right and left Multifidus, 3rd trial

Median frequencies calculated for the period 400 – 1800s of the third trial are given in Figure 39. It can be seen that the MDFs of the left and right Multifidus decrease by more than 8 Hz when the majority of impacts occurred (in time period between 1070 s and 1200 s from the beginning of the trial) demonstrating a similar effect to that seen when muscle fatigues (Merletti & Parker 2004).

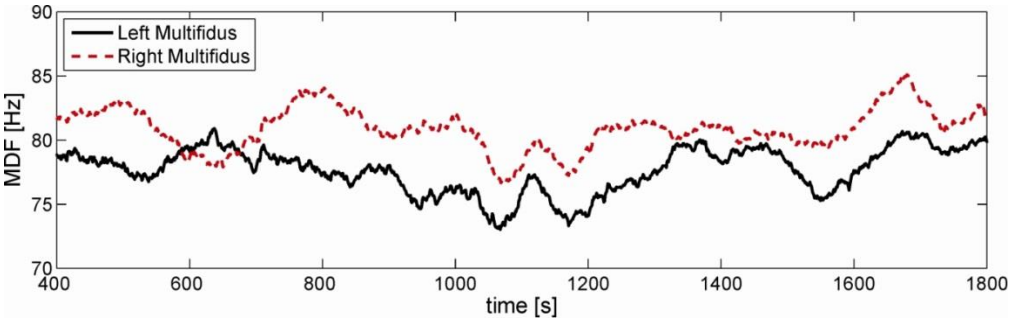

Figure 39. Median frequency of Multifidus muscles (3rd trial).

3.6.16 Rating of perceived exertion

Participants were asked to score their own RPE immediately following the transit; they were asked to indicate, using the scale, how hard they perceived they had been working at the hardest part of the transit.

The results of the Borg rate of perceived exertion test for each trial respectively are 11.5, 12 and 17 indicating that the participant's perception of the sense of effort during the sea trial, when they perceived that they were working at their hardest, was rated between somewhat hard (>11) to very hard (>15). These results concur with vibration data that illustrates the severity of the trial – as can be seen from Table 9, the vibration parameters increased from the first to the third trial.

3.6.17 Heart rate, MDF and ECG, 1st trial

The heart rate computed from the ECG and the MDF values calculated for the EMG and ECG measurements conducted before and after the first trial are given in Table 10 and Table 11 respectively. In this trial, the results of the muscle fatigue test have not demonstrated general increase of heart rate or decrease of MDF values after the trial. It could be speculated that the effect of the vibration exposure on the muscle fatigue was not significant due to slight sea conditions (Table 8) and fitness level of the participant. No heart rate data were available for trails two and three due to heart rate monitor lead failure.

Table 10. Comparison of heart rate values for the pre and post-trial muscle fatigue tests (first trial).

HR [beats/min]	min		max		mean		*SD*		range	
	pre-	post-	pre-	post-	pre-	post-	pre-	post-	pre-	post-
	63.8	**59.6**	**95.8**	**93.1**	**83.6**	**77.3**	**7.2**	**8.5**	**32**	**33.4**

Table 11. Comparison of MDF values for the pre-trial and post-trial muscle fatigue tests (first trial).

MDF [Hz]	min		max		mean		*SD*		range	
	pre-	post-	pre-	post-	pre-	post-	pre-	post-	pre-	post-
L. Trapezius	**64**	**68.6**	**75.6**	**89.2**	**68.7**	**79.2**	**2.6**	**5.6**	**11.6**	**20.6**
R. Trapezius	**58.8**	**65**	**76**	**88**	**64.9**	**73.6**	**2.4**	**3.4**	**17.2**	**23**
L. Multifidus	**76.2**	**84**	**101.7**	**104**	**88.3**	**94.4**	**6.7**	**4.9**	**25.5**	**20**
R. Multifidus	**73**	**83.8**	**110**	**115**	**91.1**	**99.1**	**9.3**	**7.3**	**37**	**31.2**

3.6.18 Ito pre- and post-test

Median frequencies of the FFT were calculated from the right and left sEMG of the upper Trapezius and Multifidus muscles. The results of the pre- and post-transit Ito test demonstrated that the trial results in fatigue as evidenced by the shift in median frequency in the Multifidus group but not the upper fibres of Trapezius (Figure 40 and Figure 41). There is a decrease in the median frequency from the start of the test to the end, the holding time is increased following the transit and the magnitude of the decrease is less post-transit.

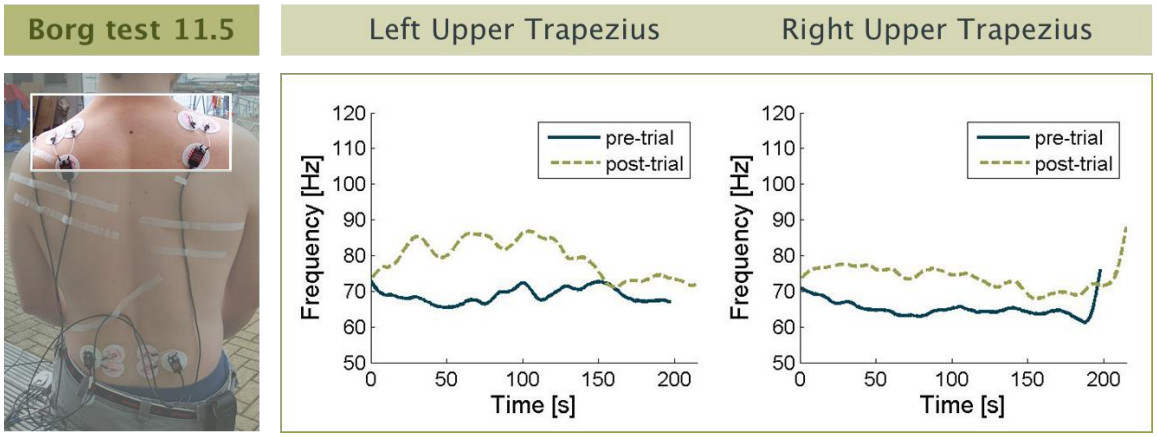

Figure 40. Result of pre and post-transit Ito fatigue test, upper fibres of Trapezius.

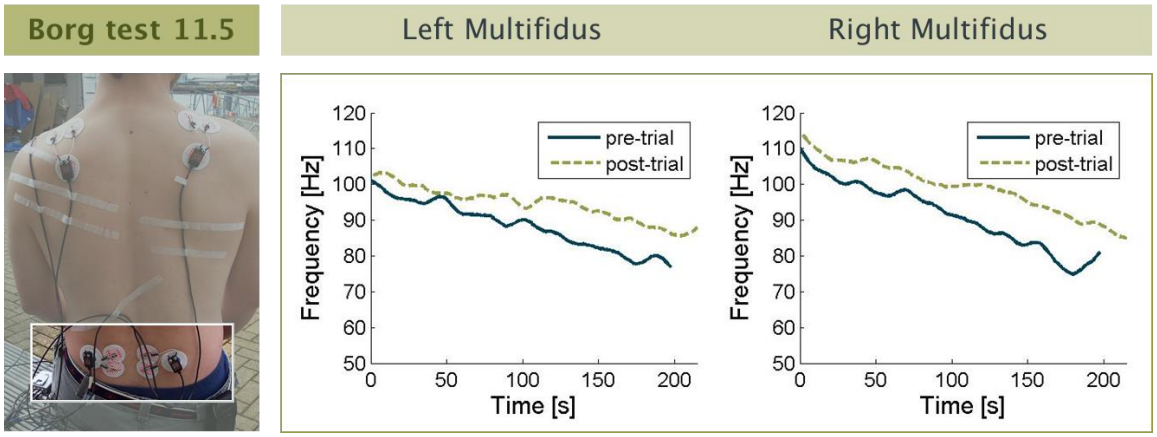

Figure 41. Result of pre and post transit Ito fatigue test for Multifidus.

On each figure, there are two plots; the dark green solid line represents the pre-trial test and the light green dashed, the post-trial.

Table 12. Pre- and Post-Transit Ito results: time to task-failure.

Pre- and Post-transit Ito times (seconds)		
Participant No.	Pre-transit	Post-transit
1	**196**	**220**
2	**220**	**217**
3	**177**	**186**

Table 12 gives data on pre- and post-transit Ito holding times/times to task-failure; it is noted that post-transit holding times exceeded the pre-transit holding time in two out of the three trials. It is also noted that the results of the analysis of MDF indicate that the rate of change in the MDF was less post-transit.

3.6.19 Discussion

A method that monitors and assesses crew performance in high-speed marine craft transits at sea has been proposed and preliminary results of the feasibility case series study are presented. These results may be of particular relevance to those, such as the RNLI crews, who are exposed to random and shock vibration as part of their daily activity. It is reported that lifeboat crews experience high levels of fatigue associated with high-speed transits. This phenomenon is not new, but this method demonstrates clearly that muscles supporting the spine are subjected to forces that result in muscle fatigue. It is also evident that the individuals in this case series recovered quickly following the high-speed-transits. The VDVs obtained in this feasibility study are compared with limit values set by current standards and legislation; thus demonstrating the high VDV that can be expected on board high-speed marine craft even in relatively calm seas with short transit times. Values would be even larger in more severe sea states and compounded by wind and tide effects. It is shown that the physiological data are correlated with vibration magnitudes during sea transits. A decrease in median frequencies of the sEMG signals associated with an increase in vibration amplitude is demonstrated for the Multifidus muscle group. For a more thorough analysis of the effects of the trials on participant's performance during the muscle fatigue tests conducted before and after trial,

it would be necessary to collect more experimental data in different sea states from more participants.

The utility of the Borg test has been demonstrated within this experiment – in general, participants were working at a rate that was consistent with their own RPE. These test results are consistent with an individual working somewhat hard (>11) to very hard (>15) during the sea trial which under normal circumstances would result in immediate post-test fatigue. This however, would be dependent on the level of fitness; in particular, the rate at which heart rate would return to normal and to what extent the increase in heart rate was at or above lactate threshold level. It is unlikely that this was the case for the participants in this study.

Results of the sEMG analysis indicate a shift in MDF which is consistent with Multifidus muscle fatigue but this was not demonstrated in Trapezius. Wearing a helmet might be the cause of cervical spine muscle fatigue in some cases but this was not demonstrated.

There was little evidence that the high-speed transit caused lasting fatigue as evidenced by the differences in the pre- and post-Ito test results. There could be a number of reasons for this; the test may not have the sensitivity required to demonstrate change in fatigue state. The plots in Figure 39 and Figure 37 also demonstrate that the MDF recovers towards the end of the transit and this was commonly seen in all trials as the boat speed dropped and due to calmer seas. This recovery is a characteristic of fatigue when the stressor ceases and any testing that is designed to demonstrate post-test fatigue should be undertaken immediately following the fatiguing task. This did not occur in this case, as there was a delay of up to 5 minutes in post-testing, during which recovery might have taken place.

It may be that the Biering-Sørensen test procedure would be more discriminating than the Ito version; however, the Biering-Sørensen test would be impracticable to administer in a marine or most work place situations. In the context of this experiment, the place of testing was several metres from pontoon at which the RIB-X Expert XT650 boat docked, there was a delay of several minutes following completion of the trail as the vessel docked and a delay in the participant reaching the testing area; during this period, recovery could have occurred.

3.6.20 Conclusion

The results of the pre- and post-transit Ito test indicate that using this procedure is suitable for a field-testing situation; myoelectric manifestation of fatigue, as a result of the test, was demonstrated in the lumbar Multifidus muscle at L4 level but not in the upper fibres of Trapezius. However, it has not been demonstrated that there was evidence of more fatigue post-transit than before; the Ito test may not demonstrate sufficient sensitivity in this situation.

Therefore the null hypothesis (3.6.4), that there is no change in the results of a standardised fatigue test, the Ito test, undertaken pre- and post-high-speed transit, is accepted as a result of this particular case series experiment.

Further studies are required using a greater number and a range of participants that better represent the population of interest. However, the methodology developed resulted in valid sEMG, ECG and vibration data being collected during high-speed-transits and myoelectric changes were seen in the sEMG signals that are consistent with muscle fatigue.

It is recommended that pre- and post-transit testing should incorporate tools with greater sensitivity to detect changes in performance degradation.

While this study has shown that the myoelectric manifestations of fatigue of a section of the Multifidus muscle can be demonstrated during a high-speed transit, it does not demonstrate any overall fatigue effect of the stabilisers of the lumbar region. These stabilisers are extensive (See Section 2.1.3.6 & 2.1.5) and so a methodology that captures data from a greater proportion of muscles that contribute to the extensor mechanism as part of a controlled experiment was developed and described in the following section.

4. Development of feasibility study methodology: Assessment of spinal muscle fatigue using multi-channel surface EMG

4.1 Introduction

Many investigators have studied fatigue using electromyography (EMG) signals recorded from muscles involved in supporting the lumbar spine during fatiguing tasks (Falkenberg, Podein, Pardo, & Iaizzo 2001; Farina, Gazzoni, & Merletti 2003a; Kankaanpaa, Taimela, Webber, Jr., Airaksinen, & Hanninen 1997; Robinson, Cassisi, O'Connor, & MacMillan 1992). Others have specifically looked at the myoelectric changes that occur during whole body vibration (Blunthner, Seidel, & Hinz 2001; Blunthner, Seidel, & Hinz 2002; de Oliveira & Nadal 2004). EMG parameters, such as amplitude and frequency are recorded and descriptions are given of typical fatiguing effects such as an increase in amplitude of the EMG signal, a shift towards lower frequencies in the frequency spectrum and changes in the MDF reported. The cause of these changes during isometric testing is thought to be related to motor unit recruitment, synchronisation and reduction in muscle fibre conduction velocity. The central governor model (CGM) would predict that these changes are due to a decrease in central drive to the motor neuron pool as part of the mechanism to maintain homeostasis.

Changes in cognitive functioning and changes in the cardiovascular, respiratory, endocrine, vestibular and metabolic systems are also reported (Griffin 1990) but these are outside the scope of this thesis.

The purpose of this feasibility study was to establish if the methodology proposed could collect fatigue data utilising multi-channel surface electromyography (sEMG). A standard test (the Biering-Sørensen test) would be used in a lab-based experiment, to collect data from sEMG sensor locations based on published anatomical data.

4.2 Aims

The aims of this feasibility study were;

1. To develop a methodology and to standardise the test procedure for a laboratory-based assessment of spinal muscle fatigue based on the Biering-Sorenson test procedure.
2. To establish if high-density electrode matrixes and arrays would be suitable for investigating surface electromyography recording from spinal muscles.
3. To establish if the electrode placements based on previous anatomical studies provided useful data.
4. To develop tools for the visualisation of the raw electromyography signal
5. To undertake analysis of the myoelectric manifestations of fatigue during high force isometric muscle contraction.

4.3 Design

A pilot quasi-experimental design to develop a methodology utilising a convenience sample.

4.4 Hypothesis

The hypothesis of this feasibility study was that;

> Electrode placement based on previous anatomical studies provided valid data from the muscles under investigation

The null hypothesis being that;

> Electrode placement based on previous anatomical studies does not provide valid data from the muscles under investigation

4.5 Method

A convenience sample of six participants volunteered for this phase to develop the methodology. Participants were included who were willing to participate in

this feasibility study provided that they had no concurrent symptoms of acute low back pain or any significant identifiable pathology e.g. spondylolisthesis. Participants attended on more than one occasion as was required in the development of the methodology and the software application.

The study conformed to the Declaration of Helsinki and was approved by ISVR safety and ethics committee as a feasibility study for the purpose of developing the methodology. Therefore, data are presented to demonstrate development of the methodology; no conclusions are drawn from any aggregation of data. All equipment was safety tested and rated appropriate for experimental purposes.

Participants attended the laboratory by arrangement and once the necessary processes had taken place to ensure that the participants fully understood the procedure they were prepared for the experiment as described (4.5.4). The experiment was repeated three times with a fifteen-minute break between each test on each occasion. There were no adverse events reported during or following the experiments and each one was conducted and completed according to the agreed protocol. A follow up of all participants at 12 months revealed that none had experienced any symptoms attributable to testing undertaken.

4.5.1 Electrode placement for multi-channel sEMG

Currently, there are no surface electromyography for the non-invasive assessment of muscles (SENIAM) guidelines for the placement of high-density sEMG electrodes for muscles of the body; guidelines exist for mono-polar or bi-polar applications only (Figure 42, Figure 43 and Figure 44) with SENIAM recommendations in quotes.

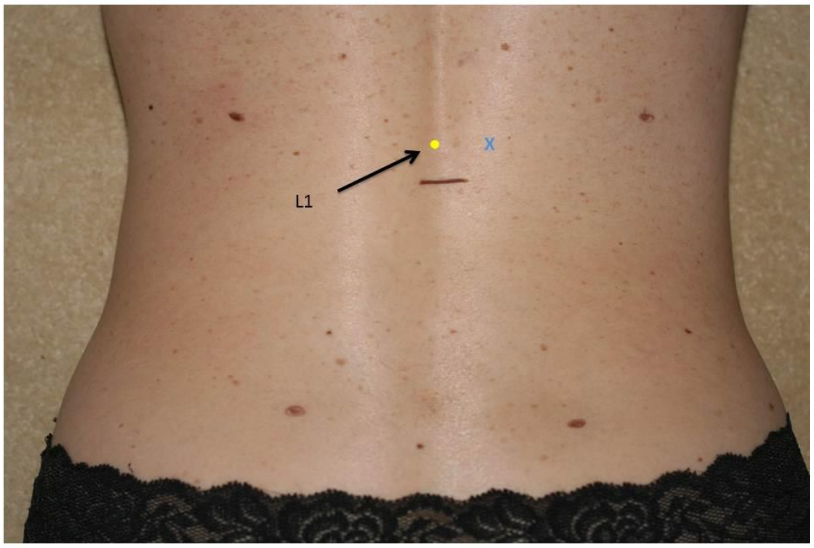

Figure 42. Longissimus SENIAM guidelines – 'Sensor positioned 2 finger widths from lateral to spinous process of L1.'

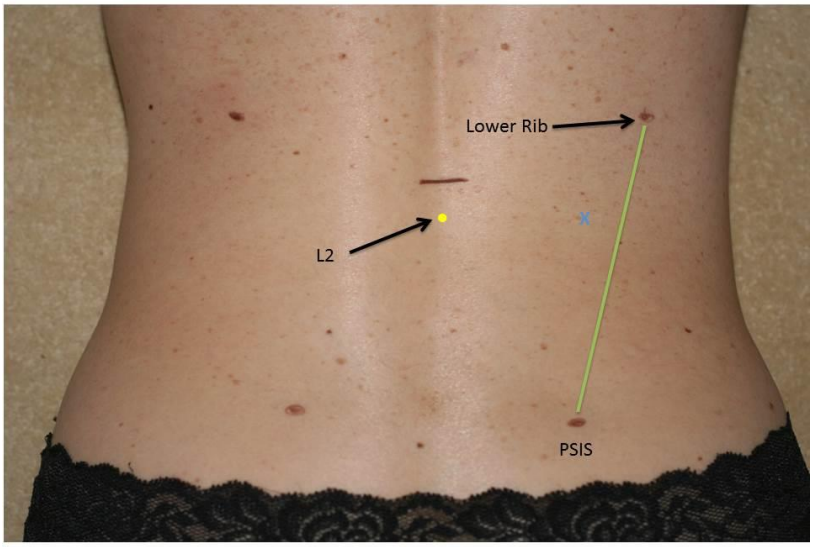

Figure 43. Iliocostalis SENIAM guidelines – 'Sensor positioned 1 finger width medial to the line from the posterior superior iliac spine to the lowest point of the lower rib, at the level of L2.'

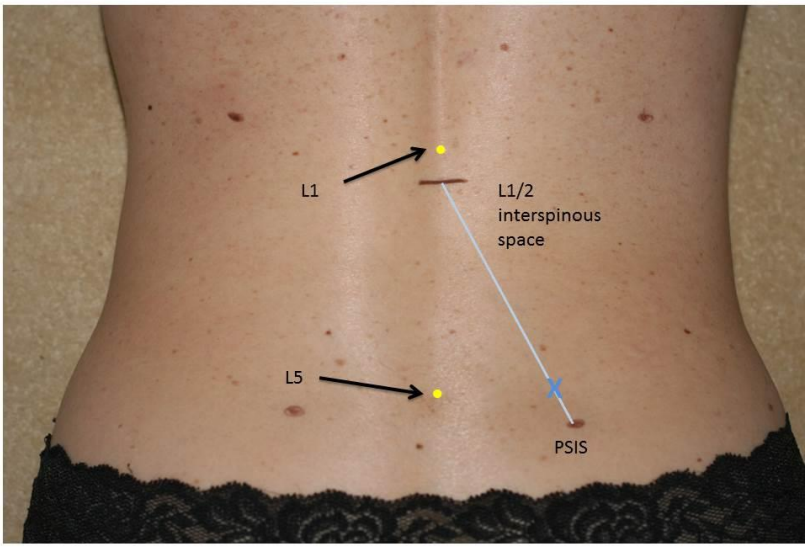

Figure 44. Multifidus SENIAM guidelines – 'Sensor aligned with a line from caudal tip of the posterior superior iliac spine to the interspace between L1 and L2 at the level of L5 spinous process (i.e. about 2 – 3 cm from the midline).'

The above positions were used to inform the process of multi-channel sEMG positioning but were considered unsuitable. The linear and matrix nature of high-density electrodes requires two dimension location information as described below; accurate electrode placement requires more precise measures than 'finger width'. It was therefore conclude that the SENIAM guidelines were unsuitable.

Certain principles apply to the location of high-density electrodes. It is recommended that high-density electrode arrays should be centred over the innervations zone of the muscle and that the electrode array should be orientated along the line of the muscle fibre (Farina, Fortunato, & Merletti 2000; Merletti, Farina, & Gazzoni 2003; Merletti, Farina, & Granata 1999). In the case of the muscles of the spine, this causes a number of issues. Due to the segmental innervation of many of the muscles of the spine, it is unlikely that identifiable innervation zones exist for each muscle. The muscles of the spine are innervated by the posterior primary rami of the spinal nerve root at each spinal level and consequently muscles that span numerous segments receive their innervation directly from more than one adjacent spinal segment. Studies have not been able to identify the locations of innervation zones of spinal muscles (Tsao, Danneels, & Hodges 2011; Tsao, Galea, & Hodges 2008)

in contrast to muscle of the limbs where innervation is via the anterior primary rami, the plexuses that are formed and the peripheral nerves; these locations are described in the SENIAM guidelines (Merletti & Hermens 2000).

Consequently, the position of high-density sEMG electrodes would need to be based on knowledge of the anatomical location of the muscle in order that these could be orientated along the longitudinal axis of muscles under investigation.

In order to collect data from muscles that contributed most to the extensor moment (i.e. Longissimus, Iliocostalis and the Multifidus) and the large surface area of muscle to be tested, multi-channel surface electromyography was chosen. This electrode format overcomes some of the issues associated with monopolar or bipolar sEMG; in particular, data from a larger surface area and from multiple spinal muscles can be achieved and post data collection signal processing can be utilised to identify innervation zones and eliminate data as required.

For this study, initial locations of the sEMG electrodes were based on two previous anatomical studies (Biedermann, DeFoa, & Forrest 1991; De Foa, Forrest, & Biedermann 1989). These studies reported that the location of the lateral edges of the muscles of interest can be defined by reference lines drawn from bony landmarks, the posterior superior iliac spines (PSIS), the lateral end of the twelfth rib and the L1/2 interspace, and from angles measured in relation to the longitudinal axis of the body, as follows; see Table 13 and Figure 45. They concluded that;

> *A line projected from the PSIS to the tip of rib 12 will identify the lateral edge of Iliocostalis Lumborum* – it is not clear if the authors were intending to describe the pars lumborum component or the pars thoracis.
>
> *A line projected horizontally from the PSIS to the L1/2 interspinous space will identify a point that is at the lateral edge of Multifidus.*
>
> *No reliable reference line could be established for Longissimus- however, reference angles were stated.*

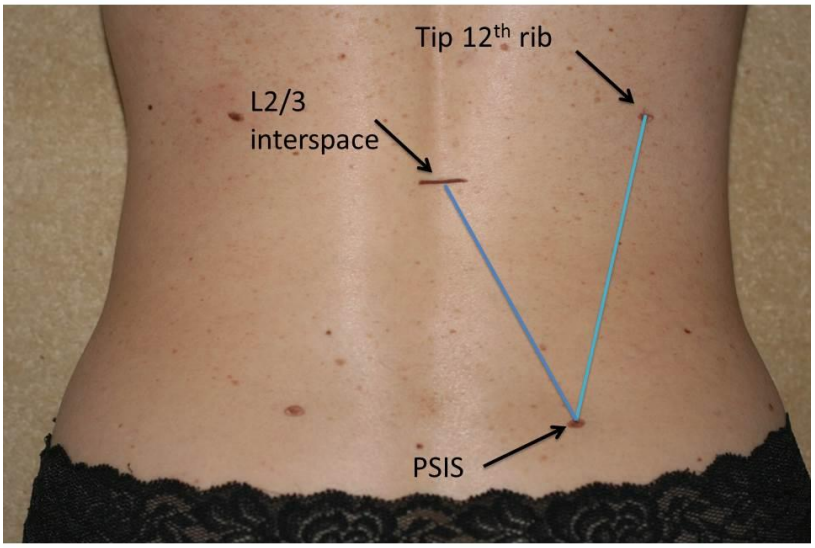

Figure 45. Lateral lines based on de Foa et al. (1989).

In these two studies (Biedermann, DeFoa, & Forrest 1991; De Foa, Forrest, & Biedermann 1989), that used data from six male and seven female embalmed cadavers, the following data were presented (Table 13). It is noted that the Longissimus and Multifidus data were obtained from four and five cadavers respectively.

It is noted that the SENIAM guidelines are remarkably similar to the recommendations of De Foa (1989) and Biedermann (1991) and when these two sets of guidelines are used in clinical practice to locate Iliocostalis and Multifidus, similar positions are located. In the case of Longissimus, the SENIAM guidelines do not concur.

Table 13. Angles of spinal muscles based on previous studies (Biedermann et al., 1991, DeFoa et al., 1989).

	M	*SD*	Range	n
Multifidus				
Males				
Fibre direction angle from spine	15.1°	1.43°	13.5° – 18.0°	4
Fibre direction angle from reference line	0.1° (m)	0.95°	± 1.0°	4
Females				
Fibre direction angle from spine	23.5°	4.50°	17.5 – 28.5	6
Fibre direction angle from reference line	0.1° (l)	1.10°	0.4° (m) – 1.2° (l)	5
Iliocostalis Lumborum				
Males				
Fibre direction angle from spine	13.0°	2.11°	11.5° – 17.0°	6
Fibre direction angle from reference line	0.4° (m)	1.50°	± 1.8°	6
Females				
Fibre direction angle from spine	12.9°	1.2°	11.0° – 14.4°	7
Fibre direction angle from reference line	4.9°	2.9°	0.5° – 8.0°	7
Longissimus Thoracis				
Males				
Fibre direction angle from spine	0.8°	7.67°	9.0° (m) – 9.81° (l)	5
Fibre direction angle from reference line	No reference line found			

(m) – medially (l) – laterally

4.5.2 Surface EMG electrodes for feasibility study

To collect sEMG data from Longissimus and from Iliocostalis, four 16-channel electrode arrays were used. These arrays, with an inter-electrode distance (IED) of 10mm were sufficiently long to accommodate the length of the muscles under investigation (Figure 16 and Figure 49).

For Iliocostalis the electrodes were initially positioned using the reference line from the PSIS to the tip of the twelfth rib (R12) to identify the lateral edge of Iliocostalis and the array was then fixed to the skin medial to this line at an angle of 13° from the spine. See right hand image Figure 46.

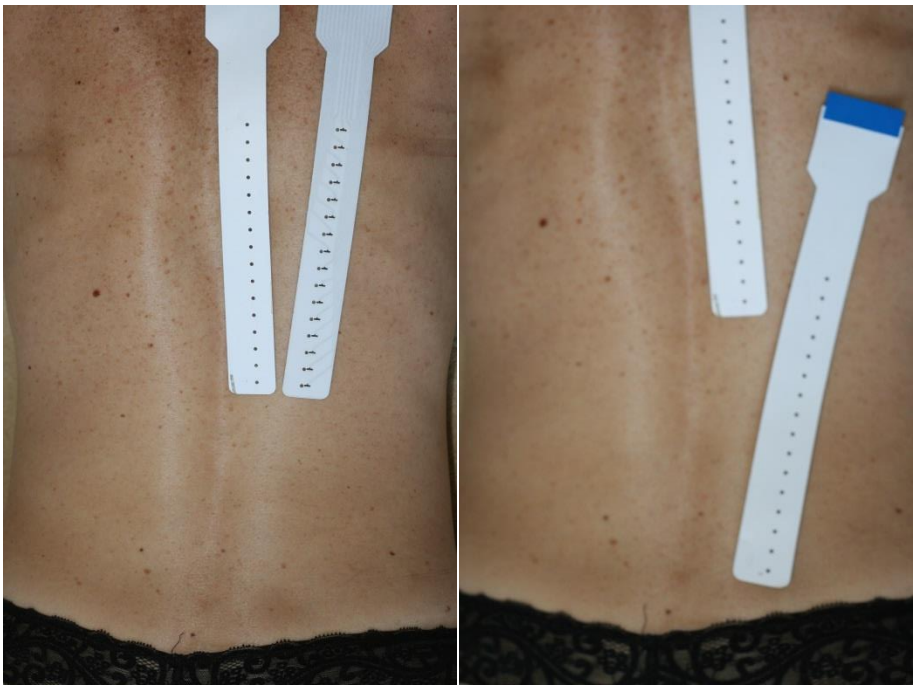

Figure 46. Initial positions for Longissimus and Iliocostalis.

For Longissimus, the electrode was fixed to the skin adjacent to the medial edge of the previously applied electrode and adjacent to the longitudinal axis of the body using a range of angles as informed by the range of previous studies. Initially, two electrodes were attached adjacent to each other (Figure 46, Figure 49 and Figure 52) as the exact location for this muscle could not be determined accurately from previous study due to lack of a reference line.

For Multifidus, the construction of the electrode sensor matrix, with an IED of 8mm, did not allow orientation along the angle of both the right and left muscles simultaneously due to the converging nature of Multifidus. The electrodes are orientated in rows and columns that are perpendicular to each other as can be seen in Figure 47, Figure 48 and Figure 49. The location of any innervation zones would be determined visually post-data collection by analysis of the sEMG signal.

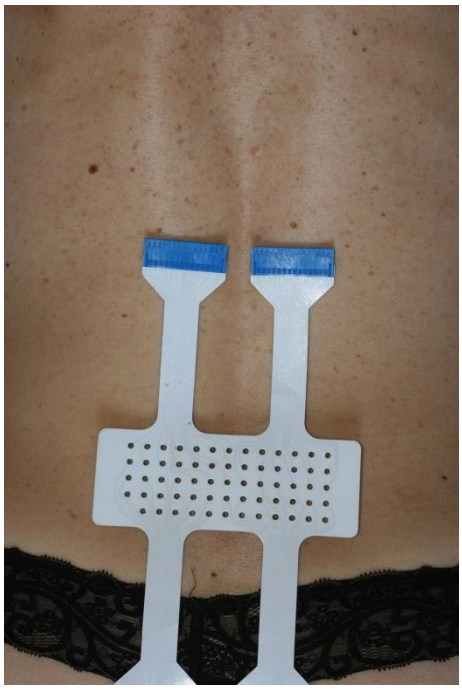

Figure 47. Multifidus matrix position.

The position of each sensor in the 64-channel matrix can be seen in Figure 48. Illustrated are 'Layout 1' and 'Layout 2'. The configuration of the channels can be seen to differ between each layout – at the commencement of this study, the supplier provided matrix electrodes with 'Layout 1' configurations; during the study 'Layout 2' configuration electrodes were supplied. A method was developed to differentiate between the different sensor configurations in the analysis post data collection. This was achieved by the development of a graphical user interface (GUI) that provided decoding of the signal into a consistent channel order which enabled a comparison to be made between data collected using either configuration.

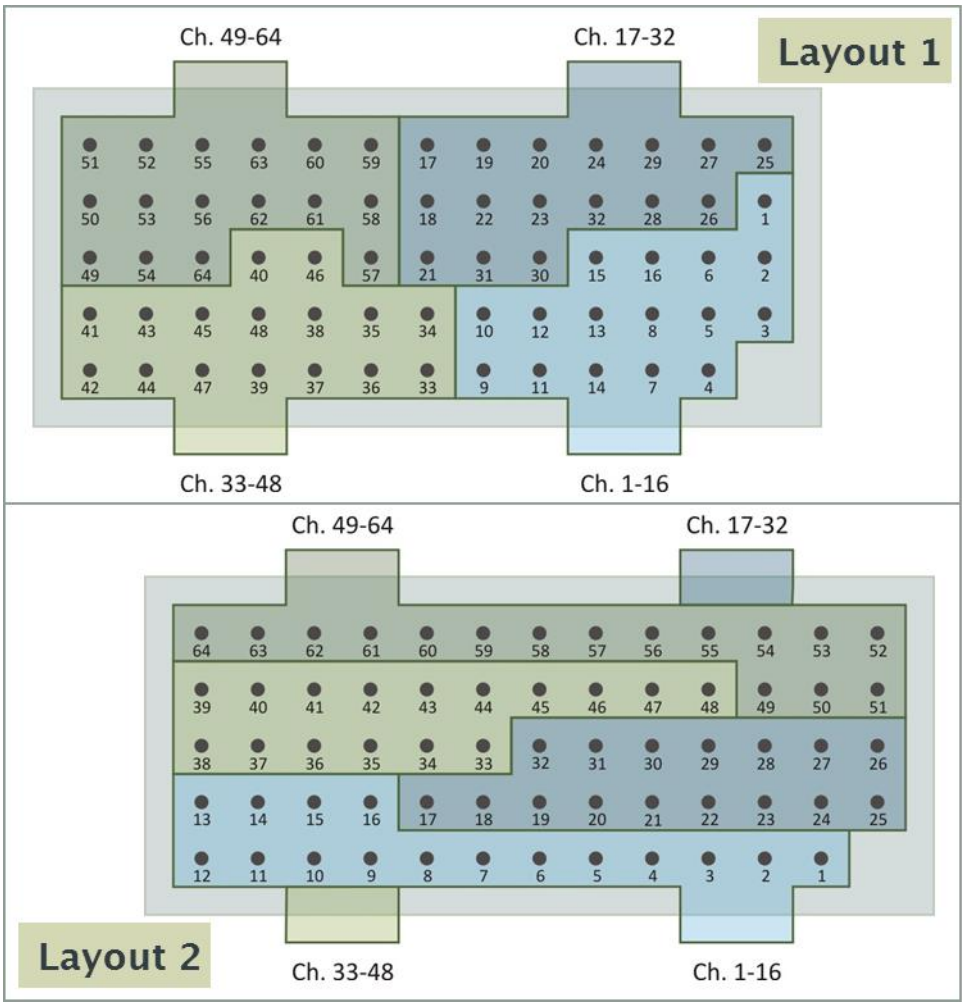

Figure 48. Layout of the 64-electrode matrix.

4.5.3 Multi-channel EMG amplifier

A 128 multi-channel EMG amplifier was used (Figure 18), this had not been configured for the particular requirements of the research experiment or the electrodes chosen; the hardware set-up could not be configured for the four 16-electrode array and the 64-electrode matrix (Figure 16, Figure 48 and Figure 49). The hardware configuration of the amplifier allowed for single differential techniques to be enabled for some electrode options; however, the electrode configuration chosen did not allow this. Therefore, monopolar data collection was the option chosen as post data capture analysis could then be undertaken where single or double differential analysis would be possible.

Neither the 64-channel matrix nor the 16-channel array electrodes had previously been used to investigate the sEMG signal from lumbar spine muscles. The matrix was not specifically developed for investigating the

Multifidus muscle and had previously been use in studying Trapezius, Biceps Brachii, Vastus Lateralis, Abductor Minimi Digiti and Abductor Policis Longus (Falla and Farina 2008; Holobar & Zazula 2007; Holobar, Farina, Gazzoni, Merletti, & Zazula 2009). However, it was considered appropriate for this experiment (Merletti 2008) and approved by ISVR ethics and safety committee.

In order to determine the end point of the test and to provide consistent feedback to the participants, a visual feedback system was developed utilising previously tested equipment (Figure 55). In previous studies (Biering-Sorensen 1984b; Latimer et al. 1999) defining the end point of the test had been problematic and not well described in the literature. In the original test, the end point of the test was determined by the operator as the point at which the unsupported upper part of the body fell -10° from the horizontal; at this point the time to task failure is determined. This precise point is difficult to determine in practice and so this aspect was automated by using an electrogoniometer and biofeedback system which provided visual feedback to the participant and recorded the point in time when the trunk fell -10° below the horizontal starting position. This also allowed the time to task failure to be determined once the test had been completed (Figure 82).

4.5.4 Method of acquisition and processing the sEMG signal.

4.5.4.1 Isometric lumbar extensor testing: Biering-Sørensen test

The Biering-Sorenson test has already been described (2.4.10) and was performed with the following requirements as previously recommended (Biering-Sorensen 1984a; Biering-Sorensen 1984b). The participant was constrained on the couch with three straps, a pillow supported the ankles, the anterior superior iliac spines were positioned level with the edge of the end of the couch, the arms were held crossed across the body and the cervical spine was maintained in a neutral position throughout the test procedure (Figure 53). The participant rested their upper body on a stool prior to the test procedure commencing, this was removed at the start of the test in order to maintain the spine in a position as close to horizontal as possible. The test end point was deemed to be when the participant was no longer able to sustain the test position within -10° of the horizontal. Participants were not verbally

encouraged to maintain the test position once the test had started. This was to ensure consistency in external factors that affect performance.

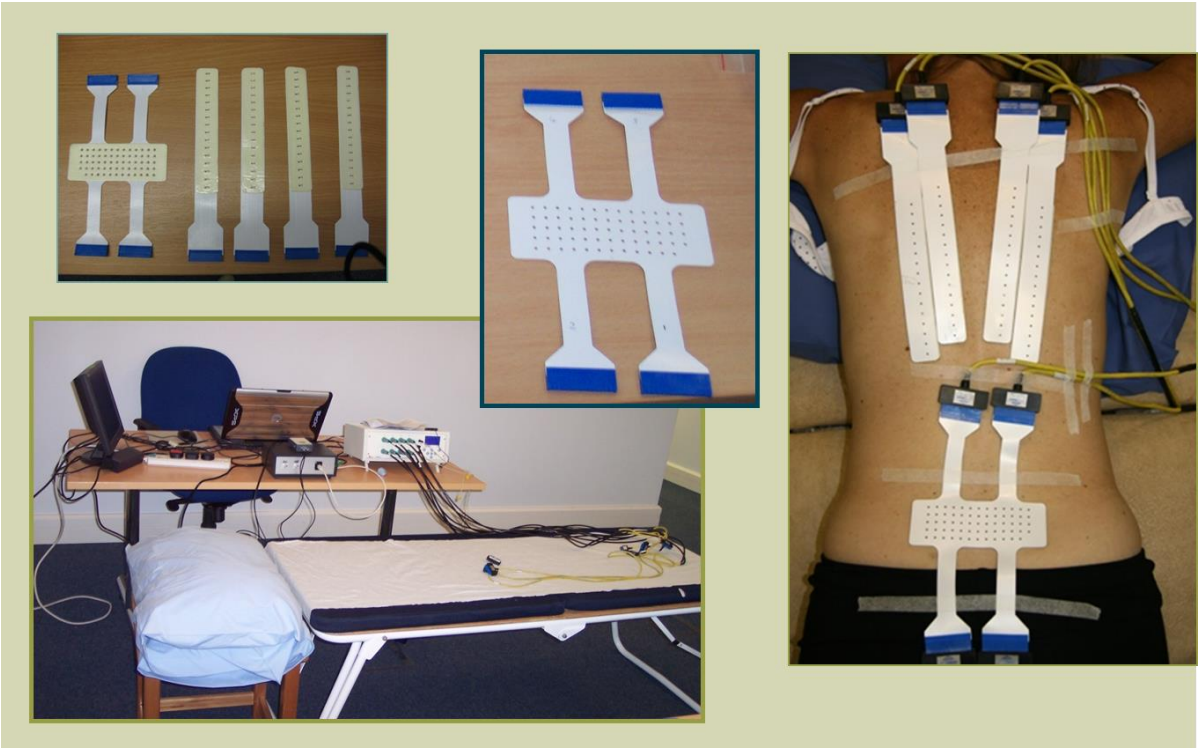

Figure 49. Experimental setup for Longissimus and Multifidus – electrode arrays and matrix.

In Figure 49 the electrodes used, the location on the participant and the proximity of the sEMG amplifier is shown.

Four 16 sensor arrays (inter-electrode distance 10mm) and a 64 sensor matrix (inter-electrode distance 8mm) were prepared by attaching adhesive pads which were pre-cut to create cells under each EMG electrode (LISiN Bioengineering Centre, Polytechnic of Turin, Department of Electronics). Having prepared the skin using SENIAM guidelines, arrays and matrix were attached to the lumbar and thoracic region using predetermined landmarks based on previous anatomical studies.

Electronic pipettes (Eppendorf Research® plus, adjustable volume) were used to fill each of the cells with a predetermined volume of 50µL electrode conducting gel to ensure correct conductivity once the sensors were firmly attached (Figure 50 and Figure 51).

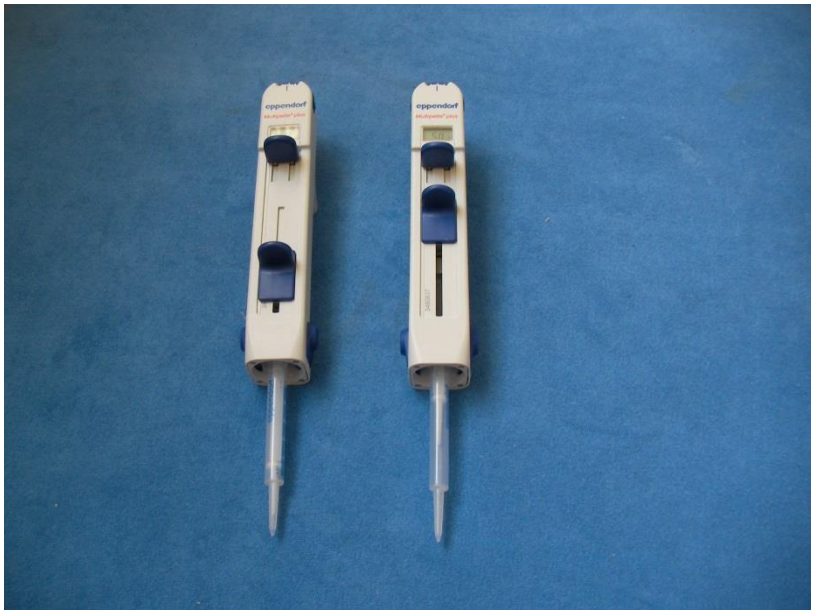

Figure 50. Electronic pipettes.

Figure 51. 50µL electrode gel per cell once matrix removed.

A bi-axial electrogoniometer (Figure 52 and Figure 55) was attached with double-sided tape; one component over the sacrum which was assumed to be stable and the other end over the junction of the thoracolumbar region. Feedback was given to the participant via a bi-axial goniometer system (Penny + Giles™; Biometrics Ltd, Gwent, UK) that provided input to a computer monitor (Figure 52, Figure 53 and Figure 55). The analogue signal from the goniometer was isolated via an optical output isolation unit and then digitised with a 12-bit analogue-to-digital (A/D) converter before providing an output for a bespoke Matlab programme that provided a 'cross hair' moving within a target for the participant. No verbal encouragement was given during the test; the instruction was to maintain the position as long as possible while keeping the cross hairs within the target. Time to completion was recorded, as was tracking data from the biofeedback system. Figure 52 illustrates the basic schema for acquiring the fatigue data using the 128-multi-channel sEMG system.

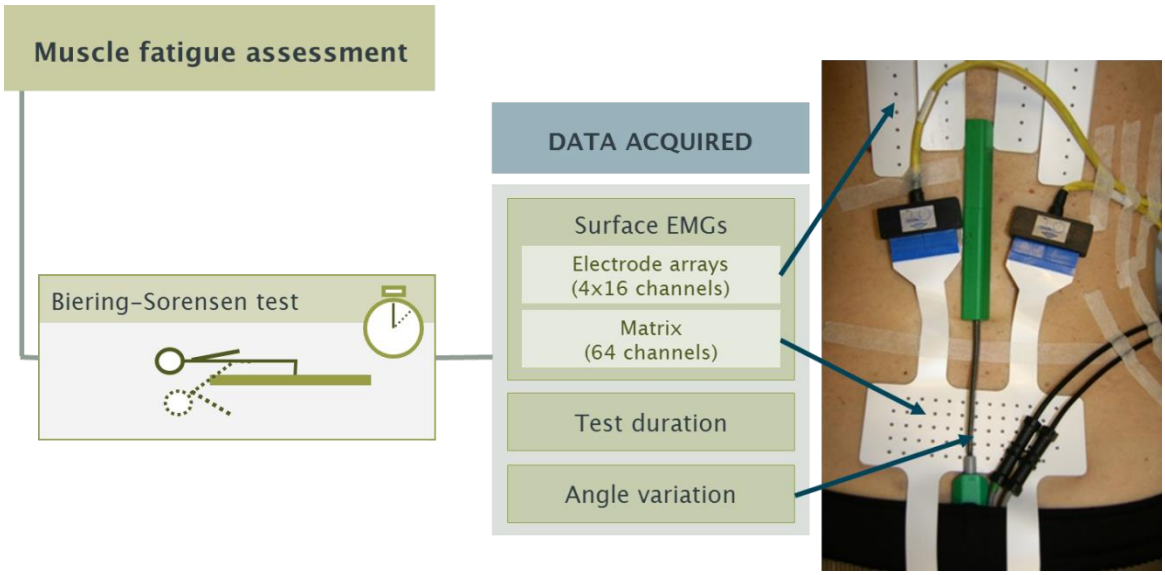

Figure 52. Schema to demonstrate experimental procedure.

The schema (Figure 52) illustrates the experimental procedure. The Biering-Sørensen test is timed and data were collected from the muslces as illustrated. The electrogoniometer is seen attached at the sacrum and at the thoroco-lumbar junction.

Once electrodes had been attached it was possible, using the acquisition software provided with the sEMG amplifier, to visualise in real time the sEMG signal. This enabled each of the 128 channels to be checked for continuity and

adjustments made as required to the adhesion of the electrodes or to the amount of conduction gel in each cell. The participant undertook a series of dorsal raises in order to activate the erector spinae (ES) muscle group.

At this point, the feedback system was returned to a value of zero, this pre-set the values used as the 'neutral' position of the spine.

Data collection then commenced; the supporting stool was removed and the participant instructed to maintain the horizontal postion for as long as possible using a standard form of words.

Figure 53. Biering-Sørensen test used in experiment.

In Figure 53, a participant can be seen undertaking the Biering-Sørensen test while data are being collected. The feedback system, whereby the participant is receiving visual feedback of whether they are maintaining the horizontal position, can also be seen in the left hand image. This system provided visual information displayed onto a monitor that provided information in the x and y axis of any deviation from a neutral position that had been pre-set during the experimental set-up (Figure 54).

Figure 54. Monitor for positional feedback.

Participants attempted to maintain a horizontal position by keeping the cross hairs on the target for as long as possible. The test end point (time to task failure) occured once the participant was no longer able to maintain the starting positon and dropped −10° below the horizontal.

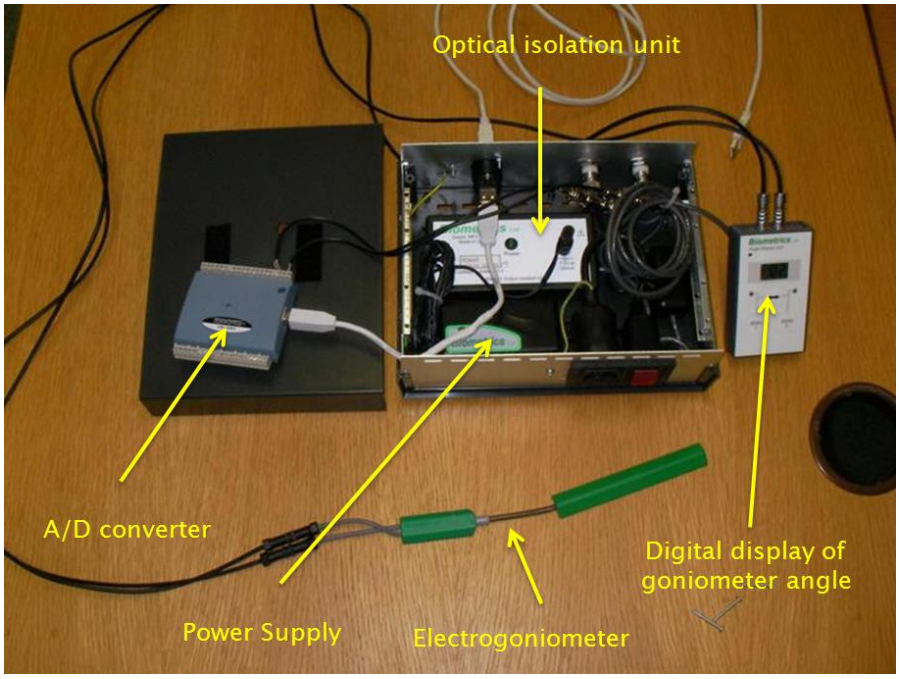

Figure 55. Electrogoniometer and participant isolation unit.

Figure 55 illustrates the system for collecting position date; the electrogoniometer can be seen at the bottom of the picture. The analogue signal is isolated via an optical isolation unit from the power supply. The 12-bit A/D converter digitises the signal. A Matlab programme enabled the cross hairs to be zeroed and a data recording made of the x and y axes of motion.

4.5.5 Data processing

4.5.5.1 Surface EMG analysis

The parameters of interest at this stage in the study were running rms value and MDF. These parameters were selected to determine if useful sEMG data, that was relevant to fatigue studies, could be collected. The rms was calculated from the consecutive 1s time windows of the sEMG signals. MDF is defined as the frequency that divides the frequency spectrum into two equal areas. This was calculated from 1s non-overlapped time windows using a fast Fourier transform algorithm (in Matlab) that was used to calculate the power spectrum. MDF values were calculated and displayed as a mean shift in the overall MDF together with changes in rms values over the entire test.

However, this level of signal analysis did not provide useful data analysis for a number of reasons;

1. The raw signal data file was not separated into data specifically from each of the electrode arrays or the matrix.
2. The raw signal was not band-pass filtered in the range that was useful for analysis and which would have reduced cable motion artefacts. In the low frequency range above 10Hz, a high-pass filter would be useful and a low-pass filter that could be set at 250Hz. This would result in a data set from a range within which most of the power of the sEMG is located.
3. No notch filtering was applied that would reduce power line noise. This resulted in a noisy signal from which it was not possible to determine if suitable data capture had occurred.
4. It was not possible to separate out, from 128 channels of data, those that specifically originated from the array or matrix electrodes. This

meant that it would not be possible to separately analyse or compare data from the separate muscles under investigation.

5. It was problematic to view, post data collection, the raw signal to determine if a successful collection of data had taken place. The acquisition software did not provide sufficient resolution of the data.
6. Frequently, post data capture, it was evident that one or more channels had either not collected any data or that there was a significant amount of noise. In these cases, it would be necessary to remove these channels before any overall analysis was undertaken as this data would contaminate or skew any analysis.

To overcome the above problems specific software was developed in order that the following data analysis could be undertaken (Figure 56);

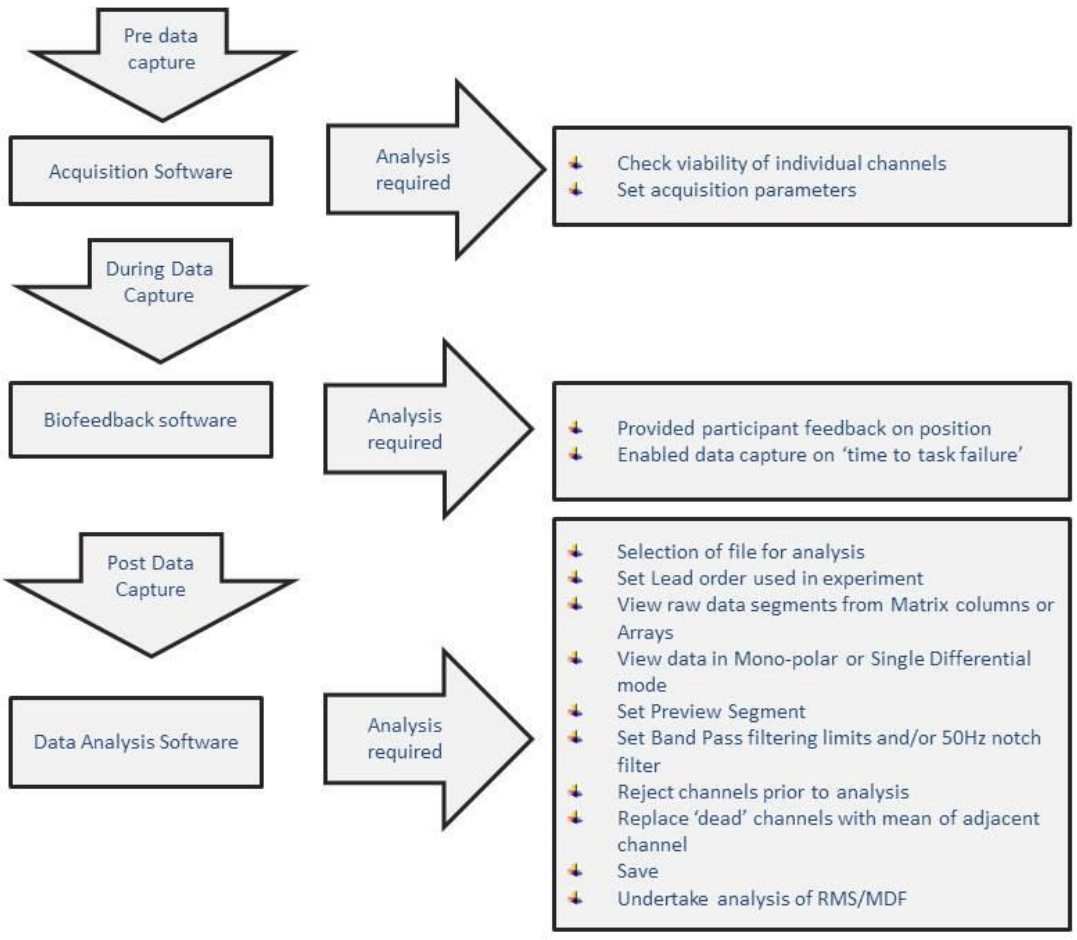

Figure 56. Flow chart of data analysis.

4.5.5.2 Development of software and graphical user interface

In order to undertake the necessary analysis, Data Analysis Software and Graphical User Interfaces (GUIs) were developed in Matlab by the Institute of Sound and Vibration (ISVR) Research Fellow under the direction of the researcher. The applications were tested and developed as part of the development of the methodology. A description follows of the various stages in data analysis.

4.5.5.2.1 Data manipulation post data capture.

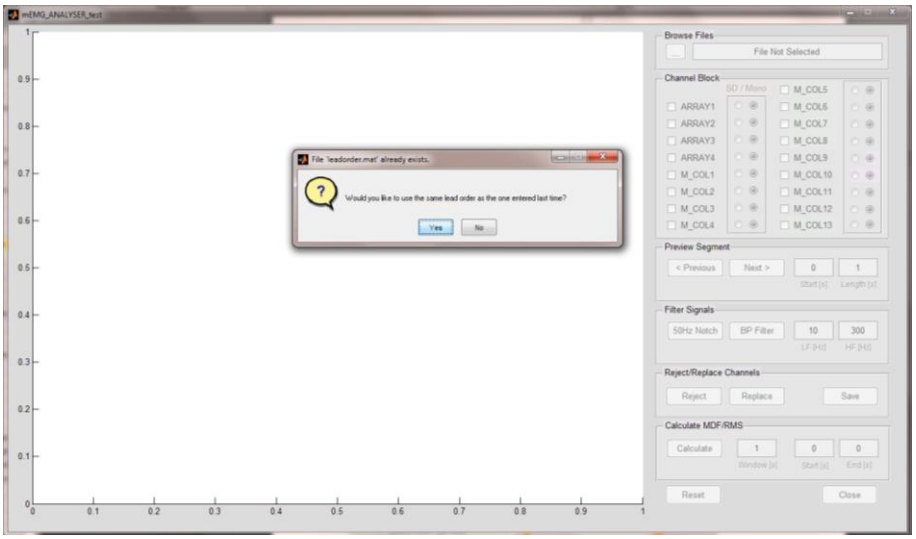

Figure 57. Option to set lead order.

When the application is first opened (Figure 57 and Figure 58), the option to select the recording lead order used in the experimental set up is offered. As part of the experimental protocol, the lead order was set (i.e. leads 1 – 4 were attached to the matrix and leads 5 – 8 to the arrays in a specified order), however, if this was not the case then the pre-set order could be changed (Figure 58). The option to select the 'old' or the 'new' matrix set up is also offered and would be selected based on which matrix electrode had been used.

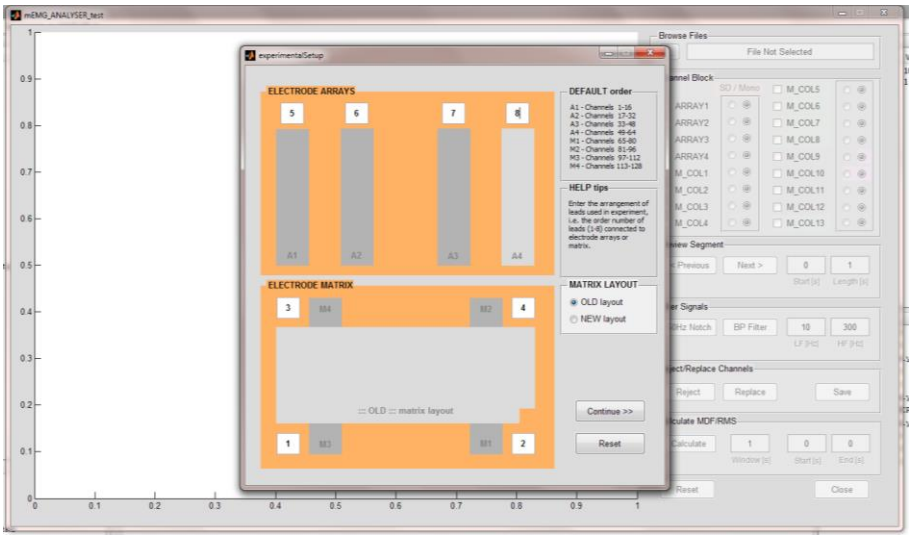

Figure 58. Setting lead order.

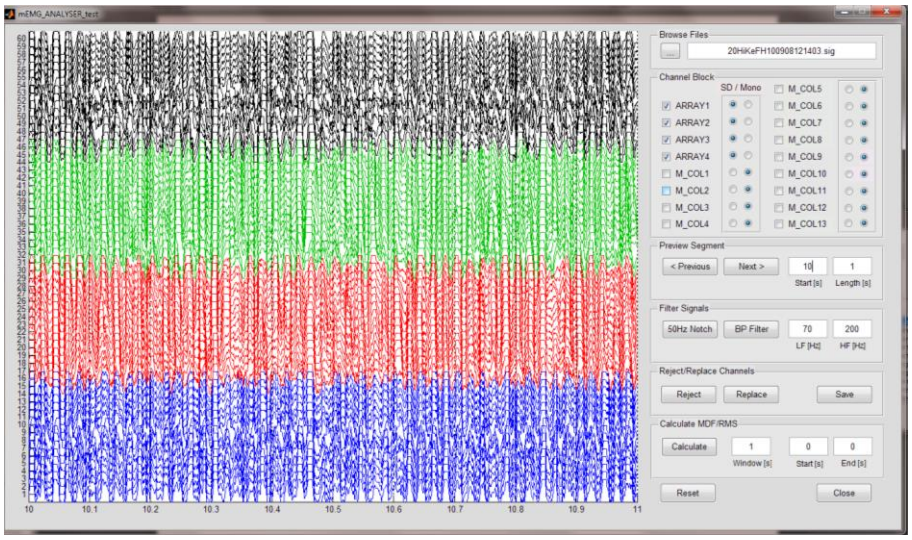

Figure 59. Raw data file opened showing array data.

Once the data file is opened, the required channels can be viewed. In Figure 59 the raw data from the four arrays is visible in single differential mode. One second of data can be seen from the 10th second from the start of the data file; the Preview Segment option allows any segment of data to be viewed. In Figure 59, the data requires some pre-processing before analysis is undertaken.

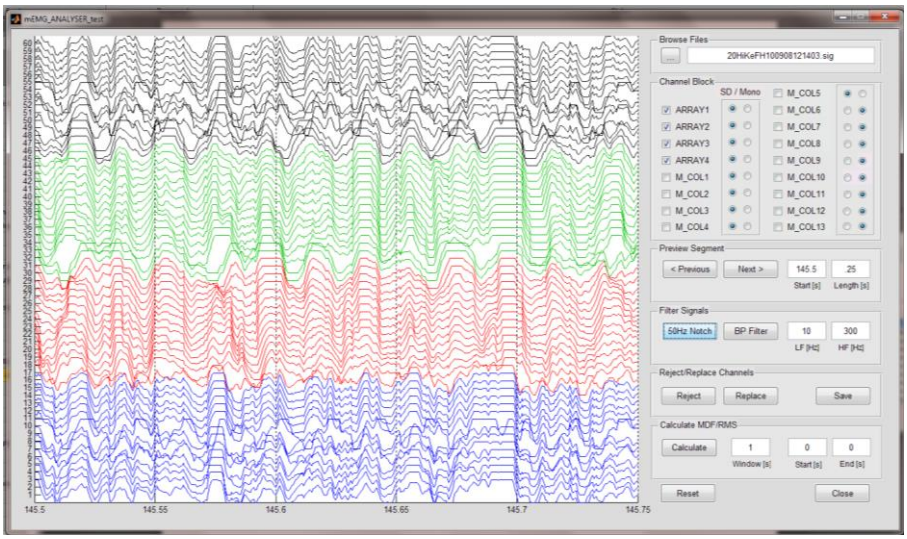

Figure 60. Segment of data prior to smoothing.

Figure 60 illustrates the effect of reducing the Preview Segment size to 0.25s, no filters have been applied. The effect of the 50Hz Notch filter can be seen in Figure 61 and the effect of the Band-pass filter in Figure 62 which provides considerable smoothing. It becomes possible to view the individual motor unit action potentials (MUAPs).

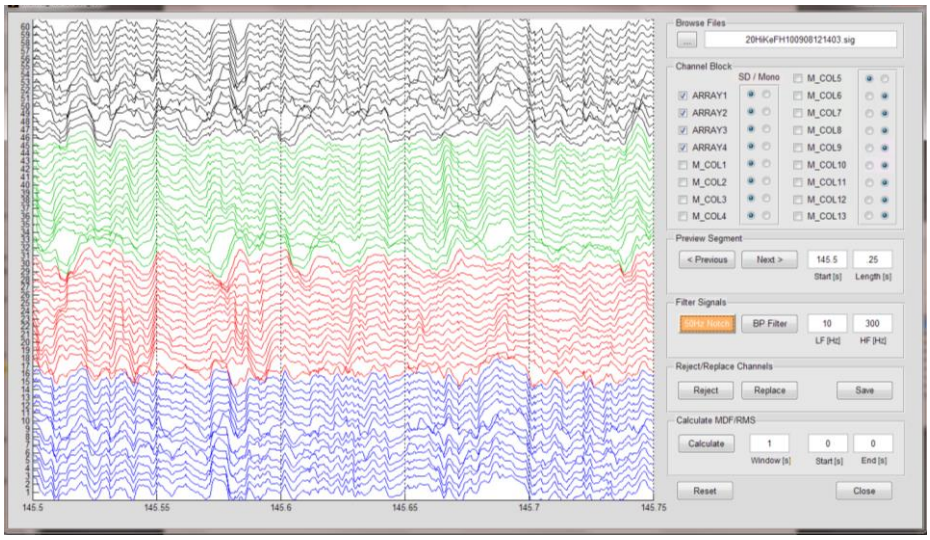

Figure 61. Effect of 50Hz notch filter.

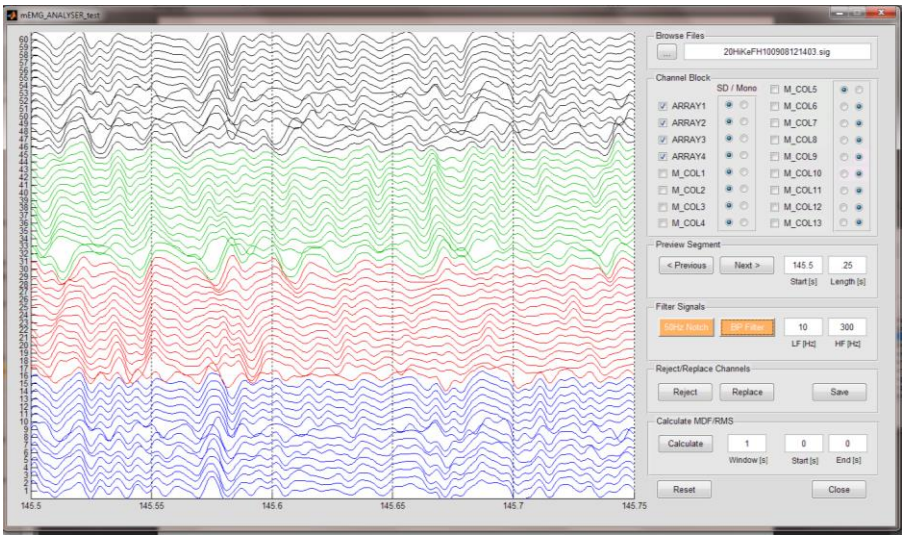

Figure 62. Effect of 10- 300Hz band-pass filter.

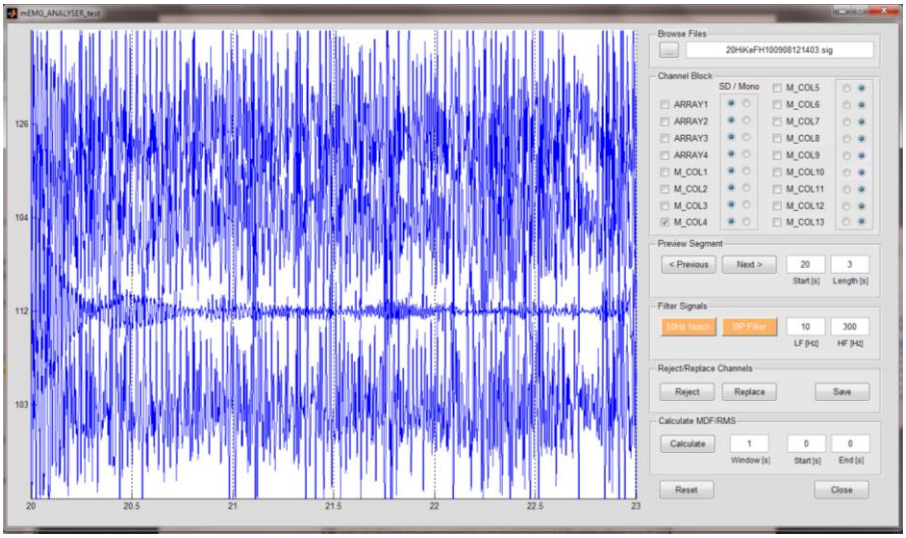

Figure 63. Viewing rogue channels.

In Figure 63, three seconds of data are shown from 20 seconds into the recording from one column (column 4) of the matrix electrode. A rogue channel is seen and reducing the Preview Segment size to 1s allows channel 112 to be identified as the rogue channel (Figure 64).

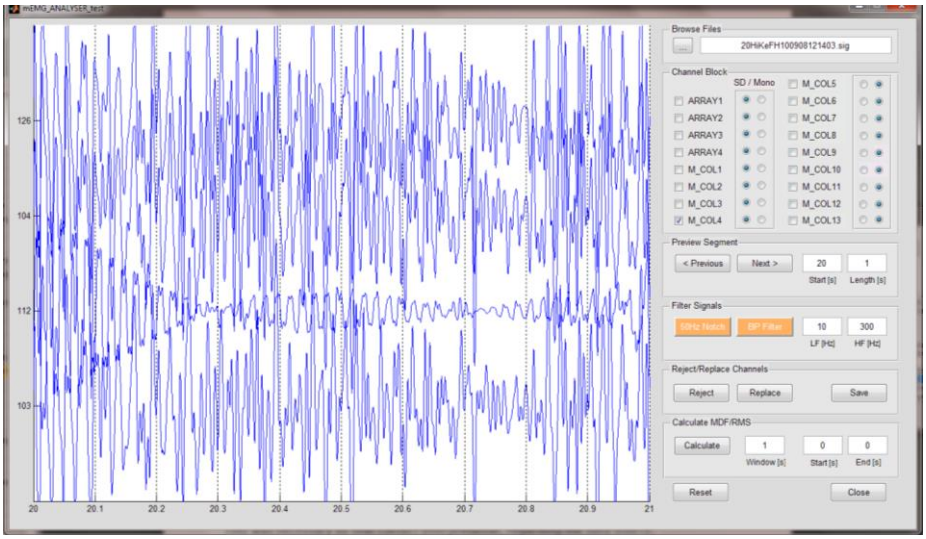

Figure 64. Identification of rogue channel.

Selecting the Replace Channel option (Figure 65) allows this channel to be replaced for analysis purposes with the mean MDF/rms values of adjacent channels.

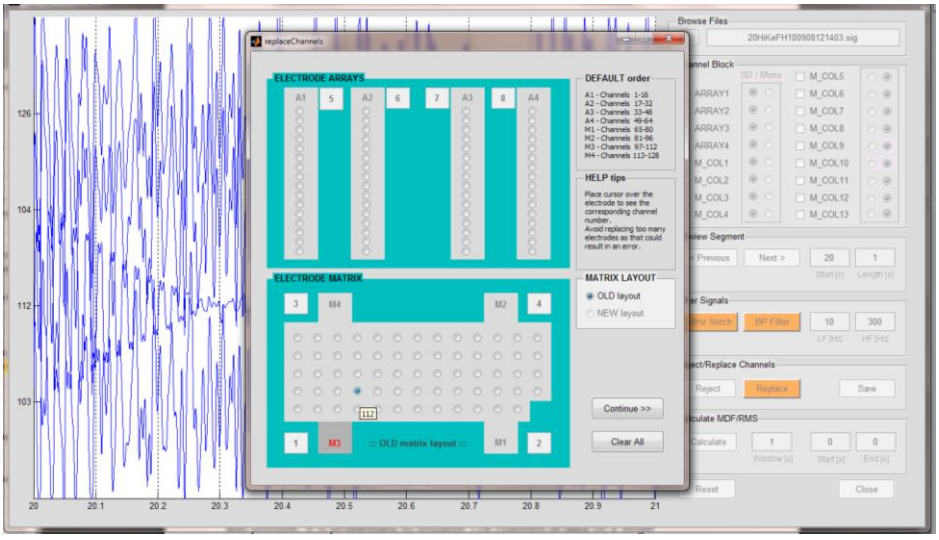

Figure 65. Replacing rogue channel.

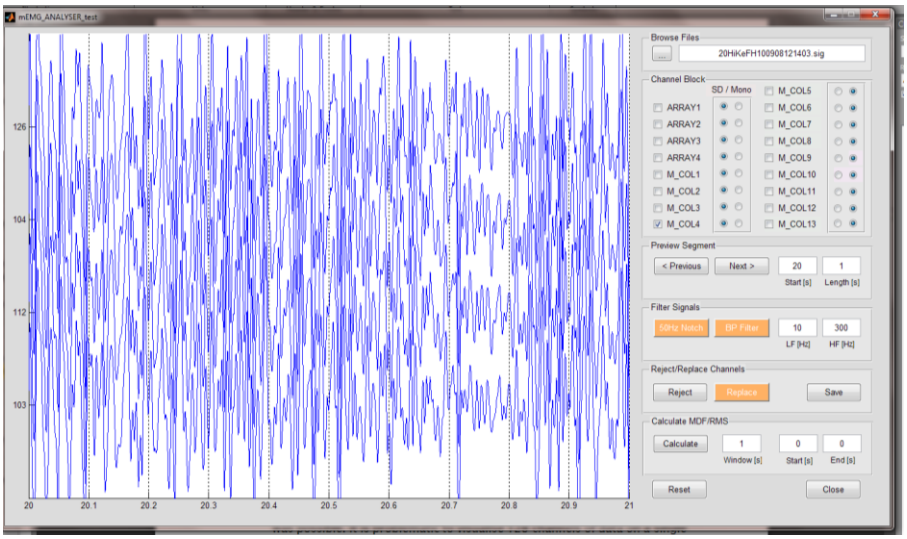

Figure 66. Post replacement of rogue channel.

Comparing Figure 64 with Figure 66, the effect of removing the rogue channel can be seen. This new file would be saved before any data analysis was undertaken using the Save opinion.

4.5.6 Procedure for data analysis

The next step would be to analyse the new data set (Figure 67). In the Calculate MDF/rms options it is possible to set the length of the window for data analysis and to set the time (in seconds) from the start of the file and from the end of the file. This function allows the beginning and end of any data set to be disregarded in the analysis, if for instance, during an experiment, there was a period before and/or after the test started/finished where no sEMG data were collected.

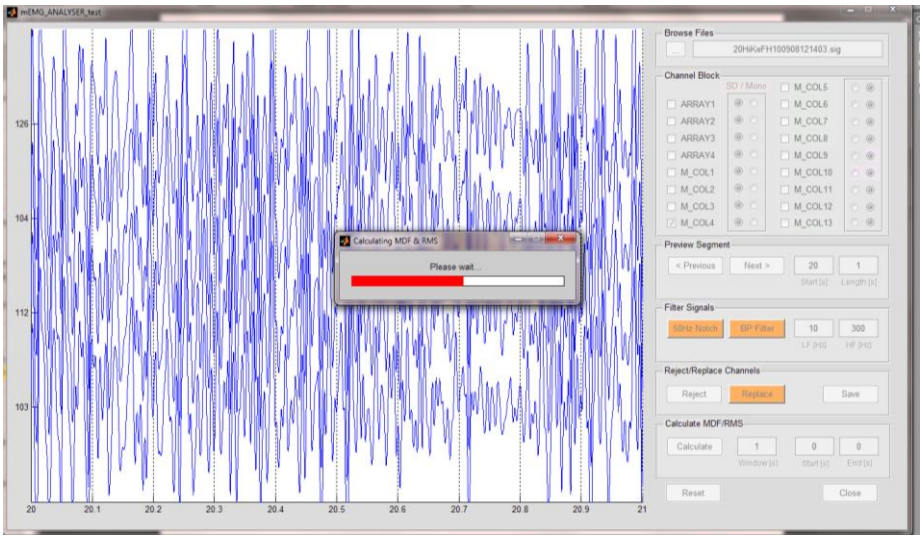

Figure 67. Running data analysis.

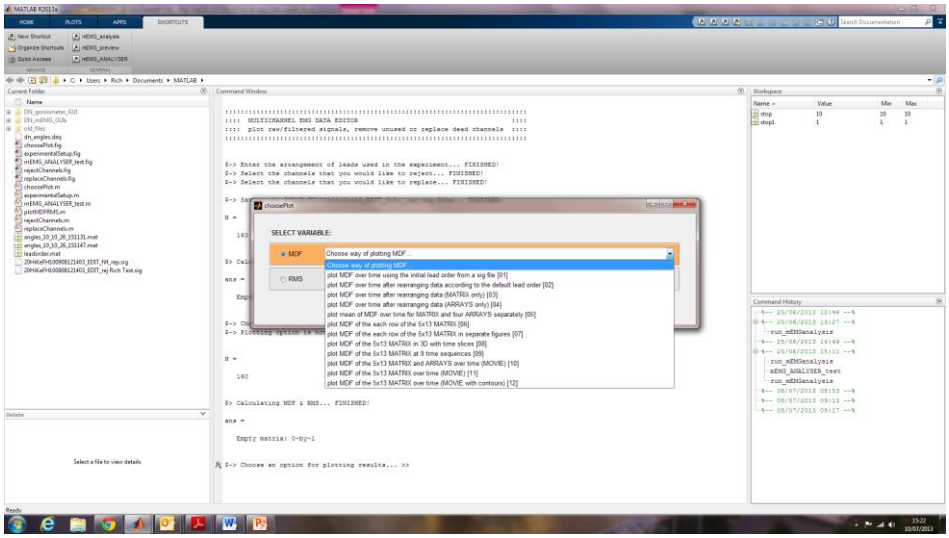

Figure 68. Choosing plotting options.

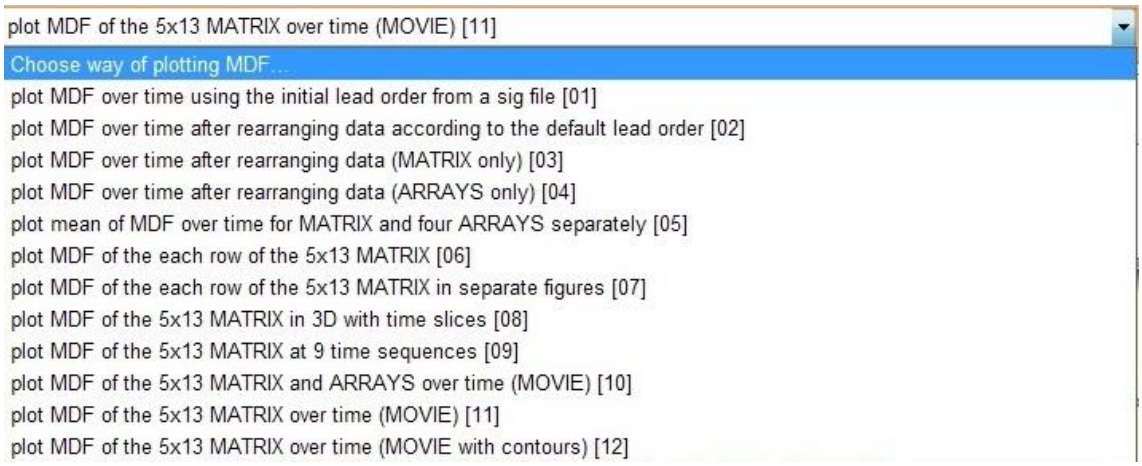

Figure 69. MDF plotting options.

The plotting options can be selected from a drop down list (Figure 68 and Figure 69) and were chosen to best illustrate the parameters of interest (only MDF options show, rms options similar). For each data point (each electrode) power spectral densities of the measured EMG signals were estimated and averaged using Welch's method (Welch 1967) with a window FFT size of 512 samples and 50% overlap. The mean MDF and rms values were then calculated for each array and matrix; this was a convenient method for displaying the overall changes that occurred during the experiment.

In Figure 70, the changes in mean of MDF over time are plotted for each array and the matrix separately. It can be seen that all measures shift over time to lower mean frequencies which would be consistent with myoelectric manifestation of fatigue (Merletti and Lo Conte 1995; Merletti and Roy 1996). It can also be seen that there is a rise in the MDF value from 0s to 5s into the plot and from 150s to the end of the plot. This represents the start and end of the test where the participant was not performing the fatigue test. This would be removed from the analysis using the option when calculating the mean MDF and would result in a plot that does not involve these sections of data (Figure 71).

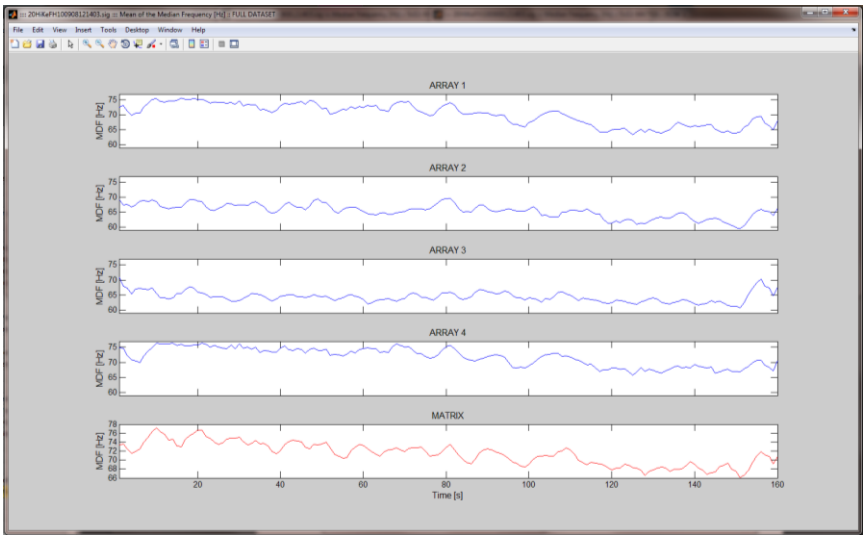

Figure 70. Plotting changes in mean of MDF for arrays and matrix separately.

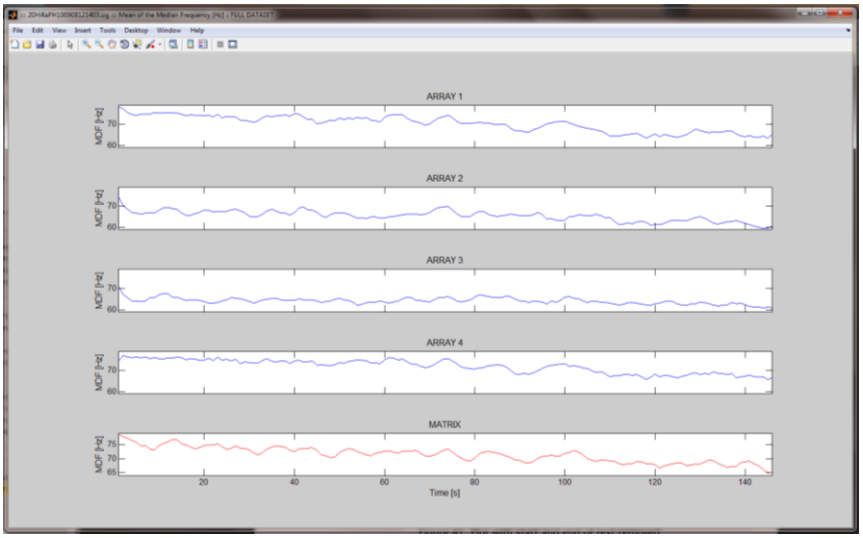

Figure 71. Plot with start and end of test removed.

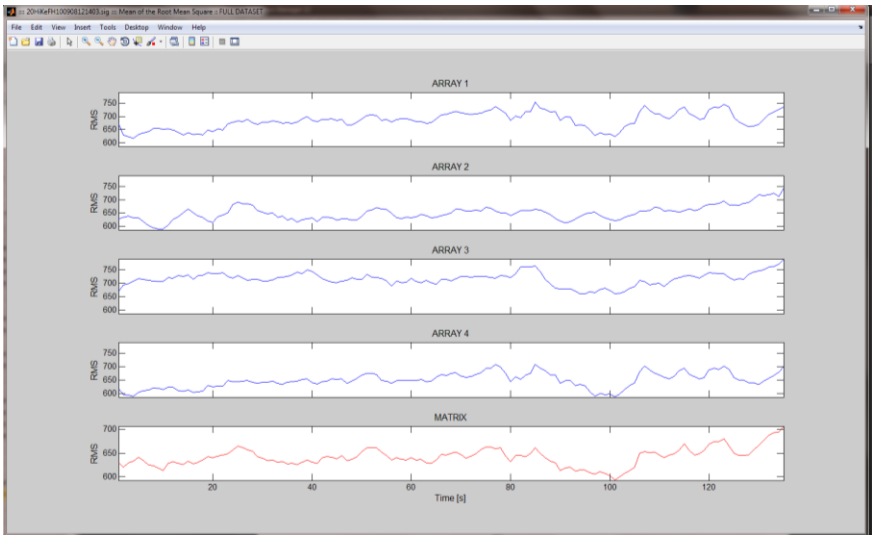

Figure 72. The rms values over time.

The rms values can be similarly plotted over time (Figure 72). These can be seen to rise and this finding is consistent with the myoelectric manifestation of fatigue (Section 2.4.2).

4.5.6.1.1 Rejecting Channels

Having undertaken experiments which followed the development of this methodology (Sections 5, 6 and 7) it was concluded that there would be the need to omit channels from any analysis where the size and location of the muscle of interest was smaller than the size of the electrode (Figure 73). In this case, it would be necessary to remove channels at the start of the data analysis based upon new information regarding the location of muscles. This is reported in Sections 5, 6 and 7.

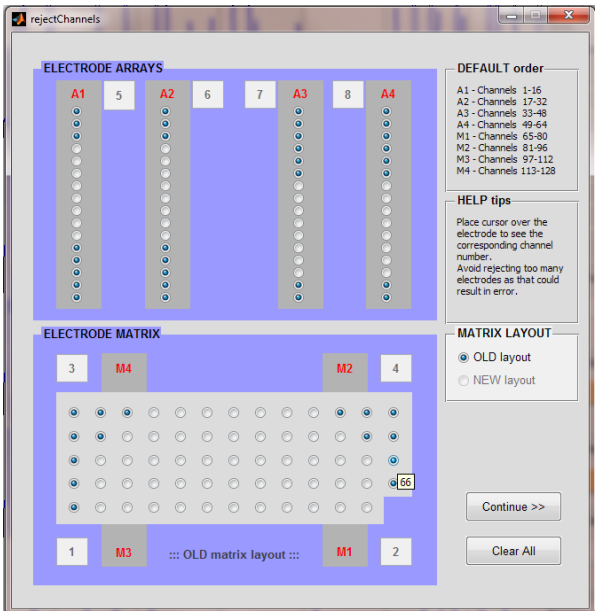

Figure 73. Rejecting channels for analysis.

Figure 73 illustrates the process of removing channels based on new information that was not available at the time of the experimental procedures described in this section. Checking the radio buttons selects channels that are rejected in the analysis.

4.6 Participants

A convenience sample of six individuals participated in the development of the methodology and data were collected and analysed for each. The population consisted of 4 female and 2 male participants (*M*=24.2, *SD* 16.4).

4.7 Results

In many of the experiments, data were contaminated by movement artefacts. No usable sEMG data were collected from the Ito or McIntosh test; the test requires the participant to extend their lumbar and thoracic spine, this caused both the matrix electrode and often the array electrodes to detach from the skin over the lumbar region. Holding times were recorded, (See Appendix 4.7.1); each test was stopped if the participant could hold for more than 240 seconds as per the original Biering-Sørensen protocol. Summary data are presented in Appendix 14.3 of the sEMG analysis from this phase.

4.7.1 Holding times for each participant

The time to task failure (holding time) is shown in Table 14. Some participants attended on more than one occasion. Results indicated that female participants had a longer mean holding time than males.

Table 14. Mean time to task failure.

	Mean time to task failure (mean of 3 tests) Biering-Sørensen Test						
	Participant No.	1 (f)	2(m)	3(m)	4(f)	5(f)	6(f)
Test No.	Mean time to task failure (seconds)						
1		**240 (test ended)**	**121**	**178**	**196**	**204**	**211**
2		**232**	**142**	**102**		**222**	**197**
3		**224**		**146**			**202**
	Mean holding times by gender (seconds) f = 214 m= 137						

	Mean time to task failure (mean of 3 tests) Ito Test						
	Participant No.	1 (f)	2(m)	3(m)	4(f)	5(f)	6(f)
Test No.	Mean time to task failure (seconds)	**240 (test ended)**	**220**	**217**	**240 (test ended)**	**189**	**240 (test ended)**
1							
	Mean holding times by gender (seconds) f = 227 m= 218						

	Mean time to task failure (mean of 3 tests) McIntosh Test						
	Participant No.	1 (f)	2(m)	3(m)	4(f)	5(f)	6(f)
Test No.	Mean time to task failure (seconds)						
1		**220**	**189**	**240 (test ended)**	**130**	**216**	**240 (test ended)**
2		**235**					
	Mean holding times by gender (seconds) f = 208 m= 214						

4.7.2 Data collection from individual sensor locations

Surface EMG data were collected from some of the participants during this phase of the study and, where possible, analysis was undertaken as part of the process of developing the testing methodology and the GUIs. The method of data analysis is described in section 4.5.5. The mean running MDF and rms values over time were obtained for each array and the matrix separately and plotted.

It can be seen in Figure 74 (taken as examples from individual tests) that the running MDF reduces over time (the regression line in the top image of Figure 74 indicates the slope of the line); in Figure 72 the rms values increases over time, these changes are consistent with the myoelectric changes seen in muscle fatigue (Luttmann, Jager, & Laurig 2000).

At each sensor site (where data were successfully collected) it was possible to decompose the EMG signal, calculate the MDF/rms values and draw a fatigue plot (e.g. See Figure 74) of either the changes in MDF or rms over time. A decrease in MDF values and increase in rms values, consistent with manifestation of fatigue were demonstrated in all of 8 of the signals that were processed (See 14.3).

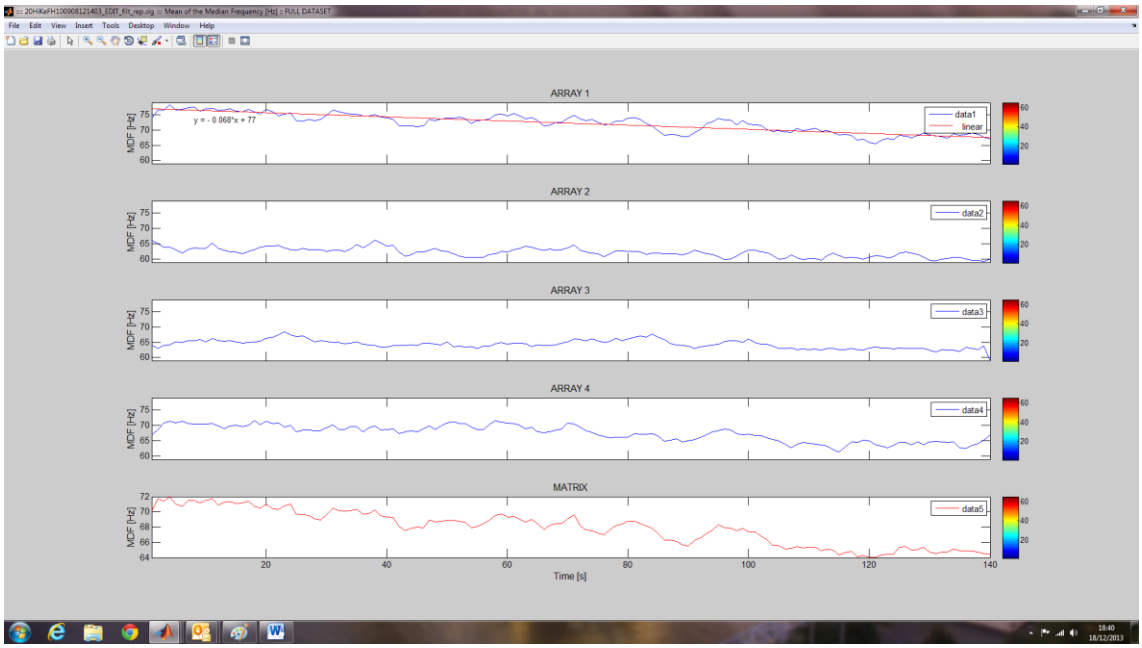

Figure 74. Fatigue plot for single points from each electrode array demonstrating shift in MDF.

4.7.3 Propagating motor unit action potentials

It became apparent, during data collection, that many of the sensors of the array electrodes were not collecting data where propagating MUAPs were evident and that a review of the location of these was necessary in order to progress the study. In Figure 75, there is evidence of a propagating MUAP in the lower part of the display (coloured blue) but in the upper part (red), there is evidence that may be consistent with end of fibre effects where the MUAP appears not to propagate and have the appearance of a standing wave. Correct location of electrodes should result in visualisation of MUAP propagation but maybe not as clearly as with limb muscles.

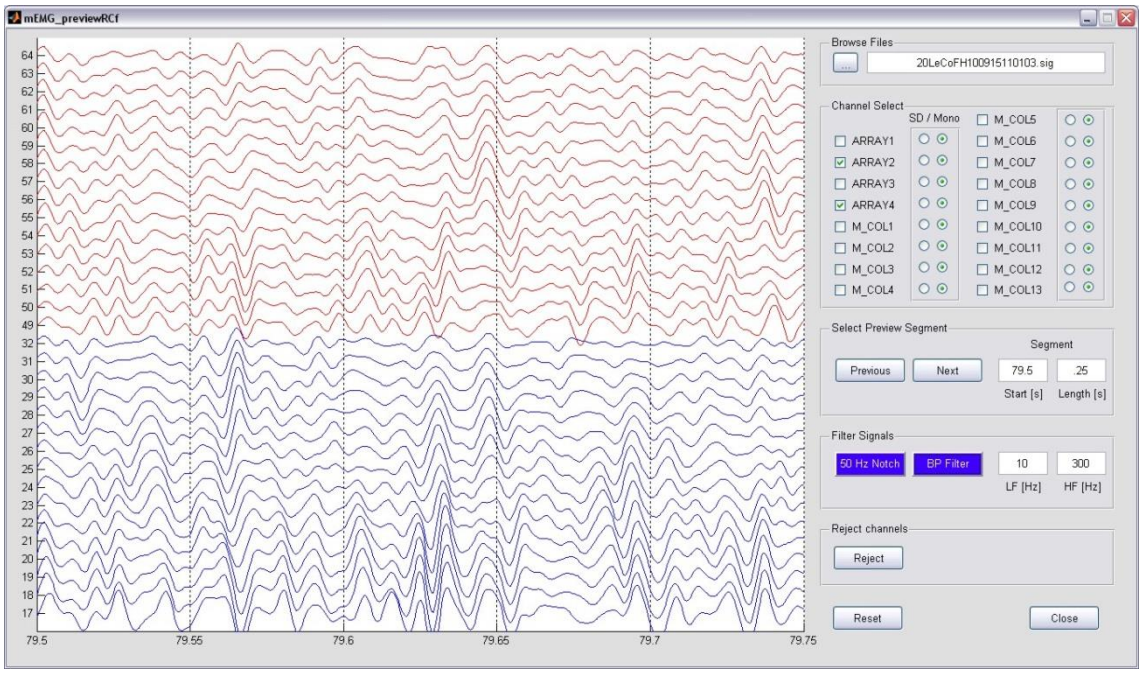

Figure 75. Visualising individual MUAPs.

4.7.4 Mean of median frequency

The following results from one participant are presented to indicate possibilities for future data analysis. The mean of the MDF was calculated for each of the array electrodes and for the matrix as a whole in Figure 76 and Figure 77.

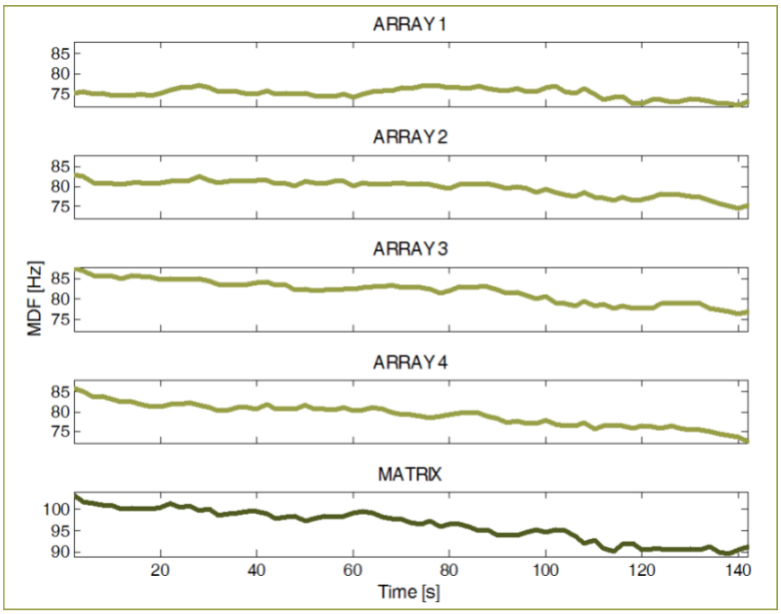

Figure 76. Mean MDF during Biering-Sørensen test.

Figure 76 illustrates the mean MDF during the Biering-Sørensen test for each of the array electrodes. The mean of the MDF can be seen for the matrix. For each of the electrodes, the mean MDF is seen to fall during the test. The mean rms values for the matrix and the arrays also demonstrate changes consistent with fatigue in that the rms value rises throughout the experiment.

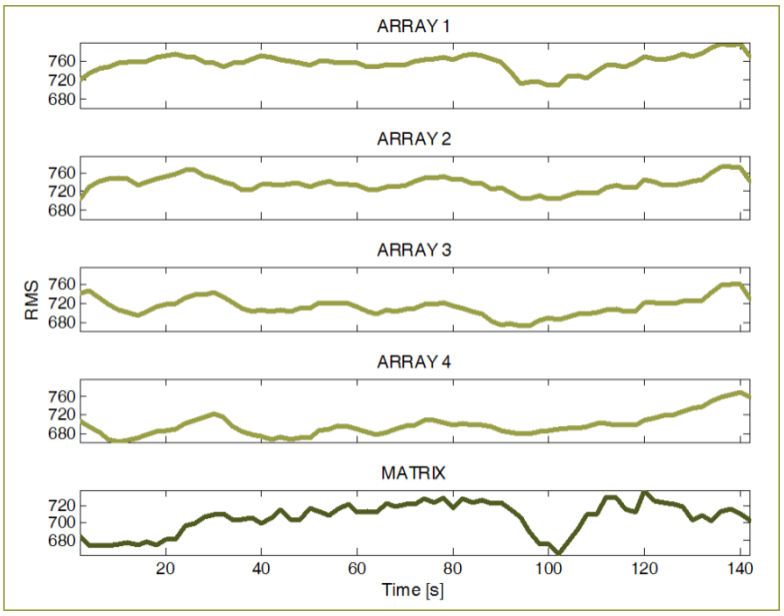

Figure 77. Mean rms during Biering-Sørensen test. The mean rms values rise during the Biering-Sørensen test.

4.7.5 Contour mapping MDF and rms

Plotting the MDF over time (Figure 79 and Figure 81) for the matrix as a contour plot, the change becomes more obvious. A change in colour from red end of the spectrum towards blue indicates a reduction in the MDF and in the contour plot which shows, in increments, the underlying architecture of the muscles becomes apparent. The centre portion of each contour map was located over or just offset of the mid-line of the lumbar spine and an approximation of the shape and angle of multifidus is apparent. MDF and rms amplitudes calculated from a 1 second non-overlapped time window of the sEMG signal; sampling frequency was 2048Hz.

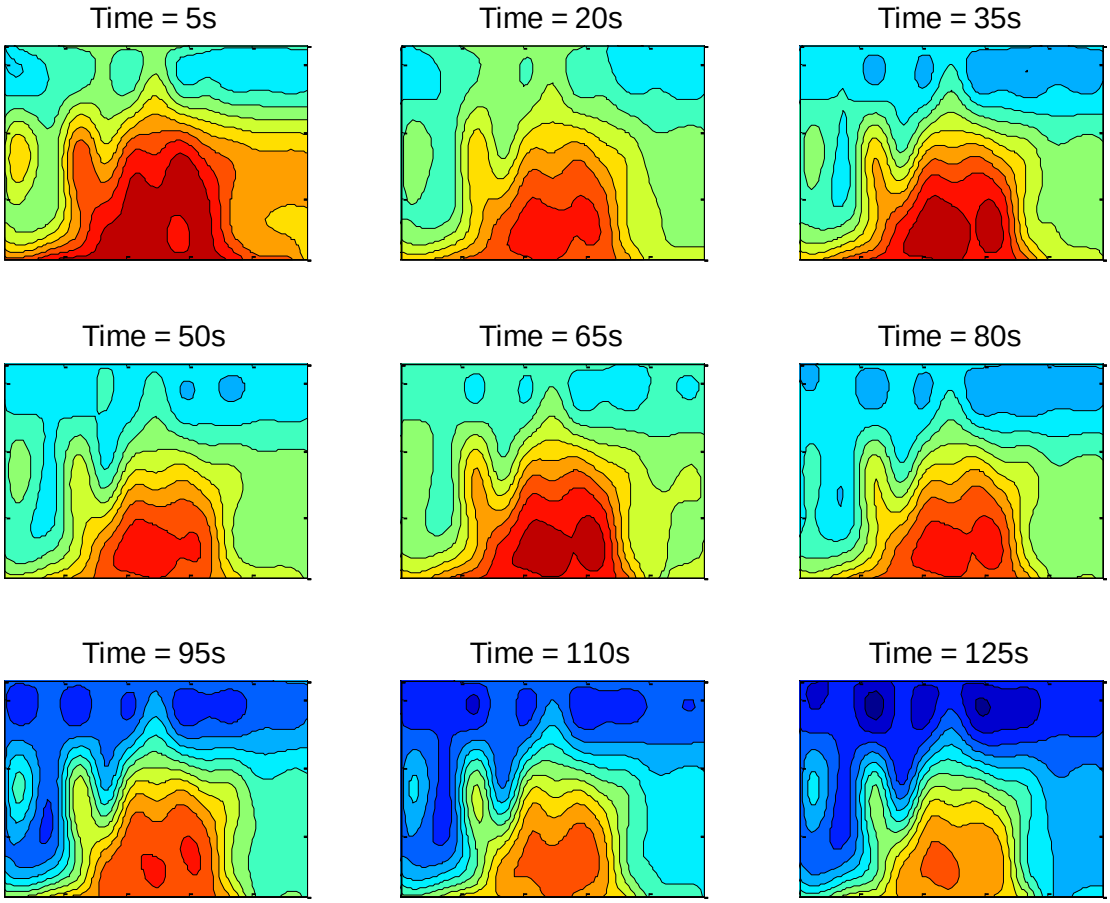

Figure 78. Contour of MDF changes during Biering-Sørensen test over time.

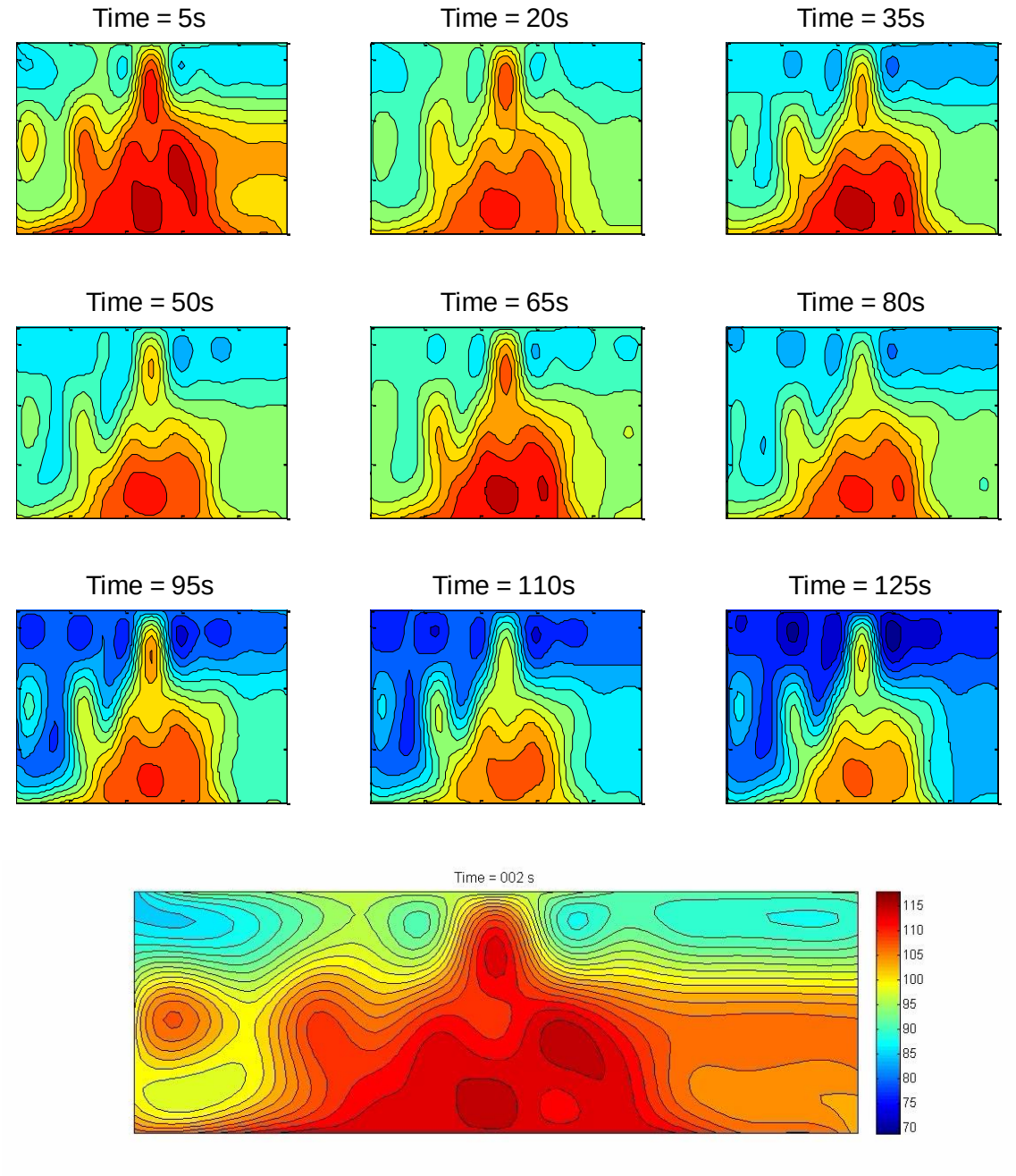

Figure 79. Contour plots of MDF changes during Biering-Sørensen test over time with movie plot screen shot.

The images in Figure 78 and Figure 79 illustrate a method for contour plotting the MDF that can be shown as a movie (see last image Figure 79 that also demonstrates scale used (Hz)). The images in Figure 78& Figure 79 demonstrate a development of the technique for contour mapping; the size of the image represents the size of the matrix array which measures 9.6 cm x 3.2 cm and covers the lower part of Multifidus. The lower edge of the image is aligned to the PSIS – PSIS line, thus the image represents part of Multifidus

from S1 and above. The extent of the image will be determined by the size of the individual.

Similar changes are also evident for rms values where the architecture can still be seen as the colour shifts from blue to red indicating an increase in the rms value.

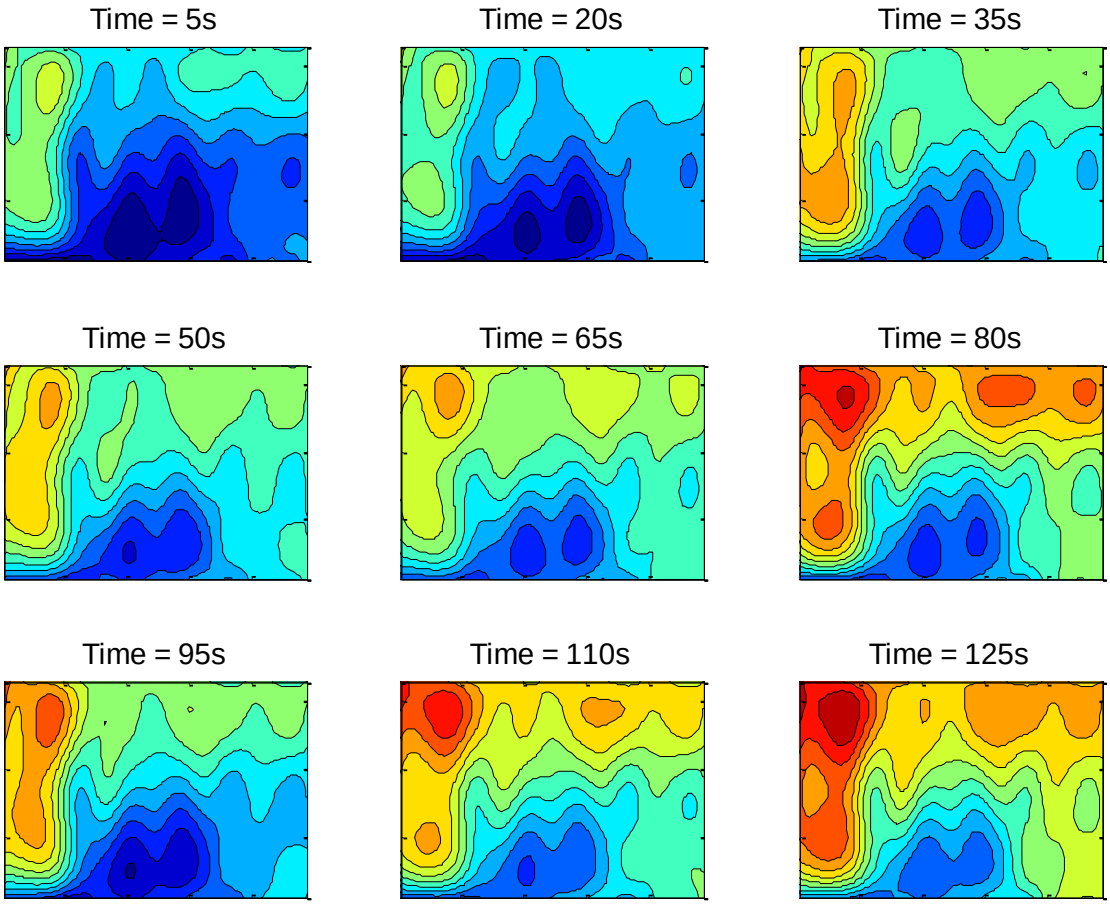

Figure 80. Contour of mean rms changes during Biering-Sørensen test over time.

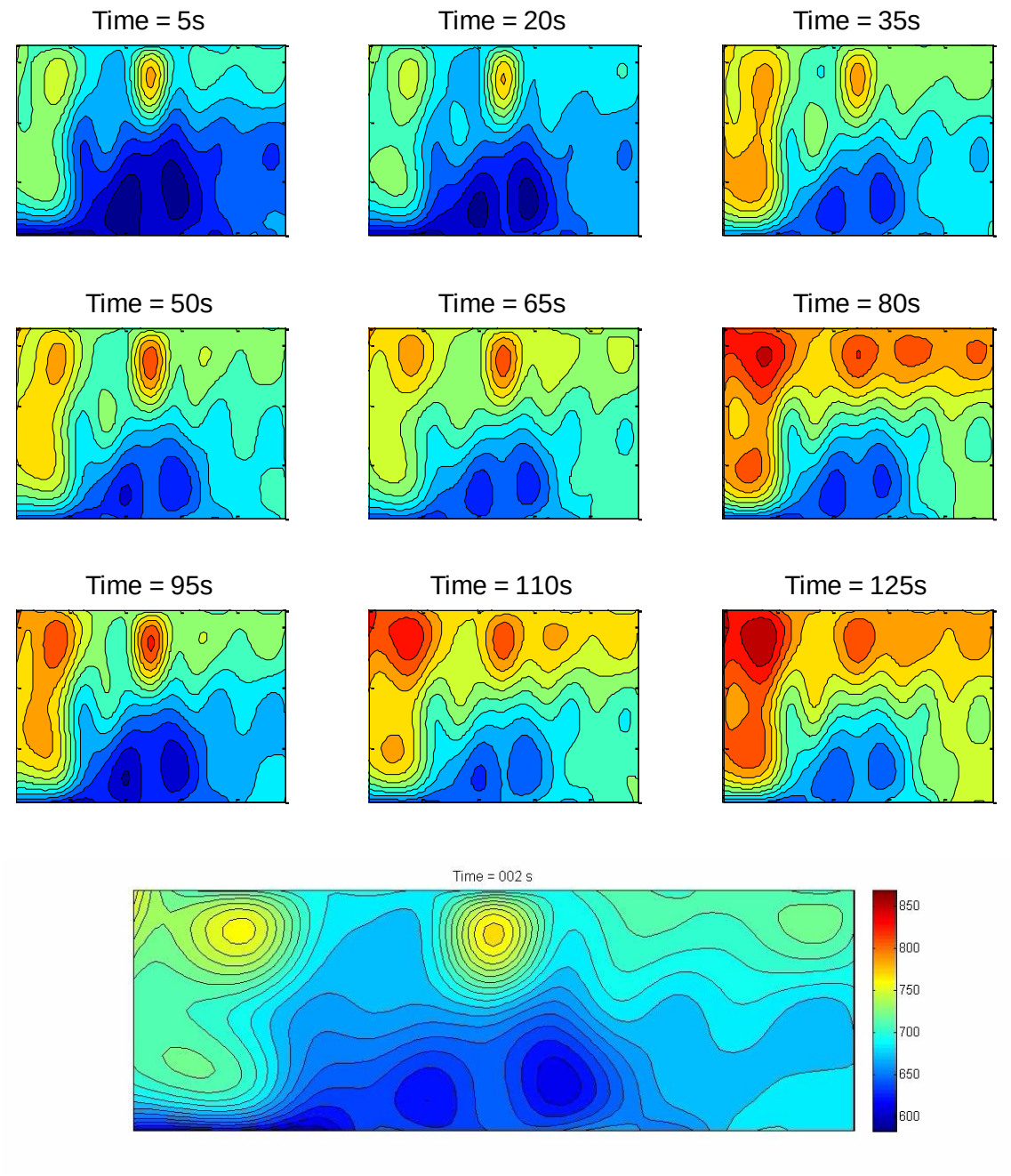

Figure 81. Contour of mean rms changes during Biering-Sørensen test over time with movie plot screen shot.

The images in Figure 80 and Figure 81 illustrate a method for contour plotting the rms values that can be shown as a movie (last image also demonstrates scale used (uV)).

4.7.6 Charting changes in tracking angle

The following figures (Figure 82, Figure 83 and Figure 84) give some indication of how the tracking angle changed during each of the different fatigue tasks. It can be seen that the point in time when the angle drops below -10° is evident from the chart. This is evident with the Biering-Sørensen and Ito test but in the case of the McIntosh test (Figure 84) the end point is almost reached at 100s into the test but then the participant recovers and completes the test. These tracking angle charts were drawn from data collected in the development of the tracking angle software.

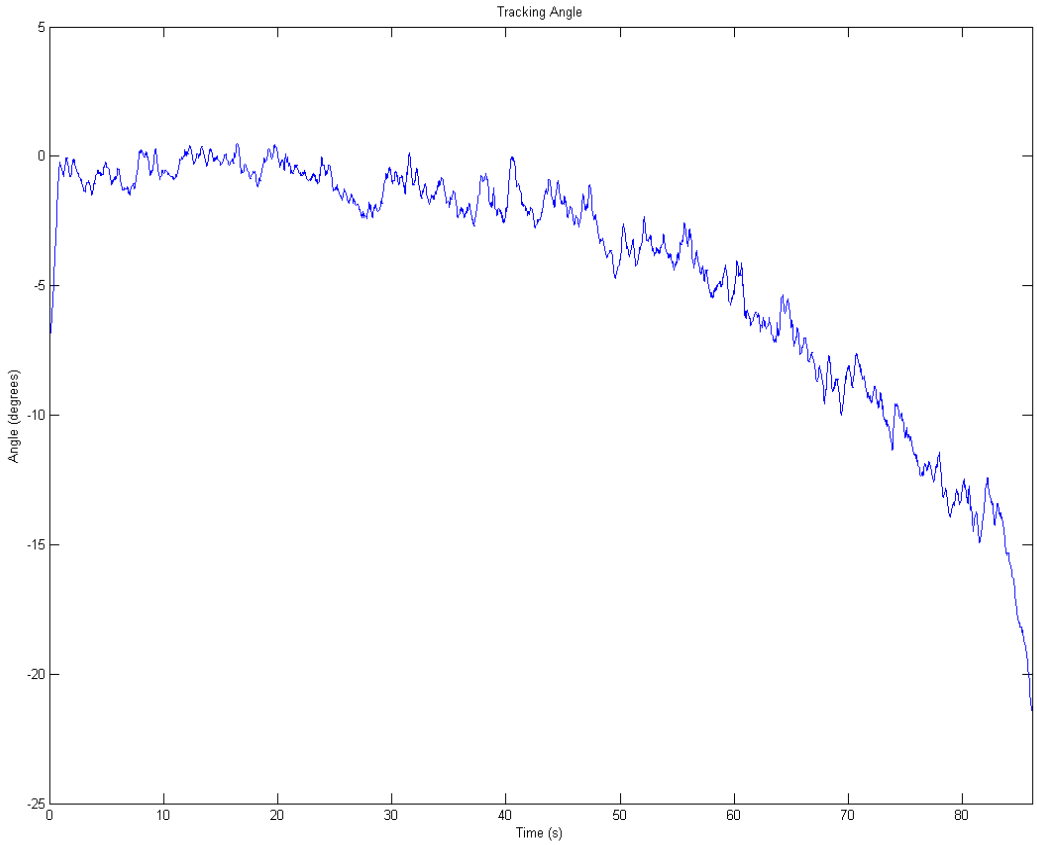

Figure 82. Tracking angle changes during Biering-Sørensen test.

In this plot drawn from the tracking angle against time the position of the participant drops from 0° to -20° by the end of the trial. The time taken to drop -10° below the horizontal occurs at around 70 seconds into the test.

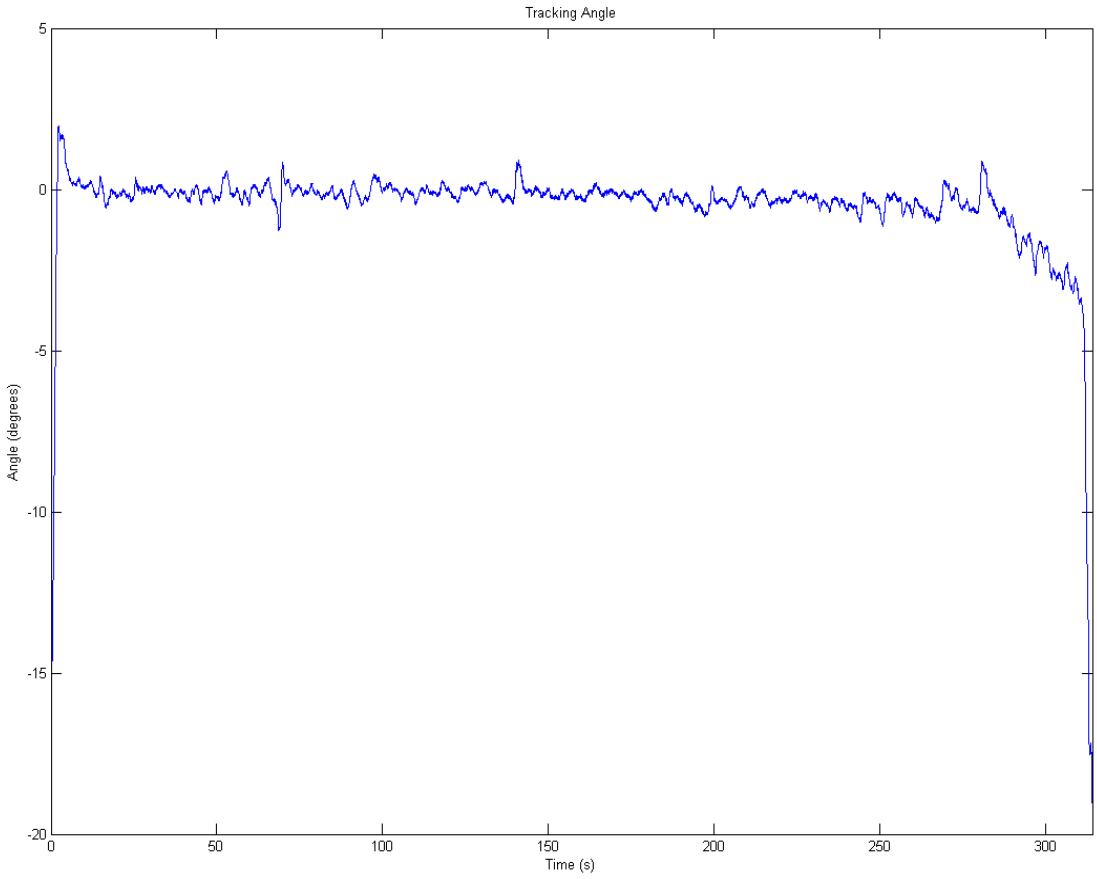

Figure 83. Tracking angle changes during the Ito test.

The tracking angle data from the Ito test shows a different pattern to the Biering-Sørensen test. In the Ito test, the participant is able to hold the test position for considerably longer and the test ends abruptly at 300 seconds.

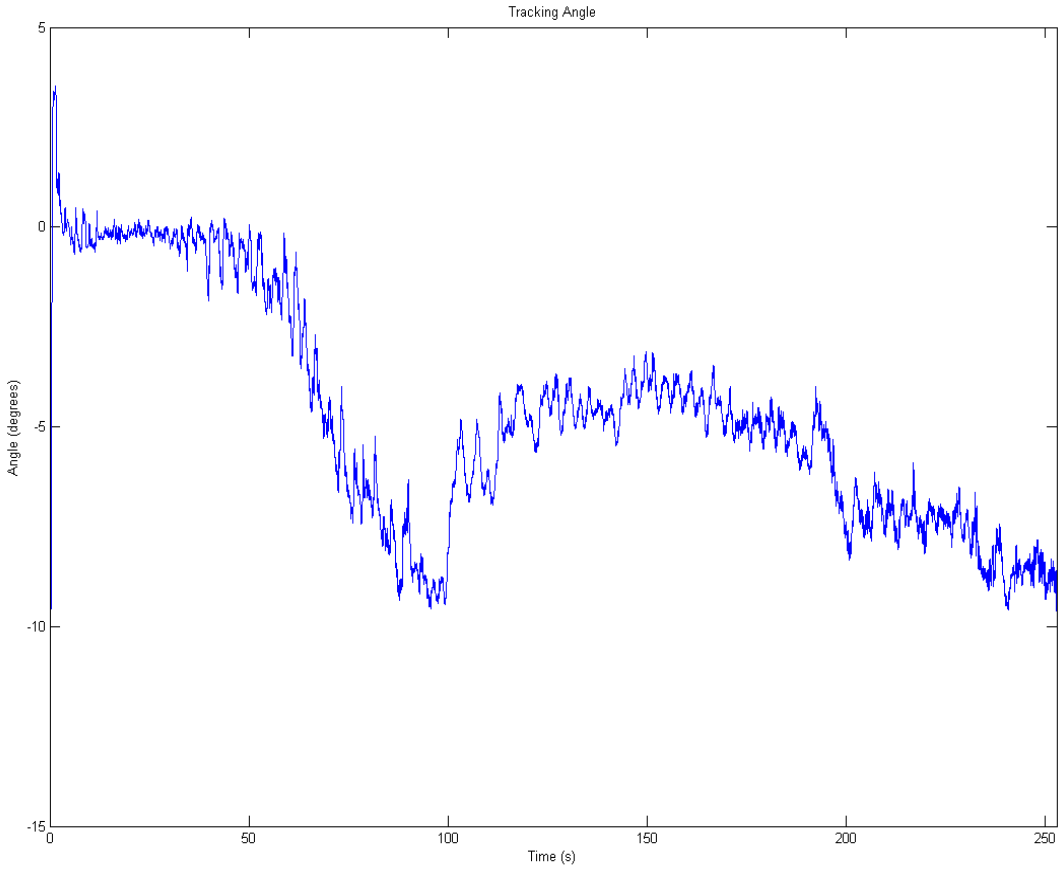

Figure 84. Tracking angle changes during the McKintosh test.

The tracking angle data from the McIntosh test is not easy to evaluate; the participant does not fall below -10° but does fail to continue at 250 seconds into the test. It can be seen that at 100 seconds the participant seemed to have dropped to -10° but continues the test. The tracking angle results are inconclusive.

4.8 Discussion

This feasibility study described the development of an experiment designed to take measurements from particular spinal muscles as they fatigue during a standard fatiguing tasks. The muscles studied contribute some 70% of force to the extensor moment and are therefore important, but not the only, stabilisers of the spine (Bogduk 1980; Bogduk & Macintosh 1984; Bogduk, Macintosh, & Pearcy 1992; McGill 2002; McGill, Childs, & Liebenson 1999). As spinal instability is a contributory factor in the aetiology of LBP better understanding

of mechanisms by which stability is lost may result in novel intervention strategies in the management of LBP.

The following aims of the feasibility study will be discussed;

1. To develop a methodology and to standardise the test procedure for a laboratory-based assessment of spinal muscle fatigue based on the Biering-Sorenson test procedure.
2. To establish if high-density electrode matrixes and arrays would be suitable for investigating sEMG recording from spinal muscles.
3. To establish if the electrode placements based on previous anatomical studies provided useful data.
4. To develop tools for the visualisation of the raw EMG signal
5. To undertake analysis of the myoelectric manifestations of fatigue during high force isometric muscle contraction.

4.8.1 To develop a methodology and to standardise the test procedure for a laboratory-based assessment of spinal muscle fatigue based on the Biering-Sorenson test procedure.

The use of multi-channel sEMG has the potential to move from the laboratory to the clinical/field-based situation and examples of its benefits are emerging (Farina et al. 2004b; Merletti, Bottin, Cescon, Farina, Gazzoni, Martina, Mesin, Pozzo, Rainoldi, & Enck 2004; Zwarts & Stegeman 2003). However, problems still exist with regard to the reliability and validity of the methodologies employed when applied to the analysis of spinal muscles. This feasibility phase has demonstrated that much work is still required before this particular technique for evaluating the fatigue characteristics of spinal muscles can be applied in clinical practice.

The Biering-Sørensen test procedure is used in many different testing environments and a standardised method of this testing procedure was chosen, for this study, as previously described (Section 2.4.10). However, many of the variations of the technique are inconsistent with the principles of standardisation. Participants for this study were restrained using a standard method as described. The arms were held crossed across the body as this position inhibited the use of the Latissimus Dorsi muscle and the shoulder girdle retractors in extending the thoracic spine. The cervical spine was

maintained in neutral. Contracting muscles other than those of interest could potentially cause crosstalk, contamination and noise in the sEMG signal, particularly the signal obtained from the array electrodes.

It was considered necessary to adapt the original description of the Biering-Sorenson test procedure in the following ways;

No verbal feedback or encouragement was provided to the participants during testing. There is evidence that to do so could result in changes to central drive to muscles (Gandevia 2001) and therefore to holding times. As the nature of verbal feedback and encouragement cannot be easily controlled only standardised written instructions were provided with the participant information.

Feedback was however provided to the participants in the form of a visual display (Figure 53 and Figure 55) for each of the three test procedures. This provided the participant with visual feedback as to how well they were maintaining the starting position. Instructions to each participant were to maintain the cross hairs on the target for as long as possible; position data in the x and y axis was recorded for later analysis. No instruction was given as when the test was to end apart from the instruction to 'please hold the test position for as long as possible'. In practice, each participant was normally able to hold the test position for the Biering-Sørensen test procedure with a steady decline in performance culminating in 'task failure' towards the end of the procedure (Figure 82).

Two additional variations of the Biering-Sørensen test procedure were also tested for their utility; the Ito and the McIntosh test procedures that are also thought to be endurance tests were also used and data recorded from muscles of interest. Neither of these tests has been used as extensively for research purposes and their overall utility was not considered to be more superior to the Biering-Sørensen test procedure.

The Ito version resulted in participants holding the test position for considerably longer time than the Biering-Sørensen test and, in some cases, participants did not reach a point of task failure and the test was terminated at 240 seconds as this was the time considered to be consistent with a normal

degree of endurance for the Biering-Sørensen test, no such normative data exists for the Ito test. It was often the case that participants rested the lower part of their thoracic cage on the plinth which resulted in longer than expected holding times. The original description of the Ito test (Ito et al. 1996) suggested that a pillow is placed under the abdomen of the participant in order to prevent hyper lordosis; in practice, participants adopt a position of extension/hyper lordosis of the lumbar spine Figure 20) even though a pillow is placed under the abdomen. Furthermore, the addition of a pillow did not prevent participants resting their rib cage on the plinth in order to extend the holding time. A loss of sEMG signal was also a problem with the Ito test; the matrix electrode was attached to the participant in prone lying but during the test procedure a loss of contact often occurred as the participant extended their lumbar spine. If the matrix was applied with the participant in an extended position it prevented a comfortable return to neutral once the test had been completed.

The McIntosh variant produced erratic results with participants being able to sustain long holding times but with considerable variation in position. In practice, this test produced highly inconsistent results and was judged not to be suitable for sEMG data collection as the active extension of the lumbar spine often resulted in disruption of the matrix electrode with resultant loss of signal.

The results of this phase of the study were affected by technical problems that are not unusual in experimentation with sEMG amplifiers; these were resolved due to a change in location and data were collected as per the method described in Section 4.5. However, additional technical problems occurred with the position plotting apparatus and no further data from this instrument was collected. It was noted however, that the Biering-Sørensen test procedure was consistently ended by the participant at the point of task failure so that the holding time that had been recorded could be taken as a consistent measure of the test duration. The Biering-Sørensen test procedure did not show the variations (Figure 82) that had been seen in the Ito and McIntosh variations (Figure 83 and Figure 84). It was decided that further testing could rely on the ‘time to task failure’ as an appropriate outcome measure although it could be argued that the plotting data from the Ito test procedure produces a clearer ‘cut off’ point at the end of the test.

4.8.2 To establish if the electrode placements based on previous anatomical studies provided useful data.

Studies by Biedermann et al. (1991) and De Foa et al. (1989), that were available at the time when the initial methodology of the sEMG study was being developed, informed the location of muscles of interest (Biedermann, DeFoa, & Forrest 1991; De Foa, Forrest, & Biedermann 1989). These studies had been undertaken in order to identify the location of the following muscles, as named by the authors; Iliocostalis Lumborum, Multifidus and Longissimus Thoracis specifically for sEMG studies. The methodology used provided data of muscles angles from palpable bony landmarks and these data were initially considered potentially useful to the multi-channel sEMG study.

A number of issues were identified with the methodology used in these studies that were taken into account in the development of the thesis methodology; the original authors used staples inserted into bony landmarks and lengths of string stretched between bony points. It is concluded that this methodology is likely to result in a lack of reliability and validity of the angles published (Table 13) and therefore, these data cannot be taken as a 'gold standard' measure against which to make other measurements, the authors themselves question the validity of this technique and cite the wide variations in individual anatomy and the methodology used as reasons to question the applicability of their approach.

The Biedermann and De Foa papers did not state if their methodology specifically identified the pars Lumborum component of Iliocostalis Lumborum or Longissimus Thoracis. In the case of Iliocostalis Lumborum it is likely that the use of a line projected from the PSIS to the tip of rib 12 to identify the lateral edge of Iliocostalis Lumborum could identify the lateral edge of the Iliocostalis Lumborum pars Lumborum rather than the pars thoracis component. If this is the case, then data collected using this reference line would be invalid.

Another consideration is that the Biedermann and De Foa reference lines only identify the lateral border of muscles of interest. In sEMG studies and in particular multi-channel sEMG studies data recording from over the mid portion of the muscle that is closest to the innervation zone is recommended.

Additionally, the use of reference lines does not give any indication where the muscle lies along that line or where, on that line, the muscle attaches to the erector spinae aponeurosis.

No reference line was established by these authors for Longissimus Thoracis so the initial pilot study described in this thesis used the SENIAM guidelines and an approximation based on known anatomy and previous sEMG studies (Lariviere, Arsenault, Gravel, Gagnon, & Loisel 2002).

Results of the pilot study indicate that useful data can be collected using electrode matrixes and arrays but that due consideration needs to be made of the exact location over the muscles of interest. The electrode matrixes and arrays are of a fixed dimension and as such may not be suitable for the normal individual variations seen. Specifically, if data are collected from the entire length of the array or area of the matrix, then there cannot be any certainty that the data are from muscles of interest. Using standard measures of fatigue (shifts in MDF and rms during a fatiguing task), a consistent finding of an analysis of sEMG was that all data points from which a usable signal was collected and analysed, showed evidence that was consistent with fatigue. The fatigue plot often showed evidence that fatigue occurred at different rates or at different time.

Within the sEMG signal, there were end of fibre effects and inconsistent evidence of propagation of MUAPs. It could be expected that end of fibre effects and propagation of MUAPs would be consistent with locations of electrodes that were correctly placed as is the case when studying other muscle groups, provided this was a consistent finding; in these experiments, there were no consistent findings. It was concluded that the best interpretation was that the muscles of interested were not being specifically analysed due to a lack of knowledge of the surface anatomy that related to the muscle of interest and that better localisation was necessary.

It was concluded, following analysis of results of the pilot study, that basing the location of electrode matrixes and arrays on previous studies was not appropriate and that it could not be concluded that any data that were collected could not, with any confidence, be considered to have arisen specifically from muscles of interest in this thesis. It was further concluded

that a specific anatomical study was required in order to have confidence in electrode placements based on surface anatomy.

4.8.3 To develop tools for the visualisation of the raw EMG signal

Tools were developed in Matlab in order to collect and visualise the raw signal in real time before signal decomposition and analysis (Figure 56). This was necessary as no software system was available at the time that was suitable for setting up a 128 channel sEMG experiment (Section 4.5.5.1). Specifically, it was necessary to ensure that each channel was providing a valid signal; 128 channels are difficult to visualise simultaneously so software was developed that allowed individual sections of data to be examined separately. This process developed novel solutions to both data visualisation and to data analysis.

The software applications developed enabled a number of steps to be undertaken in order to effectively process the data. These applications were tested rigorously and developed on an ongoing basis as the methodology was being developed.

4.8.4 To undertake analysis of the myoelectric manifestations of fatigue during high force isometric muscle contraction.

Data processing and analysis are required in order to draw conclusions from sEMG experimentation. Acquisition software was available within the hardware configuration of the EMG amplifier and a programme was available (OT Bioelettronica, C.so Unione Sovietica 312, 10135 – Torino, ITALY) that enabled setting of various acquisition parameters. No software was available that would allow data handling from 128 channels and which allowed analysis of specific sections of the signal from specifically identified electrodes located within a matrix or array. The development of this software is outlined in section 4.5.5.2. No software was available for the signal decomposition that was required, although within Matlab various routines are available to undertake the fast Fourier transform in order to be able to decompose the signal and to produce fatigue plots as required.

The parameters of interest at this stage were the running root mean squared value and median frequency. The rationale for calculating these parameters, from the signal obtained, was that changes in these measures are considered to be consistent with changes in central nervous system output that maintain homeostasis as an individual 'fatigues'. Many other parameters can be calculated such as Average Rectified Value (ARV), Normalised rms (NRMS), Mean Frequency (MNF) and variation in the fatigue plot can be draw from these that represent changes in amplitude variables, spectral variables and muscle fibre conduction velocities (CV), (Merletti and Lo Conte 1997). All these variables are interdependent and can be interpreted from data recorded from linear arrays and matrices. It was therefore the view, in the development of the methodology, that the analysis of MDF and rms would be sufficient to demonstrate changes in the frequency and amplitude domain that would be expected to be seen as a classification of muscle behaviour consistent with fatigue (Luttmann, Jager, & Laurig 2000). Fatigue plots could be drawn and rates of fatigue calculated from regression line analysis as described in the RIB trials described in a later section (Figure 38 and Section 3). Future analysis of other parameters would be possible from data collected.

Software developed and the mechanisms for data analysis were such that the sEMG signal could be visualised in real time as the experiment was being set-up. Initial data manipulation could determine if a usable signal was available and post data analysis allowed the parameters of interest to be calculated.

4.8.5 Limitations

Initially there were problems with the validity of some of the data collected; the initial location chosen for the experiment was a laboratory in ISVR and owing to the level of radio frequency (RF) noise in the environment it was often not possible to record any usable data as it was contaminated by RF noise that could not be successfully removed by filtering post data collection. The laboratory was moved to another location on site where the level of RF was significantly less. At this location experiments were repeated and useable sEMG data were collected. However, an issue with the electrogoniometer occurred; the power supply for the isolation unit produced an irregular high frequency interference that prevented any further usable position data from

being collected. Time to task failure was subsequently recorded from digital display from electrogoniometer (Figure 55).

4.9 Conclusion

It has been established so far in this study that, in the right environment, the combination of multi-channel sEMG and a standardised fatigue test results in usable data. The correct location of electrodes is essential for this procedure and to date, for Multifidus, Iliocostalis and Longissimus this is not known. It could be assumed, on the basis of these results that locating a 64 electrode matrix as per the protocol for recording from Multifidus is appropriate but it has not been demonstrated that the location of the arrays for Iliocostalis and Longissimus is correct. Indeed, it appears highly likely that the location of the arrays is not correct and a clear need exists to refine these locations through a thorough study of the underlying anatomy. Normally, locating sEMG electrodes is undertaken by palpating anatomical surface features that are known to correlate with the location of muscles of interest. Typically, the distance from a bony landmark or an angle measured in relation to one of the cardinal planes of the body from a bony landmark would be used.

The development of the GUIs allows the visualisation of the signal, which is essential in the set-up of this experiment and in the analysis. To date, analysis has been limited to the techniques described above; further analysis requires signal decomposition techniques but these should only be undertaken once confidence in the validity and reliability of the sEMG signal is high.

With regard to the utility of the use of an electrogoniometer for biofeedback, it is evident that feedback might result in a more valid experiment as it presents each participant with the same information that is not contaminated by verbal feedback. In practice, the use of the Biering-Sørensen or Ito test results in the participant reaching a definite endpoint that is evident to the clinician or experimenter. The use of a standard stopwatch to record holding times would suffice in practice.

This phase of the study has partly achieved the study aim; the methodology has been tested and tools have been developed to enable visualisation and

analysis of the raw data prior to, and post, data collection. Data were collected consistently, independent of electrode position.

> The hypothesis for this experiment cannot be accepted and consequently, the null hypothesis that…electrode placement based on previous anatomical studies does not provide valid data from the muscles under investigation… is accepted for this phase of the study.

In clinical practice, it is likely that the outcome measure used in fatigue protocols will be the time to task failure and that point will be determined by the practitioner.

Electrode placements based on previous anatomical studies are not appropriate for multi-channel surface electromyography and anatomical studies are required to provide details of the location of the muscles of interest. It should be determined if the location of underlying musculature is more accurately achieved based in relation to angles from or to bony landmarks relative to the cardinal planes of the body or on the distance from bony landmarks. The following three sections of this thesis will specifically address issues of specific muscle angles and position in relation to palpable bony landmarks.

5. A post-mortem study of muscle fibre angle of Iliocostalis Lumborum pars Thoracis and Lumbar Multifidus muscle.

5.1 Introduction

Anatomical studies detailing the angles of the paraspinal muscles in relation to the mid-line of the body are limited. In the descriptions that have been reported, a large degree of discrepancy exists, in particular related to the precise anatomy and attachments of the musculo-tendinous mass of the Erector Spinae (ES) muscle group (Bogduk 1980; Bogduk & Macintosh 1984; Daggfeldt, Huang, & Thorstensson 2000; Gray 2009; Kalimo, Rantanen, Viljanen, & Einola 1989; Macintosh & Bogduk 1987). The lack of morphological data has led to an absence in standardised sEMG protocols and inaccuracies in published studies (Bradl, Morl, Scholle, Grassme, Muller, & Grieshaber 2005; Callaghan, Patla, & McGill 1999; Elfving, Nemeth, & Arvidsson 2000; Hermans, Freriks, Merletti, Stegeman, Blok, Rau, Disselhorst-Klugg, & Hagg 1999; Hermens, Freriks, Disselhorst-Klug, & Rau 2000; Mannion et al. 1998; Oliver, Tillotson, Jones, Royal, & Greenough 1996).

De Foa et al. (De Foa, Forrest, & Biedermann 1989) devised a surface landmark derived reference line system for demarcating the angles of the Iliocostalis (ILpT) and Multifidus (LM) muscle fibres for use in sEMG; however the method has not been scrutinised or assessed for validity or reliability. This anatomical study took a series of lumbar spine dissections, from which detailed muscular descriptions (Section 6) and fibre angle measurements were taken to clarify the morphology of the Iliocostalis and Multifidus muscles. The De Foa (1989) method is based on the assumption that accurate location of surface markings of the posterior superior iliac spine (PSIS), the L2/3 interspinous space and the tip of the 12th rib is possible. If this is the case, then clinicians extrapolate lines between these points and are therefore able to identify the lateral edge location of the muscles of interest.

The conclusions from the De Foa (1989) paper are that;

A line projected horizontally from L2/3 that intersects a line from the PSIS to the tip of rib 12 will identify a point that is at the lateral edge of Iliocostalis.

A line projected horizontally from the L4/5 interspinous space that intersects a line from the PSIS to the L1/2 interspinous space will identify a point that is at the lateral edge of Multifidus.

The validity and reliability of the indirect method devised by De Foa et al. (1989) was assessed and compared to a direct method and a method utilising digital images for measuring muscle angles. These findings were used to facilitate the identification of Iliocostalis and LM and contribute to recommendations made regarding positioning of sEMG electrodes.

This section tested if the method devised by De Foa et al. (1989) could be used as a reliable and valid method for determining the muscle fibre angles of Iliocostalis Lumborum pars Thoracis and Lumbar Multifidus with sufficient accuracy and reliability that the method could be utilised with confidence in multi-channel sEMG experimentation.

5.2 Aim

To undertake serial measures of the muscle fibre angles of the Iliocostalis and Multifidus muscle.

To compare a direct digital method for measuring the muscle fibre angle of Iliocostalis and Multifidus to the De Foa method.

5.3 Design

This was a post-mortem case series anatomical study designed to provide a detailed anatomical description of the location of components of the Longissimus Thoracis pars Thoracis, Iliocostalis Lumborum pars Thoracis and lumbar Multifidus muscles in relation to palpable bony landmarks.

5.4 Hypothesis

The hypotheses of this study were;

> Measurements of angles, taken from digital images, of Iliocostalis and Multifidus using an adapted measurement method described by De Foa will be equivalent to a direct fibre angle measurement method.
>
> Digital methods for measuring muscle angles will be more discriminating in detecting differences in muscle angles compared to the De Foa indirect method; specifically with regard to differences between male and female and between right and left sides of the body.

The null hypotheses being that;

> Measurements of angles, taken from digital images, of Iliocostalis and Multifidus using an adapted measurement method described by De Foa will not be equivalent to a direct fibre angle measurement method.
>
> Digital methods for measuring muscle angles will not be discriminating in detecting differences in muscle angles compared to the De Foa indirect method.

5.5 Method

5.5.1 Dissection

The spinal muscles of three male and four female embalmed individuals aged between 73 to 95 years old (*M*= 84.3; *SD* 8.3 years) were dissected at the Centre for Learning Anatomical Sciences (CLAS), University of Southampton, UK. The bodies were embalmed in a prone position in order, as far as was practicable, not to disturbed the orientation of muscle fibre due to compressive effects. Anatomical examination was performed in accordance with the Human Tissue Act UK (2004) and Anatomy Act UK (1984) and the study was approved by the University of Southampton's Medical School ethics committee.

The dissection was performed in a serial fashion and began via a median incision along the spinous processes. The right and left Iliocostalis muscles of

the Multifidus were exposed and the superior and inferior attachments identified. Digital images were obtained (Section 5.5.3) at each stage of the dissection process were stored in accordance within the requirements of the ethics approval and CLAS procedures. The superior, inferior, and middle points of the T11 to L5 spinous processes and the S2 tubercle and posterior superior iliac spines (PSISs) were demarcated using coloured ink (Cancer Diagnostics Inc.; USA) (Figure 85). General morphology of the Iliocostalis muscle and its attachments were noted from direct observation of the cadavers.

Following identification and measurements of Iliocostalis, further dissection was undertaken to expose the Multifidus group. Digital images and measurements were obtained as described below (Section 5.5.3). Confirmation of the identity of each muscle was undertaken by the researcher and an advisor (an anatomist) for this phase of the study. As part of the inter-rater and intra-rater reliability process (Section 5.7.12) there was agreement that each muscle was correctly identified based on anatomical description of attachments and location (Bogduk 2005; Bogduk 1980) before measurement was undertaken.

5.5.2 Method for obtaining digital images

A hollow Perspex Box was placed over the lumbar region of the prone cadaver. Photographic images were captured using a digital camera (Fujifilm FinePix S100FS) mounted on the top of the box via a bracket, with the lens through a circular hole orientated in the same plane as the back musculature. Surface levels of both the Perspex box and camera were confirmed with a two-axis spirit level. The dissecting table on which the prone body of the individual was lying was also checked to ensure that it was level using a two-axis spirit level. All images were centred in the viewfinder, prior to obtaining, to ensure that the camera was positioned directly above the area of interest. This was to minimise optical angle errors due to perspective distortion which would render later measurements of angles from images inaccurate. This process enabled Digital Images to be obtained from which direct measurement of muscle angle could be taken using a variety of methods.

This process enabled Digital Images to be obtained from which direct measurement of muscle angle could be taken using a variety of methods.

5.5.3 Measurement of Iliocostalis and Multifidus muscle fibre angles

All digital images were uploaded and viewed with Microsoft Office PowerPoint 2003 (Microsoft Corporation, Redmond, WA, USA) where vertical and horizontal reference lines were added. Reference lines were drawn in order that different methods of measuring muscle angles could be compared (Figure 85 and Figure 86).

In a clinical setting, the recommendations of the De Foa method (1989) would be based on palpating bony landmarks and interpolating between these locations. Directly drawing the De Foa lines onto the digital image allows the assumptions made by that method to be compared with measures taken directly. Angles were then compared to direct measures of muscle angles from the same images in order for a method comparison to be undertaken.

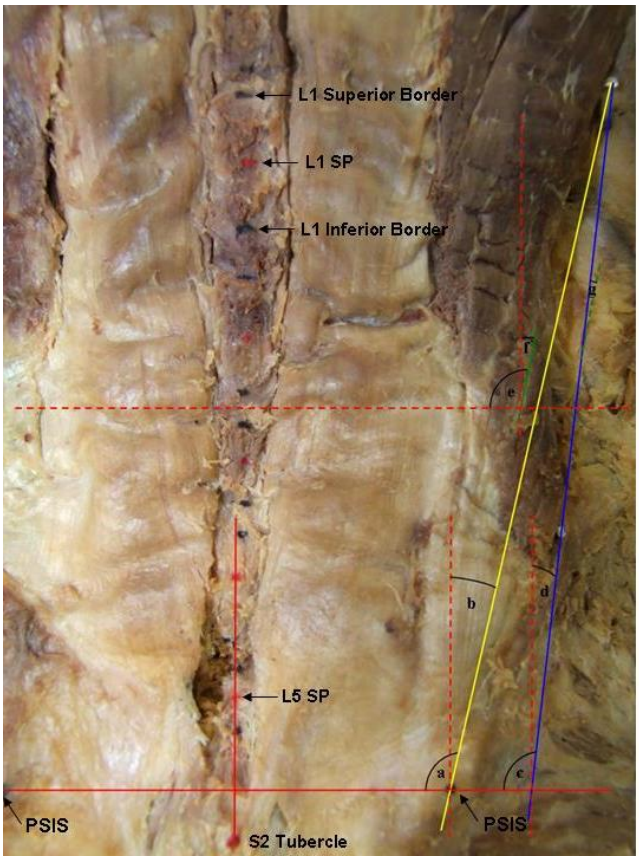

Figure 85. Digital image method – Iliocostalis Lumborum pars Thoracis.

Figure 85 demonstrates the method for marking the image of the right Iliocostalis pars Thoracis muscle with the inferior and superior lateral border

attachments (pins within the blue solid line) and middle of the spinous process (vertical red ink dots), inferior and superior borders of the spinous processes (black ink dots), right and left PSISs (green ink dots) and S2 tubercle (red ink dots) demarcated. The vertical and horizontal reference lines (dotted red lines) were transposed to facilitate the measurement of Iliocostalis muscle fibre angle with respect to the Iliocostalis lateral border (blue line), De Foa et al. (1989) reference line (yellow line) and the Iliocostalis fibre angle at L2/L3 (green line). The angles measured were De Foa-Horizontal (a), De Foa-Vertical (b), Iliocostalis lateral border-Horizontal (c), Iliocostalis lateral border-Vertical (d), L2/L3 Fibre Line-Horizontal (red horizontal dotted line) (e), L2/L3 Fibre Line-Vertical (red vertical dotted line) (f), L2/L3 Fibre Line-De Foa (g).

The following 'methods' were used to mark each digital image and are described for Iliocostalis (Figure 85);

'De Foa' method (yellow line in Figure 85)

The reference lines described by De Foa et al. (1989) ('De Foa' method) were drawn on the digital image between the prominent point of the PSIS (previously marked) and the angle of the lowest point of the twelfth rib.

'Fibre line' method (green line in Figure 85)

The best approximation of the angle of the Iliocostalis muscle fibres at the level of L2/L3 was drawn on the digital image ('Fibre Line' method) as described by De Foa et al. (1989).

Iliocostalis 'Lateral Border' method (blue line in Figure 85)

This line was demarcated on each cadaver with pins and a line between these drawn and extrapolated on each digital image.

The 'De Foa', 'Fibre Line' and 'Lateral Border' angles were measured with respect to the vertical and horizontal reference lines. These were also drawn on each digital image using a line between each PSIS as a horizontal reference line and the best approximation of a line drawn through tips of each lumbar spinous process. Angles of interest were measures using the software application ImageJ (Rasband, W.S., ImageJ, U. S. National Institutes of Health, Bethesda, Maryland, USA, http://imagej.nih.gov/ij/, 1997-2012).

Further dissection was then undertaken to expose Multifidus and further digital images obtained and vertical and horizontal reference lines added.

The following 'methods' were used to mark each digital image are described for Multifidus (Figure 86). Lines were identified as described below;

'De Foa Multifidus' method (blue line in Figure 86) drawn from PSIS to the interspinous space at L1/2.

Multifidus 'Lateral border' method (oblique yellow line in Figure 86).

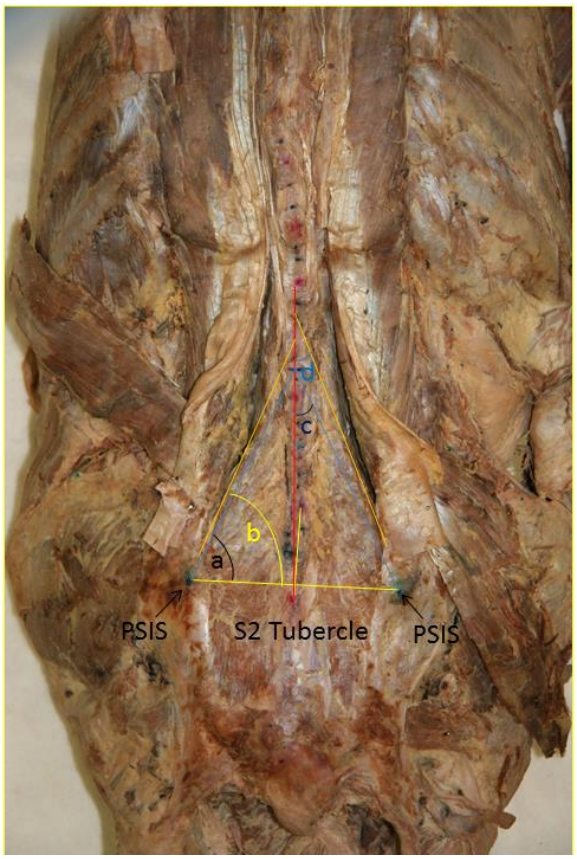

Figure 86. Digital image method – Lumbar Multifidus.

Figure 86 demonstrates the method of marking the image of Multifidus muscle. A horizontal reference line (yellow) is drawn between the PSISs (green dots). A short vertical line (yellow) is drawn between S1; a longer (red) vertical reference line is drawn between S2 and L1. The De Foa method (blue lines) are drawn from right and left PSIS respectively to the interspinous space at L1/2. Lines were drawn (yellow) along the lateral edge of the Multifidus to represent a 'best fit approximation'. Angles measured were between De Foa horizontal

line – De Foa L1/2 intersection (a), De Foa horizontal line – lateral edge Multifidus (b), vertical reference line – De Foa L1/2 intersection (c) and vertical reference line – lateral edge Multifidus (d). Measurements were taken from both right and left sides (one side only is illustrated in Figure 86).

5.6 Data analysis

5.6.1 Method agreement and reliability

To determine the method agreement of the De Foa et al. (1989) method in measuring Iliocostalis and Multifidus muscle fibre angles, the 'lateral border' method had been devised for comparison for both muscles. These data are presented below (Section 0)

For the determination of inter-observer reliability, a second trained observer performed all measurement methods (De Foa and lateral border) on the same day. For intra-observer reliability, all measurements were repeated the next day. Each observer was blinded to previous measurements (section 5.7.12).

5.6.2 Statistical analysis

The data were tabulated to indicate the extent of individual variation and presented with mean *(M)* and standard deviation (*SD*) values. Wilcoxon signed-rank and Mann-Whitney U tests were used to determine whether there was a difference in Iliocostalis fibre angle between right and left sides and female and male cadavers respectively.

Two different methods were used to test for clinical equivalence; Bland and Altman limits of agreement (Bland and Altman 1986; 1999) and equivalence testing (Schuirmann 1987). This study was seeking to establish methods for measuring angle on the same individual therefore Bland and Altman plots were an appropriate analysis; equivalence testing sets a zone of clinical indifference which is comparable to the limits of agreement approach. The study described in Section 6 also utilises equivalence testing so comparisons can be made.

Bland and Altman limits of agreement (LOA) (Bland and Altman 1986; 1999) and paired t-tests were used to estimate the agreement between the De Foa et al. (1989) methods, the Fibre Line and the Lateral Border methods for Iliocostalis muscle fibre angle with respect to both the horizontal and vertical

reference lines. For Multifidus the De Foa and Lateral border methods were compared.

Equivalence analysis was undertaken using two one-sided test procedure (TOST) (Schuirmann 1987) to establish whether the confidence intervals of the angles measured were within clinically acceptable limits (zone of clinical indifference) that would demonstrate clinical equivalence (Huson 2001; Vavken 2011). The one-sided 90% confidence interval (CI) for the difference between the two measures was set at a range of 10° (-10°, 10°).

Correlation coefficients were calculated to indicate closeness of fit between variable and displayed in scatterplots.

5.7 Results

The assumptions of the limits of agreement method were verified statistically and graphically. Intra- and inter-observer reliability were determined using intra-class correlation coefficients ICC (2,1) and ICC (3,1), respectively. A probability level of p=.05 was set as the minimum criterion of statistical significance for all tests. All analyses were performed using SPSS version 17.0 for Windows (SPSS Inc., Chicago, Illinois, USA), Microsoft Office Excel 2003 (Microsoft Corporation, Redmond, WA, USA), XLSTAT Version 2013.4.04, MedCalc ® Version 12.7.0.0 64-bit. © 1993-2013 MedCalc Software and GraphPad Prism version 6.00 for Windows, GraphPad Software, La Jolla California USA, www.graphpad.com.

5.7.1 Iliocostalis Muscle fibre angle – De Foa and Lateral Border method compared

With respect to the vertical reference line (b) (Figure 85), a mean value of 10.11° (*SD* 2.66°) and with respect to the horizontal reference line (a), a mean value of 99.67° (*SD* 4.39°) was calculated using the De Foa method. These compared to mean values of 7.69° (*SD* 3.7°) and 97.43° (*SD* 5.87°) for Lateral Border measurement method of the angle (Table 15). A comparison of all methods can be seen in Table 15.

Table 15. Iliocostalis muscle angle (°) data collation of methods. The letters in parenthesis refer to the angles noted in Figure 85.

	Lateral border measures of muscle angle (blue line)		L2–L3 Fibre line angle (green line)		De Foa measures using anatomical landmarks (yellow line)		
	Vertical (d)	**Horizontal (c)**	**Vertical (f)**	**Horizontal (e)**	**Vertical (b)**	**Horizontal (a)**	**De Foa Ref line (g)**
Mean	7.69°	97.43°	12.93°	102.49°	10.11°	99.67°	6.10°
SD	3.70°	4.94°	5.87°	8.08°	2.66°	4.39°	5.37°
Median	6.19°	96.38°	11.86°	102.78°	10.49°	101.28°	4.85°
Min	2.82°	87.89°	2.42°	83.76°	6.43°	90.60°	0.01°
Max	13.83°	106.20°	23.95°	115.24°	16.78°	105.94°	16.68°
N	7	7	7	7	7	7	7

5.7.2 Left and right differences in Iliocostalis angle (°)

Table 16. Left and right differences.

	Lateral border measures of muscle angle (blue line)		L2–L3 Fibre line angle (green line)		De Foa measures using anatomical landmarks (yellow line)		
	Vertical (d)	**Horizontal (c)**	**Vertical (f)**	**Horizontal (e)**	**Vertical (b)**	**Horizontal (a)**	**De Foa Ref line (g)**
Left							
Mean	8.07°	97.87°	13.65°	104.18°	11.18°	100.57°	7.64°
SD	4.66°	4.50°	6.65°	6.82°	2.64°	2.71°	6.06°
Right							
Mean	7.30°	96.98°	12.20°	100.79°	9.04°	98.78°	4.56°
SD	2.74°	5.67°	5.41°	9.39°	2.37°	5.71°	4.50°

There were no significant differences in Iliocostalis fibre angle between left *M*= 11.18° (*SD* 2.64°) and right *M*= 9.04° (*SD* 2.37°) sides with respect to the

vertical reference line *W*(7)= −10, Z= 1.9, *p*= .5 (Figure 87). Or left, *M*=100.57° (*SD*2.71°) and right *M*=98.78° (*SD* 5.71°) sides with respect to the horizontal reference line, *W*(7)= −14, Z= 2.1, *p*= .3 (Figure 88).

In all box and whisker plots the following are shown; median, 25th and 75th percentiles, range and any outliers.

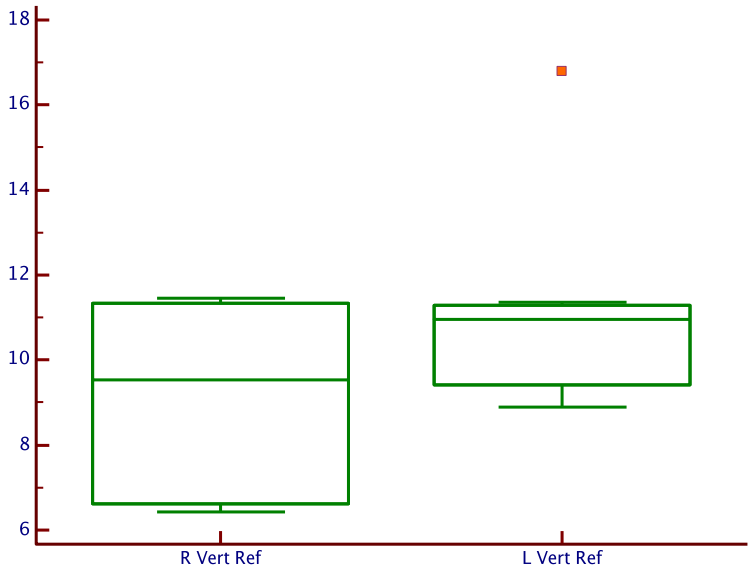

Figure 87. De Foa method, Iliocostalis left and right differences in vertical measures.

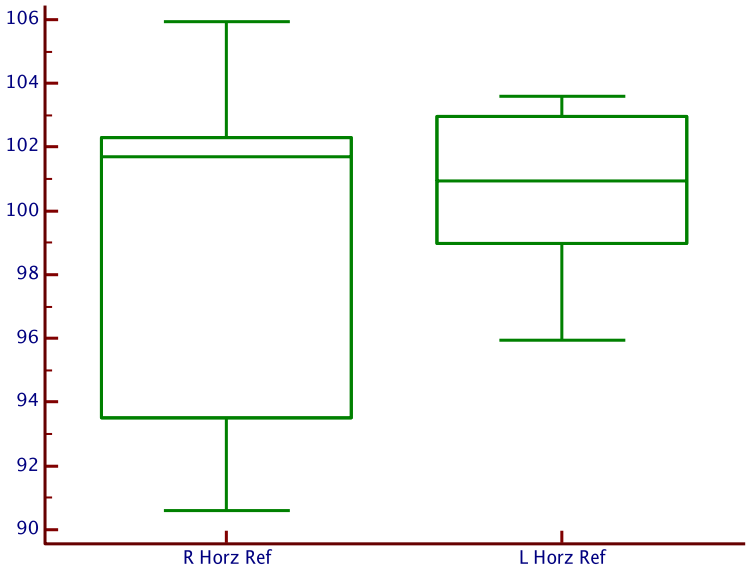

Figure 88. De Foa method, Iliocostalis left and right differences in horizontal measures.

5.7.3 Male and female differences in Iliocostalis: De Foa method

Table 17. Iliocostalis muscle fibre angle (°) measured using the DeFoa et al. (1989) method; male and female differences.

		Angle (°) of the Iliocostalis pars Thoracis muscle fibres from the:			
		Vertical reference line		Horizontal reference line	
Individual	Age (years)	Right	Left	Right	Left
Female					
1	78	6.43°	11.00°	92.69°	101.61°
3	73	6.54°	11.37°	96.03°	103.41°
5	95	6.82°	8.9°	90.6°	95.95°
6	81	9.54°	16.78°	105.94°	99.76°
Mean	81.7	7.3°	12.01°	96.31°	100.18°
(SD)	(9.4)	(1.48°)	(3.35°)	(6.79°)	(3.19°)
Male					
2	88	11.41°	10.96°	101.69°	103.61°
4	94	11.45°	9.22°	102.36°	98.71°
7	81	11.07°	10.02°	102.13°	100.95°
Mean	87.7	11.31°	10.07°	102.12°	101.09°
(SD)	(6.5)	(0.2°)	(0.87°)	(0.37°)	(2.45°)

Table 18. Iliocostalis mean data for male and female De Foa method.

	Vertical Ref	Horizontal Ref
Male	10.69°	101.61°
(SD)	0.89°	1.67°
Female	9.67°	98.25°
(SD)	3.47°	5.33°

The Iliocostalis muscle fibre angle of female specimens *M*=9.67° (*SD*=3.47°) showed no significant different to male specimens *M*=10.69° (*SD*=0.89°) with respect to the horizontal reference line *U*(14), Z=1.29; *p*= .23, or female specimens *M*=98.25° (*SD*=5.33°) to male specimens *M*=101.61°(*SD*=1.67°) with respect to the vertical reference line *U*(14), Z=1.29; *p*=.23. However, it was noted that Iliocostalis muscle fibre angle of female specimens showed greater variation (Table 17, Figure 89 and Figure 90).

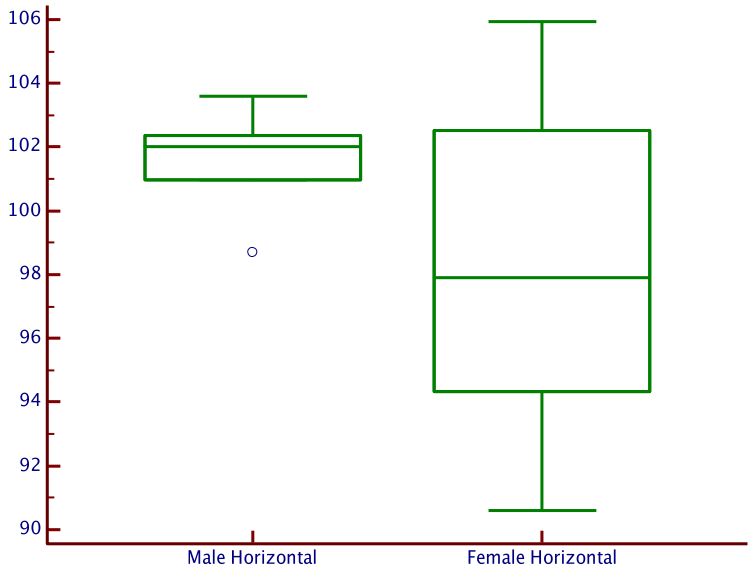

Figure 89. De Foa method, male and female differences from horizontal reference.

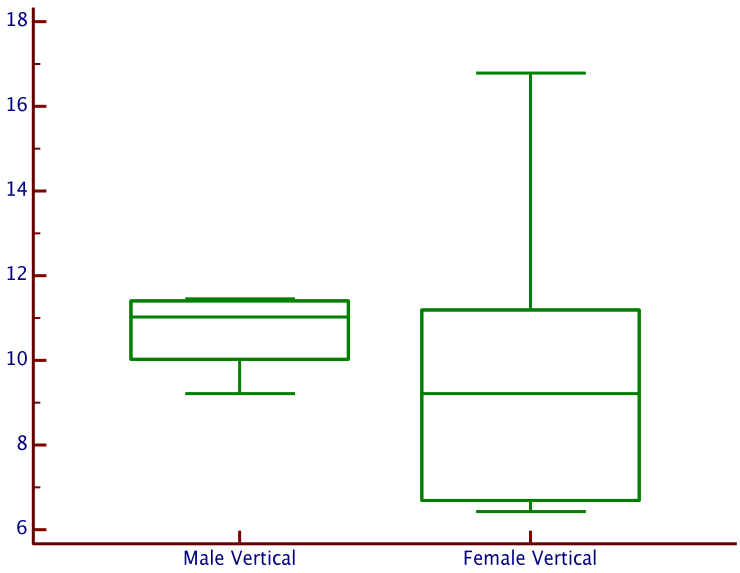

Figure 90. De Foa method, male and female differences from vertical reference.

5.7.4 Method agreement (see Figure 85 for legend)

Bland and Altman limits of agreement (Bland and Altman 1986; 1999) was used to estimate the agreement between the De Foa method, Digital Fibre Line methods and the Lateral Border method for Iliocostalis muscle fibre angle with respect to both the horizontal (Figure 92) and vertical reference lines (Figure 94). For Multifidus the De Foa and Fibre Line method were compared. Data are also presented as scatter plots for each comparison (Figure 91 and Figure 93). An assumption demonstrated above is that there are no left and right side differences between data and between male and female. This assumption will be discussed in the discussion; in order to make comparisons between methods, all data were pooled.

5.7.5 Comparing De Foa and Lateral Border method using horizontal reference line.

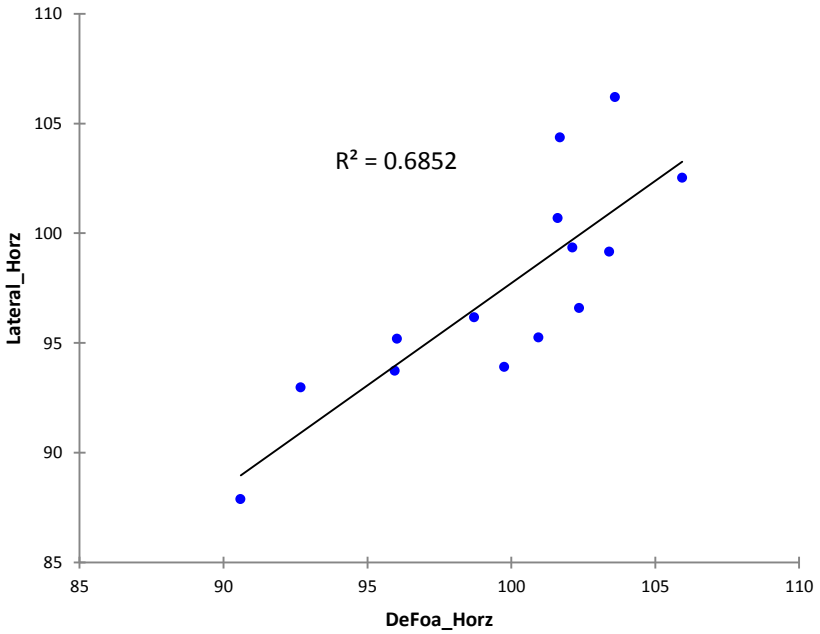

Figure 91. Scatter plot comparing De Foa and Lateral Border method using horizontal reference line.

The scatter plot indicates a moderate fit between data $t\,(13) = -3.02$, $p = .01$, overall model fit was $R^2 = 0.69$, between Lateral horizontal and De Foa horizontal method.

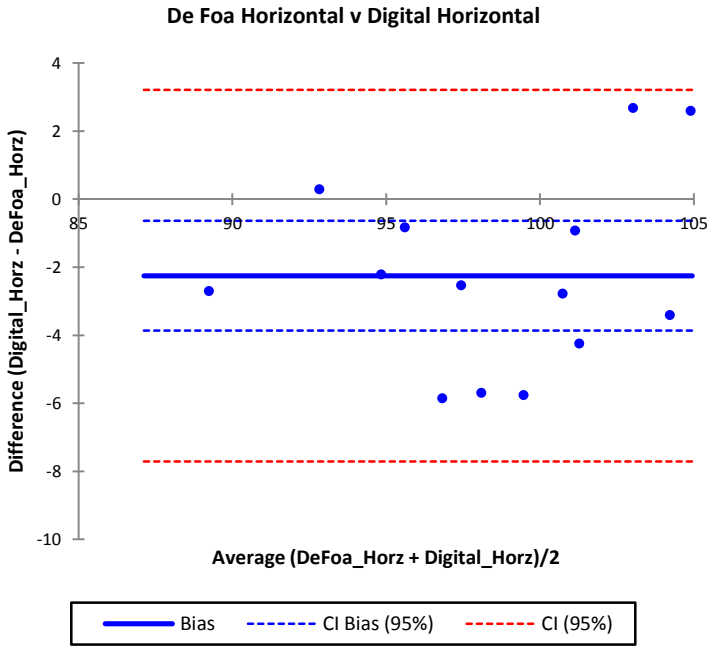

Figure 92. Limits of agreement for Iliocostalis – horizontal reference line.

For legend referring to angles (a) and (c), refer to Figure 85; limits of agreement for the De Foa method of measuring the angle of Iliocostalis muscle fibres (a) measured with respect to PSIS – PSIS horizontal reference line (c). The mean difference/bias (solid blue line) and the limits of agreement (± 1.96sd) are indicated (dashed red lines). Dotted lines indicate confidence intervals for limits of agreement (lower (blue) and upper (red) limit 95% CI).

Limits of agreement for the angles of Iliocostalis muscle fibres measured with respect to a horizontal reference line are shown in Table 19.

Table 19. Limits of agreement for Iliocostalis – horizontal reference line.

	Differences
Sample size, right and left sides	**14**
Bias	**-2.25°**
95% CI difference between means (Bias)	**-3.86 to - 0.64**
Standard error	**2.79**
Lower limit (LOA)	**3.22**
Upper limit (LOA)	**-7.71**

For legend referring to angles (b) and (d), refer to Figure 85; limits of agreement for the angle (b) of Iliocostalis muscle fibres measured with respect to a L4–S2 vertical reference line using lateral border method (d) is shown in

Figure 94. The mean difference/bias (solid blue line) and the limits of agreement (± 1.96sd) are indicated (dashed red lines). Dotted lines indicate confidence intervals for limits of agreement (lower (blue) and upper (red) limit 95% CI).

The bias of -2.25° would indicate that the two methods in this case are clinically equivalent, the limits of agreement are wide, 3.22, -7.71, this is in the order of 10° and there is a trend with limits of agreement being greater for larger angles.

Calculation of 90% confidence intervals for comparison between De Foa and lateral border method was -3.6° to -0.93°. This lies within the range of clinical indifference and with 95% confidence it can be concluded that two methods are equivalent.

5.7.6 Comparing De Foa and Lateral Border method using vertical reference line.

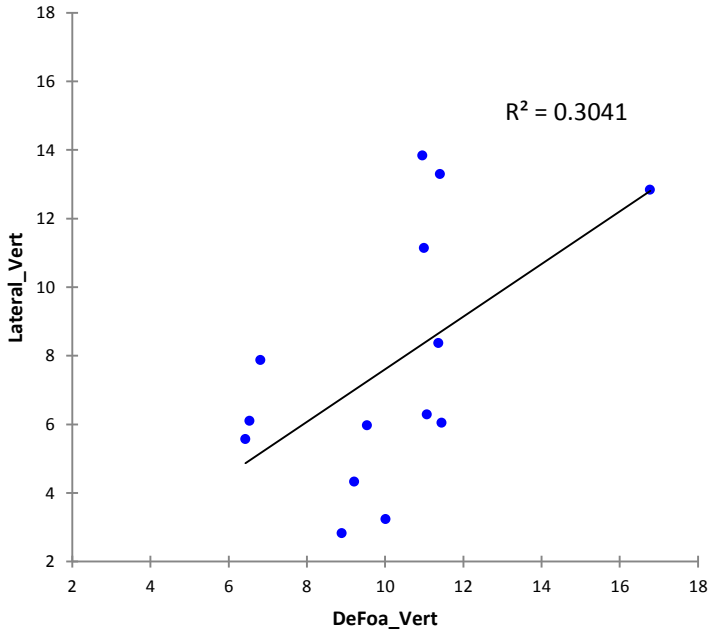

Figure 93. Scatter plot comparing De Foa and Fibre Line method using vertical reference line.

The scatter plot show a poor fit between methods for measuring using Fibre Line method and De Foa method against a vertical reference line $t(13) = -2.88$, $p = .01$, overall model fit was $R^2 = 0.3$.

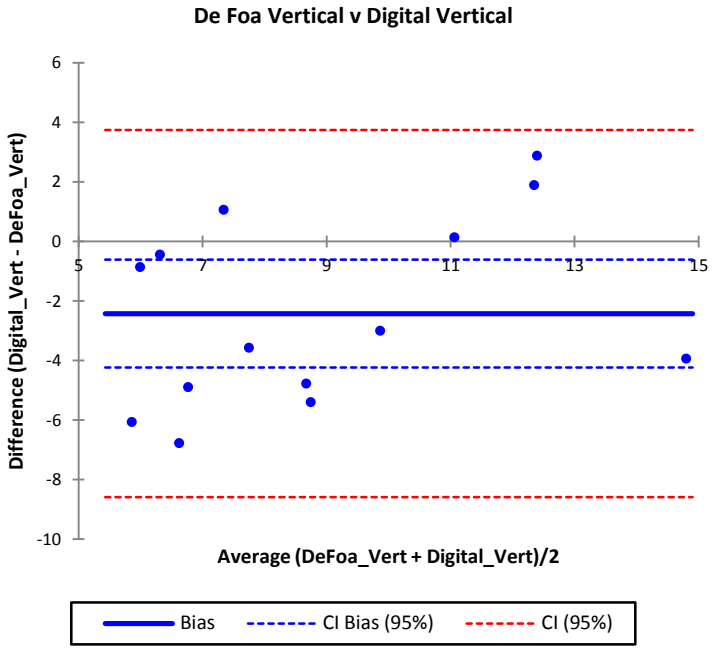

Figure 94. Limits of agreement for Iliocostalis – measured against a vertical reference line.

Table 20. Limits of agreement Iliocostalis – vertical reference line.

	Differences
Sample size, right and left sides	**14**
Bias	**-2.42°**
95% CI difference between means (Bias)	**-4.24 to - 0.61**
Standard error	**3.14**
Lower limit (LOA)	**3.74**
Upper limit (LOA)	**-8.58**

Limits of agreement for the vertical angle (b) (Figure 85) of Iliocostalis muscle fibres measured with respect to a L4–S2 vertical reference line using digital method (d) (Figure 85). The mean difference and the limits of agreement (± 1.96sd) are indicated. Blue lines (Figure 94) indicate confidence intervals for limits of agreement (lower and upper limit 95% CI), dashed red line indicate limits of agreement.

The bias of -2.42° would indicate that the two methods in this case are clinically equivalent, the limits of agreement are wide, 3.74, -8.58, this is larger than 10° and there is a trend with limits of agreement being greater for larger angles.

Calculation of 90% confidence intervals for comparison between De Foa and Lateral Border method against the vertical reference line was -3.9° to -0.93°. This lies within the range of clinical indifference and with 95% confidence it can be concluded that two methods are equivalent.

5.7.7 Comparing Fibre Line method with De Foa method against a horizontal reference line

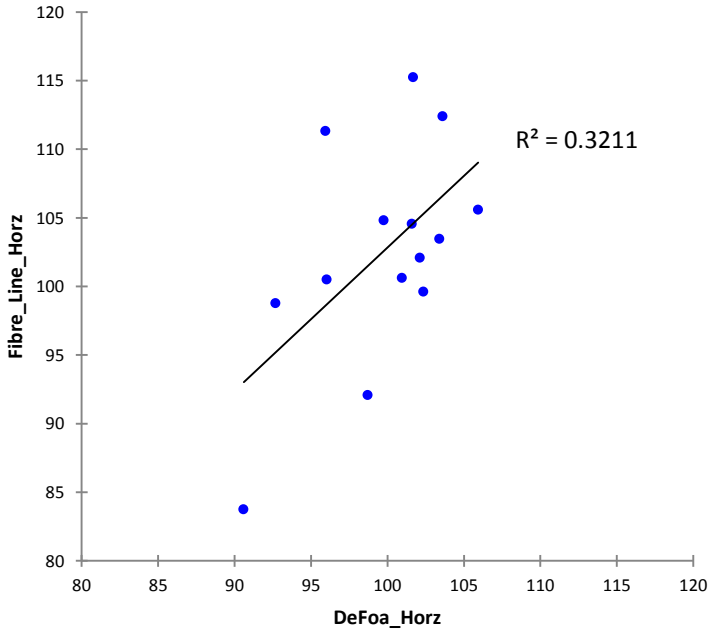

Figure 95. Scatter plot comparing Fibre Line method with De Foa method using a horizontal reference line.

The scatter plot show a poor fit between methods for measuring using L2/3 and De Foa horizontal lines $t\,(13) = 1.58$, $p = .14$, overall model fit was $R^2 = 0.32$.

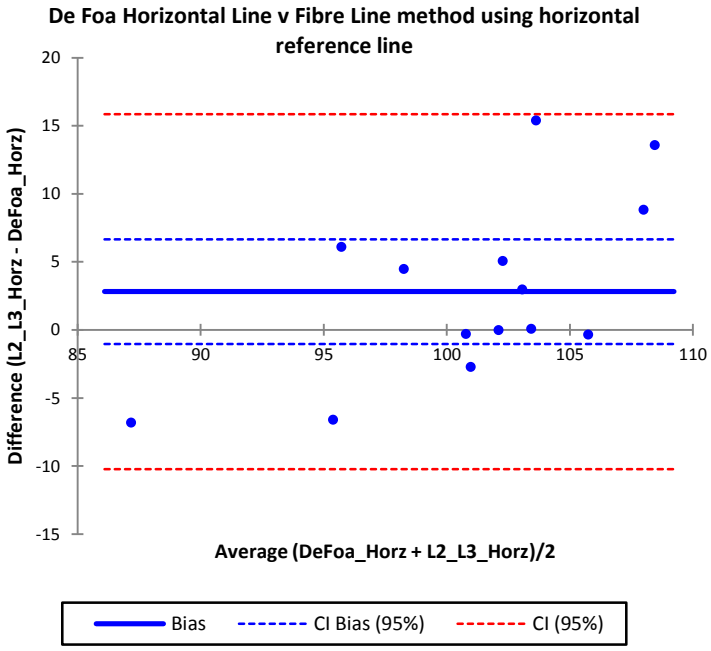

Figure 96. Limits of agreement; Fibre Line method with De Foa method using a horizontal reference line.

Table 21. Limits of agreement Fibre Line method with De Foa method using a horizontal reference line.

	Differences
Sample size, right and left sides	**14**
Bias	**2.81°**
95% CI difference between means (Bias)	**-1.03 to 6.66**
Standard error	**6.66**
Lower limit (LOA)	**-10.24**
Upper limit (LOA)	**15.86**

Limits of agreement for the De Foa Method (a) (Figure 85) and Fibre Line method (e) of Iliocostalis muscle fibres measured with respect to a horizontal reference line (Figure 85). The mean difference and the limits of agreement (± 1.96sd) are indicated. Blue lines indicate confidence intervals for limits of agreement (lower and upper limit 95% CI), dashed red line indicate limits of agreement.

The bias of 2.81° would indicate that the two methods in this case are clinically equivalent, the limits of agreement are wide, -10.24, 15.86, this is in the order of 25° and there is a trend with limits of agreement being greater for larger angles.

Calculation of 90% confidence intervals for comparison between De Foa and L2/3 Horizontal method was -0.34° to -5.96°. This lies within the range of clinical indifference and with 95% confidence it can be concluded that two methods are equivalent.

5.7.8 Comparing Fibre Line method and De Foa method against a horizontal reference line

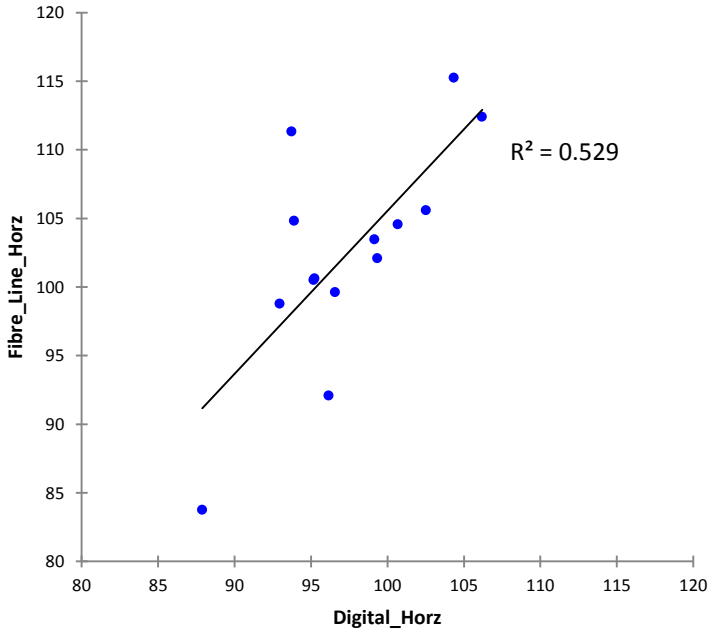

Figure 97. Digital horizontal reference line and Fibre Line method horizontal line.

The scatter plot show a fit between methods for measuring using digital horizontal reference line and Fibre Line method horizontal line t (13) = 3.37, p = .005, overall model fit was R^2 =0.53.

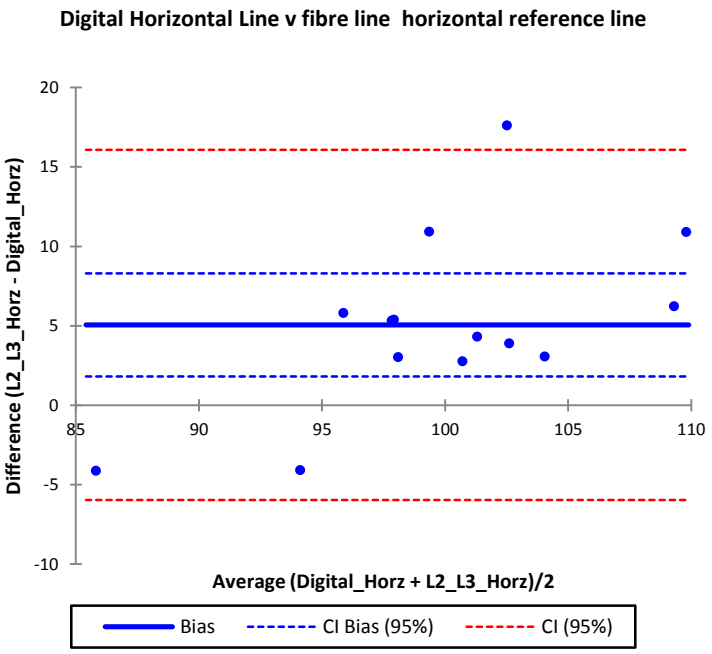

Figure 98. Digital horizontal reference line and Fibre Line method horizontal line.

Table 22. Limits of agreement digital horizontal reference line and Fibre Line method horizontal line.

	Differences
Sample size, right and left sides	**14**
Bias	**5.06°**
95% CI difference between means (Bias)	**1.8 to 8.3**
Standard error	**5.62**
Lower limit (LOA)	**-5.96**
Upper limit (LOA)	**16.08**

Limits of agreement for the Iliocostalis Lateral border horizontal line (c) of Iliocostalis muscle fibres measured with respect to a Fibre Line method horizontal reference line using digital method (e). The mean difference and the limits of agreement (± 1.96sd) are indicated. Blue lines indicate confidence intervals for limits of agreement (lower and upper limit 95% CI), dashed red line indicate limits of agreement.

The bias of 5.06° would indicate that the two methods in this case are clinically equivalent, the limits of agreement are wide, -5.96, 16.08, this is in the order of 21° and there is a trend with limits of agreement being greater for larger angles.

Calculation of 90% confidence intervals for comparison between Fibre Line method horizontal method and Digital method was 2.4° to 7.3°. This lies within the range of clinical indifference and with 95% confidence it can be concluded that two methods are equivalent.

5.7.9 Comparing Fibre Line method and Lateral Border method against a horizontal reference line

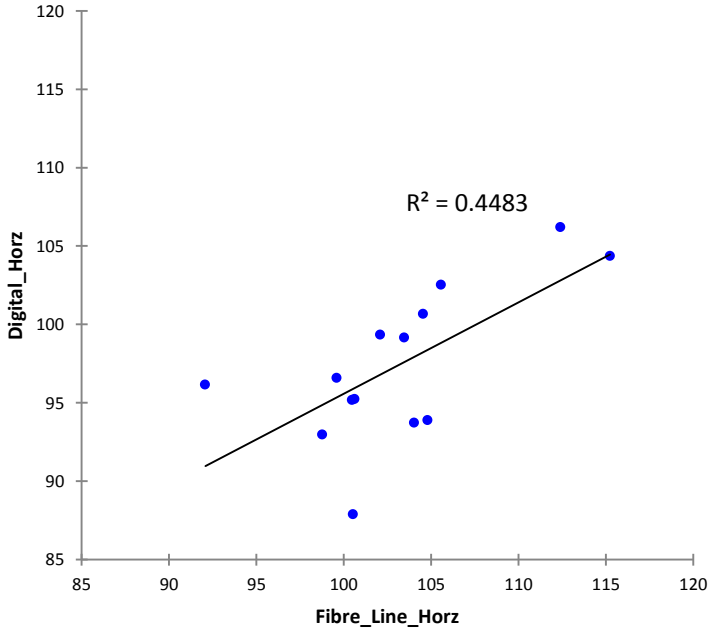

Figure 99. Comparing Fibre Line method and Lateral Border method against a horizontal reference line.

The scatter plot (Figure 99) show a fit between methods for measuring using digital horizontal reference line and Fibre Line horizontal line t (13) = 4.92, p = <.001, overall model fit was R^2 =0.45.

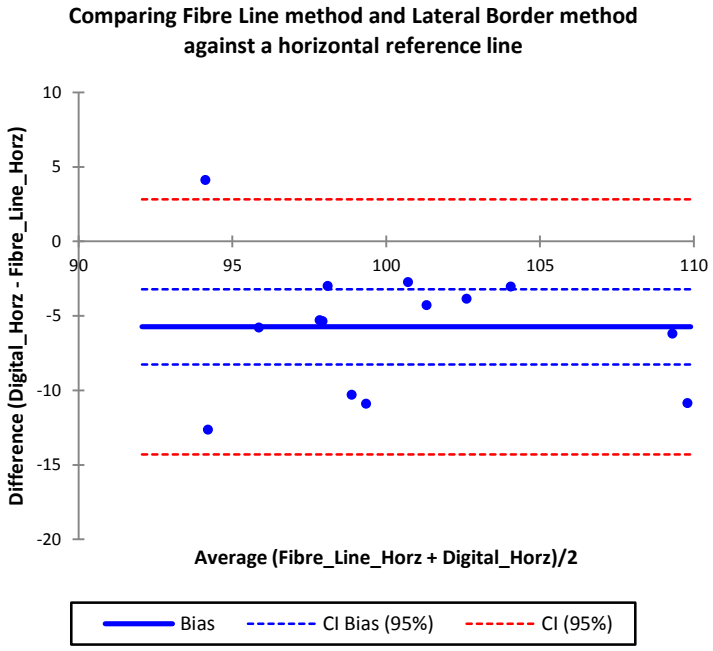

Figure 100. Bland and Altman plot comparing Fibre Line method and Lateral Border method against a horizontal reference line.

Table 23. Limits of agreement Fibre Line method and Lateral Border method against a horizontal reference line.

	Differences
Sample size, right and left sides	14
Bias	5.74
95% CI difference between means (Bias)	3.22 to 8.26
Standard error	4.37
Lower limit (LOA)	-2.82
Upper limit (LOA)	14.3

Limits of agreement for the Fibre Line method (e) and Lateral Border Method (c) against a horizontal reference line. The mean difference and the limits of agreement (± 1.96sd) are indicated. Blue lines indicate confidence intervals for limits of agreement (lower and upper limit 95% CI), dashed red line indicate limits of agreement.

The bias of 5.74° would indicate that the two methods in this case are clinically equivalent, the limits of agreement are wide, -2.82, 14.3, this is in the order of 17° and there is a trend with limits of agreement being greater for smaller angles.

Calculation of 90% confidence intervals for comparison between L2/3 horizontal method and Digital method was 2.4° to 7.3°. This lies within the range of clinical indifference and with 95% confidence it can be concluded that two methods are equivalent.

5.7.10 Comparing Fibre Line method and Lateral Border method against a vertical reference line

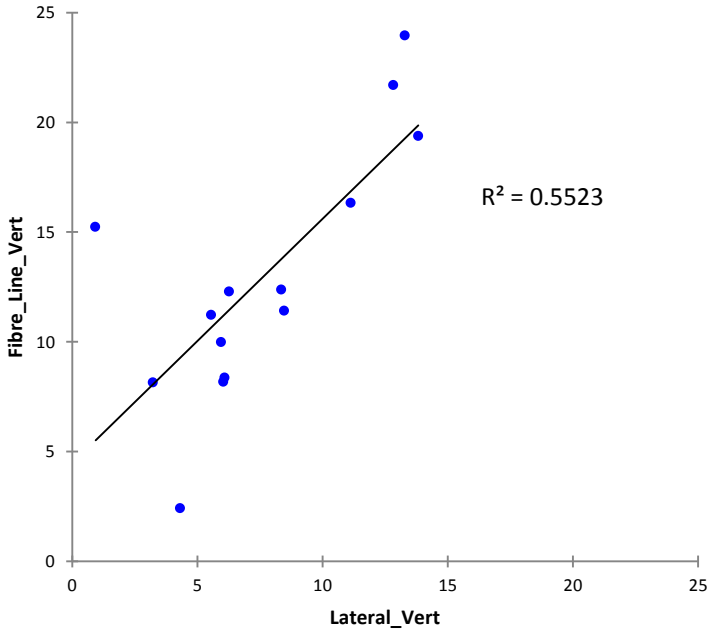

Figure 101. Comparing Fibre Line method and Lateral Border method against vertical reference line.

The scatter plot (Figure 101) show a fit between methods for measuring using digital horizontal reference line and Fibre Line horizontal line $t\,(13) = 5.05$ $p = <.001$, overall model fit was $R^2 = 0.55$.

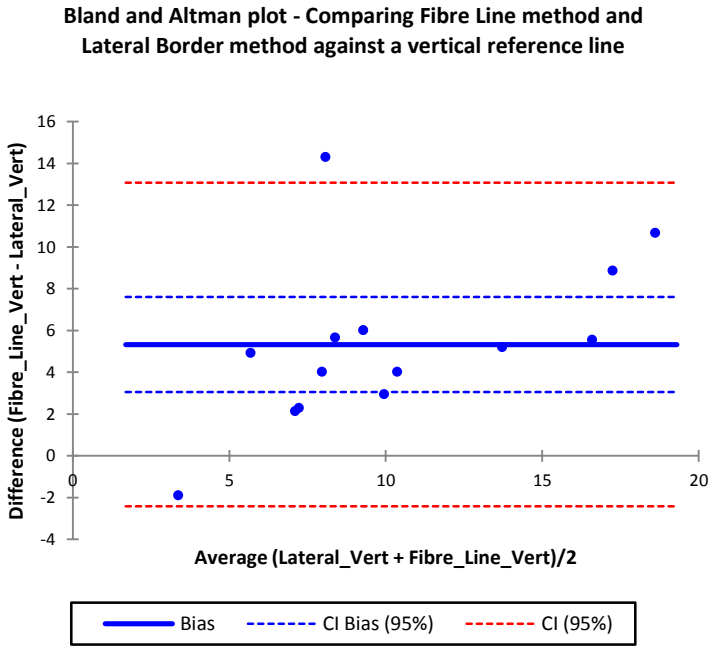

Figure 102. Comparing Fibre Line method and Lateral Border method against a vertical reference line.

Table 24. Limits of agreement Fibre Line method and Lateral Border method against a vertical reference line.

	Differences
Sample size, right and left sides	14
Bias	5.33
95% CI difference between means (Bias)	3.05 to 7.61
Standard error	3.95
Lower limit (LOA)	-2.42
Upper limit (LOA)	13.1

Limits of agreement for Fibre Line method (g) and Lateral Border method (d) against a vertical reference line. The mean difference and the limits of agreement (± 1.96sd) are indicated. Blue lines indicate confidence intervals for limits of agreement (lower and upper limit 95% CI), dashed red line indicate limits of agreement.

The bias of 5.33° would indicate that the two methods in this case are clinically equivalent, the limits of agreement are wide, -2.42, 13.1, this is in the order of 15° and there is a trend with Limits of agreement being greater for larger angles.

Calculation of 90% confidence intervals for comparison between Fibre Line method and Lateral Border method against a vertical reference line was 2.08° to 8.4°. This lies within the range of clinical indifference and with 95% confidence it can be concluded that two methods are equivalent.

5.7.11 Multifidus Results

For Multifidus the De Foa and Fibre Line method were compared.

No statistically significant differences, as analysed by Wilcoxon signed-rank test, were seen between the right and left sides when analysis either the De Foa method or the Digital Image method.

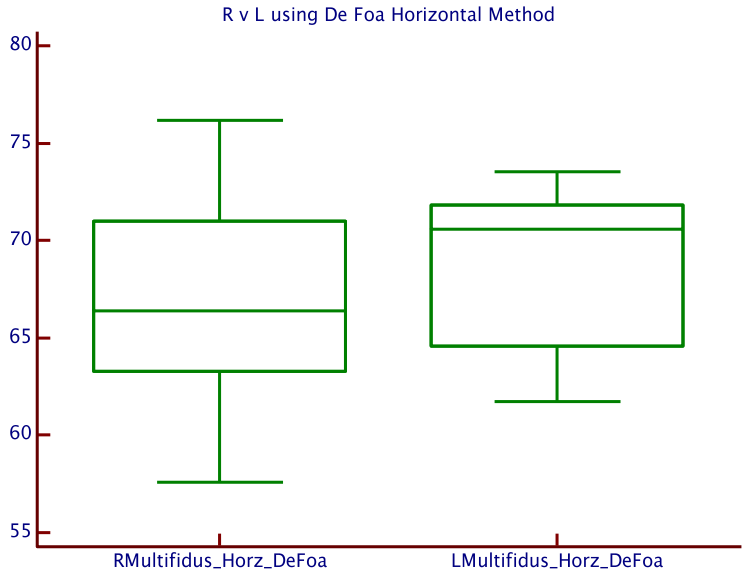

Figure 103. Right and left comparison of Multifidus using De Foa Horizontal Method.

The two sets of data do not differ significantly $W(7)= -10$, $Z= -2.3$, $p= .5$ when comparing the right and left side data for Multifidus using the De Foa Horizontal Method (Figure 103).

Calculation of 90% confidence intervals for comparison between right and left side using De Foa Horizontal method was -4.9° to 1.6°. This lies within the range of clinical indifference and with 95% confidence it can be concluded that the measures of the two sides are equivalent.

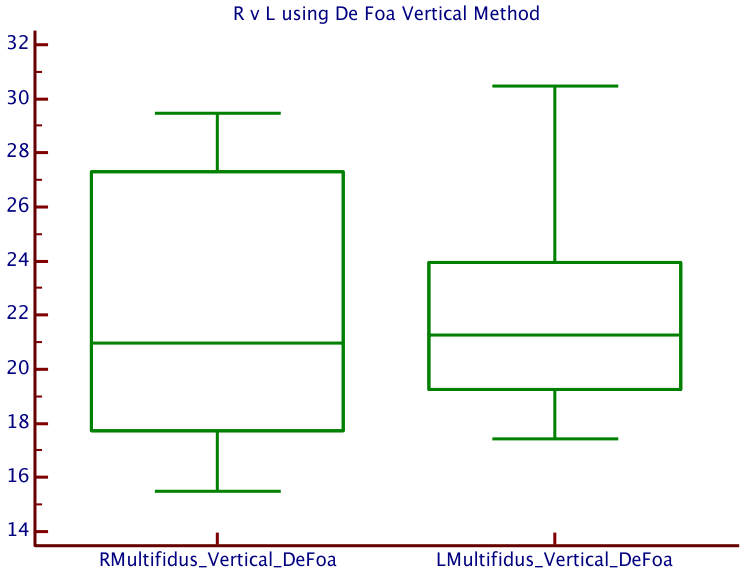

Figure 104.Right and left comparison of Multifidus using De Foa Vertical Method.

The two sets of data do not differ significantly $W(7)= 0$, $Z= -0.7$, $p= .9$ when comparing the right and left side data for Multifidus using the De Foa Vertical Method (Figure 104).

Calculation of 90% confidence intervals for comparison between right and left side using De Foa Horizontal method was -1.4° to 1.8°. This lies within the range of clinical indifference and with 95% confidence it can be concluded that two sides are equivalent.

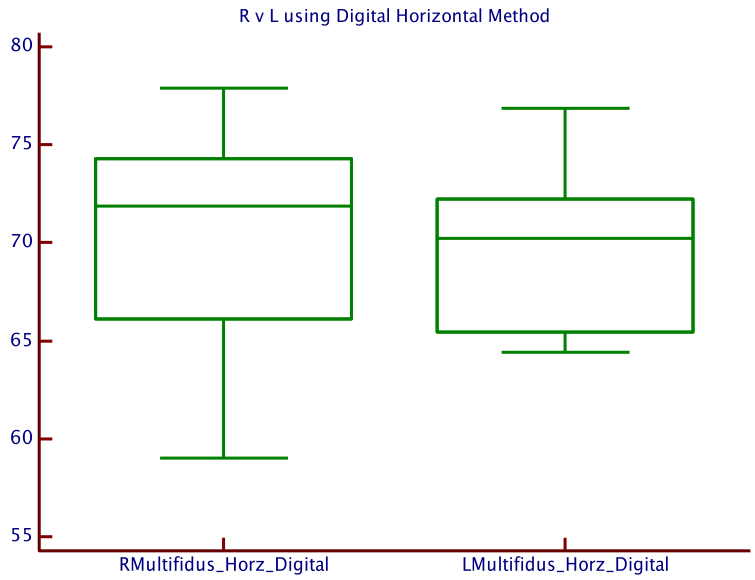

Figure 105.Right and left comparison of Multifidus using horizontal Digital Method.

The two sets of data do not differ significantly $W(7)= 6$, $Z= 1.5$, $p= .7$ when comparing the right and left side data for Multifidus using horizontal Digital Method (Figure 105).

Calculation of 90% confidence intervals for comparison between right and left side using De Foa Horizontal method was -3.8° to 4.3°. This lies within the range of clinical indifference and with 95% confidence it can be concluded that two sides are equivalent.

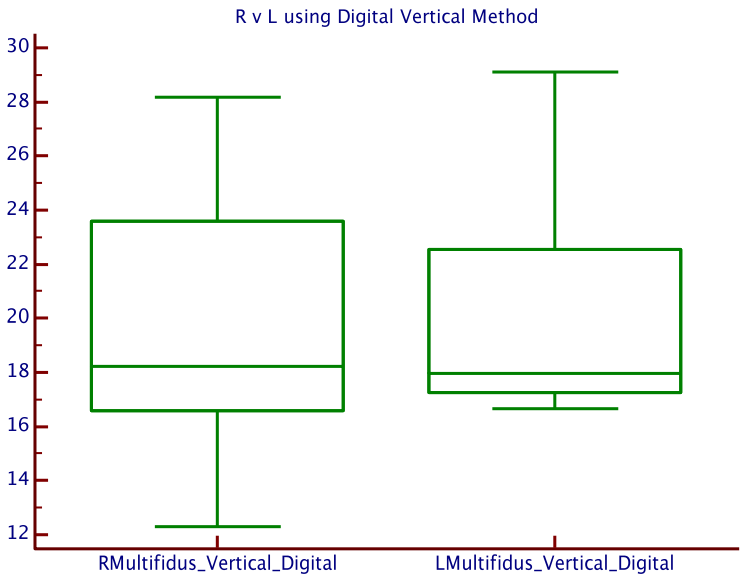

Figure 106.Right and left comparison of Multifidus using Digital Vertical Method.

The two sets of data do not differ significantly $W(7)=-8$, $Z= -0.9$, $p= .6$ when comparing the right and left side data for Multifidus using Digital Vertical Method (Figure 106).

Calculation of 90% confidence intervals for comparison between right and left side using De Foa Horizontal method was -2.5° to 1.3°. This lies within the range of clinical indifference and with 95% confidence it can be concluded that two sides are equivalent.

5.7.11.1 Male v female: Multifidus De Foa and Fibre Line method

Male v female for Multifidus using the De Foa and Fibre Line method were compared.

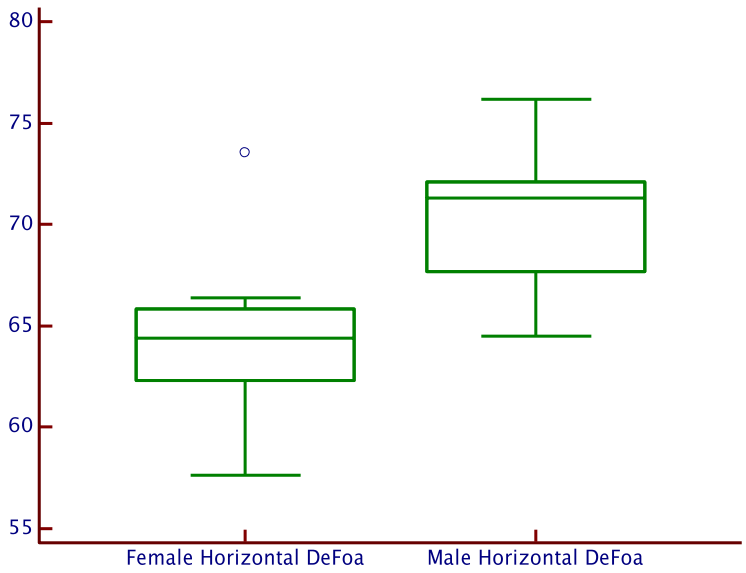

Figure 107. Male v female for Multifidus using the De Foa Horizontal Line method.

The two groups differed significantly U(14) = 7.5, Z = 2.13, p = .03 (Figure 107).

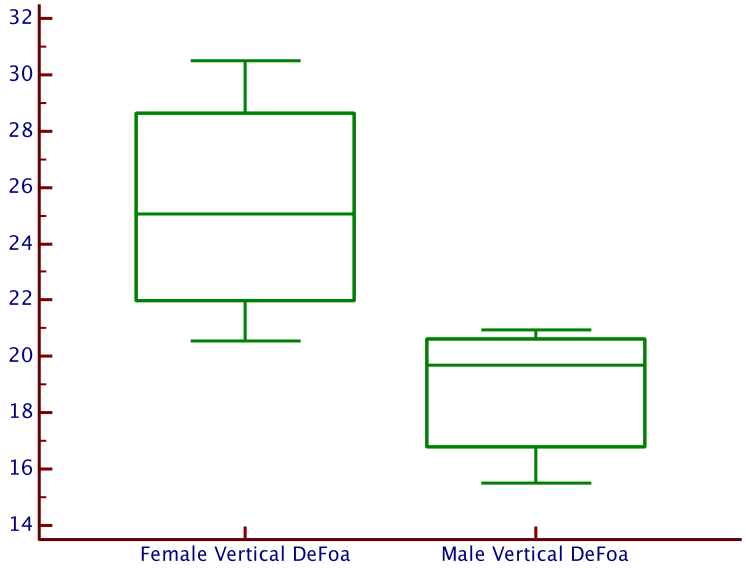

Figure 108. Male v female for Multifidus using the De Foa Vertical line method

The two groups differed significantly U(14) = 2.5, Z = 2.8, *p* = <.001 (Figure 108).

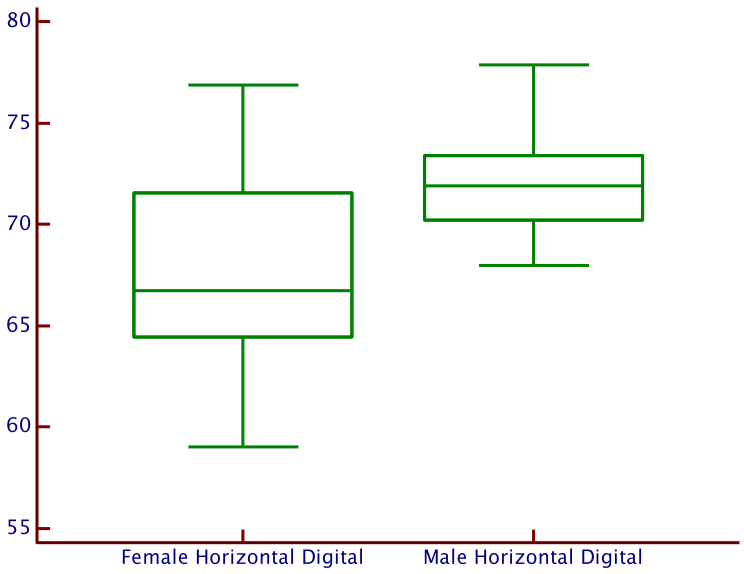

Figure 109. Male v female for Multifidus using Horizontal Digital method.

The two groups did not differ significantly U(14) = 11.5, Z = 1.6, p = .1 (Figure 109).

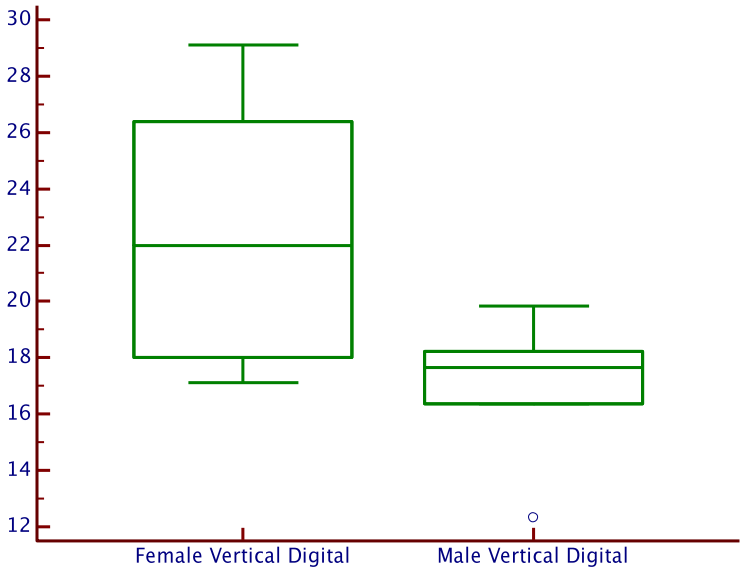

Figure 110. Male v female for Multifidus using Vertical Digital method.

The two groups differed significantly U(14) = 8.5, Z = 2.0, p = .04 (Figure 110).

5.7.12 Inter-rater and Intra-rater reliability

Intra-rater reliability (ICC (2,1) – two-way mixed – absolute agreement) for all methods measuring fibre angle from a vertical reference line were excellent, ranging from 0.94 to 0.99. Inter-rater reliability (ICC (3,1) two way random – absolute agreement) (for the De Foa and Digital Image methods was excellent (0.95 to 0.97) and for the L2/L3 Fibre Line method was good (0.77).

For angle measurements from a horizontal reference line, the intra-rater reliability (ICC (2,1) two-way mixed – absolute agreement) was excellent for all methods (0.98 to 0.99) and the inter-rater reliability (ICC (3,1) two way random – absolute agreement) was excellent for the De Foa and Digital Image methods (0.97 to 0.99) and good for the L2/L3 Fibre Line method (0.77). All reliability levels are in accordance with Shrout and Fleiss (1979).

5.8 Discussion

The aim of this study was to validate a method of fibre angle measurement for Iliocostalis to allow for greater accuracy of anatomical description and therefore to facilitate the standardisation of the positioning of sEMG electrodes for the lumbar Erector Spinae muscles.

Of particular interest was how the location of the Erector Spinae and Multifidus muscles could be determined with confidence from anatomical markings or locations on the surface of the body. Previous studies had not determined their location with sufficient accuracy for the proposed method to investigate the fatigue characteristics with multi-channel sEMG. The SENIAM guidelines (Merletti & Hermens 2000) were designed with monopolar and bipolar sEMG and given that using high-density sEMG electrodes requires great precision, an anatomical study was undertaken of the Erector Spinae muscle of interest (See Section 6);

Surface EMG for Non-Invasive Assessment of Muscles (SENIAM) (Hermens et al., 2000) produced a set of European guidelines concerning EMG sensors, their positioning criteria, EMG processing, modelling and information extraction. According to these recommendations the electrodes for the Iliocostalis muscle should be placed one finger width medial from a line from the PSIS to the

lowest point of the lower rib at the level of L2. Sensors should be orientated in the direction of the line between the PSIS and lowest point of the lower rib and the distance between corresponding electrodes should be 20 mm (IED). SENIAM guidelines are for bipolar electrodes only; currently no guidelines exist for high-density sEMG electrode positioning. The SENIAM recommendations are comparable with the De Foa et al. (1989) reference line, which runs from the PSIS to the lowest point of the twelfth rib. Results presented in this section also concur with the SENIAM recommendations as the muscle fibres of all specimens were of full thickness above the level of the L2/L3 interspinous space. According to these findings, electrode placement as described by SENIAM for the Iliocostalis muscle would detect activity specifically from the Iliocostalis muscle fibres.

Evaluation of levels of agreement and equivalence for the following; the De Foa method, Digital Fibre Line methods and the Lateral Border method for Iliocostalis muscle fibre angle with respect to both the horizontal and vertical reference lines and for Multifidus the De Foa and Fibre Line method, were undertaken. Both methods demonstrated that there was clinical equivalence between the DeFoa method as originally described and the methods devised for this study. The small number of individuals measured, the wide limits of agreement and inconsistent variability require these conclusions to be considered with some caution.

There were no significant differences between left and right sides although the muscle fibre angle of female specimens showed greater variation compared to male specimens, particularly with regards to the vertical reference line. This may be due to scoliosis (defined as a lateral curvature of the spine (Stokes 1994)), observed in all of the female specimens, which may have impacted upon the range of values obtained in the present study. This is one of the limitations of using cadavers from older people.

The digital method was devised specifically to enable measurements to be taken directly from cadavers from older people. These methods were compared with the De Foa et al. (1989) method, which was deemed more clinically applicable as the reference line was created using palpable surface landmarks. This is opposed to the muscular attachment points used for the reference lines visible only via dissection. The replication of the De Foa et al. (1989) method in this study produced comparable results to those previously

published (De Foa et al., 1989). With respect to the vertical reference line it was found that the angle of muscle fibres ranged from 6.43° to 16.78°; the angles obtained by De Foa et al. (1989) ranged from 11° to 17°. Half of the results fell within this range; all remaining angles measured were smaller relative to the vertical i.e. less oblique. Of these angles, four out of seven measurements were only marginally below the range of De Foa et al. (1989), with a maximum difference of 1.78°. The most extreme outlier was 4.57° outside the lowest range; a possible explanation for the two outliers is the presence of scoliosis observed in these cadavers although the possibility that the process of embalming, storage and dissecting could also change tissue sufficiently to alter measurement validity and accuracy.

The two new devised methods were compared with the De Foa et al. (1989) method to test the robustness of the reference line described. Furthermore the original results of De Foa et al. (1989) showed that the landmark derived reference line was sufficiently related to muscle fibre direction at the L2/L3 level (Fibre Line Method), which was concluded to be optimal as an electrode placement site with many active fibres overlain only by the thin dorsal thoracolumbar fascia. The angle of this 'Fibre Line' was therefore also compared to the De Foa et al. (1989) reference line on the digital image. The systematic bias and random error for all method comparison measurements are similar, ranging from 2.0° to 2.5° and 6.0° to 8.3°, respectively. Furthermore the ICC values for all methods except Fibre Line angle were very close to 1, demonstrating excellent intra- and inter-observer reliability.

Therefore either the vertical or horizontal reference lines could be used to obtain fibre angle measurements, and the methods may be used interchangeably. However it is suggested that the horizontal reference line is more clinically applicable as the PSISs are more easily palpated and this line minimises the possible effect of a spinal scoliosis on fibre angle measurements found with the vertical reference line.

According to Merletti (Personal Communication, 2010), the use of 2-D arrays in sEMG of paraspinal muscles reduces the problem of misalignment since 2D interpolation would allow estimation of fibre direction, even if the columns of the array are not well aligned with the fibre direction. The misalignment of a

single array by 5° to 10° would be within the range of clinical indifference. The errors obtained by method agreement are typically less than 10°; therefore the De Foa et al. (1989) reference line is shown to be suitable to demarcate and approximate Iliocostalis fibre direction for use in multi-channel sEMG.

5.9 Limitations

Limitations to the study include the difficulty in demarcating the L2/L3 fibre line (Fibre Line Method) due to subjectivity and the degree of undulation of the muscle fibres. The scoliosis observed in the female specimens may have impacted upon the results obtained. This is a limitation of using elderly cadavers and it is recommended that further research includes a greater number of specimens. A possible contribution to the level of systematic bias is the embalming procedure, which may have affected muscle fibre orientation.

Further limitations of this study are that a small convenience sample was used. This was a self-selecting sample of individuals who donated their bodies to the Centre for Learning Anatomical Sciences and as such, it cannot be assumed that they represent the wider general population. The individuals were older and it is assumed died of natural causes but their health status was unknown at the time of death; it may have been that they had been unwell for some time and muscle atrophy may have occurred during the later stages of their life.

5.10 Conclusion and recommendations

It is recommended that the SENIAM guidelines for Iliocostalis electrode placement are used solely for detection of muscle activity for these muscle fibres and not as a generic guideline for the Iliocostalis musculature. The range of clinical indifference was set at 10° as this level of accuracy is considered to be necessary for the accurate application of high-density linear array electrodes. In all cases, where comparisons have been made, the 90% CI were within the limit of clinical indifference, it is concluded that reference lines recommended by DeFoa et al. and the digital reference lines of this study are equivalent for clinical use. In practice, the clinical utility of the DeFoa reference surface markings for Iliocostalis and Multifidus has been demonstrated within the limitations of this experiment; however, further testing and research is required. No recommendation can be made for Longissimus.

6. A post-mortem study of the positional anatomy of Longissimus Thoracis pars Thoracis, Iliocostalis Lumborum pars Thoracis and Lumbar Multifidus.

6.1 Introduction

This second anatomical study followed on from the study described in Section 5 and was carried out on the same individual's bodies that had previously been dissected. Further dissection was required to identify and measure Longissimus once positional measurements had been taken of Iliocostalis and Multifidus.

6.2 Aim

The aim of this study was;

1. To provide a detailed post-mortem anatomical description of the location and relationship of specific lumbar spinal muscles to bony landmarks to inform multi-channel sEMG studies.
2. To investigate and describe the post-mortem detailed segmental morphology of the Longissimus Thoracis pars Thoracis, Iliocostalis Lumborum pars Thoracis and lumbar Multifidus muscles
3. To compare the morphology of the different regions of the Longissimus Thoracis pars Thoracis, Iliocostalis Lumborum pars Thoracis and lumbar Multifidus muscles and investigate differences between genders.
4. To examine post-mortem, the relationships between Longissimus Thoracis pars Thoracis, Iliocostalis Lumborum pars Thoracis and lumbar Multifidus and the Erector Spinae aponeurosis.

6.3 Design

This was a post-mortem case series anatomical study designed to provide a detailed anatomical description of the location of components of the

Longissimus Thoracis pars Thoracis, Iliocostalis Lumborum pars Thoracis and lumbar Multifidus muscles in relation to palpable bony landmarks.

6.4 Method

6.4.1 Cadavers

Three male and four female embalmed adult cadavers aged between 73 to 95 years old (*M*= 84.3; *SD* 8.3 years) were dissected at the Centre for Learning Anatomical Studies (CLAS) at the University of Southampton. The dissection and examination was carried out in accordance with the Human Tissue Act UK (2004) and Anatomy Act UK (1984) and the School of Medicine ethics committee approved the study, which allowed the spinal muscles to be dissected soon after embalming in order to preserve, as far as possible, the integrity of the underlying muscle architecture.

6.4.2 Procedure

Serial fashion dissections were carried out via a median incision along the spinous processes. After skin and subcutaneous tissue were removed, the right and left Iliocostalis and the Longissimus muscles were exposed; the superior and inferior attachments were identified. The superior, inferior, and middle points of the T6, T10 to L5 spinous processes and the S2 tubercle and posterior superior iliac spines (PSISs) were identified using standardised clinical palpation techniques and these were demarcated using coloured ink (Cancer Diagnostics Inc., USA).

Following measurements of Iliocostalis and Longissimus, these muscles were removed by careful dissection to expose the underlying Multifidus group of muscles from which measurements were also taken.

Bony landmarks were used throughout the study from which measurements were taken, as described below, using a digital calliper (Figure 113).

Identification of all muscle groups was undertaken by the researcher and supervisor (an anatomist) for this phase of the study and as part of the inter-rater and intra-rater reliability process there was agreement that the muscle being measured was correctly identified based on attachments and location.

6.4.3 Identification of muscle fibre components

Iliocostalis and Longissimus muscles attaches to the sacrum through an extensive aponeurosis, the Erector Spinae aponeurosis (Figure 111). This aponeurosis blends in a consistent way with muscle fibres that have attachments in the thoracic region. As an objective of this study was to describe and record the location of the most superficial muscle fibres in relation to palpable bony landmarks, serial measurements horizontally from spinous processes were taken. From observations of the individual dissections, it was observed that for the muscle groups under investigation the majority of muscle fibres were included within defined areas. At these locations, it was observed that the muscle had become aponeurotic, as can be seen in Figure 111 and Figure 112.

For Iliocostalis the superficial muscular component is quadrilateral in shape and superficial muscle fibres were consistently found to be present within clearly defined boundaries as follows. Superiorly a medial superior edge was found level with T10, a lateral superior edge level with T12, and medial inferior edge level with L2 and a lateral inferior edge level with L3.

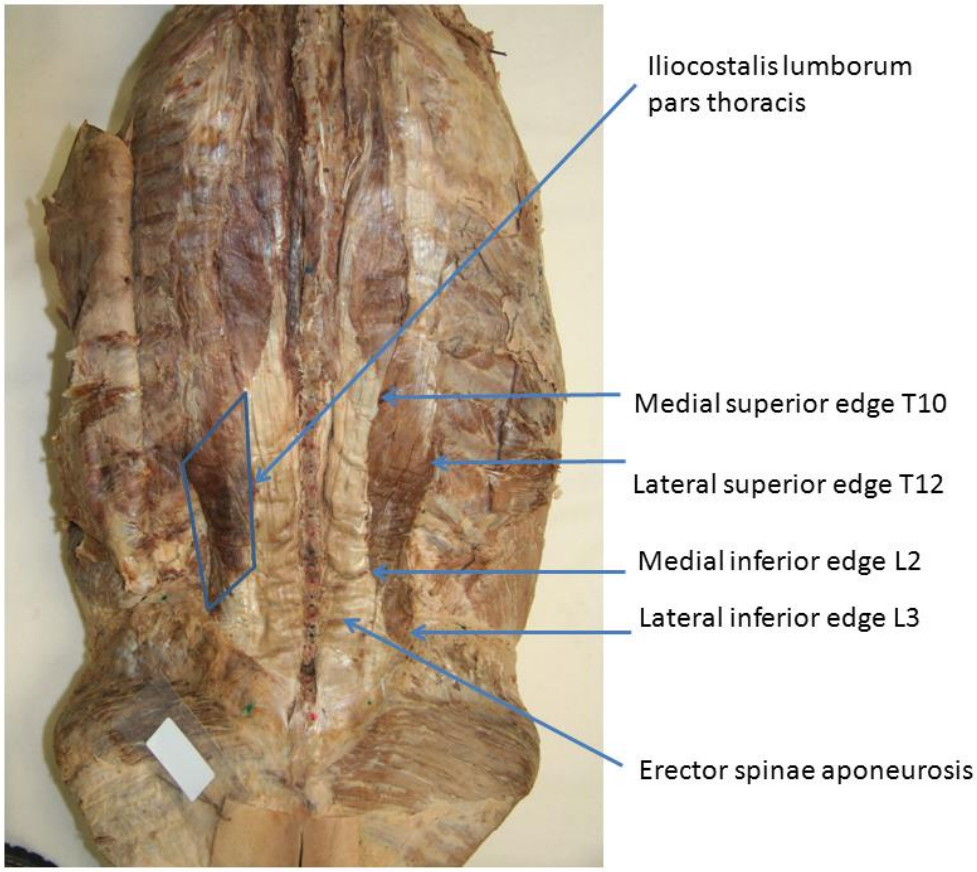

Figure 111. Iliocostalis measurements.

Figure 111 illustrates the posterior view of a dissection of the erector spine group of lumbar spine muscles to illustrate the location of Iliocostalis as defined by the medial and lateral superior edges and the medial and lateral inferior edges.

Longissimus superficial muscle fibres were also consistently found within an inverted trapezium shape defined by the following boundaries; superior medial and lateral edges level with T6 and inferior medial and lateral edges level with T10.

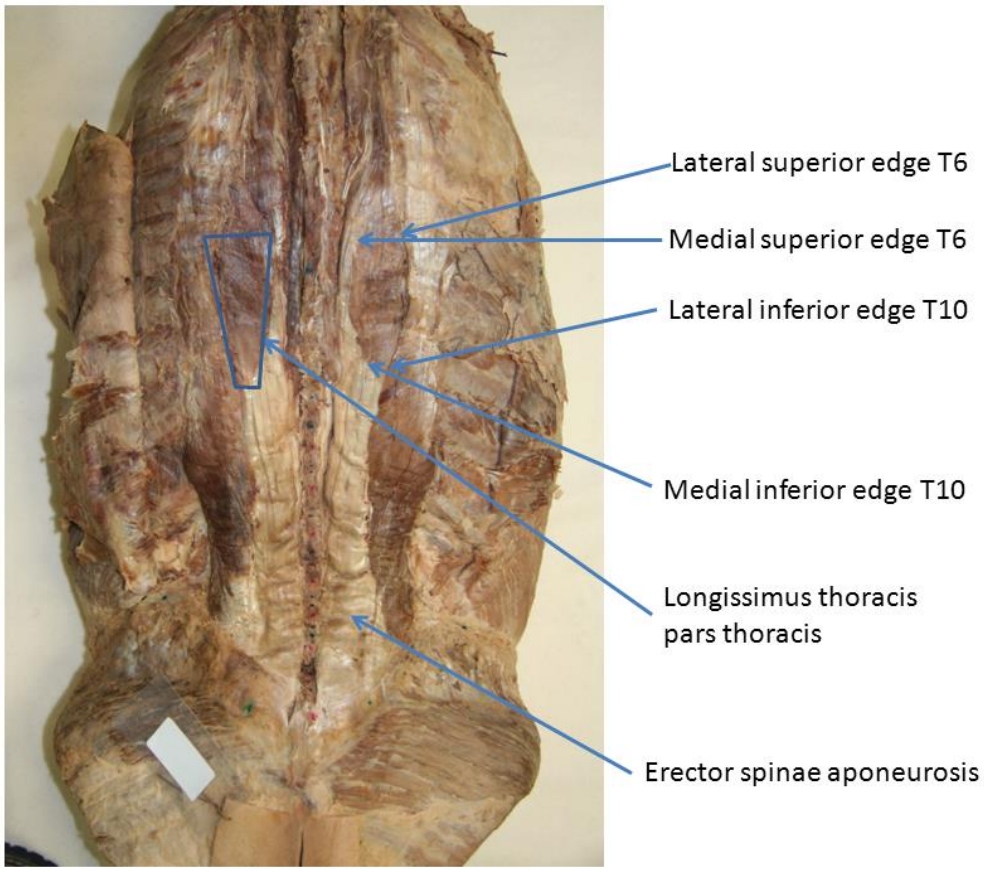

Figure 112. Longissimus measurements.

Figure 112 illustrates the posterior view of a dissection of the erector spine group of lumbar spine muscles to illustrate the location of Longissimus as defined by the medial and lateral superior edges and the medial and lateral inferior edges.

6.4.4 Measurements of Iliocostalis muscle fibre position in relation to bony landmarks

Direct measurements using digital callipers (Mitutoyo, Tokyo, Japan; accuracy 0.01mm) were taken in the horizontal plane from the centre of the spinous processes of L2 and L3 to the medial and lateral inferior borders and at T10 and T12 to the medial and lateral superior border of the right and left Iliocostalis respectively at each of these levels.

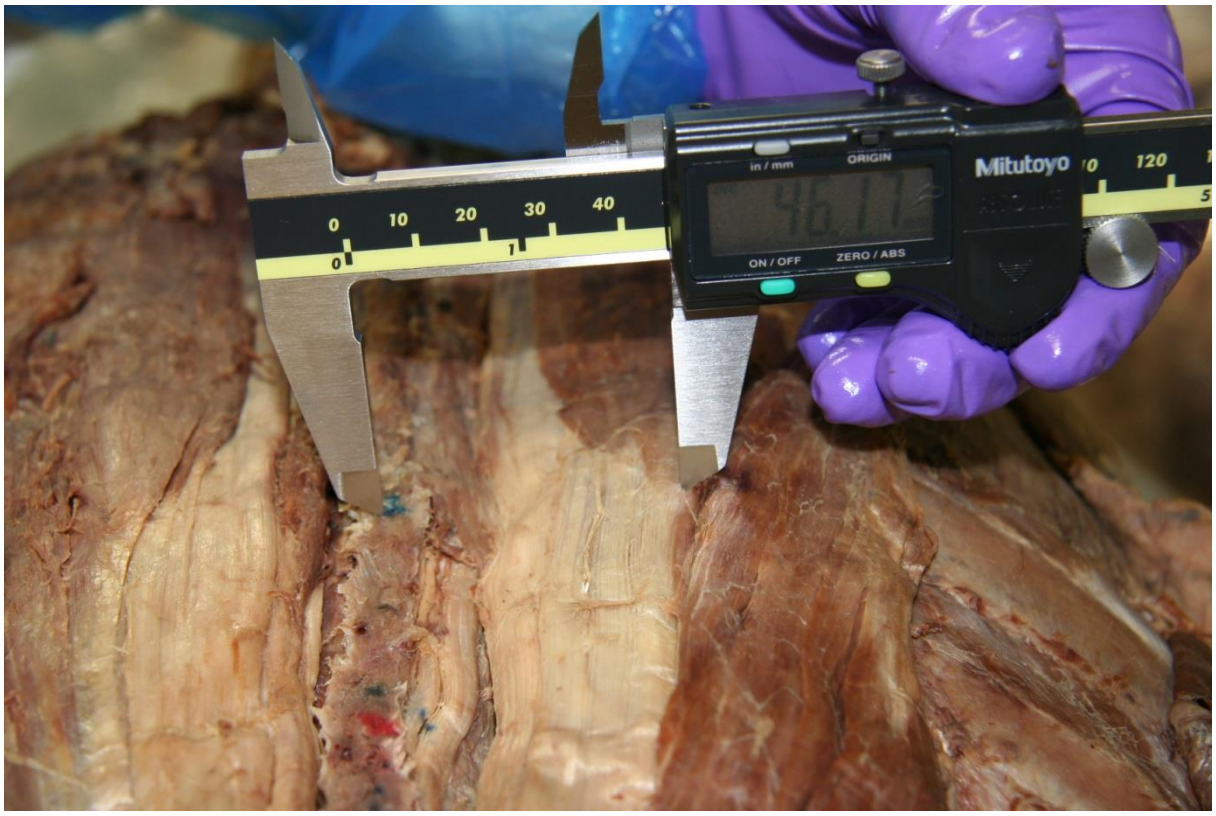

Figure 113. Measurements taken using digital calliper.

Figure 113 to illustrate the use of the digital calliper to measure the edge of a muscle from a defined bony landmark.

One investigator, blind to each value, measured each distance three times; the other investigator recorded each value and reset the calliper to zero before the next reading was taken. Inter- and intra-operator reliability assessment were conducted; inter-operator reliability on the same day and intra-operator reliability seven days after the first set of each measurements.

6.4.5 Measurements of Longissimus

Measurements were taken in the horizontal plane from the centre of the spinous processes of T10 to the medial and lateral inferior edge of the right and left Longissimus at this level and to the medial and lateral superior edges from the centre of the spinous processes at T6.

6.4.6 Measurements of Multifidus

Horizontal measurements were taken from the centre of each spinous process from S2 and L5 to L2 of the right and left Multifidus muscle (Figure 114). At

the level of L1 the fibres of Multifidus were mainly deep and a distinct lateral edge was not always identifiable; where it was possible to identify a lateral edge then measurements were taken and recorded.

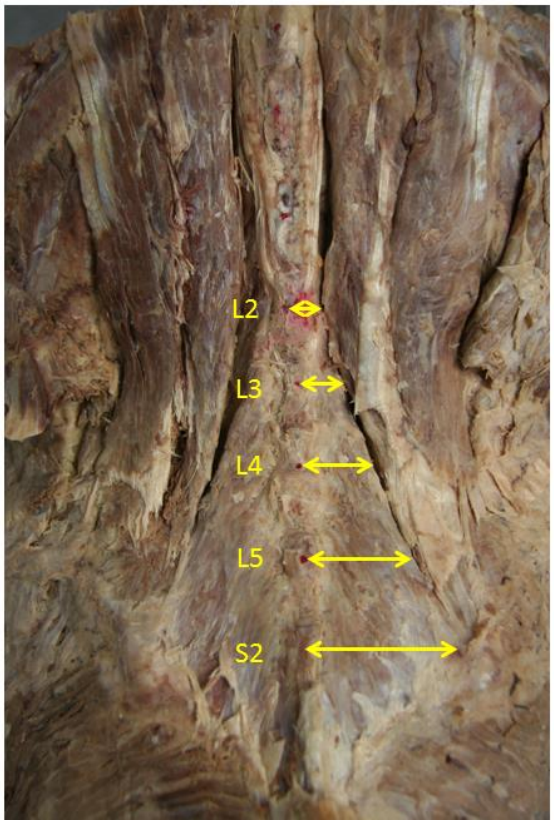

Figure 114. Measurements of Multifidus.

In the posterior view (Figure 114) of a deep dissection of the Multifidus, the lateral border is evident. Measurements were normally made at spinal segment levels as indicated.

6.4.7 Anthropomorphic data

In order to describe the body dimensions, various anthropomorphic measures were taken. Given that the stages of overall dissection differed between each individual, it was not possible to obtain a full set of body data measures in each case.

The following anthropomorphic measurements were taken from each individual;

Distance from the tip of T1 – S2 (tape measure)

Inter Posterior Superior Iliac Spine (PSIS – PSIS) distance (digital calliper)

L1 – S2 measures in mm (digital calliper)

L1 – S2 measures in cm taking into account any lordosis (tape measure)

External Occipital Protuberance – S2 (tape measure).

All measures were taken three times; the operator was blind to each measure for each method used; where practicable digital callipers were used and three measures taken. Where larger distances were involved, a standard tape measure was used and the distance included the natural curvature of the spine. In some cases, the heads of the individuals had been removed so measures from the external occipital protuberance (EOP) were not possible. Distances between the centres of the posterior superior iliac spines (PSIS) and the length of the lumbar spine using both a digital calliper and tape measure were recorded. The age and gender of each individual was also recorded.

A description of the amount of lumbar lordosis was recorded using general terminology such as '*flat'*, '*moderate'* or '*lordotic'* These terms were used purely for descriptive purposes.

6.5 Data analysis

Data were analysed under a number of areas: initial descriptive analysis of various parameters was undertaken, inferential analysis was then used to further explore the data. Analysis of differences, due to gender or body side, was undertaken.

6.5.1 Calculation of muscle mid-point

A calculation was made of the mid-point of the distal and proximal widths of Longissimus and of Iliocostalis; this was calculated as the mean of the mid-point between the lateral and medial edge of each muscle for each side using the following…

$$d = \frac{b - a}{2} + a$$

…where *d* is the distance to the mid-point from the segmental spinous process, *a* is the distance to the medial edge of the muscle of interest and *b* the distance to the lateral edge.

The width, *w* of the muscle, was calculated using…

$$w = a - b.$$

The mid-point of Iliocostalis at T11 and at the L2/3 interspace was calculated to be equidistance between the mid-point of T10 and T12 and the mid-point for L2 and L3 respectively.

For Multifidus, the distances to the lateral border only were measured. An estimation made of the angle from the distal attachment of the most lateral fascicle to the proximal attachment point at the L2/3 interspace based on the method previously described (Biedermann, DeFoa, & Forrest 1991; De Foa, Forrest, & Biedermann 1989), (Section 5).

For the inter-rater and intra-rater reliability, inter-class correlation analysis was undertaken for measures recorded.

6.5.2 Statistical analysis

Equivalence testing (5.6.2) was undertaken to establish whether the confidence intervals (CI) of the angles measured were within clinically acceptable limits that would demonstrate clinical equivalence. The 90% CI for the difference between the two measures was set at ±5mm for Longissimus and Iliocostalis and at ±4mm for Multifidus. The rationale for this range is that it represents half the inter-electrode distance of the array and matrix electrodes respectively and is considered to be the level of accuracy required for clinical application of sEMG sensors.

6.6 Results

Dimensions are presented as means (*M*), standard deviations *(SD)*, medians and ranges. A probability level of p=.05 was set as the minimum criterion of statistical significance in tests.

Statistical analysis was performed using SPSS version 17.0 for Windows (SPSS Inc., Chicago, Illinois, USA) and Microsoft Excel 2010 (Microsoft Corporation, Redmond, WA, USA), XLSTAT Version 2013.4.04, MedCalc ® Version 12.7.0.0 64-bit. © 1993-2013 MedCalc Software and GraphPad Prism version 6.00 for Windows, GraphPad Software, La Jolla California USA, www.graphpad.com.

6.6.1 Individuals

The mean age of the seven individuals was 84.3 years (*SD* 8.3). The mean age of the males was 87.6 years (*SD* 6.5) and the females 81.75 years (*SD* 9.4). Anthropomorphic data were collected for each individual and are presented in Table 25 and differences by gender in Table 26. The requirements of working under the various legislative and ethical considerations prevented data, such as weight or any other details that could have identified the individual, from being collected.

Table 25. Anthropomorphic data analysis of individuals.

Measurements from defined bony landmarks			
	n	**Mean (mm)** ***(SD)***	**Median (mm)** **(range)**
Distance from the tip of T1 – S2	**7**	**477** **(47.3)**	**481** **(404 – 545)**
PSIS – PSIS distance	**7**	**92.6** **(12.57)**	**89.6** **(73.9 – 114.6)**
L1 – S2 measures	**7**	**139.5** **(31.20)**	**147** **(85.59 – 175.22)**
L1 – S2 measures in cm taking into account any lordosis	**7**	**143** **(30.3)**	**151** **(94.0 – 177.1)**
External Occipital Protuberance – S2	**4**	**598** **(66)**	**594** **(522 – 682)**

Table 26. Measurements from defined bony landmarks by gender.

Measurements from defined bony landmarks by gender		
	Female n = 4 **Mean (mm)** ***(SD)***	**Male n = 3** **Mean (mm)** ***(SD)***
Distance from the tip of T1 – S2	**456** **(43.6)**	**505** **(32)**
PSIS – PSIS distance	**96.5** **(13.4)**	**105.4** **(10.6)**
L1 – S2 measures	**125.8** **(2.6)**	**166.0** **(12.0)**

6.6.2 Iliocostalis

The mean *(SD)* and median (range) values from the bony landmarks, (L2, L3 T10 and T12) to the medial and lateral, superior and inferior edges of the muscles are given in Table 27. The muscle width and the muscle mid-points are given in Table 28 and Table 29 respectively. The mid-point is given as a measurement from the L2/3 interspace and T11 as these two points represent the mid-points between the respective bony landmarks.

Table 27. Iliocostalis: measurement from spinous process.

Measurements from spinous process to muscle edge			
	n	**Mean (mm)** ***(SD)***	**Median (mm)** **(range)**
Medial Inferior Edge L2	**7**	**35.8** **(4.04)**	**36.17** **(28.38 – 42.52)**
Lateral Inferior Edge L3	**7**	**63.65** **(4.68)**	**63.44** **(55.39 – 72.19)**
Medial Superior Edge T10	**7**	**45.97** **(6.10)**	**46.09** **(37.40 – 59.91)**
Lateral Superior Edge T12	**7**	**74.61** **(6.65)**	**73.20** **(63.62 – 84.80)**

Table 28. Iliocostalis muscle width.

Iliocostalis Muscle Width			
	n	Mean (mm) *(SD)*	Median (mm) (range)
Width Superior	7	28.64 (8.34)	31.15 (3.71 – 36.30)
Width Inferior	7	27.85 (6.12)	26.29 (21.67 – 43.80)

Table 29. Iliocostalis muscle mid-point from bony landmarks.

Iliocostalis Muscle Mid-Point			
	n	Mean (mm) *(SD)*	Median (mm) (range)
Mid-Point Superior T11	7	60.29 (4.84)	60.33 (51.41 – 67.41)
Mid-Point Inferior L2/3 interspace	7	49.72 (3.13)	49.95 (44.00 – 56.28)

6.6.3 Iliocostalis male v female variation

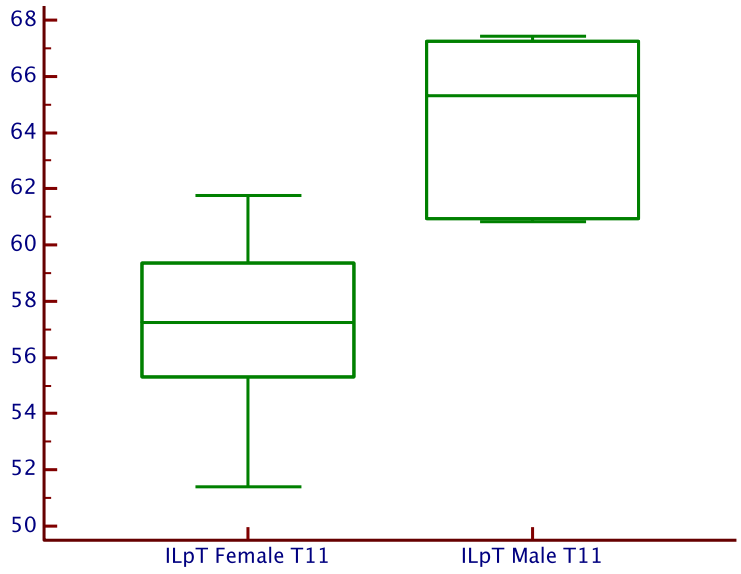

Figure 115. Iliocostalis male v female at T11 mid-point.

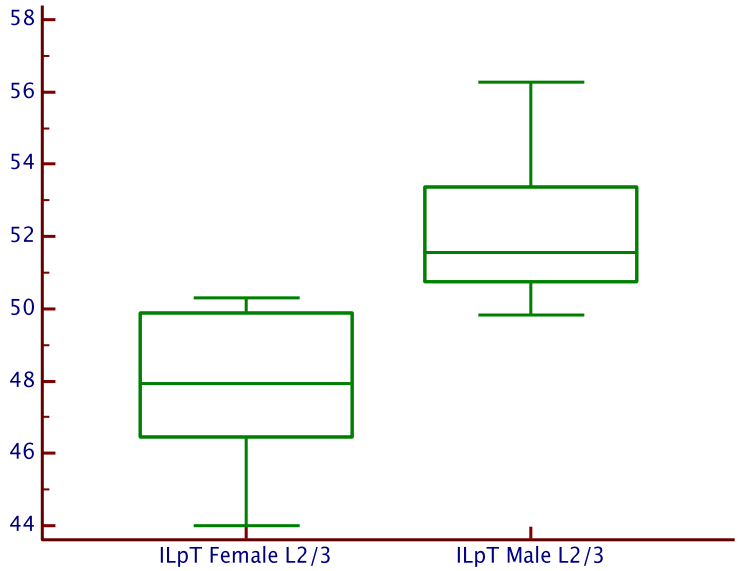

Figure 116. Iliocostalis male v female at L2/3 mid-point.

Figure 115 and Figure 116, illustrates the differences in Iliocostalis mid-point between male and female measured at L2/3 junction and adjacent to T11. The two groups differed significantly, at T11, U(13) = 2.0, Z = 2.8, p = .0045 and at L2/3, U(13) = 2.0, Z = 2.84, p = .0045.

6.6.4 Longissimus

The mean *(SD)* and median (range) values from the bony landmarks, (T10 and T6) to the medial and lateral, superior and inferior edges of the muscles are given in Table 30. The muscle width and the muscle mid-points are given in Table 31 and Table 32 respectively. The mid-point is given as a measurement from T6 and T10.

Table 30. Longissimus.

		Measurements from spinous process to muscle edge	
	n	**Mean (mm) *(SD)***	**Median (mm) (range)**
Medial Superior Edge T6	7	20.29 (6.63)	20.24 (12.71 – 33.56)
Lateral Superior Edge T6	7	46.94 (5.69)	48.10 (35.33 – 54.77)
Medial Inferior Edge T10	7	27.03 (7.47)	24.88 (17.31 – 44.15)
Lateral Inferior Edge T10	7	52.01 (8.97)	53.44 (27.98 – 64.10)

Table 31. Longissimus muscle width.

		Longissimus Muscle Width	
	n	**Mean (mm) *(SD)***	**Median (mm) (range)**
Width Superior T6	7	26.65 (5.73)	24.91 (15.81 – 37.36)
Width Inferior T10	7 Aponeurosis only at T10 in one individual	24.98 (9.49)	25.85 (4.79 – 39.50)

Table 32. Longissimus muscle mid-point from bony landmarks.

	Longissimus Muscle Mid-Point		
	n	Mean (mm) *(SD)*	Median (mm) (range)
Mid-Point Superior T6	7	33.62 (5.47)	34.30 (24.11 – 42.68)
Mid-Point Inferior T10	7 Aponeurosis only at T10 in one individual	39.52 (6.75)	38.62 (25.59 – 52.03)

6.6.5 Longissimus: male v female comparison

Figure 117 and Figure 118, illustrates the differences in Longissimus mid-point between male and female measured adjacent to T6 and T10. The two groups did not differ significantly at T6 $U(13) = 22.0$, $Z = 0.26$, $p = .7$, but at T10, the two groups differed significantly $U(14) = 8.0$, $Z = 2.07$, $p = .039$

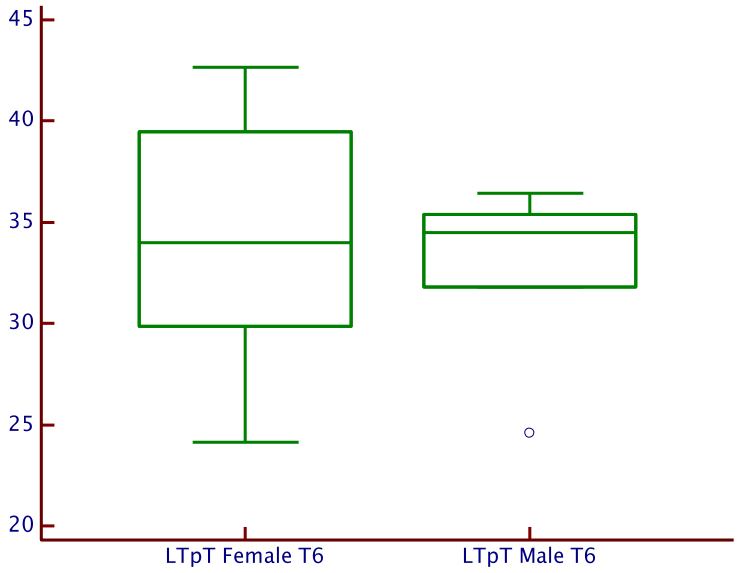

Figure 117. Longissimus: female v male at T6.

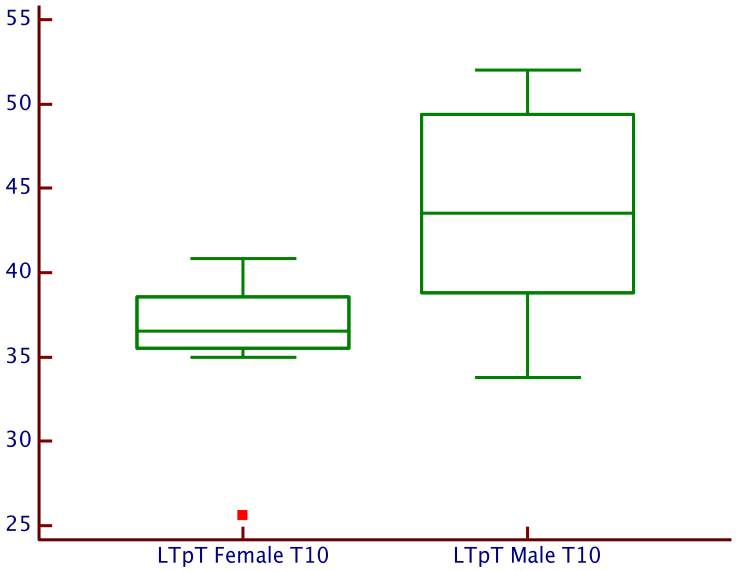

Figure 118. Longissimus: female v male at T10.

6.6.6 Multifidus

The data for Multifidus is presented as the mean, *(SD)* and median, (range) values from the bony landmarks, (S2, L5 to L1 where appropriate) to the lateral edges of the muscles are given in Table 33. The number of sides is indicated rather than the usual number of individuals as it was not always possible to identify muscle tissue at some levels.

Table 33. Multifidus.

		Measurements from spinous process to lateral muscle edge	
	n (right and left sides are recorded)	**Mean (mm) *(SD)***	**Median (mm) (range)**
Lateral edge S2	**14**	**36.39 (5.52)**	**36.66 (26.18 – 45.97)**
Lateral edge L5	**14**	**34.85 (6.51)**	**33.56 (24.65 – 46.27)**
Lateral edge L4	**14**	**27.71 (6.50)**	**29.09 (15.52 – 37.31)**
Lateral edge L3	**13**	**21.24 (4.36)**	**21.15 (12.52 – 29.27)**
Lateral edge L2	**12**	**17.10 (3.43)**	**17.52 (11.77 – 25.25)**
Lateral edge L1	**2**	**18.43 (4.68)**	**18.43 (15.12 – 21.74)**

6.6.7 Multifidus female v male comparison.

Figure 119 shows male and female comparison at S2 segmental level, the two groups differed significantly U(13) = 5.0, $Z = 2.45$, p = .014.

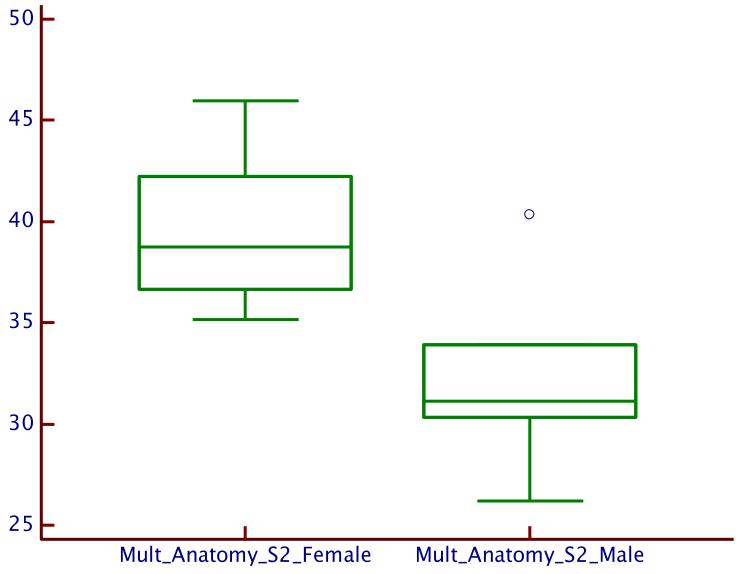

Figure 119. Multifidus: female v male comparison at S2.

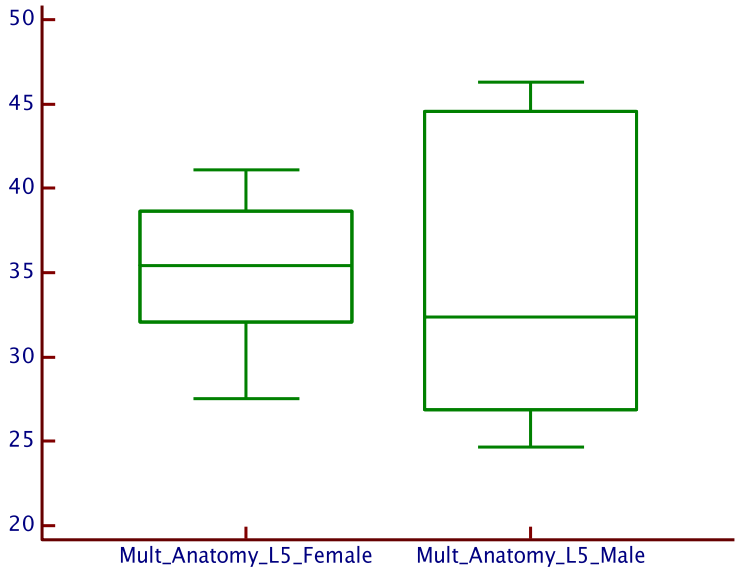

Figure 120. Multifidus: female v male comparison at L5.

Figure 120 shows male and female comparison at L5 segmental, the two groups did not differ significantly U(13) = 21, Z = 0.38, p = .7.

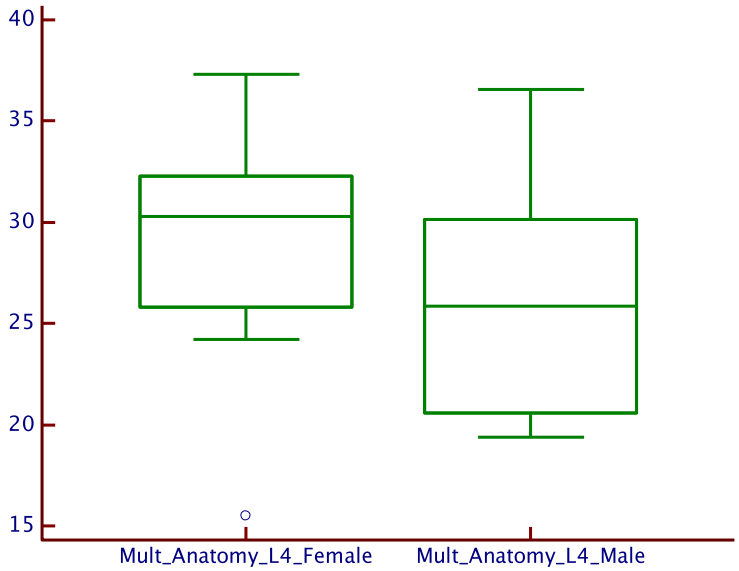

Figure 121. Multifidus: female v male comparison at L4.

Figure 121 shows male and female comparison at L4, the two groups did not differ significantly U(13) = 18, Z = 0.77, p = .4.

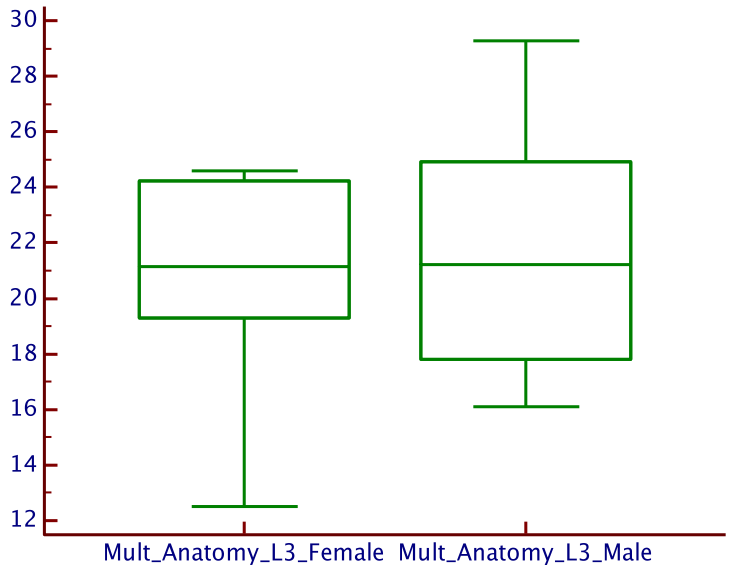

Figure 122. Multifidus: female v male comparison at L3.

Figure 122 shows male and female comparison at L3, the two groups did not differ significantly U(13) = 19, Z = 0.29, p = .8.

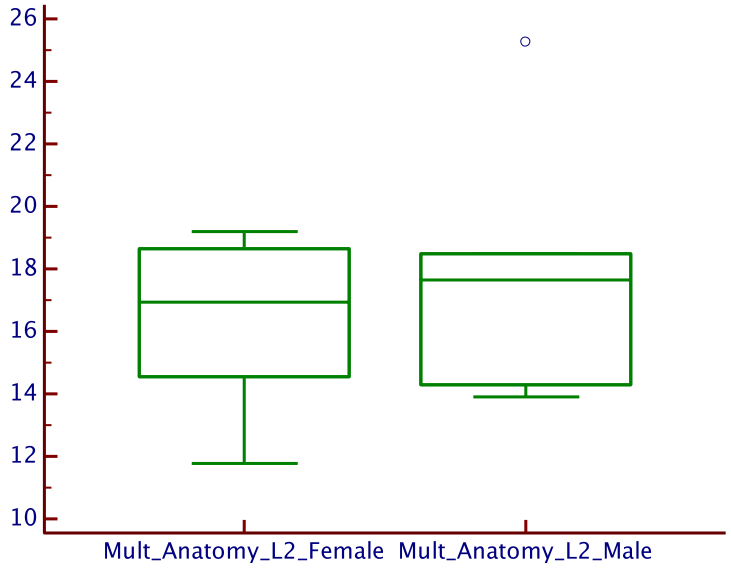

Figure 123. Multifidus: female v male comparison at L2.

Figure 123 shows male and female comparison at L2, the two groups did not differ significantly U(13) = 16, Z = 0.32, p = .75. At L1, missing data prevented analysis.

6.6.8 Inter-rater and intra-rater reliability

Interclass correlation was calculated for the inter-rater and intra-rater reliability and this is presented in Table 34.

Table 34. Inter-rater and intra-rater reliability.

	Muscle width	
	ICC (2,1)	ICC (3,1)
Observer	Intra-observer	Inter-observer
Iliocostalis	**.99 (.99-1.00)**	**.95 (.88-.98)**
Longissimus	**1.00 (1.00-1.00)**	**1.00 (.99-1.00)**
Multifidus	**.97 (.95-.99)**	**.98 (.95-0.99)**

ICCs given are the Average values (with 95% confidence intervals)
ICC (2,1) – two-way mixed – absolute agreement
ICC (3,1) – two-way random – absolute agreement

6.7 Discussion

This study aim was achieved within the constraints of the experimental set up. A methodology was developed and tested to identify the bony landmarks that would be required by a clinician in practice. The accuracy of palpation of spinous processes by suitably trained individuals has been shown to be good to moderate depending on whether symptom reproduction and signs of movement abnormalities were being examined (Jull, Bogduk, & Marsland 1988; Phillips, Barnard, Mullee, & Hurley 2009; Phillips and Twomey 1996). Sensitivity in the order of 63% to 94% is achieved and depends on whether verbal subject's responses are used to indicate symptomatic levels. In a study where signs and symptoms reproduction were excluded from the test, accuracy of palpation is reduced with kappa, using standards of strength (Landis and Koch 1977), of 0.18 (slight) and 0.48 (moderate) for accurate palpation of radiologically identified C7 and L5 respectively (Robinson, Robinson, Bjorke, & Kvale 2009). In another study (Harlick, Milosavljevic, & Milburn 2007), experienced manual therapists accurately identified the correct spinous process with 47% accuracy and were within one segmental level 72% of the time, no kappa statistical analysis was undertaken in this study.

This level of accuracy is problematic in clinical practice when using palpation of bony landmarks for correctly identifying segmental levels of interest. If clinicians are unable to accurately identify the correct vertebral level in practice then inaccurate measurement or treatment is likely.

In this anatomical study, the identification of segmental level was not considered to be in doubt. All spinous processes could be visualised by both the researcher and supervisor and no individuals in the study exhibited abnormalities such as lumbarisation of a sacral segment or additional lumbar or thoracic vertebrae. Agreement as to which spinous segment was being palpated was achieved by agreement between researcher and supervisor and based on agreed methodology (Phillips et al. 2009). Furthermore, the mid-point of each spinous process was identified and marked so that a fixed point could be used for all measures, in clinical practice, this level of accuracy and identification is not likely to be possible. This could be problematic for taking study results forward to clinical practice.

Identification of each muscle was achieved by researcher and supervisor agreeing on identity of muscle during the process of dissection. The identification of the lateral and medial edges of muscles of interest at each segmental level was also by agreement. This process was repeated throughout each dissection and also repeated for the inter-rater reliability process.

Results of this case study series indicate that the methodology used to measure the location of the edges of muscles is reliable both for inter-rater and intra-rater. The use of interpolation of muscle mid-point calculated from measures of the superior, inferior, lateral and medial extent of a muscle is based on the assumptions that the mid-point is equidistant from the two points measured.

6.7.1 Functional independence of Erector Spinae

It is claimed that the morphology and the functionality of the two parts of the lumbar Erector Spinae aponeurosis and Multifidus are distinct with no discernable connection (Bogduk 1980) although this position is contested by some (Daggfeldt, Huang, & Thorstensson 2000). In this study, a connection

between these structures was consistently found for all individuals on both sides and at all levels of the lumbar region.

In each of the images below (Figure 124) the Erector Spinae aponeurosis has been reflected to reveal the presence of muscle and fibrous attachments to the underlying Multifidus muscle. No histological investigation was undertaken of the junctions between the attachments and the Erector Spinae aponeurosis so no conclusion can be drawn as to the nature of the connective tissue, however, in all cases, the tissue had features consistent with muscle fibres and their presence would be consistent with a model where the functionality of the lumbar Multifidus and the Erector Spinae aponeurosis are interdependent.

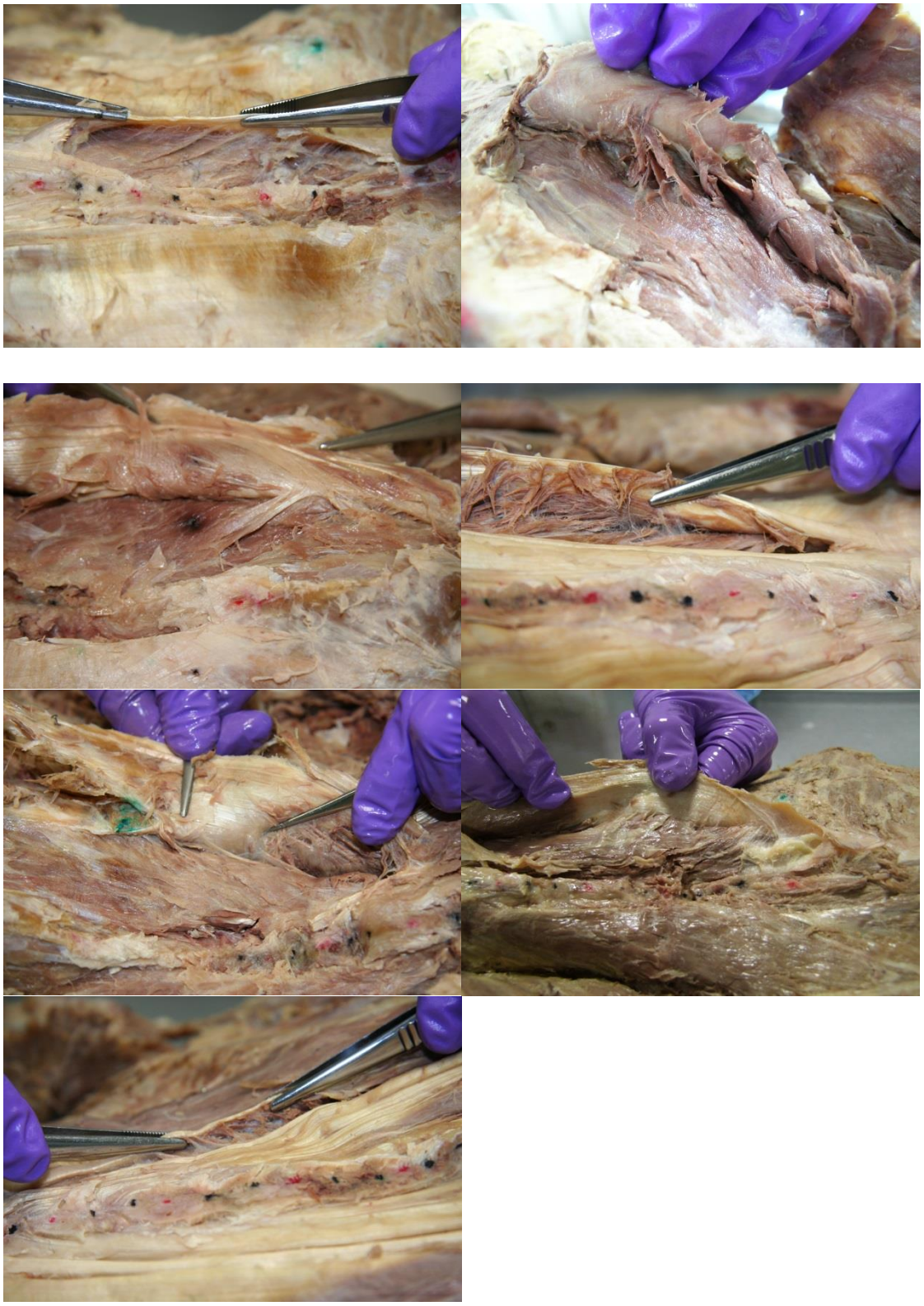

Figure 124. Physical connection between Erector Spinae aponeurosis and Multifidus.

6.8 Recommendations for practice

Based on the results of this case series, the following electrode placements could be utilised in adult populations; in practice, the use of values in parenthesis is more practicable (Table 35, Table 36 and Table 37). Adhesive dots used in following illustrations are 5mm in diameter and therefore represent the measure of clinical indifference used for Iliocostalis and Longissimus.

Table 35. Location of Multifidus lateral edge based on anatomy study.

	Location of lateral edge Multifidus based on anatomy study (mm)	
Lateral Edge distance from segmental level	**Calculated position**	**Recommended position**
S2	36.39	36
L5	34.85	35
L4	27.71	28
L3	21.24	21
L2	17.10	17
L1	18.43	18

Figure 125. Location of lateral edge Multifidus based on anatomy study.

Figure 125 illustrates the positions of S2 – T11 and right PSIS and left PSIS (red dots), the tip of rib 12 (purple dot), the location of SENIAM guidelines for Multifidus, Iliocostalis and Longissimus (blue dots) and the location of the lateral edge of Multifidus (green dots) at each of the segmental levels.

Table 36. Location of Iliocostalis muscle mid-point from bony landmarks, based on anatomy study.

	Location of Iliocostalis muscle mid-point from bony landmarks, based on anatomy study (mm)	
Iliocostalis muscle mid-point from segmental level	**Calculated position**	**Recommended position**
Mid-point superior at T11	60.29	60
Mid-point inferior at L2/3	49.72	50

Figure 126. Location of Iliocostalis muscle mid-point from bony landmarks, based on anatomy study.

In Figure 126, the additional purple dots (compare with Figure 125) mark the location of the mid-point of Iliocostalis based on the anatomy study (Table 36).

Table 37. Location of Longissimus muscle mid-point from bony landmarks, based on anatomy study.

	Location of Longissimus muscle mid-point from bony landmarks, based on anatomy study (mm)	
Longissimus muscle mid-point from segmental level	**Calculated position**	**Recommended position**
Mid-point superior at T6	33.62	34
Mid-point inferior at T10	39.52	40

Figure 127. Location of Longissimus muscle mid-point from bony landmarks, based on anatomy study.

Figure 127 indicates the positions of the mid-point of Longissimus lateral to T6 and T11 respectively (Table 37).

In order to apply these electrode placements in a clinical situation, measurements would be taken from palpable bony landmarks and distances to the muscle mid-points or lateral edge in the horizontal plane made. The mid-point of the Iliocostalis muscle is marked on the skin as demonstrated from the L2/3 interspace (Figure 128).

A line could be extended between these two points to aid aligning the array electrodes (Figure 129 and Figure 130).

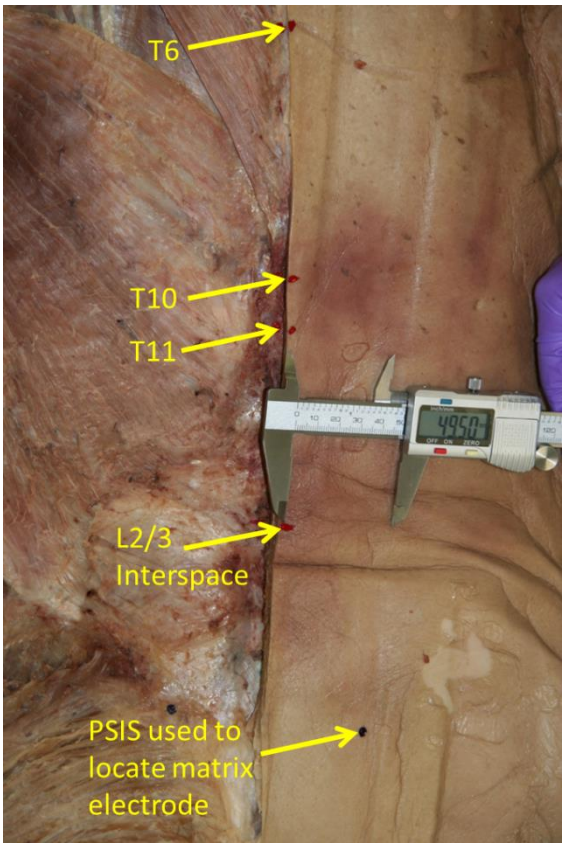

Figure 128. Demonstration of location of muscle mid-point.

Figure 128 illustrates the method of identifying the mid-point of each muscle based on the data from this case series.

Array electrodes would be then lined up on the mid-points of the muscle with the mid-point of the array being over the mid-point between the lower and upper extent of the muscle.

In the Figure 129, the alignment of the array electrodes is demonstrated. The muscle bulk of Trapezius and Latissimus Dorsi have been resected in order to show the Erector Spinae muscle group that is covered by Serratus Posterior and fascia.

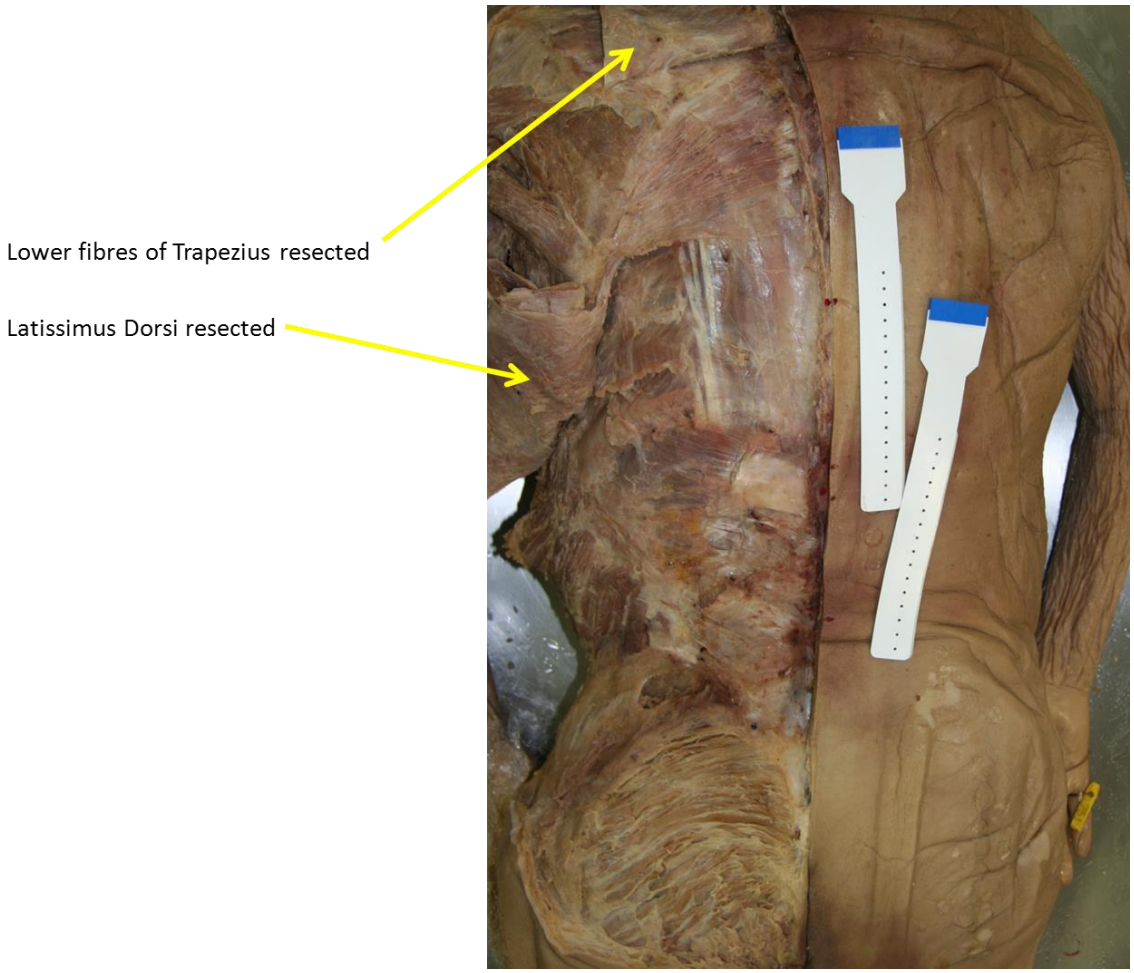

Figure 129. Location of electrode array based on mid-point measurements.

Figure 129 illustrates the recommended position of the electrode arrays based on this anatomy study.

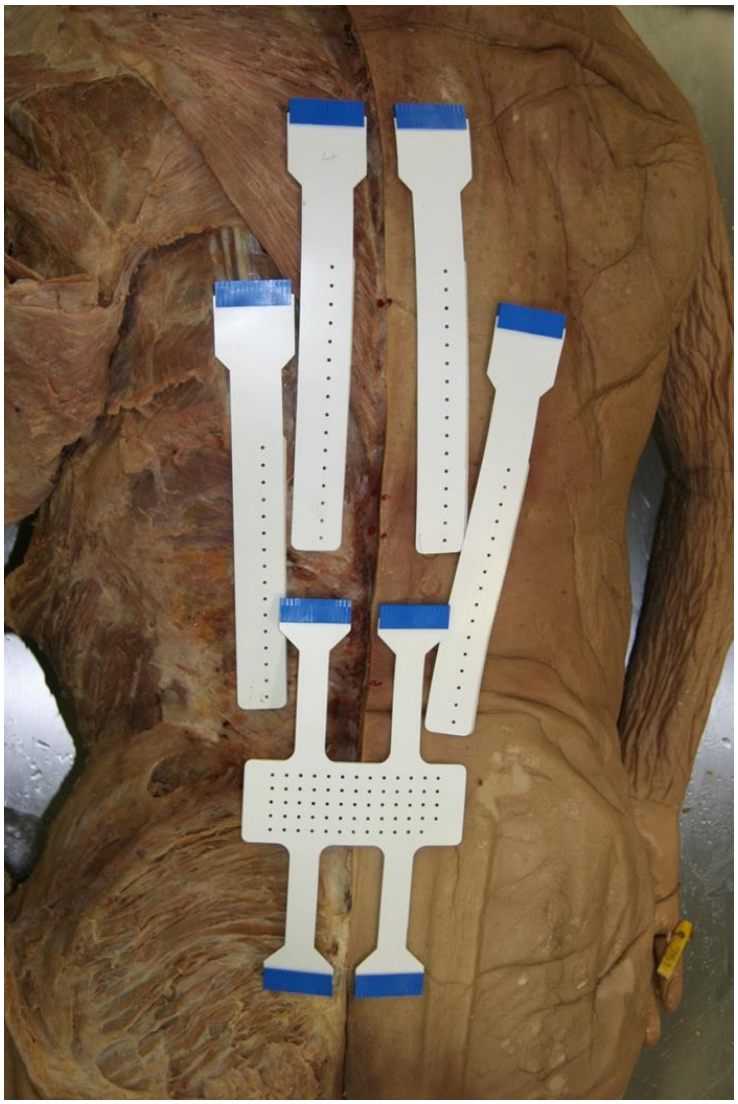

Figure 130. Location of array and matrix – bilateral set up.

Figure 130 represents the positions of both the array and the matrix electrodes based on the study results.

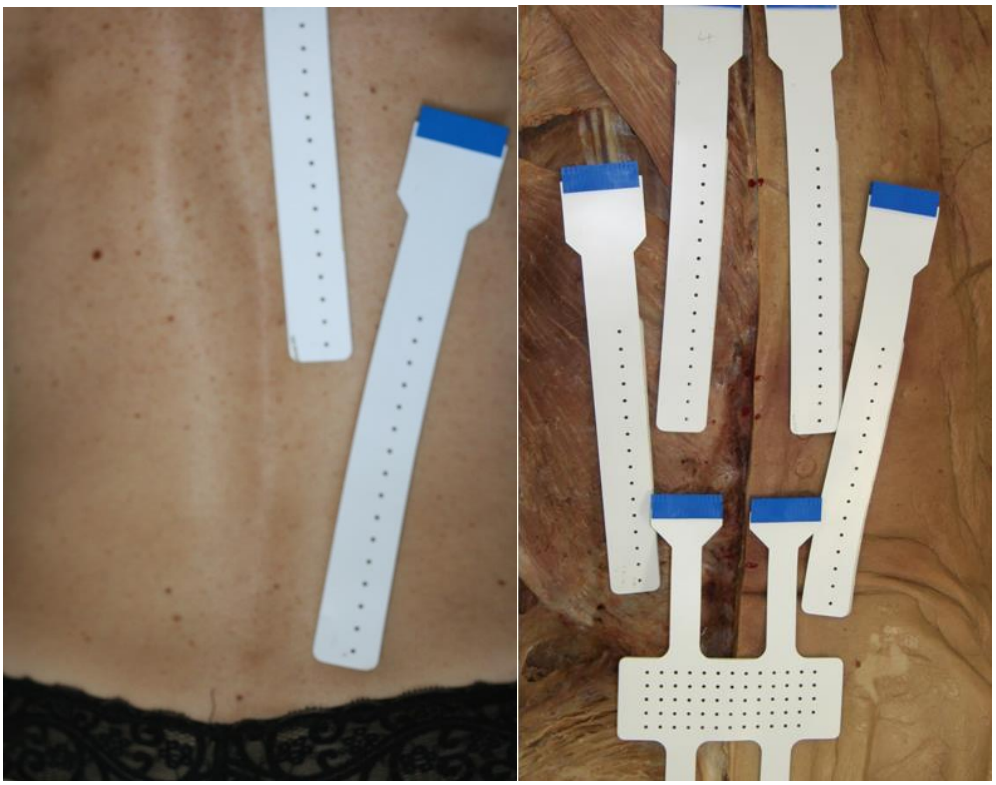

Figure 131. Comparison of sEMG positions based on experimental data and original DeFoa paper.

In Figure 131 a side by side comparison is made of the arrangements of array and matrix electrodes based on the left and utilising angles to measure the position of muscles and on the right the position of electrodes based on the results of this case series. It can be seen that the angle of the array electrodes that cover Longissimus differs in that they converges caudally and that the arrays that cover Iliocostalis are located lower, more laterally and at a wider angle. The position of the matrix electrode covering Multifidus has not been altered.

This side by side comparisons shows the position of electrodes based on Biedermann and De Foa (left) and the positions recommended by this study (right). There is considerable visual similarity. However, the methodology described requires that data are only collected from sensor locations that are between the boundaries of each muscle. This will vary between individuals and can only be determined during the experiment and post data analysis.

6.9 Limitations

A limitation of this study is that a small convenience sample was used. This was a self-selecting sample of individuals who donated their bodies to the Centre for Learning Anatomical Sciences and as such, it cannot be assumed that they represent the general population. The individuals were older and it is assumed died of natural causes. However, their health status was unknown at the time of their death; they may have been unwell for some time and muscle atrophy may have occurred during the later stages of life.

A further limitation concerns the calculation of Iliocostalis mid-position based on the mean measures of the lateral and medial edges between T10 and T12, and between L2 and L3 (Section 6.5.1); this results in a positional error. The assumption that the distance calculated between these points does not take into account the difference in segmental levels. Specifically, the lines between the medial superior edge at T10 and the lateral superior edge at T12, and the medial inferior edge at L2 and the lateral inferior edge at L3 are not perpendicular to the longitudinal axis of the body. They lie on a line that is oblique to that perpendicular line and as such, that distance is greater than that calculated by a few millimetres.

A solution to this positional error would be to plot the superior lateral and superior medial, and the inferior lateral and inferior medial distances to the muscle edges of Iliocostalis and then to interpolate lines between these. Taking a point half-way between the superior edges and the inferior edges, it would be possible to identify the mid-position between these points.

The application of adhesive dots represents another of the problems of applying these results in clinical practice; tips of each spinous process were palpated using standard clinical palpation procedures for identifying bony landmarks and the adhesive dot fixed centrally on each process. An analogue calliper was set at the distance required and this used to measure from the centre of the dot over each spinous process to the muscle mid-position. Once the muscle mid-point was identified, another adhesive dot was applied. In clinical practice, the application of marks to the individual's skin, that would then enable electrodes to be applied, is recommended although it is acknowledged that this introduces a possible source of operator error.

6.10 Conclusion

This case series study has resulted in new data on which to base a further study of the sEMG characteristics of the stabilising muscles of the lumbar region but these data require validation in order to generalise results to a living population and a validation should include age ranges that are representative of the populations likely to be investigated by sEMG.

The results of this case series are comparable with similar studies that have been undertaken (Biedermann, DeFoa, & Forrest 1991; De Foa, Forrest, & Biedermann 1989), with the addition of measurements and results that are applicable to the clinical environment. If the conclusions reached are validated by further investigation, they have implications for the study of sEMG using high-density electrodes but only if coupled with appropriate expertise in signal decomposition, electrode placement and appropriate fatigue testing protocols.

The following study (Section 7) aim to validate these conclusions using a retrospective sample of MRI images.

7. A study of the anatomical features of Longissimus Thoracis pars Thoracis, Iliocostalis Lumborum pars Thoracis and lumbar Multifidus utilising Magnetic Resonance Images.

7.1 Introduction

Identifying the location of Longissimus, Iliocostalis and Multifidus using magnetic resonance images (MRI) provides a possible alternative to anatomical dissection. The technique has already been used; previous studies using MRI to identified the position of the Multifidus-Longissimus cleavage planes (Palmer, Allen, Williams, Voss, Jadhav, Wu, & Cheng 2011; Wu, Fu, Jiang, & Yu 2012). These studies took measures at the intersegmental level, as defined by the inter-body joint, as this was most easily visualised in an MRI and reported that a reliable measure from the interspinous space could be used in surgical procedures to find the multifidus-longissimus cleavage planes in the lumbar spine. These two studies, with remarkably similar titles and methodologies, took measurements from 200 MRIs each and reported that the junction between Multifidus and Longissimus (presumably Longissimus Thoracis pars Lumborum) could be readily found. Neither study concluded that there was any correlation between body mass index, age or height and the distance to the multifidus-longissimus cleavage planes but that mean distances were significantly greater in females (1 – 2mm). Both studies measured the midline to muscle edge distance from the inter-body joint as determined from the MRI. This would be difficult to replicate clinically as the inter-body joint is not palpable.

Table 38. Summary of inter-body to Multifidus-Longissimus cleavage plane (Palmer et al., 2011; Wu et al., 2012).

Inter-body segmental level	Palmer et al.	Wu et al.
	Inter body to cleavage plane distance (mm)	
L5-S1	**37.8**	**33.56**
L4-L5	**28.4**	**29.85**
L3-L4	**16.2**	**24.97**
L2-L3	**10.4**	**19.91**
L1-L2	**7.9**	**16.17**

Table 38 summarises the main findings from previous studies (Palmer et al. 2011; Wu et al. 2012). Despite similar methodologies, these studies report clinically significant differences; the measure to the cleavage plane is analogous with the mid-line of the body (spinous process) to lateral edge of multifidus.

In this thesis, the segmental level was defined as the level that the spinous process could be palpated in clinical practice as this provided the most utility. No previous MRI analysis of Iliocostalis or Longissimus was available for comparison.

In clinical or experimental practice, when utilising sEMG to record data from underlying muscle, it is necessary to position the surface sensor accurately. The degree of accuracy that it is possible to achieve will depend on the skill of the operator. In the case of high-density sEMG electrode arrays and matrixes with IED of 10mm and 8 mm then accuracies of ±5mm and ±4mm respectively should be the intention.

7.2 Aim

The study had two aims;

First aim: to identify if the location of Longissimus Thoracis pars Thoracis, Iliocostalis Lumborum pars Thoracis and lumbar Multifidus showed equivalence between the measures obtained from the anatomical study and measures taken from an MRI image in an age and gender comparable population.

This aim was achieved by measuring the position and calculating the width of Longissimus, Iliocostalis and Multifidus from a series of MRI images; these data were compare to the anatomical study previously described (Section 6).

Second aim: to identify if the location of Longissimus, Iliocostalis and Multifidus show equivalence between the measures obtained from MRI in samples selected from populations aged 70 – 90 and 25 – 45 years.

7.3 Study design

The study utilised an observational study design of;

1. A sample of retrospective Lumbar and Thoracic spine MRI axial series from individuals with an age range 70 – 90 years old. Two groups were identified based on gender; stratified randomisation was used to ensure equal numbers.

2. A sample of retrospective Lumbar and Thoracis spine MRI axial series from individuals with an age range 25 – 45 years old. Two groups were identified based on gender; stratified randomisation was used to ensure equal numbers.

7.3.1 Participant selection

The selection process followed a number of stages; MRI scans were available on the picture archiving and communications system (PACS) database based at a local university hospital and represented a sample from the local population.

A co-investigator ran searches on the PACS database using predetermined search criteria in order to limit the search to those MRI images from individuals with the age and gender specifications required as illustrated below.

7.3.2 Sample

Four specific samples were identified;

Two series of T1-weighted axial MRI scans where images of the lumbar and thoracic spine were available using the age and gender criteria as follows; 6 male aged 70 – 90 and 6 female aged 70 – 90.

Two series of T1-weighted axial MRI scans where images of the lumbar and Thoracis spine were available, using the age and gender criteria as follows; 6 male aged 25 – 45 and 6 female aged 25 – 45.

The following procedure was used to determine the four sample groups.

1. Searches were undertaken to identify a series of T1 weighted axial MRI spinal image scans for each the following groups:

    Males aged 25 – 45

    Males aged 70 – 90

    Females aged 25 – 45

    Females aged 70 – 90

From these results, if the radiology report confirms that no exclusion criteria applied then stratified randomisation was used to identify 12 axial scan series for each group.

2. All axial MRI scans were anonymised by co-investigators who removed all references and any radiology report that could identify the individual.

3. Each axial scan series was scrutinised by the applicant and specific images at the spinal segments of interest were identified. Specifically, well defined axial images of the following muscles were required for the following segmental levels of spinous processes;

    Iliocostalis – L2, L3, T10 and T12

    Longissimus – T10 and T6

    Multifidus – S2, L5, L4, L3, L2 and L1

4. If at this stage the required axial scan images were not suitable for measurement purposes the series was rejected and further stratified randomisation from the original searches was utilised to select another MRI series.

5. Once a series was accepted for inclusion into the study images were stored according to current Hospital Trust policies and measurements were obtained, see method.

7.3.3 Inclusion criteria

MRIs were included for this study if;

T1-weighted axial MRI scans of the lumbar and thoracic spine where the age and gender met the study criteria.

There was no report of significant musculoskeletal, soft tissue or vascular disease or spinal deformity.

The image series included segments of interest from the second sacral segment to the sixth thoracic segment and the muscles of interest were clearly identifiable on the MRI image.

A radiologist report was available for the images; this report was removed by co-investigator prior to the applicant taking measurements from each image.

7.3.4 Exclusion criteria

MRIs were excluded for this study if there were;

Significant musculoskeletal, soft tissue or vascular disease process reported or evident on the selected MRI.

Spinal deformity such as a significant scoliosis i.e. spinal curvature greater than 10° (Trobisch et al. 2010) as measured by Cobb method (Facanha-Filho et al. 2001), kyphosis greater 40° measured in the sagittal plane and hyper-lordosis.

Image series where the muscles of interest were not clearly identified, for example, as a result of anomalies or the effects of degenerative processes.

No radiology report.

7.3.5 Participant recruitment

The research was approved and monitored by the Ethics and Research Governance Committee at the University of Southampton (approval no. 5005) and sponsored by Southampton University Hospital Trust Research and Development. Approval has been given for this study to take place without the consent of the individuals concerned. No personal data was used or was visible to the researcher. All images and MRI image series were anonymised.

This was a retrospective study of images that were already stored in the PACS database. Consequently, no participants were directly recruited to the study.

7.3.6 Sample size calculation

No sample size calculation was undertaken as this was a convenience sample. As is common practice in the initial (pilot) phase of a study, a small sample was sought in order to establish if the methodology proposed was likely to provide the data required and to provide information from which a sample size calculation could be made at a future date (Arnold et al. 2009;Thabane et al. 2010). 24 image series in total were analysed, 12 from the age range 25 – 45 and 12 from the age range 70– 90. This number was considered sufficient to match the aims of the study.

7.4 Hypotheses

The following hypotheses were tested by this experiment for each of the following muscles; Iliocostalis, Longissimus and Multifidus;

> Measures taken from MRI of the boundaries of Iliocostalis, Longissimus and the lateral edge of Multifidus at segmental levels S2, L5 – L1 and subsequent calculations of mid-position of muscles will be clinically equivalent, in an age comparable population, to data from previous anatomy study.
>
> Measures and calculations taken from the right and left side from the MRI will be clinically equivalent.

Measures and calculations taken from the MRIs of female and males will be clinically equivalent.

Measures and calculations taken from the MRIs of 70 – 90 and 25 – 45 age ranges will be clinically equivalent.

The null hypothesis is that there is no equivalence.

7.5 Method

Sagittal views of each image series were scrutinised with MRI cut-lines enabled, this allowed identification of segmental levels where spinous processes were clearly identifiable. The following (Figure 132) illustrates this; the thoracic spinal segmental levels are clearly seen. The level of the cut-lines (labelled as part of the axial segments '5' in Figure 132) can be seen to be through the T10 spinous segmental level (this segmental level is required for Iliocostalis).

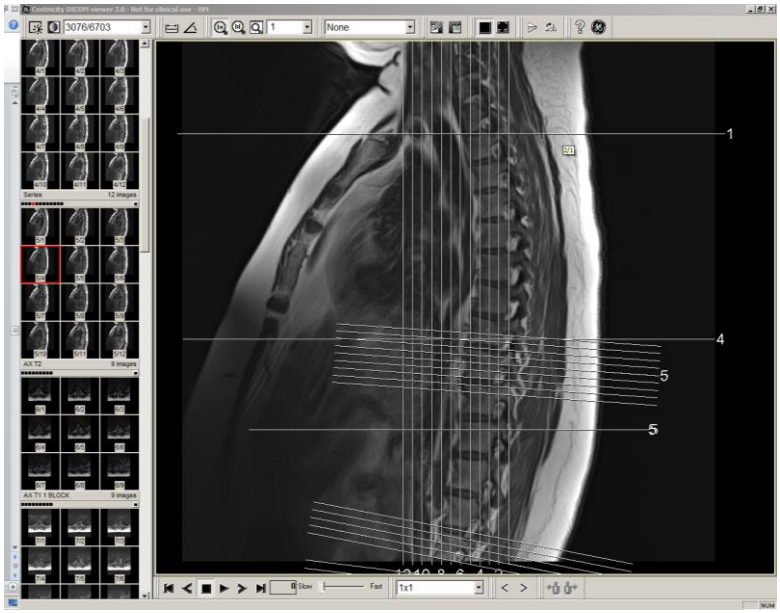

Figure 132. Method for MRI image selection.

Measurements were taken directly from the MRI scans using the proprietary linear measurement tool (calliper function) that is built into the MR imaging software (Centricity™ DICOM© viewer, GE Medical Systems). Clicking on the cut-line at the spinous process level reveals the axial section (Figure 133) from which the calliper function (Figure 134) could be utilised (once the cut-line

feature had been turned off). This tool measures distances with a pixel level degree of accuracy between defined points. In this study, these points were defined bony landmarks (spinous processes) and the edges of specific muscles. As previous studies have reported (Palmer et al. 2011; Wu et al. 2012) the intermuscular plane between muscles is curvilinear (See Figure 134, Figure 135 and Figure 136) in the axial plan, the concavity tending to face towards or away from the spinal segment, this made standardisation of the method problematic. For this study the most lateral or medial edge was used as this most accurately replicated the method used in the previous anatomy study. Identification of each muscle utilised a similar procedure as in the anatomy study phase. Colleague agreement and specialist advice from a consultant radiologist concurred.

Operator blinding was not possible as the calliper function provides immediate visual measurement; therefore the following procedure was used to reduce the possibility of previous measurement bias. From the reference MRI, where all cut lines were visible as in Figure 132, images where the segmental levels of interest were identified i.e. S2 – L1, T12, T11 and T6, and a copy of each image was made. Each image were labelled with a random file number and stored in a computer folder. The files in this folder were ordered using the file name to ensure that all images were in a random order. Measurements were taken from each image in turn; firstly for the right side and when all these data were recorded then the left side was measured, this procedure was repeated three times. This method ensured that both right and left side of all images were measured three time with the operator blind to previous measures as data were entered into a different sheet of the spreadsheet on each occasion. Inter- and intra- rater reliability utilised the same procedure. The means of three measures were calculated for each side.

Data were stored onto separate sheets in Microsoft Excel © and once all data were collected, data were merged and analysed using functions in the spreadsheet. All image files were then deleted in accordance with Hospital Trust policy.

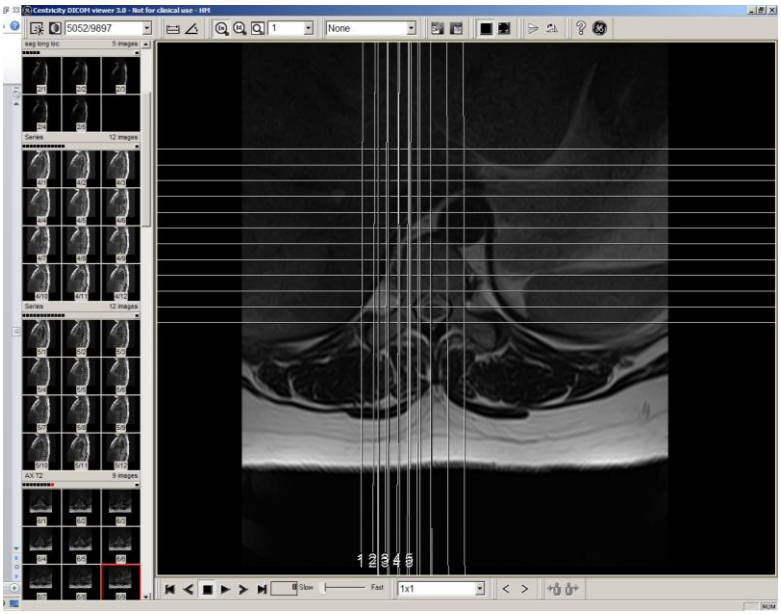

Figure 133. Axial section through T10.

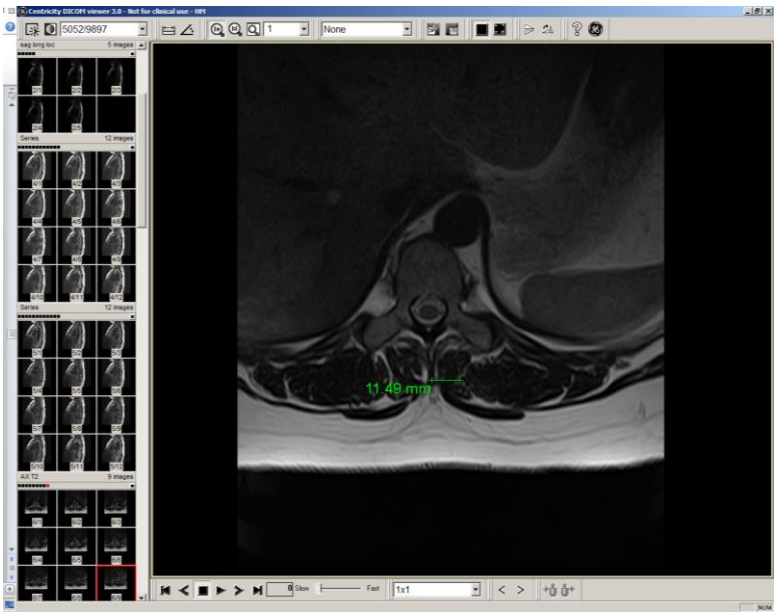

Figure 134. Calliper function for direct measurement.

In the axial view of the lumbar spine at L5 and L1 the spinous process and the lateral edge of Multifidus is clearly identifiable. The software allows measurement between points to be displayed on the screen. In Figure 135, a line has been extrapolated from the spinous process to act as a reference for the mid-point.

Figure 135. Illustrates measurement of Multifidus at the level of L5.

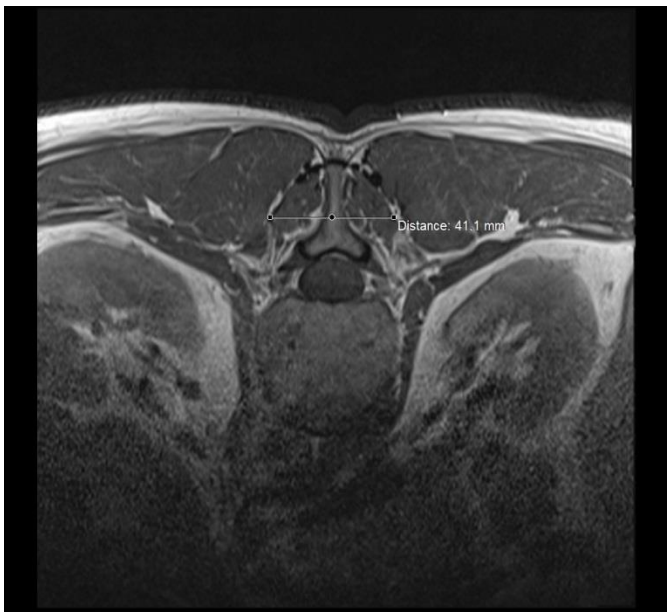

Figure 136. Illustrates measurement of Multifidus at the level of L1.

7.6 Population

Two series of T1 weighted axial MRI scans where images of the lumbar and Thoracis spine were available; 6 male aged 70 – 90 (*M*= 80.3, *SD* 4.2) and 6 female aged 70 – 90 (*M*= 78.4, *SD* 7.6).

Two series of T1 weighted axial MRI scans where images of the lumbar and Thoracis spine were available; 6 male aged 25 – 45 (*M*= 37.2, *SD* 4.8) and 6 female aged 25 – 45 (*M*= 36.7, *SD* 6.5).

Data were rejected from a number of scans due to a lack of suitable images. Many images did not include images of the thoracic spine, this prevented measurement from Iliocostalis or Longissimus. Images that did not include upper lumbar spine prevented measurements from Multifidus and in a number of individuals there were features that precluded inclusion in the study (Appendix 14.2). No other information, such as dominant hand, was available on any individual and all ages were given to the nearest integer so the calculation of mean age and *SD* may not present a valid representation of age ranges.

7.7 Data analysis

7.7.1 Method agreement and reliability

An intra-rater and an inter-rater reliability analysis (ICC) were undertaken comparing each of the three measurements.

7.7.2 Statistical analysis

Data were calculated as follows;

A calculation was made of the width of each muscle and the mid-point of the distal and proximal edges of Longissimus and of Iliocostalis; this was calculated as the mean of the mid-point between the lateral and medial edge of each muscle for each side using the method previously described (Section 6.5). Differences between side and between genders were calculated.

The data were tabulated to indicate the extent of individual variation and presented with mean and standard deviation values. Independent and dependent t-tests were used to determine whether there is a difference in Iliocostalis, Longissimus and Multifidus mid-point position of each muscle, between; the anatomy and the MRI study, right and left sides (although

dominant hand was unknown) and between female and males. Right and left side correlation was also investigated.

Equivalence testing was undertaken in order to test the hypothesis that mean measures from different sides, gender and age groups are interchangeable. The measure of clinical indifference was set at 5mm when analysing data from Iliocostalis and Longissimus; this is equivalent to the radius of the receptive field of the sEMG array electrode (IED 10mm). The measure of clinical indifference was set at 4mm when analysing data from Multifidus when the sEMG matrix electrode was used to collect data (IED 8mm).

7.8 Results

7.8.1 Muscle mid-position and width data: anatomy and MRI studies

7.8.1.1 Iliocostalis

Calculations were made of the boundaries of muscles of interest using data collected as described above. Data for each age group are presented with the anatomy study data for comparison. Width and mid-point results are presented; methodology for the calculation was as previously described in the anatomy study (Section 6).

Table 39. Iliocostalis muscle width. MRI v anatomy.

Iliocostalis Muscle Width MRI and anatomy data

	Mean (mm) 25 – 45 *(SD)* N = 12	**Mean (mm) 70 – 90 *(SD)* N = 12**	**Mean (mm) Anatomy study *(SD)* N = 7**
Width Superior T11	12.21 (4.76)	17.12 (3.61)	28.64 (8.34)
Width Inferior L2/3 Interspace	23.8 (3.21)	34.07 (3.09)	27.85 (6.12)

Table 40. MRI 25 – 45 age group: Iliocostalis mid-point.

Iliocostalis Muscle Mid-Point 25 – 45 based on mean measures and compared to anatomy data

	Mean (mm) n=12	Anatomy data n=7
Mid-Point Superior T11	62.22 (1.56)	60.29 (4.84)
Mid-Point Inferior L2/3 interspace	61.25 (2.57)	49.72 (3.13)

Table 41. MRI 70 – 90 age group, Iliocostalis mid-point.

Iliocostalis Muscle Mid-Point 70 – 90 based on mean measures and compared to anatomy data

	Mean (mm) n=12	Anatomy data n=7
Mid-Point Superior T11	63.29 (4.79)	60.29 (4.84)
Mid-Point Inferior L2/3 interspace	55.57 (3.86)	49.72 (3.13)

7.8.1.2 Longissimus

Table 42. Longissimus muscle width: MRI v anatomy.

Longissimus Muscle width MRI and anatomy data

	Mean (mm) 25 – 45 *(SD)* N = 12	Mean (mm) 70 – 90 *(SD)* N = 12	Mean (mm) Anatomy study *(SD)* N = 7
Width Superior T6	41.42 (10.32)	59.02 (4.46)	26.65 (5.73)
Width Inferior T10	49.06 (11.09)	39.35 (3.32)	24.98 (9.49)

Table 43. MRI 25 – 45 age group, Longissimus mid-point.

Longissimus Mid-Point 25 – 45 v Anatomy data		
	Mean (mm) *(SD)* **n=12**	**Anatomy data (mm)** *(SD)* **n=7**
Mid-Point Superior T6	30.52 (6.53)	33.62 (5.47)
Mid-Point Inferior T10	34.20 (4.47)	39.52 (6.75)

Table 44. MRI 70 – 90 age group, Longissimus mid-point.

Longissimus Mid-Point 70 – v Anatomy data		
	Mean (mm) *(SD)* **n=12**	**Anatomy data (mm)** *(SD)* **n=7**
Mid-Point Superior T6	37.56 (2.96)	33.62 (5.47)
Mid-Point Inferior T10	35.57 (3.6) n =10 (missing data for R side in 2)	39.52 (6.75)

7.8.1.3 Multifidus: Lateral edge from spinous process

Table 45. MRI – 25– 45 and 70 –90 age group.

	Measurements from spinous process to lateral muscle edge		
	Mean MRI 25 – 45 Age Group ***(SD)*** **n = 12**	**Mean MRI** 70 – 90 Age Group ***(SD)*** **n = 12**	**Mean Anatomy Study *(SD)* n = 7**
Lateral edge S2	**49.71 (2.22)**	**40.43 (5.98)**	**36.39 (5.52)**
Lateral edge L5	**48.34 (6.78)**	**37.63 (5.54)**	**34.85 (6.51)**
Lateral edge L4	**35.45 (3.00)**	**32.40 (4.70)**	**27.71 (6.50)**
Lateral edge L3	**29.35 (3.56)**	**26.49 (3.50)**	**21.24 (4.36)**
Lateral edge L2	**24.67 (3.09)**	**22.93 (3.33)**	**17.10 (3.43)**
Lateral edge L1	**18.98 (1.84)**	**20.77 (3.78)**	**18.43 (4.68)**

7.8.2 Equivalence analysis

Equivalence analysis was undertaken and results summarised below, see appendix 14.1 for full details of analysis. In the case of Iliocostalis and Longissimus, the CI range was set at (–5, 5) and for Multifidus (–4, 4). In the following tables, results where equivalence was demonstrated are indicated**.

7.8.2.1 Anatomy v MRI 70 – 90 age range

Table 46. Anatomy v MRI 70 – 90 age range.

Iliocostalis Mid–position MRI 70– 90	T11	L2/3		**Longissimus Mid–position MRI 70– 90**	T6	T10
CI (–5, 5)	–13.38 to –6.74	–10.12 to –5.27		CI (–5, 5)	0.35 to 6.12	–2.14 to 7.13

Multifidus Lateral Edge MRI 70– 90	S2	L5	L4	L3	L2	L1
CI (–4, 4)	–10.28 to –5.23	–9.82 to –3.21	–7.87 to –3.69	–7.86 to –4.55	–7.37 to –4.40	–5.23 to 1.28

A comparison of this data did not demonstrate equivalence between the anatomy study and the MRI 70 – 90 age group (Table 46).

7.8.2.2 MRI right v left all ages

Table 47. MRI right v left all ages.

Iliocostalis Mid-position	T11	L2/3
CI (-5, 5)	**-0.16 to -0.56****	**2.3 to 3.7****

Longissimus Mid-position	T6	T10
CI (-5, 5)	**-0.29 to 1.0****	**-2.08 to -0.51****

Multifidus Pooled data	Lateral Edge
MRI 70 – 90, CI (-4, 4)	**0.97 to 0.98****
MRI 25 – 45, CI (-4, 4)	**0.97 to 0.98****

Equivalence was demonstrated between the right and left sides of pooled data for all muscles (Table 47).

7.8.2.3 MRI male v female 70 -90

Table 48. MRI male v female 70 -90.

Iliocostalis Mid-position MRI 70- 90	T11	L2/3
CI (-5, 5)	-14.26 to -4.7	-9.38 to -4.3

Longissimus Mid-position MRI 70- 90	T6	T10
CI (-5, 5)	7.05 to 10.53	**-1.56 to 2.15****

Multifidus Lateral Edge MRI 70- 90	S2	L5	L4	L3	L2	L1
CI (-4, 4)	**-0.36 to 2.36****	**0.24 to 3.46****	**-0.43 to 1.91****	**0.08 to 1.63****	**-0.04 to 1.81****	2.15 to 4.35

In the comparison between genders in the 70 – 90 age range, equivalence is not demonstrated (apart from at T10) for Iliocostalis or Longissimus but for Multifidus, there is equivalence (apart from at L1) (Table 48).

7.8.2.4 MRI male v female 25 – 45

Table 49. MRI male v female 25 – 45.

Iliocostalis Mid-position MRI 25 – 45	T11	L2/3		**Longissimus Mid-position MRI 25 – 45**	T6	T10
CI (–5, 5)	**0.28 to 3.7****	3.9 to 5.8		CI (–5, 5)	–7.89 to –1.4	–9.9 to –6.7

Multifidus Lateral Edge MRI 25 – 45	S2	L5	L4	L3	L2	L1
CI (–4, 4)	**0.67 to 3.2****	–4.9 to 3.4	**–1.23 to 2.6****	**–2.2 to 2.35****	**–1.13 to 2.79****	**1.16 to 3.41****

In the comparison between genders in the 25 – 45 age range, equivalence is not demonstrated (apart from at T11) for Iliocostalis or Longissimus but for Multifidus, there is equivalence (apart from at L5) (Table 49).

7.8.2.5 MRI 25 – 45 v 70 – 90 Age ranges

Table 50. MRI 25 – 45 v 70 – 90 Age ranges.

Iliocostalis Mid-position MRI 70– 90	T11	L2/3		**Longissimus Mid-position MRI 70– 90**	T6	T10
CI (–5, 5)	**–4.0 to 1.8****	3.0 to 8.3		CI (–5, 5)	–7.19 to 1.4	**–3.7 to 1.4****

Multifidus	Lateral Edge
CI (–4, 4)	2.38 to 5.32

A comparison between age groups demonstrates no equivalence apart from at T10 (Table 50).

7.8.3 Inter-rater and intra-rater reliability

Inter-rater reliability for methods measuring edge of muscle distance from a line extrapolated from tip of spinous process at each level line for Multifidus was excellent, 0.99 (ICC (3,1) two-way random – absolute agreement). Inter-

rater reliability for methods measuring to edges of Iliocostalis and Longissimus were 0.97(ICC (3,1) two-way random – absolute agreement) and 0.98(ICC (3,1) two-way random – absolute agreement) respectively.

Intra-rater reliability for measuring Iliocostalis were 0.99 (ICC 2,1) two way mixed – absolute agreement). Intra-rater reliability for methods measuring to edges of Iliocostalis and Longissimus were 0.96(ICC 2,1) two way mixed – absolute agreement) and 0.97(ICC (ICC 2,1) two way mixed – absolute agreement) respectively.

7.9 Discussion

The data set collected is a small sample collected from a database of MRI images that were intended to support clinical diagnosis. Stratified randomisation was employed to ensure that a random selection of images was selected from the database for each group; however, results cannot represent a wider population as the initial selection of images from the data-base was not randomised.

Intra- and inter-rater reliability was excellent; the method used for selecting and taking measures from the MRI images was robust and concurred with colleagues.

The same methodology used to calculate the mid-point of muscles of interest in the anatomy study was used to calculate the mid-point in this study and as such it can be considered a comparable method; the level of accuracy is sufficient for clinical practice. However, a positional error is caused by the method of calculating the mid position of Iliocostalis and while reliability has been demonstrated, the validity of this calculation has not been.

Values obtained from this study indicate that mean values from the anatomy study were not equivalent to the mean values from the MRI study. In the case of Iliocostalis, the mean mid-position of the muscle was calculated to be 3 mm more lateral to T11 and 5.85 mm more lateral to L2/3 interspinous space. Muscle width calculations for Iliocostalis also show considerable variation; an intriguing possibility for future investigation is that Iliocostalis might atrophy more quickly than other spinal muscles as a result of LBP.

In the case of Longissimus and Multifidus, muscle width in the MRI study was greater than in the anatomy study; a possible explanation for this is that the embalming process dehydrates muscle and the dissecting process removes fascia, fat and vessels that, on MRI, could be identified as part of the muscle edge. In the MRI study, individual muscles were perfused with circulating body fluids and had tone.

The mid-point of Longissimus in the MRI study was found to be more medial, compared to the anatomy study, in both age groups with the exception of at T6 in the 70 – 90 age group. Muscle width was consistently greater in the MRI study and this too could be a reason for a mismatch in the data sets. In the anatomy study, it was necessary to dissect Longissimus away from the more medial structures; this could have overestimated its lateral position. The lateral edge of Multifidus was found to be more lateral to relevant spinous processes in the MRI study. This too could be due to shrinkage of muscle due to the embalming process.

Results of the equivalence between right and left side show significant correlation for all muscles studied. The range of clinical indifference was set at 5mm and 4mm and the 90% confidence intervals were all less than 2mm. For clinical practice, no left or right variation in electrode placement would be required on the basis of these results.

The analysis of the mid-point data by gender was split further by age group. For Iliocostalis in both age groups there was a significant difference. The range of the female muscle dimensions was significantly greater and the male mid-point more lateral to the relevant spinous process. Analysis of equivalence in the 70 -90 age range found equivalence at T10 (Iliocostalis) and in the 25 – 45 age group equivalence was demonstrated at T11 (Longissimus). For Multifidus, in both age groups, equivalence was demonstrated for all levels apart from L1 in the 70 – 90 age group and for L5 in the 25 0- 45 age group.

Multifidus analysis by gender and age; at L5 and L1 there were significant differences from spinous processes to lateral edge between gender in the 70 – 90 age group but not in the 25 – 45 age group. The difference at L1 may be a result of an inconsistent muscle at this level. In both the anatomy study and the MRI in both age groups, Multifidus was often absent (resulting in rejected

series) or only partially present at this level; this finding requires further confirmation but could result in skewed data. There is equivalence between genders at all spinal levels in groups aged between 70 – 90 and 25 – 45 apart from at L5.

These results add to data from those of previous studies (Biedermann, DeFoa, & Forrest 1991; De Foa, Forrest, & Biedermann 1989) that informed SENIAM guidelines that only recommend that a finger width is used as a measure from spinous processes. This study makes specific recommendations from palpable bony landmarks that can readily be applied in clinical practice using simple measuring devise such as an analogue calliper or tape measure.

7.10 Recommendations for practice

Based on the results of this MRI study, the following electrode placements could be utilised in adult populations (anatomy data also presented for comparison);

Iliocostalis muscle mid-point from bony landmarks;

Table 51. Location of mid-position of Iliocostalis based on MRI study.

	Location of mid-position of Iliocostalis based on MRI study (mm)		
Mid position distance from segmental level	**Calculated position 25 – 45 Age Group**	**Calculated position 70 – 90 Age Group**	**Anatomy Study Recommended**
T11	62.22	63.29	60
L2/3	61.25	55.57	50

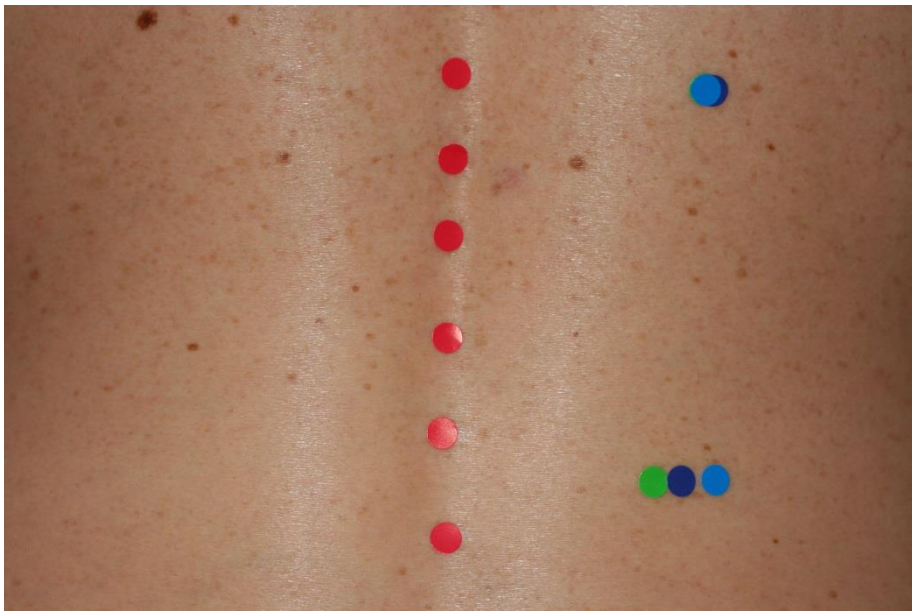

Figure 137. Location of mid-position of Iliocostalis based on MRI study.

The location of the mid-position of Iliocostalis is shown to the right of the spine at T11 and at L2/3 in Figure 137 and Table 51, illustrates the fit between these data. The anatomy data (green), the MRI 25 – 45 age group (light blue dots) and the MRI 70 – 90 age group (dark blue dots) overlap at T11 but not at L2/3. In a younger or female population, the use of a wider electrode placement at L2/3 could be used.

Table 52. Longissimus muscle mid-point from bony landmarks.

	Location of mid-position of Longissimus based on MRI study (mm)		
Mid position distance from segmental level	Calculated position 25 – 45 Age Group	Calculated position 70 – 90 Age Group	Anatomy Study Recommended
T6	30.52	37.56	34
T10	34.20	35.57	40

Figure 138. Longissimus muscle mid-point from bony landmarks

Figure 138 and Table 52 show position and illustrate close fit between these data. The anatomy data (green), the MRI 25 – 45 age group (light blue dots) and the MRI 70 – 90 age group (dark blue dots) overlap at both levels.

Table 53. Multifidus lateral edge from bony landmarks.

	Location of lateral edge Multifidus based on MRI study (mm)		
Lateral Edge distance from segmental level	Calculated position 25 – 45 Age Group	Calculated position 70 – 90 Age Group	Anatomy Study Recommended
S2	49.71	40.43	36
L5	48.34	37.63	35
L4	35.45	32.4	28
L3	29.35	26.49	21
L2	24.67	22.93	17
L1	18.98	20.77	18

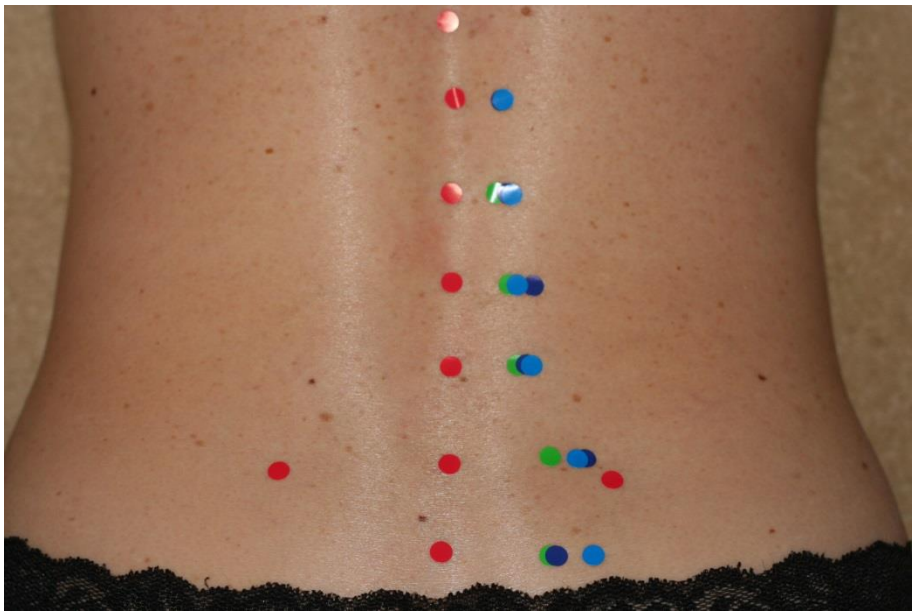

Figure 139. Multifidus lateral edge from bony landmarks; anatomy and MRI study, 25 – 45 and 70 – 90 age group data.

In Figure 139, the positions of the anatomy study (green dots), the MRI 25 – 45 age group (light blue dots) and the MRI 70 – 90 age group (dark blue dots) are shown. The diameter of the dots in 5mm and is therefore greater than the limit of clinical indifference of 4mm.

7.11 Limitations

This pilot study used retrospective data from a local PACS database; this limits the generalisability of the study conclusions. The use of a retrospective database limited the availability of suitable images and there was considerable variation in image quality and a lack of standardisation of imaging technique. No clinical details were available but a reasonable conclusion was that many of the individuals would be being investigated with MRI as part of the diagnostic procedures for pain of spinal origin. It is not unreasonable to assume that the population studied did not come from the normal population but instead may have been a sub-population of individuals with spinal pain or other musculoskeletal disorders. It is also not known what the 'handedness' of each individual was although results would indicate that the right and left side data are equivalent.

The identification of segmental levels using cut lines in the MRIs could result in incorrect measurements. Diverging cut lines are used in lumbar spine MRI that correspond to the curvature of the lumbar lordosis while in the thoracic region, cut lines were often parallel despite the degree of thoracic kyphosis (Figure 132). Identifying a cut line that passed through the relevant spinous process was normally possible; however, as the plane of the cut line was often in an oblique horizontal plane, the point of measuring the edges of the muscle may not have always been as precise as in the anatomy study.

The positional error described in 5.9 will have occurred in this study as the medial edge of Iliocostalis was not measured at the segmental level that corresponded to the level of the lateral edge. However, the same methodology to estimate the mid-position of this muscle was used in both the MRI study and the anatomy study. These results are therefore comparable but validity is not claimed.

Given that it is known that LBP causes inhibition and muscle atrophy; then the results of a study that seeks information regarding the architecture of muscles should be cautious about any assumptions regarding how these conclusions could be extrapolated to a normal population.

There is a possibility of author bias despite measures to ensure blinding of results during measurement process.

7.12 Conclusion

With regard to the specific hypotheses;

1. Measures taken from MRI of the boundaries of Iliocostalis, Longissimus and the lateral edge of Multifidus at segmental levels S2, L5 – 1 and subsequent calculations of mid-position of muscles will be clinically equivalent, in an age comparable population, to data from previous anatomy study.

This hypothesis was **not** proven for Iliocostalis, Longissimus or Multifidus. The null hypothesis is accepted

2. Measures and calculations taken from the right and left side from the MRI will be clinically equivalent.

This hypothesis was **proven** and is accepted.

3. Measures and calculations taken from the MRIs of female and males will be clinically equivalent.

This hypothesis was **not** proven for Iliocostalis in the 70 -90 age range.

This hypothesis was **not** proven for Longissimus (apart from at T10).

This hypothesis was **proven** and is accepted for Multifidus in the 70 -90 age range with the exception at L1 segmental level.

This hypothesis was **not** proven for Iliocostalis in the 25 – 45 age range (apart from at T11).

This hypothesis was **not** proven for Longissimus in the 25 – 45 age range.

This hypothesis was **proven** and is accepted for Multifidus in the 25 – 45 age range with the exception at L5 segmental level.

4. Measures and calculations taken from the MRIs of 70 – 90 and 25 – 45 age ranges will be clinically equivalent.

This hypothesis was not proven (apart from Iliocostalis at T11 and Longissimus at T10)

This is a small-scale study that has demonstrated that measurements can be taken from MRIs. A prospective study, utilising a standing MRI scanner with appropriate selection and stratified randomisation, could establish the validity of the results presented in this thesis. Such data could be used to inform studies of individuals in occupational situations where more accurate and specific data could then be collected.

Further studies are required with a representative sample and a standardised method of MRI examination.

8. Discussion

The central aim of this thesis is to add to the understanding of how particular spinal muscles fatigue when exposed to either a standardised fatiguing test or a task known to cause degradation in performance, this is particularly relevant in the aetiology of low back pain. The thesis describes the process by which tools and methodologies were developed in order to address specific study aims that arose. These specific study aims have been discussed within relevant sections of this thesis.

An evaluation of the literature on fatigue leads to an interpretation that the CNS drive to muscles is determined by a non-linear complex integrated control system in which all physiological systems interact continuously in a deterministic manner (Lambert, St Clair, & Noakes 2005; Noakes 2012; Noakes, St Clair, & Lambert 2005; Swart et al. 2009). An interpretation of this model suggests that the CNS drive to motor units and muscles will vary continuously and that surface electromyography (sEMG) data will also vary continuously. This interpretation could result in any number of different motor unit firing strategies in order to maintain homeostasis. The consequence of this interpretation is that the resultant sEMG signal may differ each time a muscle contracts and each time a test is undertaken. This thesis has not demonstrated that this is the case as this level of sEMG analysis has not been undertaken.

This discussion will focus on the unique contribution that this thesis makes to the body of knowledge.

The rigid inflatable boat (RIB) trials did not demonstrate the clinical utility of a standardised fatiguing task. In this case the Ito version (Ito et al. 1996) of the Biering-Sørensen (Biering-Sorensen 1984b) test was used to determine if exposure to random and shock vibration resulted in a degradation of performance as evidenced by differences in the rate of fatigue, pre- and post-transit in the boat. The differences in rate were measured using a standard time measure and sEMG from Multifidus and upper fibres of Trapezius, before, during and post-test. The rationale of using a high-speed RIB transit was that by recording vibration and calculating the vibration dose value (VDV) it could

be determined with some accuracy how much energy had been absorbed by the individual during the experiment. This study did demonstrate that usable data can be collected in a harsh marine environment and that further testing is feasible. The utility of the experimental methodology is such that it could be adapted to other occupational situations where fatigue data collection is required, such as on an automobile production line or in helicopter flying. This study did, however, identify the need to better understand the mechanism of lumbar spine stability and about fatigue of muscles that are involved in providing global and segmental stability to the lumbar region.

The development of the fatigue protocol in Section 4 was based on established tests and is not unique; however, combining the Biering-Sørensen test with multi-channel sEMG analysis to specifically study the fatigue characteristics of Iliocostalis, Longissimus and Multifidus is unique. This combination has the potential to provide useful data on mechanisms of fatigue such as sequence and rate. The development of specific signal processing tools that select and analyse sEMG data is unique and has applications in analysing data from occupational, clinical as well as laboratory based experiments. The utility of these tools was tested on a convenience sample and shown to be capable of analysing sEMG data to provide appropriate measures of fatigue such as changes in frequency and amplitude variables. Once data are collected, other analysis is possible that will further improve understanding of muscle fatigue.

The correct placement of electrodes is essential if meaningful data are to be collected and analysed and in this thesis two different methods are described that specifically identify and describe how and where muscles are located in relation to known and easily palpable bony landmarks; this is essential if the results of this thesis have applicability for practice.

The anatomy study described in this thesis (See Section 5 & 6) is the first to undertake detailed measurements of the position and angles of those muscles of interest that contribute to the extensor moment of the lumbar spine. As such it builds on the studies undertaken by De Foa and Biedermann (Biedermann, DeFoa, & Forrest 1991; De Foa, Forrest, & Biedermann 1989); this study has been able to concur and add to the findings of these authors. The use of the DeFoa and Biedermann studies alone does not provide sufficiently valid data on which to accurately position electrodes for multi-channel sEMG;

the results of the anatomy study provides data for more accurate electrode placement but requires further validation.

The anatomy study used robust and valid tests to establish the parameters of muscles of interest, based on visual identification of the borders of muscle. In particular, the anatomy study established evidence for the upper and lower boundaries in relation to palpable bony landmarks. These data will enable sEMG sensors to be placed with greater accuracy and could be utilised in further studies into how task specific fatigue could affect individuals with low back pain LBP. This is important in evaluating rehabilitation or treatment approaches that specifically address lack of endurance capacity and build muscle fatigue resistance.

The use of angles measured from reference lines interpolated from bony landmarks is not considered to have sufficient utility for clinical or experimental use (Gajdosik and Bohannon 1987). Typically, a compass or some form of protractor or goniometer is used to determine the projected line determined to be at an angle from a reference line. Any error due to the angle of viewing of the angular scale (parallax errors) or errors due to rounding up or down of the desired angle to be projected will be magnified at a distance. The magnification of any angular error over distance is a function of the error of the angle. The angle of clinical indifference in this thesis was set at 10° as had been considered to be acceptable for the application of sEMG electrodes. The results of this phase of the study need to be view with some caution as an angle of ±10° from the true muscle angle could result in additional magnification of angular errors at the location where it was assumed that the electrode should be located. This level of error may not be acceptable in clinical practice or experimental studies where it could be argued that a smaller angle of clinical indifference should be used.

The use of palpable bony landmarks has been demonstrated to be accurate and specific with regard to the location of the bony landmark (Jull, Bogduk, & Marsland 1988; Phillips et al. 2009; Phillips & Twomey 1996; Robinson et al. 2009). Also, in clinical studies of anthropometric measures of the body, linear measures are considered to be sufficiently accurate for practice (Gajdosik & Bohannon 1987; Hoyle, Latour, & Bohannon 1991). The conclusion of this

thesis is that accuracy of measures in the order of 4 – 5mm is within the range of clinical indifference. There is prima fascia evidence that the use of a digital or analogue calliper would result in sufficient accuracy provided that any measure is taken perpendicular to the centre line of the spine/longitudinal axis of the body or to a horizontal or longitudinal reference line.

The assumption and subsequent calculation that the mid-position between the upper and lower boundaries of Iliocostalis and Longissimus is the correct location from which to reliably collect sEMG data has not been demonstrated. It is assumed that individual muscle innervation zones will be located at the mid-point of a muscle but these zones have yet to be demonstrated for spinal muscles (Tsao, Danneels, & Hodges 2011; Tsao, Galea, & Hodges 2008). Detection of the innervation zone utilising a silver bar electrode array would have previously been problematic as the precise location of muscles was not known; this study has established the parameters of each muscle and so the detection of possible innervation zones with a silver bar electrode array could now be undertaken with greater confidence. This assumes that an innervation zone is possible to detect; the fasicular nature of Iliocostalis and Longissimus may preclude this.

For Multifidus the mid-position was not calculated. The architecture of this muscle is such that it consists of multiple fascicles, arising from deep mamillary processes, that attach to spinous processes throughout the lumbar region. The lateral limit of Multifidus as a group has been described in this study; the use of 2-dimensional matrix electodes enables post-data collection analysis of the sEMG signal. It is the premise of this thesis that the innervation zones of Multifidus are not likely to be readily accessable to sEMG data collection; the EMG signal is likely to consist of superimposed motor unit action potentials (MUAPs) from multiple fascicles that are independently innervated. This is in keeping with the function of Multifidus as a segmental stabiliser of the spine.

The accuracy and validity of data collected from any post-mortem anatomical study will normally need to be interpreted with caution; the process of embalming, subsequent dehydration of tissue and the process of dissection can disrupt the size, position and alignment of tissue. In the anatomical study, the protocol dictated that cadavers were embalmed and stored in the prone position in order, as far as is practicable, to preserve the integrity of the

muscles as in the supine position; considerable deformation of tissue occurs due to body weight. It is not known if the measured positions accurately reflect the normal anatomical position of muscles as there is no gold standard against which to evaluate the validity of this study data.

An issue with post-mortem studies is that any study that seeks data from donated bodies will be examining a self-selecting population that may not be representative of the normal population. Studies of this nature are limited by the availability of individuals; in the literature, small-scale anatomical studies are the norm and this study is no different. It is comparable to the De Foa and Biedermann (Biedermann, DeFoa, & Forrest 1991; De Foa, Forrest, & Biedermann 1989) studies in terms of numbers of individuals; however, the study in this thesis adopted robust and valid measurement techniques and ensured blinding of assessors. This data is therefore considered to be more valid for the population studied than previous studies.

The magnetic resonance imaging (MRI) study resulted in data that is considered to be complementary to the anatomy study in this thesis. The sample was a convenience sample selected from the picture archiving and communications system (PACS) database that used randomised stratification to ensure that the required number of image series were analysed for each age and gender group. Analysis of these studies was that there was no clinical equivalence between the results of the anatomy study and the MRI study. The results however demonstrated that there are trends between data from the two experiments; any differences could be explained as a result of differences between individuals and the methodology utilised in the collection of data. These conclusions require validation.

Results from the MRI study demonstrate clinical equivalence between right and left side and between a 70 – 90 age range and a 25 – 45 age range. Implications for this are that if these data are used for sEMG studies, and results are interpolated between age ranges, then the same relative positions could be used for all age ranges. The between gender equivalence was equivocal; these results require further investigation.

The combination of data on the upper and lower boundaries from the anatomy study and the confirmation of the data on distance from bony landmarks from

the MRI study have be combined in a recommendation for future sEMG studies (See Section 7.10). It is likely that a smaller number of sensors would be required than the 128 used in this study; the exact number will be determined by future studies based on results using the software developed here for in-depth analysis of the sEMG signals.

9. Recommendations for future research

Results presented in this thesis should now be reappraised with appropriately powered prospective or retrospective MRI studies to validate the recommended sensor positions in more representative populations. The use of standing MRI scanners would improve the accuracy of edge location for future studies, particularly where analysis of individuals undertaking activities in an upright position was proposed.

Further post-mortem anatomical studies are unlikely to be undertaken as they are time-consuming and availability of donated bodies is limited. The use of imaging studies is more likely to provide valid data of muscle positions across a wide range of ages more representative of the population with LBP. Virtual reality techniques similar to those used in the Visible Human Project (Ackerman 1998; Ackerman 1999; Ackerman and Banvard 2000; Ackerman, Yoo, & Jenkins 2001) could be developed that enable more specific sensor positions to be determined.

Clinical studies, utilising the recommended sensor positions and the Biering-Sørensen or Ito variation are required to establish the fatigue characteristics of Iliocostalis, Longissimus and Multifidus and in particular to evaluate their individual contribution to spinal stability as they fatigue. These studies should test the validity of using the mid-position between the upper and lower boundaries as the best location for sEMG data collection.

Future studies should employ additional signal decomposition techniques that investigate sEMG features associated with fatigue. These techniques will investigate further changes in amplitude variables, spectral variables and muscle fibre conduction velocities.

10. Final conclusions

This thesis has described a number of interlinked studies that build on and develop previous knowledge further.

Conclusions from the literature review and summary of fatigue and low back pain lead to the conclusion that testing for evidence of poor endurance capacity is complex and complicated. The non-linear nature of the central nervous system's response, in situations where homeostasis is threatened, results in sEMG data that may not be consistent when standardised testing is undertaken, therefore caution is required in interpretation results.

The study in a marine environment demonstrated the feasibility of measuring human physiology in the harsh environment caused by high-speed boat transits. The results indicate that similar testing would be possible in other occupational situations but that more sensitive tools are required to determine if the exposure to a fatiguing activity causes any short-term or long-term degradation in performance.

Development of software was undertaken in order that better evaluation and analyse of multi-channel sEMG signals would be possible in future studies. This was necessary as no software application was available that could undertake the level of analysis required. The feasibility study described in Section 4, concluded that basing sEMG studies on previously recommended sEMG locations, i.e. the SENIAM guidelines, was not appropriate and that new knowledge was required; furthermore, in Sections 5, 6 & 7 , the SENIAM guidelines have been shown to contain inaccuracies.

The findings of two previous anatomical studies ((Biedermann, DeFoa, & Forrest 1991) (De Foa, Forrest, & Biedermann 1989)) were compared in a post-mortem anatomical study. This study used robust and valid measures; validity and reliability of the data were tested by an additional MRI study. These two studies add to the body of knowledge in this area and contribute to the advancement of this area of clinical science.

The results presented in this thesis provide specific recommendations for the location of electrodes for studies of sEMG data collection using high-density,

mono-polar or bi-polar electrodes. The use of high-density electrodes, in combination with multi-channel amplifiers and appropriate analysis, has the capacity to provide the researcher or clinician with more representative data on muscle fatigue. This approach is more complex to employ and may not always be appropriate for clinical situations. However, future developments in sensor technology and in particular bespoke sensors for specific muscles would improve the utility of this technology.

The results detailed in this thesis also challenge the validity of the SENIAM guidelines, particularly in relation to Longissimus where results of this study and the guidelines differ significantly; if SENIAM guidelines are followed then data would more likely be collected from Multifidus adjacent to L1, not Longissimus. In the case of Multifidus, the SENIAM guidelines will only provide data from muscle activity adjacent to L5. In the case of Iliocostalis, the guidelines are likely to provide data from the mid-portion of this muscle.

The identification of the position of Iliocostalis, Longissimus and Multifidus requires the use of simple measurement devices that can locate a surface point with an accuracy of one millimetre; a simple analogue or digital calliper will suffice. However, the palpation skills of the clinician will determine how accurate bony landmarks are located.

The use of any instrument for measuring angles from reference lines may result in more inaccuracy in the clinical situation as have been described. However, results of this study conclude that this method has validity for identifying the lateral edge of Iliocostalis and Multifidus but not the mid-point of these muscles.

Rehabilitation approaches should be developed that are targeted specifically to address the fatigue characteristics of specific spinal muscles; these muscle characteristics could be identified by multi-channel sEMG analysis based on the results of this study. Furthermore, the effects of any intervention could be tested more accurately as this study has provided more clarity as to the specific location of Iliocostalis, Longissimus and Multifidus muscles in relation to known and palpable bony landmarks.

Performance degradation due to fatigue is costly, causes pain and loss of independence. Results of this study will be used to better understand fatigue characteristics and develop strategies to improve performance.

11. References

Abbott, F.V., Franklin, K.B., & Melzack, R. 1996. Comments on Detweiler et al. (Pain 63 (1995) 251-254). *Pain*, 67, (1) 220-225.

Ackerman, M.J. 1998. The Visible Human Project: a resource for anatomical visualization. *Medinfo.*, 9 Pt 2, 1030-1032.

Ackerman, M.J. 1999. The Visible Human Project: a resource for education. *Acad.Med.*, 74, (6) 667-670.

Ackerman, M.J. & Banvard, R.A. 2000. Imaging outcomes from the National Library of Medicine's Visible Human Project. *Comput.Med.Imaging Graph.*, 24, (3) 125-126.

Ackerman, M.J., Spitzer, V.M., Scherzinger, A.L., & Whitlock, D.G. 1995. The Visible Human data set: an image resource for anatomical visualization. *Medinfo.*, 8 Pt 2, 1195-1198.

Ackerman, M.J., Yoo, T., & Jenkins, D. 2001. From data to knowledge--the Visible Human Project continues. *Medinfo.*, 10, (Pt 2) 887-890.

Adams, M.A., Bogduck, N., Burton, K., & Dolan, P. 2006. *The Biomechanics of Back Pain*, 2nd ed. Churchill Livingstone Elselvier.

Adams, M.A., Mannion, A.F., & Dolan, P. 1999. Personal risk factors for first-time low back pain. *Spine*, 24, (23) 2497-2505.

Adams, M.A. & Roughley, P.J. 2006. What is intervertebral disc degeneration, and what causes it? *Spine (Phila Pa 1976.)*, 31, (18) 2151-2161.

Airaksinen, O., Brox, J.I., Cedraschi, C., Hildebrandt, J., Klaber-Moffett, J., Kovacs, F., Mannion, A.F., Reis, S., Staal, J.B., Ursin, H., & Zanoli, G. 2006. Chapter 4. European guidelines for the management of chronic nonspecific low back pain. *Eur.Spine J.*, 15 Suppl 2, S192-S300.

Alaranta, H., Luoto, S., Heliovaara, M., & Hurri, H. 1995. Static back endurance and the risk of low-back pain. *Clin.Biomech.(Bristol., Avon.)*, 10, (6) 323-324.

Albert, W.J., Sleivert, G.G., Neary, J.P., & Bhambhani, Y.N. 2004. Monitoring individual erector spinae fatigue responses using electromyography and near infrared spectroscopy. *Can.J Appl.Physiol*, 29, (4) 363-378.

Anderson-Putz, V., Bernard, B. P., Burt, S., Cole, L. L., Fairfield-Estill, C., Fin, L. J., & Grant, K. A. 1997, *Musculoskeletal Disorders and Workplace Factors: A Critical Review of Epidemiologic Evidence for Work-Related Musculoskeletal Disorders of the Neck, Upper Extremity, and Low Back*, U.S. DEPARTMENT OF HEALTH AND HUMAN SERVICES, Cincinnati, DHHS (NIOSH) Publication No. 97B141.

Andreassen, S. & Arendt-Nielsen, L. 1987. Muscle fibre conduction velocity in motor units of the human anterior tibial muscle: a new size principle parameter. *J.Physiol*, 391, 561-571.

Apter, J.T. 1966. Models in medical research. "Muscles are motors". *JAMA*, 195, (11) 931-934.

Arjmand, N., Gagnon, D., Plamondon, A., Shirazi-Adl, A., & Lariviere, C. 2009. Comparison of trunk muscle forces and spinal loads estimated by two biomechanical models. *Clin.Biomech.(Bristol., Avon.)*, 24, (7) 533-541.

Arnall, F.A., Koumantakis, G.A., Oldham, J.A., & Cooper, R.G. 2002. Between-days reliability of electromyographic measures of paraspinal muscle fatigue at 40, 50 and 60% levels of maximal voluntary contractile force. *Clin.Rehabil.*, 16, (7) 761-771.

Arthritis Research Campaign. 2002, *Arthritis the big picture.*

Assendelft, W.J., Morton, S.C., Yu, E.I., Suttorp, M.J., & Shekelle, P.G. 2004. Spinal manipulative therapy for low back pain. *Cochrane.Database.Syst.Rev.* (1) CD000447.

Bergmark, A. 1989. Stability of the lumbar spine. A study in mechanical engineering. *Acta Orthop.Scand.Suppl*, 230, 1-54.

Bevan, S., Passmore, E., & Mahon, M. 2009, *Fit for Work? Musculoskeletal disorders and labour market participation. London:* The Work Foundation.

Biedermann, H.J., DeFoa, J.L., & Forrest, W.J. 1991. Muscle fibre directions of iliocostalis and multifidus: male-female differences. *J.Anat.*, 179, 163-167.

Biering-Sorensen, F. 1982. Low back trouble in a general population of 30-, 40-, 50-, and 60-year-old men and women. Study design, representativeness and basic results. *Dan.Med.Bull.*, 29, (6) 289-299.

Biering-Sorensen, F. 1983. A prospective study of low back pain in a general population. I. Occurrence, recurrence and aetiology. *Scand.J.Rehabil.Med.*, 15, (2) 71-79.

Biering-Sorensen, F. 1984a. A one-year prospective study of low back trouble in a general population. The prognostic value of low back history and physical measurements. *Dan.Med.Bull.*, 31, (5) 362-375.

Biering-Sorensen, F. 1984b. Physical measurements as risk indicators for low-back trouble over a one-year period. *Spine*, 9, (2) 106-119.

Biering-Sorensen, F. & Hilden, J. 1984. Reproducibility of the history of low-back trouble. *Spine*, 9, (3) 280-286.

Bigland-Ritchie, B., Donovan, E.F., & Roussos, C.S. 1981. Conduction velocity and EMG power spectrum changes in fatigue of sustained maximal efforts. *J Appl.Physiol*, 51, (5) 1300-1305.

Bigland-Ritchie, B. & Woods, J.J. 1984. Changes in muscle contractile properties and neural control during human muscular fatigue. *Muscle Nerve*, 7, (9) 691-699.

Bigos, S.J., McKee, J.E., Holland, J.P., Holland, C.L., & Hildebrandt, J. 2001. Back pain, the uncomfortable truth - assurance and activity problem. *Schmerz.*, 15, (6) 430-434.

Blunthner, R., Seidel, S., & Hinz, B. 2001. Examination of the myoelectric activity of back muscles during random vibration - methodical approach and first results. *Clinical Biomechanics*, 16, (Supplement 1) S25-S30.

Blunthner, R., Seidel, S., & Hinz, B. 2002. Myoelectric response of back muscles to vertical random whole-body vibration with different magnitudes at different postures. *Journal of Sound and Vibration*, 253, (1) 37-56.

Bogduk, N. 2005. *Clinical Anatomy of the Lumbar Spine and Sacrum*, 4th ed. Elsevier.

Bogduk, N. & Twomey, L. 1987. *Clinical Anatomy of the Lumbar Spine*, 1st ed. New York, Churchil Livingstone.

Bogduk, N. 1980. A reappraisal of the anatomy of the human lumbar erector spinae. *J.Anat.*, 131, (Pt 3) 525-540.

Bogduk, N. 1983. The innervation of the lumbar spine. *Spine*, 8, (3) 286-293.

Bogduk, N. 2004. Management of chronic low back pain. *Med.J.Aust.*, 180, (2) 79-83.

Bogduk, N. & Macintosh, J.E. 1984. The applied anatomy of the thoracolumbar fascia. *Spine*, 9, (2) 164-170.

Bogduk, N., Macintosh, J.E., & Pearcy, M.J. 1992. A universal model of the lumbar back muscles in the upright position. *Spine*, 17, (8) 897-913.

Bogduk, N., Wilson, A.S., & Tynan, W. 1982. The human lumbar dorsal rami. *J Anat.*, 134, (Pt 2) 383-397.

Booth, F.W. & Thomason, D.B. 1991. Molecular and cellular adaptation of muscle in response to exercise: perspectives of various models. *Physiol Rev.*, 71, (2) 541-585.

Borg G 1998. *Borg's Perceived Exertion and Pain Scales*, 1 ed. Human Kinetics.

Boshuizen, H.C., Bongers, P.M., & Hulshof, C.T.J. 1990. Back disorders and occupational exposure to whole-body vibration. *International Journal of Industrial Ergonomics*, 6, (1) 55-59.

Bovenzi, M. 1996. Low back pain disorders and exposure to whole-body vibration in the workplace. *Semin.Perinatol.*, 20, (1) 38-53.

Bovenzi, M. & Hulshof, C.T. 1999. An updated review of epidemiologic studies on the relationship between exposure to whole-body vibration and low back pain (1986-1997). *Int.Arch.Occup.Environ.Health*, 72, (6) 351-365.

Bradl, I., Morl, F., Scholle, H.C., Grassme, R., Muller, R., & Grieshaber, R. 2005. Back muscle activation pattern and spectrum in defined load situations. *Pathophysiology.*, 12, (4) 275-280.

Brody, L.R., Pollock, M.T., Roy, S.H., De Luca, C.J., & Celli, B. 1991. pH-induced effects on median frequency and conduction velocity of the myoelectric signal. *J.Appl.Physiol*, 71, (5) 1878-1885.

BSI 6841 1987, *British Standards Institution : Measurement and evaluation of human exposure to whole-body mechanical vibration and repeated shock 1987:6841*.

Buer, N. & Linton, S.J. 2002. Fear-avoidance beliefs and catastrophizing: occurrence and risk factor in back pain and ADL in the general population. *Pain*, 99, (3) 485-491.

Burton, A.K. & Waddell, G. 1998. Clinical guidelines in the management of low back pain. *Baillieres Clin.Rheumatol.*, 12, (1) 17-35.

Burton, A.K., Waddell, G., Tillotson, K.M., & Summerton, N. 1999. Information and advice to patients with back pain can have a positive effect. A randomized controlled trial of a novel educational booklet in primary care. *Spine*, 24, (23) 2484-2491.

Callaghan, J.P., Patla, A.E., & McGill, S.M. 1999. Low back three-dimensional joint forces, kinematics, and kinetics during walking. *Clin.Biomech.(Bristol., Avon.)*, 14, (3) 203-216.

Cardozo, A.C., Goncalves, M., & Dolan, P. 2011. Back extensor muscle fatigue at submaximal workloads assessed using frequency banding of the electromyographic signal. *Clin.Biomech.(Bristol., Avon.)*.

Carpenter, R. 2003. *Neurophysiology*, 4th ed. Arnold.

Cescon, C., Venturi, S., Merletti, R., Bonfiglioli, R., & Violante, F. 2004, Neuromuscular assessment of Fatigue of low back muscles in elderly nurses, C. Cescon & S. Lecce, eds., pp. 43-45.

Cescon, C., Gazzoni, M., Gobbo, M., Orizio, C., & Farina, D. 2004. Non-invasive assessment of single motor unit mechanomyographic response and twitch force by spike-triggered averaging. *Med.Biol.Eng Comput.*, 42, (4) 496-501.

Cescon, C., Rebecchi, P., & Merletti, R. 2007. Effect of electrode array position and subcutaneous tissue thickness on conduction velocity estimation in upper trapezius muscle. *J.Electromyogr.Kinesiol.*

Cescon, C., Sguazzi, E., Merletti, R., & Farina, D. 2006. Non-invasive characterization of single motor unit electromyographic and mechanomyographic activities in the biceps brachii muscle. *J Electromyogr.Kinesiol.*, 16, (1) 17-24.

Choi, B.K., Verbeek, J.H., Tam, W.W., & Jiang, J.Y. 2010. Exercises for prevention of recurrences of low-back pain. *Cochrane.Database.Syst.Rev.* (1) CD006555.

Cholewicki, J. & McGill, S.M. 1996. Mechanical stability of the in vivo lumbar spine: implications for injury and chronic low back pain. *Clin.Biomech.(Bristol., Avon.)*, 11, (1) 1-15.

Cifrek, M., Medved, V., Tonkovic, S., & Ostojic, S. 2009. Surface EMG based muscle fatigue evaluation in biomechanics. *Clin.Biomech.(Bristol., Avon.)*, 24, (4) 327-340.

Cohen, J.E., Goel, V., Frank, J.W., & Gibson, E.S. 1994. Predicting risk of back injuries, work absenteeism, and chronic disability. The shortcomings of preplacement screening. *J Occup.Med*, 36, (10) 1093-1099.

Corin, G., Strutton, P.H., & McGregor, A.H. 2005. Establishment of a protocol to test fatigue of the trunk muscles. *Br.J.Sports Med.*, 39, (10) 731-735.

Cripps, R., Cain, C., Philips, H., Rees, S., & Richards, D. 2008, *Development of a new crew seat for all weather lifeboats*.

Crossman, K., Mahon, M., Watson, P.J., Oldham, J.A., & Cooper, R.G. 2004. Chronic low back pain-associated paraspinal muscle dysfunction is not the result of a constitutionally determined "adverse" fiber-type composition. *Spine*, 29, (6) 628-634.

Dagenais, S., Tricco, A.C., & Haldeman, S. 2010. Synthesis of recommendations for the assessment and management of low back pain from recent clinical practice guidelines. *Spine J.*, 10, (6) 514-529.

Daggfeldt, K., Huang, Q.M., & Thorstensson, A. 2000. The visible human anatomy of the lumbar erector spinae. *Spine*, 25, (21) 2719-2725.

Dalsgaard, M.K. & Secher, N.H. 2007. The brain at work: a cerebral metabolic manifestation of central fatigue? *J.Neurosci.Res.*, 85, (15) 3334-3339.

De Foa, J.L., Forrest, W., & Biedermann, H.J. 1989. Muscle fibre direction of longissimus, iliocostalis and multifidus: landmark-derived reference lines. *J Anat.*, 163, 243-247.

De Luca, C.J. 1984. Myoelectrical manifestations of localized muscular fatigue in humans. *Crit Rev.Biomed.Eng*, 11, (4) 251-279.

de Oliveira, C.G. & Nadal, J. 2004. Back muscle EMG of helicopter pilots in flight: effects of fatigue, vibration, and posture. *Aviat.Space Environ.Med.*, 75, (4) 317-322.

Deliagina, T.G., Beloozerova, I.N., Zelenin, P.V., & Orlovsky, G.N. 2008. Spinal and supraspinal postural networks. *Brain Res.Rev.*, 57, (1) 212-221.

Deliagina, T.G. & Orlovsky, G.N. 2002. Comparative neurobiology of postural control. *Curr.Opin.Neurobiol.*, 12, (6) 652-657.

Deliagina, T.G., Orlovsky, G.N., Zelenin, P.V., & Beloozerova, I.N. 2006. Neural bases of postural control. *Physiology.(Bethesda.)*, 21, 216-225.

Delp, S.L., Suryanarayanan, S., Murray, W.M., Uhlir, J., & Triolo, R.J. 2001. Architecture of the rectus abdominis, quadratus lumborum, and erector spinae. *J.Biomech.*, 34, (3) 371-375.

Deyo, R.A. & Tsui-Wu, Y.J. 1987. Descriptive epidemiology of low-back pain and its related medical care in the United States. *Spine*, 12, (3) 264-268.

Deyo, R.A. & Weinstein, J.N. 2001. Low back pain. *N.Engl.J Med*, 344, (5) 363-370.

Di Giulio, C., Daniele, F., & Tipton, C.M. 2006. Angelo Mosso and muscular fatigue: 116 years after the first Congress of Physiologists: IUPS commemoration. *Adv.Physiol Educ.*, 30, (2) 51-57.

Directive 2002/44/EC 2002, *The European Parliament and the Council of the European Union. On the minimum health and safety requirements regarding the exposure of workers to the risks arising from physical agents (vibration). Directive 2002/44/EC. Official Journal of the European Communities 6 July 2002;L177/13-19*.

Dolan, P., Mannion, A.F., & Adams, M.A. 1995. Fatigue of the erector spinae muscles. A quantitative assessment using "frequency banding" of the surface electromyography signal. *Spine*, 20, (2) 149-159.

Dreyfuss, P., Halbrook, B., Pauza, K., Joshi, A., McLarty, J., & Bogduk, N. 2000. Efficacy and validity of radiofrequency neurotomy for chronic lumbar zygapophysial joint pain. *Spine*, 25, (10) 1270-1277.

Dunn, K.M. 2010. Extending conceptual frameworks: life course epidemiology for the study of back pain. *BMC.Musculoskelet.Disord.*, 11, 23.

Dunn, K.M. & Croft, P.R. 2004. Epidemiology and natural history of low back pain. *Eura.Medicophys.*, 40, (1) 9-13.

Edwards, R.H. 1981. Human muscle function and fatigue. *Ciba Found.Symp.*, 82, 1-18.

Ehrlich, G.E. 2003. Back pain. *J.Rheumatol.Suppl*, 67, 26-31.

Elfving, B. & Dedering, S. 2007. Task dependency in back muscle fatigue - Correlations between two test methods. *Clin.Biomech.(Bristol., Avon.)*, 22, (1) 28-33.

Elfving, B., Nemeth, G., & Arvidsson, I. 2000. Back muscle fatigue in healthy men and women studied by electromyography spectral parameters and subjective ratings. *Scand.J.Rehabil.Med.*, 32, (3) 117-123.

Elfving, B., Nemeth, G., Arvidsson, I., & Lamontagne, M. 1999. Reliability of EMG spectral parameters in repeated measurements of back muscle fatigue. *J.Electromyogr.Kinesiol.*, 9, (4) 235-243.

Enoka, R.M. & Duchateau, J. 2008. Muscle fatigue: what, why and how it influences muscle function. *J.Physiol*, 586, (1) 11-23.

Enoka, R.M. & Fuglevand, A.J. 2001. Motor unit physiology: some unresolved issues. *Muscle Nerve*, 24, (1) 4-17.

Enoka, R.M. & Stuart, D.G. 1992. Neurobiology of muscle fatigue. *J.Appl.Physiol*, 72, (5) 1631-1648.

Faas, A., Van Eijk, J.T., Chavannes, A.W., & Gubbels, J.W. 1995. A randomized trial of exercise therapy in patients with acute low back pain. Efficacy on sickness absence. *Spine*, 20, (8) 941-947.

Falkenberg, J., Podein, R.J., Pardo, X., & Iaizzo, P.A. 2001. Surface EMG activity of the back musculature during axial spinal unloading using an LTX 3000 Lumbar Rehabilitation System. *Electromyogr.Clin.Neurophysiol.*, 41, (7) 419-427.

Falla, D. & Farina, D. 2008. Non-uniform adaptation of motor unit discharge rates during sustained static contraction of the upper trapezius muscle. *Exp.Brain Res.*, 191, (3) 363-370.

Farina, D., Fortunato, E., & Merletti, R. 2000. Noninvasive estimation of motor unit conduction velocity distribution using linear electrode arrays. *IEEE Trans.Biomed.Eng*, 47, (3) 380-388.

Farina, D., Gazzoni, M., & Merletti, R. 2003a. Assessment of low back muscle fatigue by surface EMG signal analysis: methodological aspects. *J Electromyogr.Kinesiol.*, 13, (4) 319-332.

Farina, D., Kallenberg, L.A., Merletti, R., & Hermens, H.J. 2003. Effect of side dominance on myoelectric manifestations of muscle fatigue in the human upper trapezius muscle. *Eur.J Appl.Physiol*, 90, (5-6) 480-488.

Farina, D., Madeleine, P., Graven-Nielsen, T., Merletti, R., & rendt-Nielsen, L. 2002. Standardising surface electromyogram recordings for assessment of activity and fatigue in the human upper trapezius muscle. *Eur.J Appl.Physiol*, 86, (6) 469-478.

Farina, D. & Merletti, R. 2004a. Estimation of average muscle fiber conduction velocity from two-dimensional surface EMG recordings. *J Neurosci.Methods*, 134, (2) 199-208.

Farina, D. & Merletti, R. 2004b. Methods for estimating muscle fibre conduction velocity from surface electromyographic signals. *Med Biol.Eng Comput.*, 42, (4) 432-445.

Farina, D., Merletti, R., & Enoka, R.M. 2004. The extraction of neural strategies from the surface EMG. *J Appl.Physiol*, 96, (4) 1486-1495.

Farina, D., Merletti, R., Rainoldi, A., Buonocore, M., & Casale, R. 1999. Two methods for the measurement of voluntary contraction torque in the biceps brachii muscle. *Med Eng Phys.*, 21, (8) 533-540.

Farina, D. & Negro, F. 2012. Accessing the neural drive to muscle and translation to neurorehabilitation technologies. *IEEE Rev.Biomed.Eng*, 5, 3-14.

Farina, D., Negro, F., Gazzoni, M., & Enoka, R.M. 2008. Detecting the unique representation of motor-unit action potentials in the surface electromyogram. *J.Neurophysiol.*, 100, (3) 1223-1233.

Farina, D., Pozzo, M., Merlo, E., Bottin, A., & Merletti, R. 2004. Assessment of average muscle fiber conduction velocity from surface EMG signals during fatiguing dynamic contractions. *IEEE Trans.Biomed.Eng*, 51, (8) 1383-1393.

Farina, D., rendt-Nielsen, L., Merletti, R., & Graven-Nielsen, T. 2002. Assessment of single motor unit conduction velocity during sustained contractions of the tibialis anterior muscle with advanced spike triggered averaging. *J Neurosci.Methods*, 115, (1) 1-12.

Farina, D., rendt-Nielsen, L., Merletti, R., Indino, B., & Graven-Nielsen, T. 2003. Selectivity of spatial filters for surface EMG detection from the tibialis anterior muscle. *IEEE Trans.Biomed.Eng*, 50, (3) 354-364.

Farina, D., Zagari, D., Gazzoni, M., & Merletti, R. 2004a. Reproducibility of muscle-fiber conduction velocity estimates using multichannel surface EMG techniques. *Muscle Nerve*, 29, (2) 282-291.

Farina, D., Zagari, D., Gazzoni, M., & Merletti, R. 2004b. Reproducibility of muscle-fiber conduction velocity estimates using multichannel surface EMG techniques. *Muscle Nerve*, 29, (2) 282-291.

Farina, D., Zennaro, D., Pozzo, M., Merletti, R., & Laubli, T. 2006. Single motor unit and spectral surface EMG analysis during low-force, sustained contractions of the upper trapezius muscle. *Eur.J Appl.Physiol*, 96, (2) 157-164.

Farina, D., Gazzoni, M., & Merletti, R. 2003b. Assessment of low back muscle fatigue by surface EMG signal analysis: methodological aspects. *Journal of Electromyography and Kinesiology*, 13, (4) 319-332.

Fletcher, W.M. 1907. Lactic acid in amphibian muscle. *J.Physiol*, 35, (4) 247-309.

Frank, J.W., Brooker, A.S., DeMaio, S.E., Kerr, M.S., Maetzel, A., Shannon, H.S., Sullivan, T.J., Norman, R.W., & Wells, R.P. 1996. Disability resulting from occupational low back pain. Part II: What do we know about secondary prevention? A review of the scientific evidence on prevention after disability begins. *Spine (Phila Pa 1976.)*, 21, (24) 2918-2929.

Frank, J.W., Kerr, M.S., Brooker, A.S., DeMaio, S.E., Maetzel, A., Shannon, H.S., Sullivan, T.J., Norman, R.W., & Wells, R.P. 1996. Disability resulting from occupational low back pain. Part I: What do we know about primary prevention? A review of the scientific evidence on prevention before disability begins. *Spine (Phila Pa 1976.)*, 21, (24) 2908-2917.

Gajdosik, R.L. & Bohannon, R.W. 1987. Clinical measurement of range of motion. Review of goniometry emphasizing reliability and validity. *Phys.Ther.*, 67, (12) 1867-1872.

Gandevia, S.C. 2001. Spinal and supraspinal factors in human muscle fatigue. *Physiol Rev.*, 81, (4) 1725-1789.

Garland, S.J., Garner, S.H., & McComas, A.J. 1988. Reduced voluntary electromyographic activity after fatiguing stimulation of human muscle. *J.Physiol*, 401, 547-556.

Gibbons, L.E., Videman, T., & Battie, M.C. 1997. Determinants of isokinetic and psychophysical lifting strength and static back muscle endurance: a study of male monozygotic twins. *Spine (Phila Pa 1976.)*, 22, (24) 2983-2990.

Goldfinch, D. 2012, *Mitigating against the effects of shock*.

Gray, H. 2009. *Gray's Anatomy*, 40 ed. Churchill Livingstone.

Griffin, M.J. 1990. *Handbook of human vibration* London, Academic Press.

Griffin, M.J. 1998. Predicting the hazards of whole-body vibration--considerations of a standard. *Ind.Health*, 36, (2) 83-91.

Griffin, M.J. 2004. Minimum health and safety requirements for workers exposed to hand-transmitted vibration and whole-body vibration in the European Union; a review. *Occup.Environ.Med*, 61, (5) 387-397.

Grillner, S., Wallen, P., Saitoh, K., Kozlov, A., & Robertson, B. 2008. Neural bases of goal-directed locomotion in vertebrates--an overview. *Brain Res.Rev.*, 57, (1) 2-12.

Hansen, J. 1964. Postoperative management in Lumbar disc protrusions. I. Indications, Method and Results. II Follow-up on a trained and an untrained group of patients. *Acta Orthop.Scand.Suppl* SUPPL-47.

Harlick, J.C., Milosavljevic, S., & Milburn, P.D. 2007. Palpation identification of spinous processes in the lumbar spine. *Man.Ther.*, 12, (1) 56-62.

Hayden, J.A., van Tulder, M.W., Malmivaara, A.V., & Koes, B.W. 2005. Meta-analysis: exercise therapy for nonspecific low back pain. *Ann.Intern.Med.*, 142, (9) 765-775.

Hayden, J.A., van Tulder, M.W., & Tomlinson, G. 2005. Systematic review: strategies for using exercise therapy to improve outcomes in chronic low back pain. *Ann.Intern.Med.*, 142, (9) 776-785.

Hermans, H., Freriks, B., Merletti, R., Stegeman, D., Blok, J., Rau, J., Disselhorst-Klugg, C., & Hagg, G. 1999. European recommendations for surface electromyography. Roessingh research and development. Enschede. The Netherlands. *SENIAM*.

Hermens, H.J., Freriks, B., Disselhorst-Klug, C., & Rau, G. 2000. Development of recommendations for SEMG sensors and sensor placement procedures. *J.Electromyogr.Kinesiol.*, 10, (5) 361-374.

Hestbaek, L., Leboeuf-Yde, C., Engberg, M., Lauritzen, T., Bruun, N.H., & Manniche, C. 2003. The course of low back pain in a general population. Results from a 5-year prospective study. *J Manipulative Physiol Ther.*, 26, (4) 213-219.

Hestbaek, L., Leboeuf-Yde, C., & Manniche, C. 2003. Low back pain: what is the long-term course? A review of studies of general patient populations. *Eur.Spine J*, 12, (2) 149-165.

Hides, J., Wilson, S., Stanton, W., McMahon, S., Keto, H., McMahon, K., Bryant, M., & Richardson, C. 2006. An MRI investigation into the function of the transversus abdominis muscle during "drawing-in" of the abdominal wall. *Spine*, 31, (6) E175-E178.

Hides, J.A., Jull, G.A., & Richardson, C.A. 2001. Long-term effects of specific stabilizing exercises for first-episode low back pain. *Spine*, 26, (11) E243-E248.

Hides, J.A., Richardson, C.A., & Jull, G.A. 1996. Multifidus muscle recovery is not automatic after resolution of acute, first-episode low back pain. *Spine*, 21, (23) 2763-2769.

Hides, J.A., Stokes, M.J., Saide, M., Jull, G.A., & Cooper, D.H. 1994. Evidence of lumbar multifidus muscle wasting ipsilateral to symptoms in patients with acute/subacute low back pain. *Spine*, 19, (2) 165-172.

Hill, A.V. 1924. Muscular Activity and Carbohydrate Metabolism. *Science*, 60, (1562) 505-514.

Hodges, P.W. 2003. Core stability exercise in chronic low back pain. *Orthop.Clin.North Am*, 34, (2) 245-254.

Hodges, P.W., Gurfinkel, V.S., Brumagne, S., Smith, T.C., & Cordo, P.C. 2002. Coexistence of stability and mobility in postural control: evidence from postural compensation for respiration. *Exp.Brain Res.*, 144, (3) 293-302.

Hodges, P.W. & Richardson, C.A. 1997. Feedforward contraction of transversus abdominis is not influenced by the direction of arm movement. *Exp.Brain Res.*, 114, (2) 362-370.

Holmstrom, E., Moritz, U., & Andersson, M. 1992. Trunk muscle strength and back muscle endurance in construction workers with and without low back disorders. *Scand.J Rehabil.Med*, 24, (1) 3-10.

Holobar, A. & Zazula, D. 2007. Multichannel blind source separation using convolution kernal compensation. *IEEE Trans Sig Process*, 55, 4487-4496.

Holobar, A., Farina, D., Gazzoni, M., Merletti, R., & Zazula, D. 2009. Estimating motor unit discharge patterns from high-density surface electromyogram. *Clin.Neurophysiol.*, 120, (3) 551-562.

Hoyle, D.A., Latour, M., & Bohannon, R.W. 1991. Intraexaminer, interexaminer, and interdevice comparability of leg length measurements obtained with measuring tape and metrecom. *J Orthop.Sports Phys.Ther.*, 14, (6) 263-268.

Huson, L. 2001. Statistical Assessment of Superiority, Equivalence and Non-Inferiority in Clinical Trials. *Clinical Research Focus*, 12, (5).

ISO 2631-1 1997, *International Organization for Standardization. Mechanical vibration and shock—evaluation of human exposure to whole-body vibration. Part 1: General requirements. International Standard. ISO, 1997:2631-1.*

Ito, T., Shirado, O., Suzuki, H., Takahashi, M., Kaneda, K., & Strax, T.E. 1996. Lumbar trunk muscle endurance testing: an inexpensive alternative to a machine for evaluation. *Arch.Phys.Med.Rehabil.*, 77, (1) 75-79.

Jones, D.A. 1981. Muscle fatigue due to changes beyond the neuromuscular junction. *Ciba Found.Symp.*, 82, 178-196.

Jones, D.A. 1996. High-and low-frequency fatigue revisited. *Acta Physiol Scand.*, 156, (3) 265-270.

Jordan, L.M., Liu, J., Hedlund, P.B., Akay, T., & Pearson, K.G. 2008. Descending command systems for the initiation of locomotion in mammals. *Brain Res.Rev.*, 57, (1) 183-191.

Jorgensen, K. 1997. Human trunk extensor muscles physiology and ergonomics. *Acta Physiol Scand.Suppl*, 637, 1-58.

Jorgensen, K., Nicholaisen, T., & Kato, M. 1993. Muscle fiber distribution, capillary density, and enzymatic activities in the lumbar paravertebral muscles of young men. Significance for isometric endurance. *Spine (Phila Pa 1976.)*, 18, (11) 1439-1450.

Jorgensen, K. & Nicolaisen, T. 1986. Two methods for determining trunk extensor endurance. A comparative study. *Eur.J.Appl.Physiol Occup.Physiol*, 55, (6) 639-644.

Jull, G., Bogduk, N., & Marsland, A. 1988. The accuracy of manual diagnosis for cervical zygapophysial joint pain syndromes. *Med J Aust.*, 148, (5) 233-236.

Kalimo, H., Rantanen, J., Viljanen, T., & Einola, S. 1989. Lumbar muscles: structure and function. *Ann.Med*, 21, (5) 353-359.

Kankaanpaa, M., Laaksonen, D., Taimela, S., Kokko, S.M., Airaksinen, O., & Hanninen, O. 1998. Age, sex, and body mass index as determinants of back and hip extensor fatigue in the isometric Sorensen back endurance test. *Arch.Phys.Med.Rehabil.*, 79, (9) 1069-1075.

Kankaanpaa, M., Taimela, S., Laaksonen, D., Hanninen, O., & Airaksinen, O. 1998. Back and hip extensor fatigability in chronic low back pain patients and controls. *Arch.Phys.Med.Rehabil.*, 79, (4) 412-417.

Kankaanpaa, M., Taimela, S., Webber, C.L., Jr., Airaksinen, O., & Hanninen, O. 1997. Lumbar paraspinal muscle fatigability in repetitive isoinertial loading: EMG spectral indices, Borg scale and endurance time. *Eur.J.Appl.Physiol Occup.Physiol*, 76, (3) 236-242.

Kapandji, I.A. 2008. *The Physiology of the Joints: The Trunk and the Vertebral Column, Volume 3*, 6 ed. Churchill Livingstone.

Kirkaldy-Willis, W.H. 1988. *Managing Low Back Pain* New York, NY; Churchill Livingstone Inc.

Klingenstierna, U. & Pope, M.H. 1987. Body height changes from vibration. *Spine (Phila Pa 1976.)*, 12, (6) 566-568.

Koes, B.W., van, T.M., Lin, C.W., Macedo, L.G., McAuley, J., & Maher, C. 2010. An updated overview of clinical guidelines for the management of non-specific low back pain in primary care. *Eur.Spine J.*, 19, (12) 2075-2094.

Kujala, U.M., Taimela, S., Viljanen, T., Jutila, H., Viitasalo, J.T., Videman, T., & Battie, M.C. 1996. Physical loading and performance as predictors of back pain in healthy adults. A 5-year prospective study. *Eur.J Appl.Physiol Occup.Physiol*, 73, (5) 452-458.

Lambert, E.V., St Clair, G.A., & Noakes, T.D. 2005. Complex systems model of fatigue: integrative homoeostatic control of peripheral physiological systems during exercise in humans. *Br J Sports Med*, 39, (1) 52-62.

Landis, J.R. & Koch, G.G. 1977. The measurement of observer agreement for categorical data. *Biometrics*, 33, (1) 159-174.

Lariviere, C., Arsenault, A.B., Gravel, D., Gagnon, D., & Loisel, P. 2002. Evaluation of measurement strategies to increase the reliability of EMG indices to assess back muscle fatigue and recovery. *J.Electromyogr.Kinesiol.*, 12, (2) 91-102.

Latimer, J., Maher, C.G., Refshauge, K., & Colaco, I. 1999. The reliability and validity of the Biering-Sorensen test in asymptomatic subjects and subjects reporting current or previous nonspecific low back pain. *Spine*, 24, (20) 2085-2089.

Leclere, H., Beaulieu, M.D., Bordage, G., Sindon, A., & Couillard, M. 1990. Why are clinical problems difficult? General practitioners' opinions concerning 24 clinical problems. *CMAJ.*, 143, (12) 1305-1315.

Lederman, E. 2010. The myth of core stability. *J Bodyw.Mov Ther.*, 14, (1) 84-98.

Liddle, S.D., Baxter, G.D., & Gracey, J.H. 2004. Exercise and chronic low back pain: what works? *Pain*, 107, (1-2) 176-190.

Liddle, S.D., Gracey, J.H., & Baxter, G.D. 2007. Advice for the management of low back pain: a systematic review of randomised controlled trials. *Man.Ther.*, 12, (4) 310-327.

Lin, C.W., Haas, M., Maher, C.G., Machado, L.A., & van Tulder, M.W. 2011a. Cost-effectiveness of general practice care for low back pain: a systematic review. *Eur.Spine J.*, 20, (7) 1012-1023.

Lin, C.W., Haas, M., Maher, C.G., Machado, L.A., & van Tulder, M.W. 2011b. Cost-effectiveness of guideline-endorsed treatments for low back pain: a systematic review. *Eur.Spine J.*, 20, (7) 1024-1038.

Lings, S. & Leboeuf-Yde, C. 1998. [Whole body vibrations and low back pain]. *Ugeskr.Laeger*, 160, (29) 4298-4301.

Lings, S. & Leboeuf-Yde, C. 2000. Whole-body vibration and low back pain: a systematic, critical review of the epidemiological literature 1992-1999. *Int.Arch.Occup.Environ.Health*, 73, (5) 290-297.

Luttmann, A., Jager, M., & Laurig, W. 2000. Electromyographical indication of muscular fatigue in occupational field studies. *International Journal of Industrial Ergonomics*, 25, 645-660.

Macintosh, J.E. & Bogduk, N. 1987. 1987 Volvo award in basic science. The morphology of the lumbar erector spinae. *Spine*, 12, (7) 658-668.

Macintosh, J.E. & Bogduk, N. 1991. The attachments of the lumbar erector spinae. *Spine (Phila Pa 1976.)*, 16, (7) 783-792.

Madeleine, P., Farina, D., Merletti, R., & rendt-Nielsen, L. 2002. Upper trapezius muscle mechanomyographic and electromyographic activity in humans during low force fatiguing and non-fatiguing contractions. *Eur.J Appl.Physiol*, 87, (4-5) 327-336.

Maniadakis, N. & Gray, A. 2000. The economic burden of back pain in the UK. *Pain*, 84, (1) 95-103.

Mannion, A.F. 1999a. Fibre type characteristics and function of the human paraspinal muscles: normal values and changes in association with low back pain. *J.Electromyogr.Kinesiol.*, 9, (6) 363-377.

Mannion, A.F. 1999b. Fibre type characteristics and function of the human paraspinal muscles: normal values and changes in association with low back pain. [Review] [116 refs]. *Journal of Electromyography & Kinesiology.9(6):363-77*.

Mannion, A.F., Connolly, B., Wood, K., & Dolan, P. 1997. The use of surface EMG power spectral analysis in the evaluation of back muscle function. *J.Rehabil.Res.Dev.*, 34, (4) 427-439.

Mannion, A.F. & Dolan, P. 1994. Electromyographic median frequency changes during isometric contraction of the back extensors to fatigue. *Spine*, 19, (11) 1223-1229.

Mannion, A.F., Dumas, G.A., Cooper, R.G., Espinosa, F.J., Faris, M.W., & Stevenson, J.M. 1997a. Muscle fibre size and type distribution in thoracic and lumbar regions of erector spinae in healthy subjects without low back pain: normal values and sex differences. *J.Anat.*, 190 (Pt 4), 505-513.

Mannion, A.F., Dumas, G.A., Cooper, R.G., Espinosa, F.J., Faris, M.W., & Stevenson, J.M. 1997b. Muscle fibre size and type distribution in thoracic and

lumbar regions of erector spinae in healthy subjects without low back pain: normal values and sex differences. *J.Anat.*, 190 (Pt 4), 505-513.

Mannion, A.F., Dumas, G.A., Stevenson, J.M., & Cooper, R.G. 1998. The influence of muscle fiber size and type distribution on electromyographic measures of back muscle fatigability. *Spine*, 23, (5) 576-584.

Mannion, A.F., Kaser, L., Weber, E., Rhyner, A., Dvorak, J., & Muntener, M. 2000. Influence of age and duration of symptoms on fibre type distribution and size of the back muscles in chronic low back pain patients. *Eur.Spine J.*, 9, (4) 273-281.

Mannion, A.F., Weber, B.R., Dvorak, J., Grob, D., & Muntener, M. 1997. Fibre type characteristics of the lumbar paraspinal muscles in normal healthy subjects and in patients with low back pain. *J.Orthop.Res.*, 15, (6) 881-887.

Marsden, C.D., Meadows, J.C., & Merton, P.A. 1983. "Muscular wisdom" that minimizes fatigue during prolonged effort in man: peak rates of motoneuron discharge and slowing of discharge during fatigue. *Adv.Neurol.*, 39, 169-211.

Masuda, T., Miyano, H., & Sadoyama, T. 1983. The distribution of myoneural junctions in the biceps brachii investigated by surface electromyography. *Electroencephalogr.Clin.Neurophysiol.*, 56, (6) 597-603.

Mayer, C., Latimer, J., & Refshauge, K. 2000. *Atlas of clincal tests and measures for low back pain*.

Mayer, T., Gatchel, R., Betancur, J., & Bovasso, E. 1995. Trunk muscle endurance measurement. Isometric contrasted to isokinetic testing in normal subjects. *Spine (Phila Pa 1976.)*, 20, (8) 920-926.

McGill, S.M. 2002. *Low back Disorders - evidenced-based prevention and rehabilitation* Human Kinetics.

McGill, S.M., Childs, A., & Liebenson, C. 1999. Endurance times for low back stabilization exercises: clinical targets for testing and training from a normal database. *Arch.Phys.Med.Rehabil.*, 80, (8) 941-944.

McGill, S.M., Patt, N., & Norman, R.W. 1988. Measurement of the trunk musculature of active males using CT scan radiography: implications for force and moment generating capacity about the L4/L5 joint. *J.Biomech.*, 21, (4) 329-341.

McIntosh, G., Wilson, L., Affieck, M., & Hall, H. 1998. Trunk and lower extremity muscle endurance: normative data for adults. *J Rehabil Outcome Meas* (2) 20-39.

McNeill, T., Warwick, D., Andersson, G., & Schultz, A. 1980. Trunk strengths in attempted flexion, extension, and lateral bending in healthy subjects and patients with low-back disorders. *Spine (Phila Pa 1976.)*, 5, (6) 529-538.

Meeusen, R., Watson, P., Hasegawa, H., Roelands, B., & Piacentini, M.F. 2006. Central fatigue: the serotonin hypothesis and beyond. *Sports Med.*, 36, (10) 881-909.

Merletti, R. Use of 128 sEMG amplifier for spinal muscle data collection. 2008. Ref Type: Personal Communication

Merletti, R. & Parker, P.A. 2004. *Electromyography – Physiology, Engineering and Noninvasive Applications* New Jersey, John Wiley&Sons, Inc. Hoboken.

Merletti, R., Aventaggiato, M., Botter, A., Holobar, A., Marateb, H., & Vieira, T.M. 2010. Advances in surface EMG: recent progress in detection and processing techniques. *Crit Rev.Biomed.Eng*, 38, (4) 305-345.

Merletti, R., Biey, D., Biey, M., Prato, G., & Orusa, A. 1985. On-line monitoring of the median frequency of the surface EMG power spectrum. *IEEE Trans.Biomed.Eng*, 32, (1) 1-7.

Merletti, R., Bottin, A., Cescon, C., Farina, D., Gazzoni, M., Martina, S., Mesin, L., Pozzo, M., Rainoldi, A., & Enck, P. 2004. Multichannel surface EMG for the non-invasive assessment of the anal sphincter muscle. *Digestion*, 69, (2) 112-122.

Merletti, R., Farina, D., & Gazzoni, M. 2003. The linear electrode array: a useful tool with many applications. *J Electromyogr.Kinesiol.*, 13, (1) 37-47.

Merletti, R., Farina, D., & Granata, A. 1999. Non-invasive assessment of motor unit properties with linear electrode arrays. *Electroencephalogr.Clin.Neurophysiol.Suppl*, 50, 293-300.

Merletti, R. & Hermens, H. 2000. Introduction to the special issue on the SENIAM European Concerted Action. *J Electromyogr.Kinesiol.*, 10, (5) 283-286.

Merletti, R., Holobar, A., & Farina, D. 2008. Analysis of motor units with high-density surface electromyography. *J Electromyogr.Kinesiol.*, 18, (6) 879-890.

Merletti, R. & Lo Conte, L.R. 1995. Advances in processing of surface myoelectric signals: Part 1. *Med Biol.Eng Comput.*, 33, (3 Spec No) 362-372.

Merletti, R. & Lo Conte, L.R. 1997. Surface EMG signal processing during isometric contractions. *J Electromyogr.Kinesiol.*, 7, (4) 241-250.

Merletti, R., Rainoldi, A., & Farina, D. 2001. Surface electromyography for noninvasive characterization of muscle. *Exerc.Sport Sci.Rev.*, 29, (1) 20-25.

Merletti, R. & Roy, S. 1996. Myoelectric and mechanical manifestations of muscle fatigue in voluntary contractions. *J Orthop.Sports Phys.Ther.*, 24, (6) 342-353.

Merlo, A., Farina, D., & Merletti, R. 2003. A fast and reliable technique for muscle activity detection from surface EMG signals. *IEEE Trans.Biomed.Eng*, 50, (3) 316-323.

Mesin, L., Merletti, R., & Rainoldi, A. 2009. Surface EMG: the issue of electrode location. *J.Electromyogr.Kinesiol.*, 19, (5) 719-726.

Moffroid, M., Reid, S., Henry, S.M., Haugh, L.D., & Ricamato, A. 1994. Some endurance measures in persons with chronic low back pain. *J.Orthop.Sports Phys.Ther.*, 20, (2) 81-87.

Moreau, C.E., Green, B.N., Johnson, C.D., & Moreau, S.R. 2001. Isometric back extension endurance tests: a review of the literature. *J.Manipulative Physiol Ther.*, 24, (2) 110-122.

Morris, JM., Lucas, D.B., & Bresler, B. 1961. Role of the Trunk in Stability of the Spine. *Journal of Bone and Joint Surgery*, 43, (3) 327-351.

Moseley, G.L., Hodges, P.W., & Gandevia, S.C. 2002. Deep and superficial fibers of the lumbar multifidus muscle are differentially active during voluntary arm movements. *Spine*, 27, (2) E29-E36.

Mosso, A. 1915. *Fatigue* London, Allen & Unwin Ltd.

Muller, R., Strassle, K., & Wirth, B. 2010. Isometric back muscle endurance: an EMG study on the criterion validity of the Ito test. *J.Electromyogr.Kinesiol.*, 20, (5) 845-850.

Myers, S.D., Dobbins, T.D., King, S., Hall, B., Ayling, R.M., Holmes, S.R., Gunston, T., & Dyson, R. 2011. Physiological consequences of military high-speed boat transits. *European journal of applied physiology*, 111, (9) 2041-2049.

Nachemson, A. 1966. The load on lumbar disks in different positions of the body. *Clin.Orthop.Relat Res.*, 45, 107-122.

Negro, F. & Farina, D. 2012. Factors influencing the estimates of correlation between motor unit activities in humans. *PLoS.One.*, 7, (9) e44894.

Ng, J.K. & Richardson, C.A. 1996. Reliability of electromyographic power spectral analysis of back muscle endurance in healthy subjects. *Arch.Phys.Med.Rehabil.*, 77, (3) 259-264.

Ng, J.K., Richardson, C.A., Parnianpour, M., & Kippers, V. 2002. Fatigue-related changes in torque output and electromyographic parameters of trunk muscles during isometric axial rotation exertion: an investigation in patients with back pain and in healthy subjects. *Spine*, 27, (6) 637-646.

NHLBI 1990. NHLBI Workshop summary. Respiratory muscle fatigue. Report of the Respiratory Muscle Fatigue Workshop Group. *Am.Rev.Respir.Dis.*, 142, (2) 474-480.

Noakes, T.D. 2000. Physiological models to understand exercise fatigue and the adaptations that predict or enhance athletic performance. *Scand.J.Med.Sci.Sports*, 10, (3) 123-145.

Noakes, T.D. 2011a. Is it time to retire the A.V. Hill Model?: A rebuttal to the article by Professor Roy Shephard. *Sports Med.*, 41, (4) 263-277.

Noakes, T.D. 2011b. Time to move beyond a brainless exercise physiology: the evidence for complex regulation of human exercise performance. *Appl.Physiol Nutr.Metab*, 36, (1) 23-35.

Noakes, T.D. 2012. Fatigue is a Brain-Derived Emotion that Regulates the Exercise Behavior to Ensure the Protection of Whole Body Homeostasis. *Front Physiol*, 3, 82.

Noakes, T.D. & St Clair, G.A. 2004. Logical limitations to the "catastrophe" models of fatigue during exercise in humans. *Br.J.Sports Med.*, 38, (5) 648-649.

Noakes, T.D., St Clair, G.A., & Lambert, E.V. 2004. From catastrophe to complexity: a novel model of integrative central neural regulation of effort and fatigue during exercise in humans. *Br.J.Sports Med.*, 38, (4) 511-514.

Noakes, T.D., St Clair, G.A., & Lambert, E.V. 2005. From catastrophe to complexity: a novel model of integrative central neural regulation of effort and fatigue during exercise in humans: summary and conclusions. *Br.J.Sports Med.*, 39, (2) 120-124.

O'Sullivan, P.B., Twomey, L., & Allison, G.T. 1998. Altered abdominal muscle recruitment in patients with chronic back pain following a specific exercise intervention. *J Orthop.Sports Phys.Ther.*, 27, (2) 114-124.

Oddsson, L.I. & De Luca, C.J. 2003. Activation imbalances in lumbar spine muscles in the presence of chronic low back pain. *J.Appl.Physiol*, 94, (4) 1410-1420.

Okano, A.H., Fontes, E.B., Montenegro, R.A., Farinatti, P.D., Cyrino, E.S., Li, L.M., Bikson, M., & Noakes, T.D. 2013. Brain stimulation modulates the autonomic nervous system, rating of perceived exertion and performance during maximal exercise. *Br.J Sports Med*.

Oliver, C.W., Tillotson, K.M., Jones, A.P., Royal, R.A., & Greenough, C.G. 1996. Reproducibility of lumbar paraspinal surface electromyogram power spectra. *Clin.Biomech.(Bristol., Avon.)*, 11, (6) 317-321.

Omnibus Survey, O. f. N. S. 1. 1998, *Adults experiencing back pain: by age and total time suffered in previous 12 months, 1998: Social Trends 30*.

Palmer, D.K., Allen, J.L., Williams, P.A., Voss, A.E., Jadhav, V., Wu, D.S., & Cheng, W.K. 2011. Multilevel magnetic resonance imaging analysis of multifidus-longissimus cleavage planes in the lumbar spine and potential clinical applications to Wiltse's paraspinal approach. *Spine (Phila Pa 1976.)*, 36, (16) 1263-1267.

Panjabi, M.M. 1992a. The stabilizing system of the spine. Part I. Function, dysfunction, adaptation, and enhancement. *J Spinal Disord.*, 5, (4) 383-389.

Panjabi, M.M. 1992b. The stabilizing system of the spine. Part II. Neutral zone and instability hypothesis. *J Spinal Disord.*, 5, (4) 390-396.

Papageorgiou, A.C., Croft, P.R., Ferry, S., Jayson, M.I., & Silman, A.J. 1995. Estimating the prevalence of low back pain in the general population. Evidence from the South Manchester Back Pain Survey. *Spine*, 20, (17) 1889-1894.

Phillips, D.R., Barnard, S., Mullee, M.A., & Hurley, M.V. 2009. Simple anatomical information improves the accuracy of locating specific spinous processes during manual examination of the low back. *Man.Ther.*, 14, (3) 346-350.

Phillips, D.R. & Twomey, L.T. 1996. A comparison of manual diagnosis with a diagnosis established by a uni-level lumbar spinal block procedure. *Man.Ther.*, 1, (2) 82-87.

Plamondon, A., Trimble, K., Lariviere, C., & Desjardins, P. 2004. Back muscle fatigue during intermittent prone back extension exercise. *Scand.J.Med.Sci.Sports*, 14, (4) 221-230.

Pope, M.H., Magnusson, M.L., & Wilder, D.G. 1998. Kappa Delta Award. Low back pain and whole body vibration. *Clin.Orthop.* (354) 241-248.

Pope, M.H., Wilder, D.G., & Magnusson, M.L. 1998. Possible mechanisms of low back pain due to whole-body vibration. *Journal of Sound and Vibration*, 215, (4) 687-697.

Pope, M.H., Wilder, D.G., & Magnusson, M.L. 1999. A review of studies on seated whole body vibration and low back pain. *Proc.Inst.Mech.Eng [H.]*, 213, (6) 435-446.

Rainoldi, A., Galardi, G., Maderna, L., Comi, G., Lo, C.L., & Merletti, R. 1999. Repeatability of surface EMG variables during voluntary isometric contractions of the biceps brachii muscle. *J Electromyogr.Kinesiol.*, 9, (2) 105-119.

Reucher, H., Rau, G., & Silny, J. 1987. Spatial filtering of noninvasive multielectrode EMG: Part I--Introduction to measuring technique and applications. *IEEE Trans Biomed.Eng*, 34, (2) 98-105.

Rhodes, R. & Bell, D.R. 2014. *Medical Physiology*, 4th ed. Wolters Klewer.

Robinson, M.E., Cassisi, J.E., O'Connor, P.D., & MacMillan, M. 1992. Lumbar iEMG during isotonic exercise: chronic low back pain patients versus controls. *J.Spinal Disord.*, 5, (1) 8-15.

Robinson, R., Robinson, H.S., Bjorke, G., & Kvale, A. 2009. Reliability and validity of a palpation technique for identifying the spinous processes of C7 and L5. *Man.Ther.*, 14, (4) 409-414.

Savigny, P., Kuntze, S., Watson, P., & Underwood, M. 2009, *Low back pain: early management of persistent non-specific low back pain*, National Collaborating Centre for Primary Care and Royal College of General Practitioners., London.

Savigny, P., Watson, P., & Underwood, M. 2009. Early management of persistent non-specific low back pain: summary of NICE guidance. *BMJ*, 338, b1805.

Schuirmann, D.J. 1987. A comparison of the two one-sided tests procedure and the power approach for assessing the equivalence of average bioavailability. *J Pharmacokinet.Biopharm.*, 15, (6) 657-680.

Shephard, R.J. 2009. Is it time to retire the 'central governor'? *Sports Med.*, 39, (9) 709-721.

Simmonds, M.J., Olson, S.L., Jones, S., Hussein, T., Lee, C.E., Novy, D., & Radwan, H. 1998. Psychometric characteristics and clinical usefulness of physical performance tests in patients with low back pain. *Spine (Phila Pa 1976.)*, 23, (22) 2412-2421.

Singh, D.K., Bailey, M., & Lee, R.Y. 2011. Ageing modifies the fibre angle and biomechanical function of the lumbar extensor muscles. *Clin.Biomech.(Bristol., Avon.)*, 26, (6) 543-547.

Sirca, A. & Kostevc, V. 1985. The fibre type composition of thoracic and lumbar paravertebral muscles in man. *J.Anat.*, 141, 131-137.

Smith, L.J., Nerurkar, N.L., Choi, K.S., Harfe, B.D., & Elliott, D.M. 2011. Degeneration and regeneration of the intervertebral disc: lessons from development. *Disease Models & Mechanisms*, 4, (1) 31-41.

Spitzer, V., Ackerman, M.J., Scherzinger, A.L., & Whitlock, D. 1996. The visible human male: a technical report. *J.Am.Med.Inform.Assoc.*, 3, (2) 118-130.

St Clair, G.A., Baden, D.A., Lambert, M.I., Lambert, E.V., Harley, Y.X., Hampson, D., Russell, V.A., & Noakes, T.D. 2003. The conscious perception of the sensation of fatigue. *Sports Med.*, 33, (3) 167-176.

St Clair, G.A. & Noakes, T.D. 2004. Evidence for complex system integration and dynamic neural regulation of skeletal muscle recruitment during exercise in humans. *Br.J.Sports Med.*, 38, (6) 797-806.

Staerkle, R., Mannion, A.F., Elfering, A., Junge, A., Semmer, N.K., Jacobshagen, N., Grob, D., Dvorak, J., & Boos, N. 2004. Longitudinal validation of the fear-avoidance beliefs questionnaire (FABQ) in a Swiss-German sample of low back pain patients. *Eur.Spine J.*, 13, (4) 332-340.

Stokes, I.A. 1994. Three-dimensional terminology of spinal deformity. A report presented to the Scoliosis Research Society by the Scoliosis Research Society Working Group on 3-D terminology of spinal deformity. *Spine (Phila Pa 1976.)*, 19, (2) 236-248.

Sung, P.S., Lammers, A.R., & Danial, P. 2009. Different parts of erector spinae muscle fatigability in subjects with and without low back pain. *Spine J*, 9, (2) 115-120.

Suter, E. & Lindsay, D. 2001. Back muscle fatigability is associated with knee extensor inhibition in subjects with low back pain. *Spine (Phila Pa 1976.)*, 26, (16) E361-E366.

Svensson, H.O., Andersson, G.B., Johansson, S., Wilhelmsson, C., & Vedin, A. 1988. A retrospective study of low-back pain in 38- to 64-year-old women. Frequency of occurrence and impact on medical services. *Spine (Phila Pa 1976.)*, 13, (5) 548-552.

Swart, J., Lamberts, R.P., Lambert, M.I., St Clair, G.A., Lambert, E.V., Skowno, J., & Noakes, T.D. 2009. Exercising with reserve: evidence that the central nervous system regulates prolonged exercise performance. *Br.J.Sports Med.*, 43, (10) 782-788.

Tsao, H., Danneels, L., & Hodges, P.W. 2011. Individual fascicles of the paraspinal muscles are activated by discrete cortical networks in humans. *Clin.Neurophysiol.*, 122, (8) 1580-1587.

Tsao, H., Galea, M.P., & Hodges, P.W. 2008. Reorganization of the motor cortex is associated with postural control deficits in recurrent low back pain. *Brain*, 131, (Pt 8) 2161-2171.

Tsao, H., Galea, M.P., & Hodges, P.W. 2009. How fast are feedforward postural adjustments of the abdominal muscles? *Behav.Neurosci.*, 123, (3) 687-693.

Tsuboi, T., Satou, T., Egawa, K., Izumi, Y., & Miyazaki, M. 1994. Spectral analysis of electromyogram in lumbar muscles: fatigue induced endurance contraction. *Eur.J.Appl.Physiol Occup.Physiol*, 69, (4) 361-366.

Ulmer, H.V. 1996. Concept of an extracellular regulation of muscular metabolic rate during heavy exercise in humans by psychophysiological feedback. *Experientia*, 52, (5) 416-420.

van Tulder, M.W., Koes, B.W., & Bouter, L.M. 1997. Conservative treatment of acute and chronic nonspecific low back pain. A systematic review of randomized controlled trials of the most common interventions. *Spine*, 22, (18) 2128-2156.

Vavken, P. 2011. Rationale for and methods of superiority, noninferiority, or equivalence designs in orthopaedic, controlled trials. *Clin.Orthop.Relat Res.*, 469, (9) 2645-2653.

Waddell, G. & Burton, A.K. 2005. Concepts of rehabilitation for the management of low back pain. *Best.Pract.Res.Clin.Rheumatol.*, 19, (4) 655-670.

Waddell, G., Feder, G., & Lewis, M. 1997. Systematic reviews of bed rest and advice to stay active for acute low back pain. *Br J Gen.Pract.*, 47, (423) 647-652.

Walker, B.F. 2000. The prevalence of low back pain: a systematic review of the literature from 1966 to 1998. *J.Spinal Disord.*, 13, (3) 205-217.

Wasserman, D.E., Wilder, D.G., Pope, M.H., Magnusson, M.L., Aleksiev, A.R., & Wasserman, J.F. 1997. Whole-body vibration exposure and occupational work-hardening. *J.Occup.Environ.Med.*, 39, (5) 403-407.

Webb, R., Brammah, T., Lunt, M., Urwin, M., Allison, T., & Symmons, D. 2003. Prevalence and predictors of intense, chronic, and disabling neck and back pain in the UK general population. *Spine (Phila Pa 1976.)*, 28, (11) 1195-1202.

Weir, J.P., Beck, T.W., Cramer, J.T., & Housh, T.J. 2006. Is fatigue all in your head? A critical review of the central governor model. *Br.J.Sports Med.*, 40, (7) 573-586.

Welch, P. 1967. The Use of Fast Fourier Transform for the Estimation of Power Spectra: A Method Based on Time Averaging Over Short, Modified Periodograms. *IEEE Transactions on Audio Electroacoustics*, AU-15 (June 1967), 70-73.

Woolf, A.D. & Pfleger, B. 2003. Burden of major musculoskeletal conditions. *Bull.World Health Organ*, 81, (9) 646-656.

Wu, H., Fu, C., Jiang, R., & Yu, W. 2012. Multilevel magnetic resonance amaging analysis of multifidus-longissimus cleavage planes in the lumbar spine and clinical applilcation to the Wiltse approach. *Pak J Med Sci*, 28, (5) 839-841.

Zwarts, M.J. & Stegeman, D.F. 2003. Multichannel surface EMG: basic aspects and clinical utility. *Muscle Nerve*, 28, (1) 1-17.

12. List of tables

13.List of figures

14. Appendices

14.1 Equivalence Analysis

The following section provides a detailed breakdown of equivalence testing and analysis.

14.1.1 Equivalence Analysis of Anatomy v MRI 70 – 90 age group comparisons

14.1.1.1 Iliocostalis comparison at T11 Anatomy v MRI study

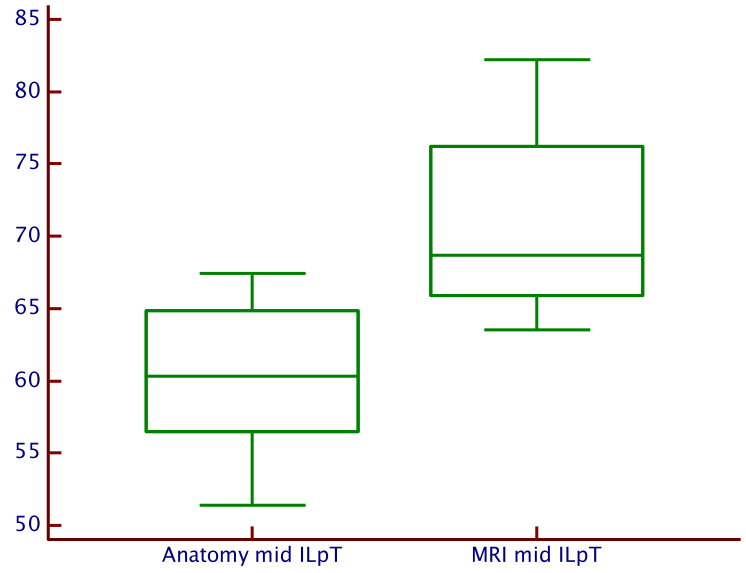

Figure 140. Comparison between Anatomy and MRI at T11, 70 -90 age group.

Calculation of 90% confidence intervals for comparison between the anatomy study and MRI mid-position at T11 was -13.38 to -6.74, this value is outside the range of clinical indifference (-5 to 5mm), it can be concluded that the two methods are not equivalent.

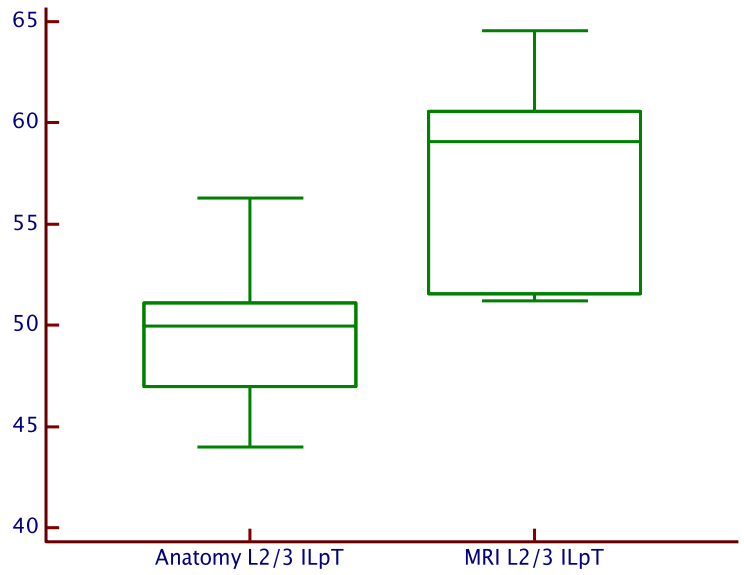

Figure 141. Comparison between Anatomy and MRI at L2/3, 70 -90 age group.

At L2/3 the 90% confidence intervals were -10.12 to -5.27, this value is outside the range of clinical indifference, it can be concluded that the two methods are not equivalent.

14.1.1.2 Longissimus comparison Anatomy v MRI mid-position study

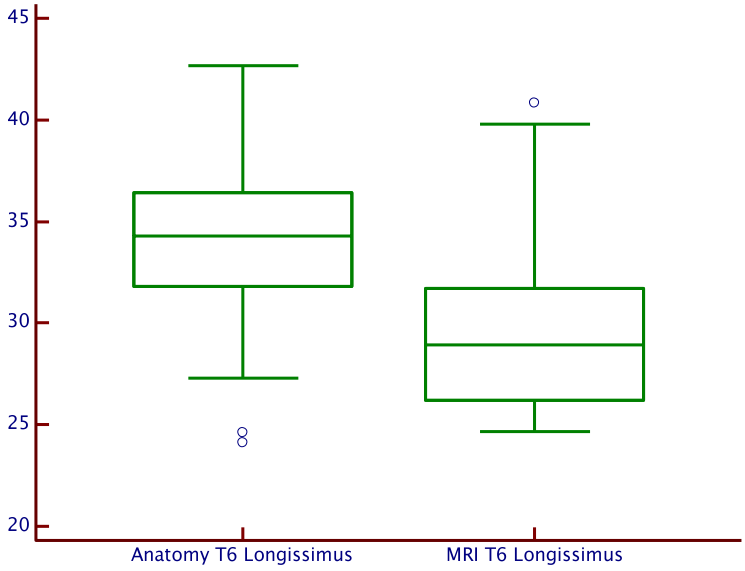

Figure 142. Comparison between Anatomy and MRI mid-position at T6

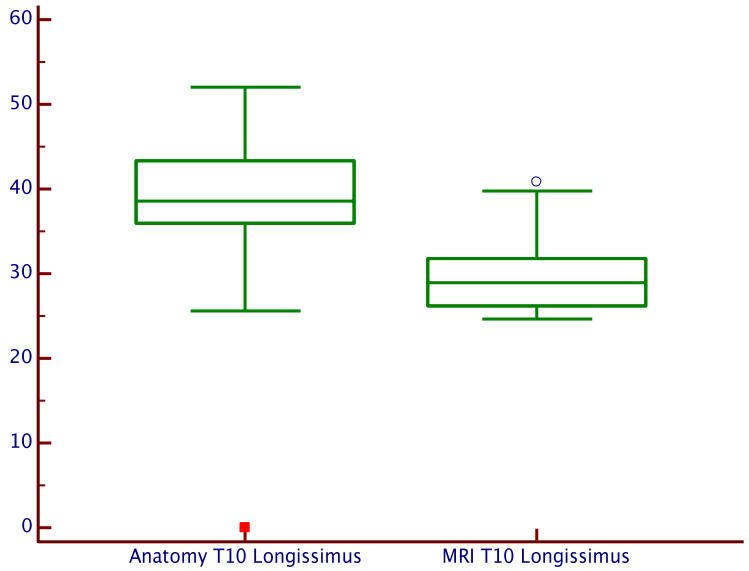

Figure 143.Comparison between Anatomy and MRI mid-position at T10

Calculation of 90% confidence intervals for comparison between the anatomy study and MRI mid-position at T6 was 0.35 to 6.12 and at T10 was -2.14 to 7.13, these values are outside the range of clinical indifference it can be concluded that the two methods are not equivalent.

14.1.1.3 Multifidus comparison Anatomy v MRI study

Calculations of 90% confidence intervals for comparison between anatomy study and MRI lateral edge of Multifidus were at;

S2: -10.28 to -5.23

L5: -9.82 to -3.21

L4: -7.87 to -3.69

L3: -7.86 to -4.55

L2: -7.37 to -4.40

L1: -5.23 to 1.28

These values are outside the range of clinical indifference (-4 to 4mm), it cannot be concluded that the two methods are equivalent.

14.1.2 Right v left comparison grouped MRI data for all ages

14.1.2.1 MRI Iliocostalis mid-position: right v left comparison

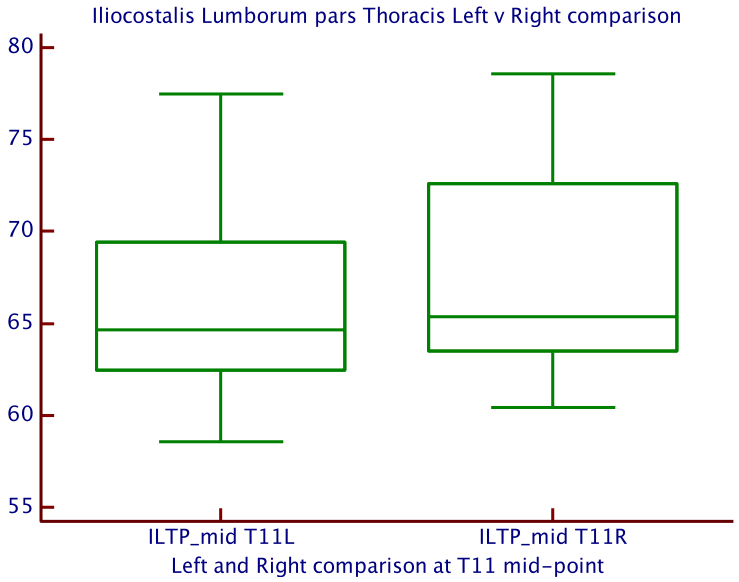

Figure 144. Iliocostalis T11 mid-position: left v right comparison.

The correlation between the right and left side data is significant, $r(23) = .96$, $p < .0001$.

At mid-position T11 the 90% confidence intervals were -0.16 to -0.56, this lies within the range of clinical indifference and with 95% confidence it can be concluded that two measures are equivalent.

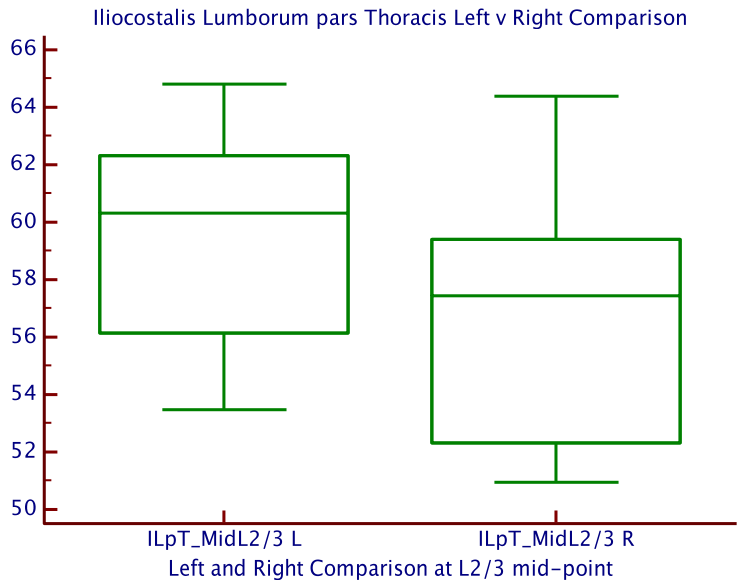

Figure 145. Iliocostalis L2/3 mid-position left v right comparison.

The correlation between the right and left side data is significant, $r(23) = .91$, $p < .0001$.

At mid position L2/3 the 90% confidence intervals were 2.3 to 3.7, this lies within the range of clinical indifference and with 95% confidence it can be concluded that measures are equivalent.

14.1.2.2 MRI Longissimus mid-position: left v right comparison

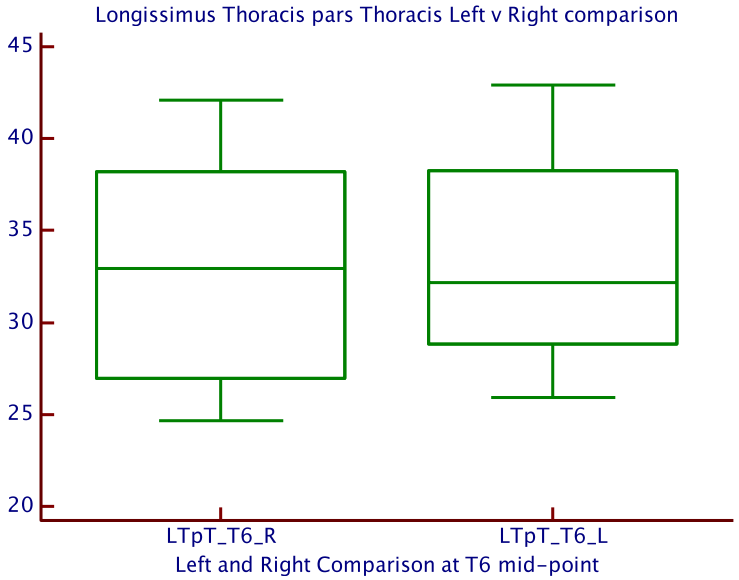

Figure 146. Longissimus T6 mid-position left v right comparison.

The correlation between the right and left side data is significant, $r(23) = .95$, $p < .0001$.

At mid-position T6 the 90% confidence intervals were -0.29 to 1.0, this lies within the range of clinical indifference and with 95% confidence it can be concluded that two measures are equivalent.

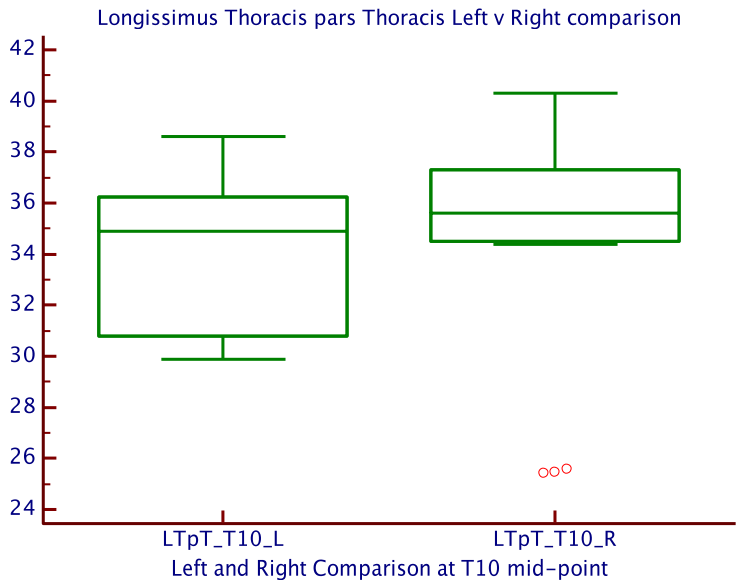

Figure 147. Longissimus T10 mid-position left v right comparison.

The correlation between the right and left side data is significant, r(23) = .89, p < .0001 .

At mid position T10 the confidence intervals were -2.08 to -0.51, this lies within the range of clinical indifference and with 95% confidence it can be concluded that two measures are equivalent.

14.1.2.3 MRI Multifidus right v left comparison

The pooled right and left side data from Multifidus for the 70 – 90 age range were compared. Correlation between side was r(142) =.97, *p< .0001*.

The 90% confidence intervals were 0.97 to 0.98, this lies within the range of clinical indifference and with 95% confidence it can be concluded that the two measures are equivalent.

The pooled right and left side data from Multifidus for the 25 – 45 age range were compared. Correlation between side is significant, r(142) =.98, *p< .0001*.

The 90% confidence intervals were 0.97 to 0.98, this lies within the range of clinical indifference and with 95% confidence it can be concluded that the two measures are equivalent.

14.1.3 Male v female comparison 70 – 90 age group

14.1.3.1 Iliocostalis: male v female comparison

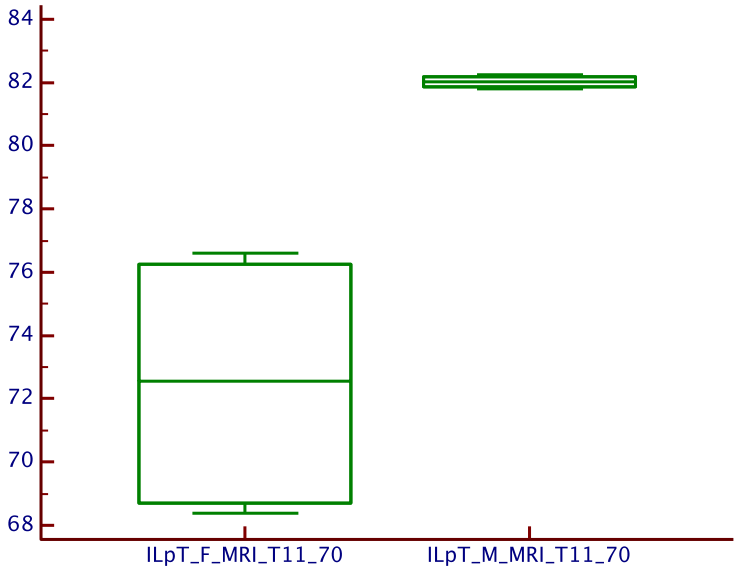

Figure 148. Iliocostalis male v female at T11, 70 – 90 age group.

The two groups differed significantly at T11 U(24) = 0.0, Z = 2.32, p = .02.

The 90% confidence intervals, at mid-position T11, between female and males in the 70 – 90 age range were -14.26 to -4.7, this lies outside the range of clinical indifference and with 95% confidence; it cannot be concluded that the measures between gender groups are equivalent.

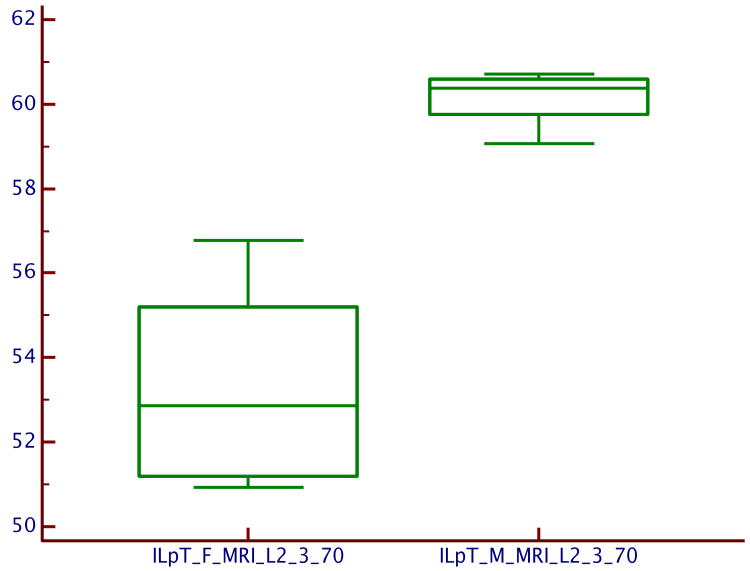

Figure 149. Iliocostalis male v female at L2/3, 70 – 90 age group.

The two groups differed significantly at L2/3 U(24) = 0.0, Z = 3.37, p <.0001.

The 90% confidence intervals, at mid-position L2/3, between female and males in the 70 – 90 age range were -9.38 to -4.3, this lies outside the range of clinical indifference; it cannot be concluded that the measures between gender groups are equivalent.

14.1.3.2 Longissimus female v male comparison

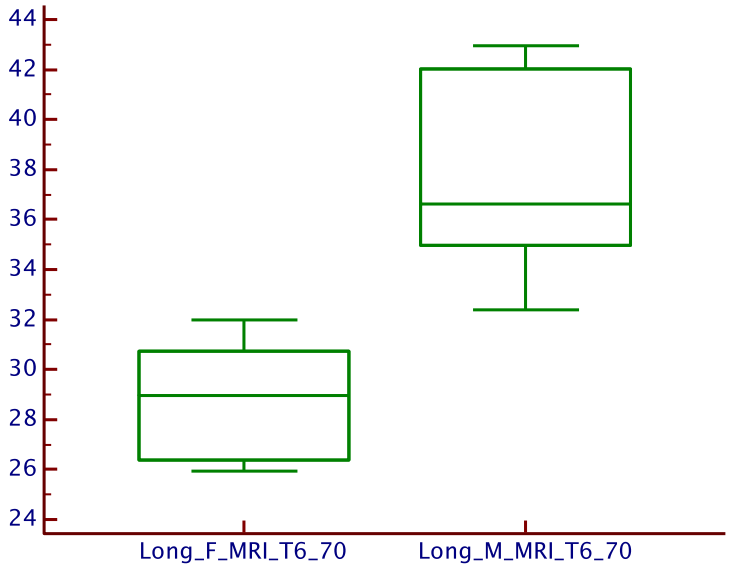

Figure 150. Female v male at T6, 70 – 90 age group.

The two groups differ significantly at T6 U(24) = 0.0, $Z = 5.13$, $p < .0001$.

The 90% confidence intervals, at mid-position T6, between female and males in the 70 – 90 age range were 7.05 to 10.53, this does not lie within the range of clinical indifference and it cannot be concluded that the measures between gender groups are equivalent.

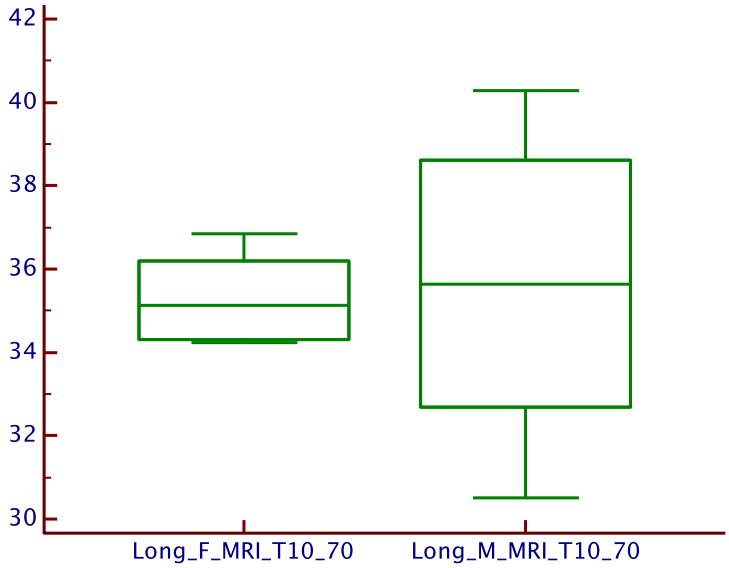

Figure 151. Longissimus female v male in 70 – 90 at T10, 70 – 90 age group..

The two groups did not differ significantly at T10 U(24) = 60, Z = 0.69, p = .48.

The 90% confidence intervals, at mid-position T10, between female and males in the 70 - 90 age range were -1.56 to 2.15, this lies within the range of clinical indifference and with 95% confidence it can be concluded that the measures between gender groups are equivalent.

14.1.3.3 Multifidus male v female comparison

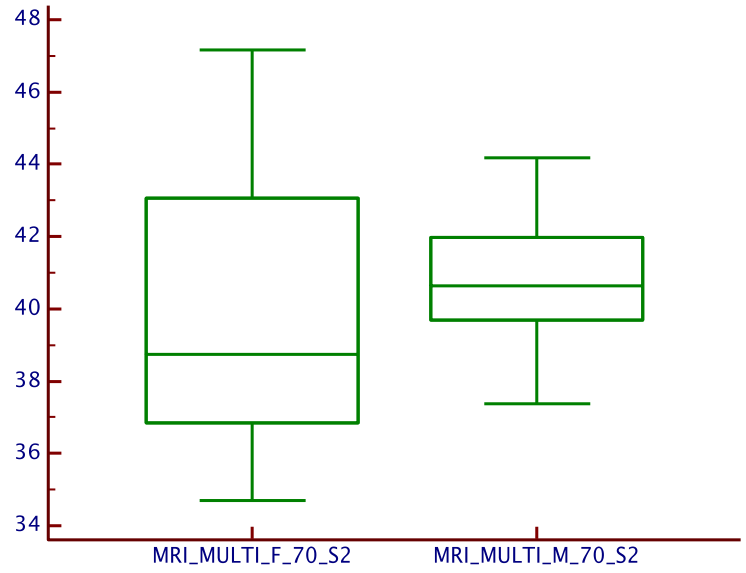

Figure 152. Multifidus male v female comparison at S2, 70 - 90 age group.

The two groups did not differ significantly at S2 U(24) = 272, Z = 1.53, p = .13.

The 90% confidence intervals, at mid-position S2, between female and males in the 70 - 90 age range were -0.36 to 2.36, this lies within the range of clinical indifference and with 95% confidence it can be concluded that the measures between gender groups are equivalent.

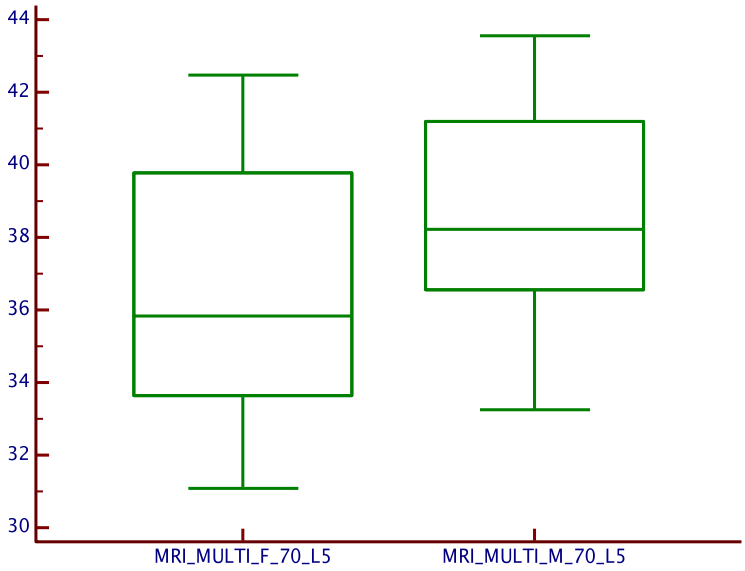

Figure 153. Multifidus male v female comparison at L5, 70 – 90 age group.

The two groups differ significantly at L5 U(24) = 235, Z = 1.97, p = .05.

The 90% confidence intervals, at mid-position L5, between female and males in the 70 – 90 age range were 0.24 to 3.46, this lies within the range of clinical indifference and with 95% confidence it can be concluded that the measures between gender groups are equivalent.

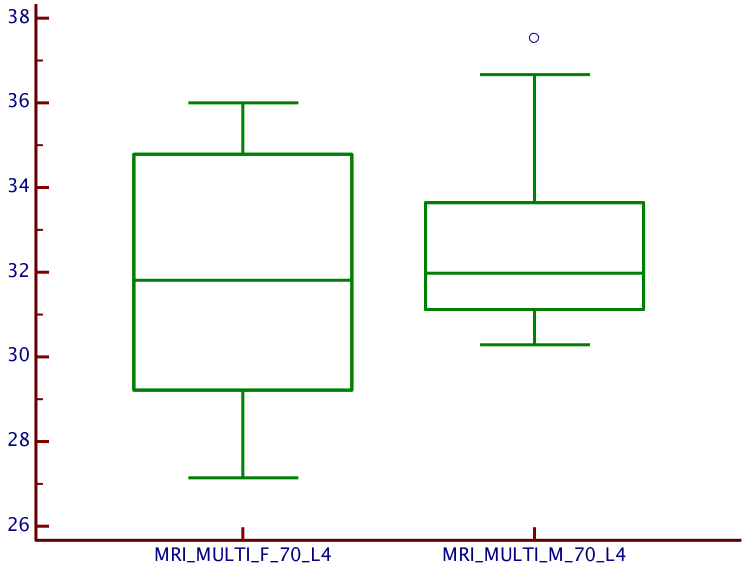

Figure 154. Multifidus male v female comparison at L4, 70 – 90 age group.

The two groups did not differ significantly at L4 U(24) = 316.5, Z = 0.76, p = .45.

The 90% confidence intervals, at mid-position L4, between female and males in the 70 – 90 age range were -0.43 to 1.91, this lies within the range of clinical indifference and with 95% confidence it can be concluded that the measures between gender groups are equivalent.

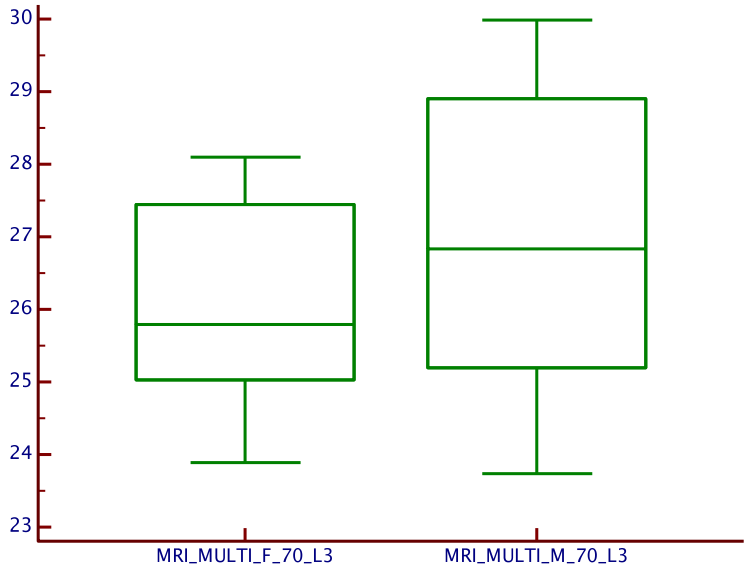

Figure 155. Multifidus male v female comparison at L3, 70 – 90 age group.

The two groups did not differ significantly at L3 U(24) = 269, $Z = 1.58$, p = .11.

The 90% confidence intervals, at mid-position L3, between female and males in the 70 – 90 age range were 0.08 to 1.63, this lies within the range of clinical indifference and with 95% confidence it can be concluded that the measures between gender groups are equivalent.

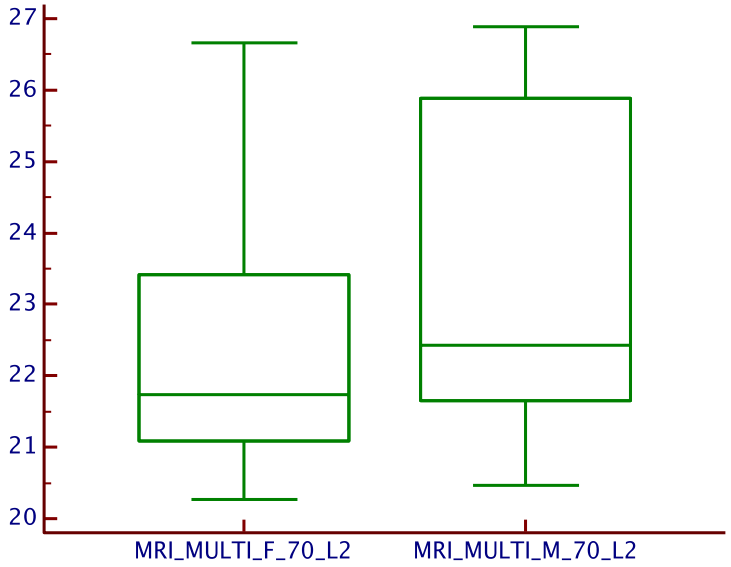

Figure 156. Multifidus male v female comparison at L2, 70 – 90 age group.

The two groups did not differ significantly at L2 U(24) = 263.5, Z = 1.68, p = .09.

The 90% confidence intervals, at mid-position L2, between female and males in the 70 – 90 age range were -0.04 to 1.81, this lies within the range of clinical indifference and with 95% confidence it can be concluded that the measures between gender groups are equivalent.

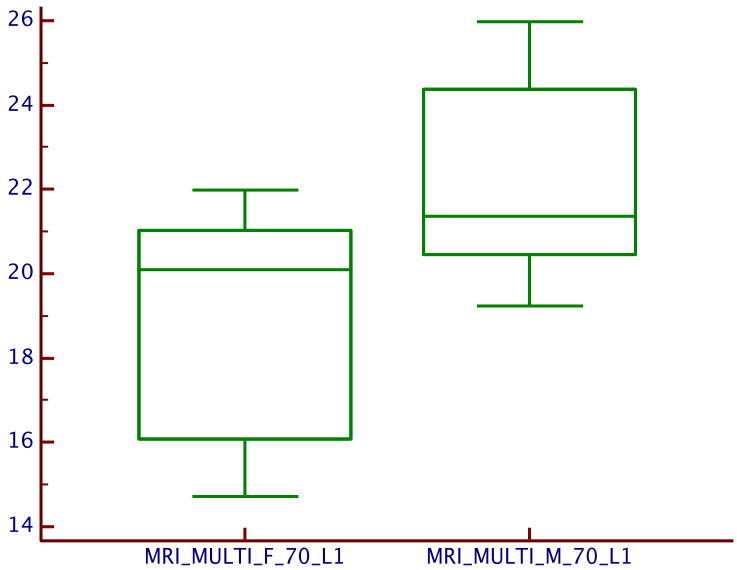

Figure 157. Multifidus male v female comparison at L1, 70 – 90 age group.

The two groups differed significantly at L1 U(24) = 157, Z = 3.53, p = .0004.

The 90% confidence intervals, at mid-position L1, between female and males in the 70 – 90 age range were 2.15 to 4.35, this lies outside the range of clinical indifference and with 95% confidence it cannot be concluded that the measures between gender groups are equivalent.

14.1.4 Male v female comparison: 25 – 45 age group

14.1.4.1 Male v female comparison: Iliocostalis 25 – 45 age range

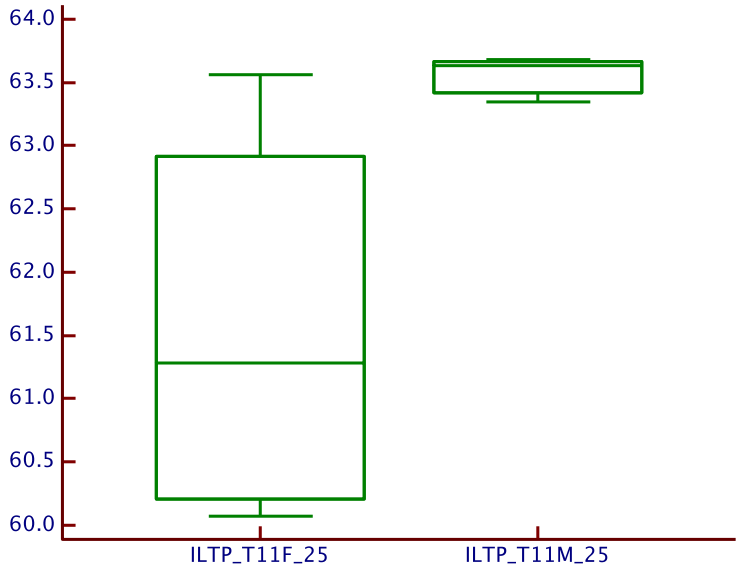

Figure 158. Iliocostalis male v female at T11, 25 – 45 age group.

The two groups differed significantly at T11 U(24) = 1, Z = 2.07, p = .03.

The 90% confidence intervals, at mid-position T11, between female and males were 0.28 to 3.7, this lies within the range of clinical indifference and with 95% confidence it can be concluded that the measures between gender groups are equivalent.

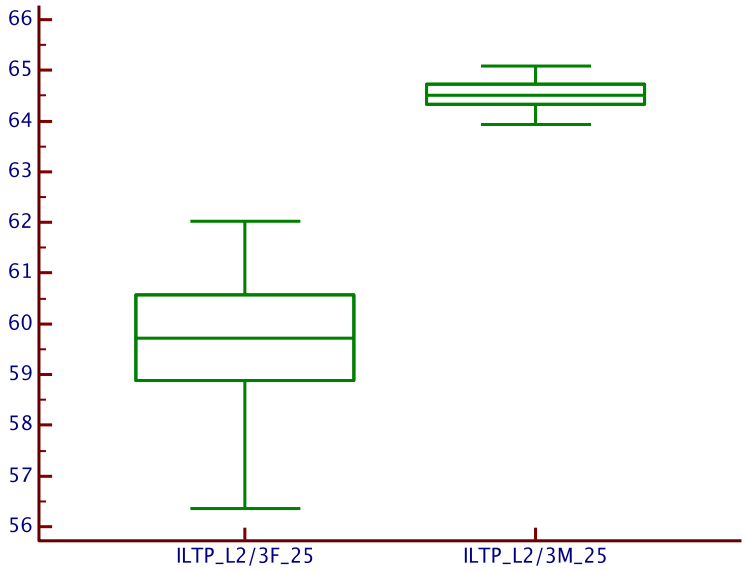

Figure 159. Iliocostalis male v female at L2/3, 25 – 45 age group

The two groups differed significantly at L2/3 U(24) = 0, Z = 4.17, p = .<.0001.

The 90% confidence intervals, at mid-position L2/3, between female and males were 3.9 to 5.8, this value is outside the range of clinical indifference, it can be concluded that the two measures are not equivalent.

14.1.4.2 Male v female comparison Longissimus 25 – 45 age range

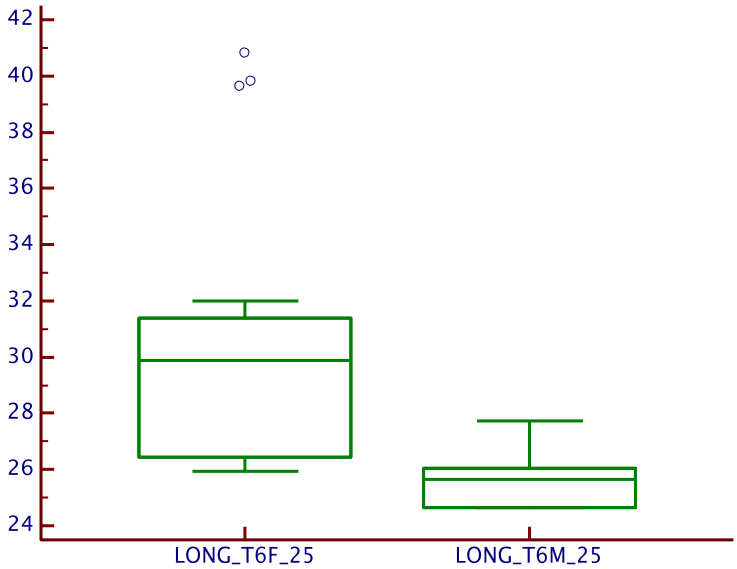

Figure 160. Longissimus male v female at T6, 25 – 45 age group.

The two groups differed significantly at T6 U(24) = 11.0, Z = 3.03, p = .0024.

The 90% confidence intervals, at mid-position T6, between female and males were -7.89 to -1.4, this value is outside the range of clinical indifference, it can be concluded that the two measures are not equivalent.

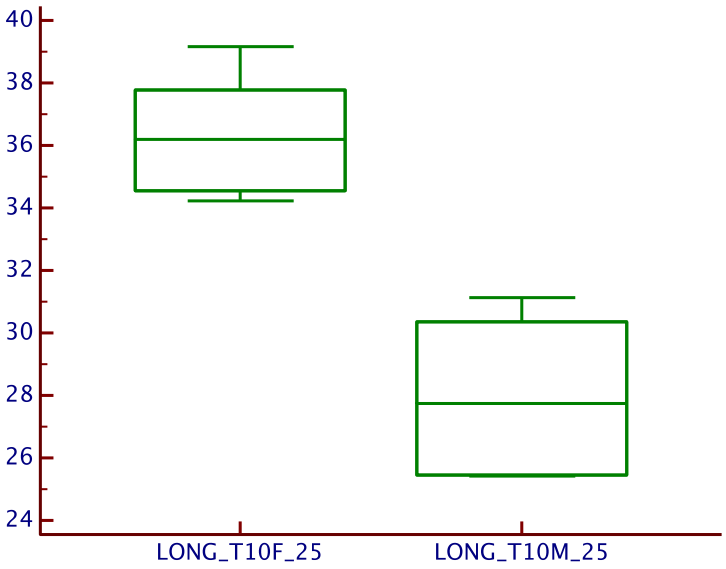

Figure 161. . Longissimus male v female at T10, 25 - 45 age group.

The two groups differed significantly at T10 U(24) = 0.0, Z = 3.6, p = .0003.

The 90% confidence intervals, at mid-position T6, between female and males were -9.9 to -6.7, this lies within the range of clinical indifference and with 95% confidence it can be concluded that two measures are equivalent.

14.1.4.3 Male v female comparison Multifidus 25 – 45 age range

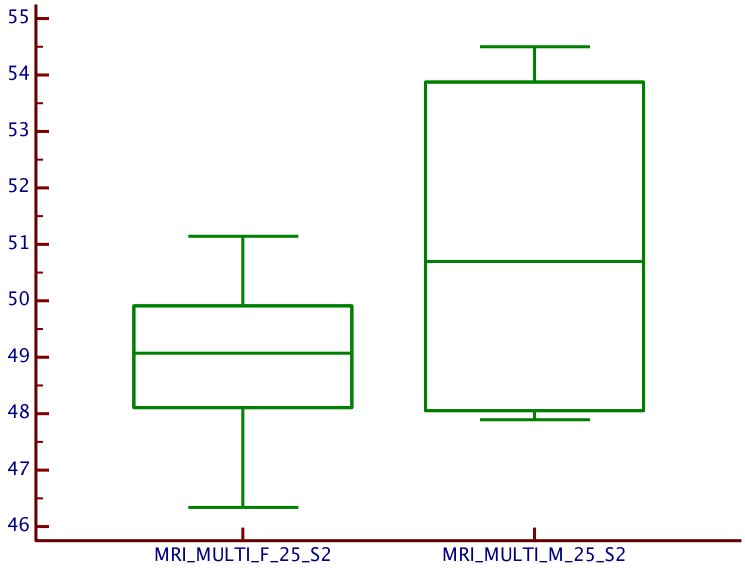

Figure 162. Multifidus male v female at S2, 25 – 45 age group.

The two groups did not differ significantly at S2 U(24) = 87, Z = 1.28, p = .19.

The 90% confidence intervals, at mid-position S2, between female and males in the 25 – 45 age range were 0.67 to 3.2, this lies within the range of clinical indifference and with 95% confidence it can be concluded that the measures between gender groups at this segmental level are equivalent.

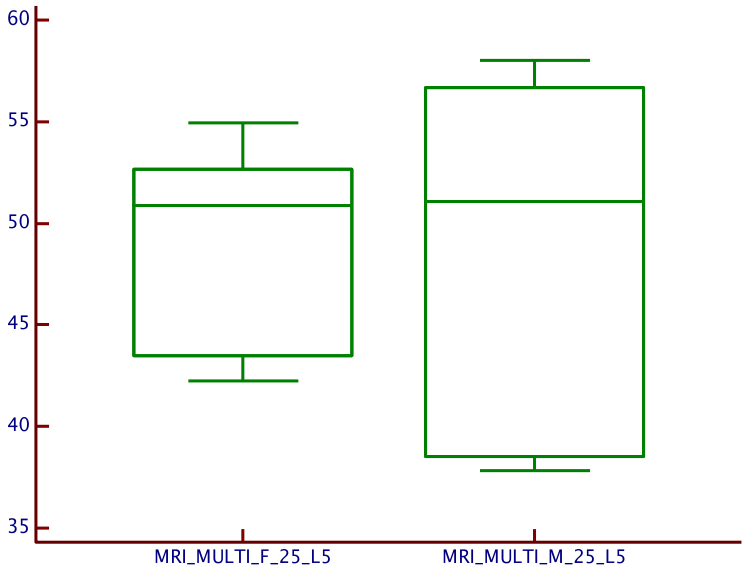

Figure 163. Multifidus male v female at L5, 25 – 45 age group.

The two groups did not differ significantly at L5 U(24) = 129, Z = .018, p = .98.

The 90% confidence intervals, at mid-position L5, between female and males in the 25 - 45 age range were -4.9 to 3.4, this value is outside the range of clinical indifference, it can be concluded that the two measures at this segmental level are not equivalent.

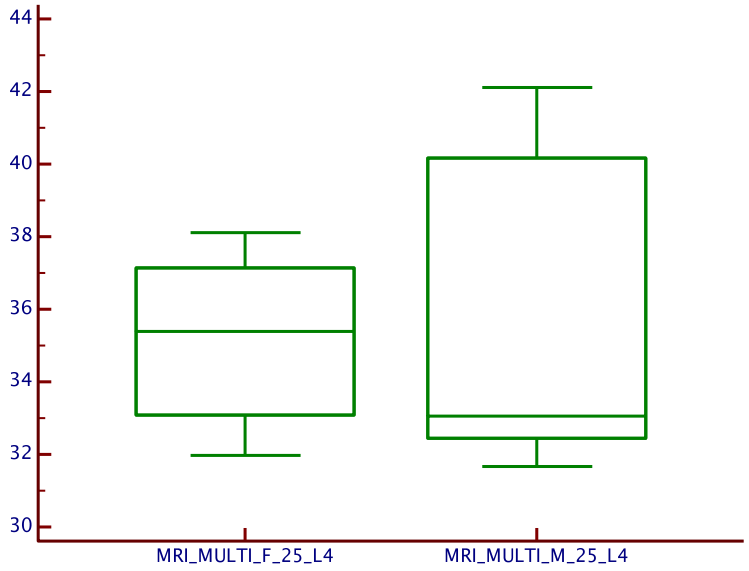

Figure 164. Multifidus male v female at L4, 25 - 45 age group.

The two groups did not differ significantly at L4 U(24) = 117, Z = .097, p = .92.

The 90% confidence intervals, at mid-position L4, between female and males in the 25 - 45 age range were -1.23 to 2.6, this lies within the range of clinical indifference and with 95% confidence it can be concluded that the measures between gender groups at this segmental level are equivalent.

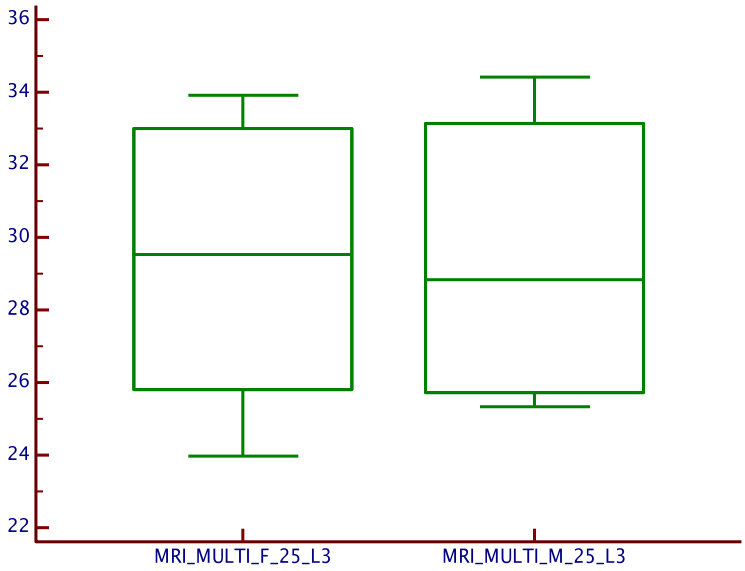

Figure 165. Multifidus male v female at L3, 25 – 45 age group.

The two groups did not differ significantly at L3 U(24) = 111, Z = .35, p = .73.

The 90% confidence intervals, at mid-position L3, between female and males in the 25 – 45 age range were -2.2 to 2.35, this lies within the range of clinical indifference and with 95% confidence it can be concluded that the measures between gender groups at this segmental level are equivalent.

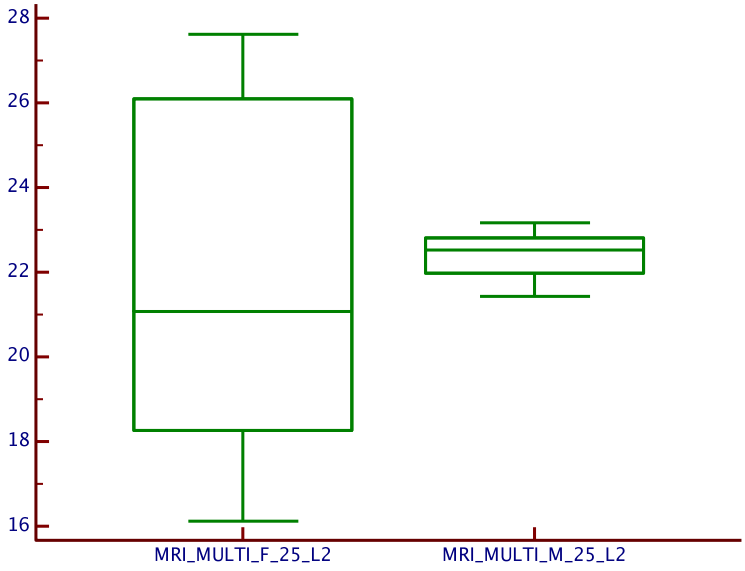

Figure 166.Multifidus male v female at L2, 25 – 45 age group.

The two groups did not differ significantly at L2 U(24) = 90, Z = 1.17, p = .24.

The 90% confidence intervals, at mid-position L2, between female and males in the 25 – 45 age range were -1.13 to 2.79, this lies within the range of clinical indifference and with 95% confidence it can be concluded that the measures between gender groups at this segmental level are equivalent.

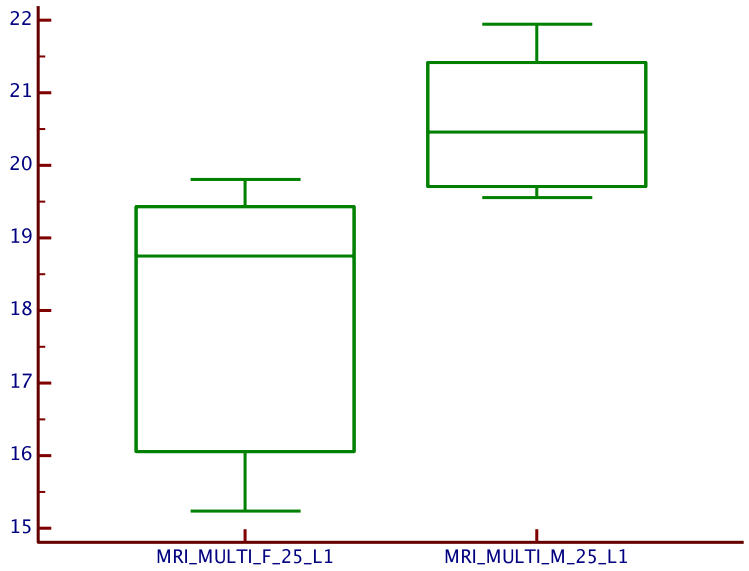

Figure 167.Multifidus: male v female at L1, 25 – 45 age group.

The two groups differ significantly at L1 U(24) = 9.5, Z = 4.3, p = < .0001.

The 90% confidence intervals, at mid-position L1, between female and males in the 25 – 45 age range were 1.16 to 3.41, this lies within the range of clinical indifference and with 95% confidence it can be concluded that the measures between gender groups at this segmental level are equivalent.

14.1.5 70 – 90 and 25 – 45 age range comparison

14.1.5.1 Iliocostalis 70 – 90 v 25 – 45 age range comparison

The correlation between the 70 – 90 age group and the 25 – 45 age group at L2/3 was 0.49 (p = .17) and at T11 was 0.47 (p= .2)

The 90% confidence intervals, at T11, between the two age ranges were -4.0 to 1.8, this is within the range of clinical indifference and it is concluded that the measures of the two sides are equivalent.

The 90% confidence intervals, at L2/3, between the two age ranges were 3.0 to 8.3, this does not lie within the range of clinical indifference and it cannot concluded that the measures of the two sides are equivalent.

14.1.5.2 Longissimus 70 – 90 v 25 – 45 age range comparison

The correlation between the 70 – 90 age group and the 25 – 45 age group at T6 was 0.24 (p = .33) and 0.34 (p = .27) at T10.

The 90% confidence intervals, at T6, between the two age ranges was -7.19 to 1.4, this does not lie within the range of clinical indifference and it cannot concluded that the measures of the two sides are equivalent.

The 90% confidence intervals, at T10, between the two age ranges was -3.7 to 1.4, this does lie within the range of clinical indifference and it can be concluded that the measures of the two sides are equivalent.

14.1.5.3 Multifidus 70 – 90 v 25 – 45 age range comparison

The 90% confidence intervals between the pooled data for the two age ranges were 2.38 to 5.32, this does not lie within the range of clinical indifference and with 95% confidence; it cannot be concluded that measures from the two age ranges are equivalent.

14.2 MRI rejected series

The following table lists the MRI series that were not suitable for analysis and the reasons are stated.

Rejected series	Reason Multifidus	Reason Iliocostalis	Reason Longissimus
R1	√	√	no thoracic
R2	√	no thoracic	no thoracic
R3	√	√	no thoracic
R4	√	no thoracic	no thoracic
R5	√	no thoracic	no thoracic
R6	no upper Lx	no thoracic	√
R7	√	no thoracic	no thoracic
R8	no upper Lx	no thoracic	no thoracic
R9	√	no thoracic	no thoracic
R10	no upper Lx	no thoracic	no thoracic
R11	√	no thoracic	no thoracic
R12	pedicle screws	no thoracic	no thoracic
R13	√	no thoracic	no thoracic
R14	fused L2/3	√	poor image
R15	scoliosis	no thoracolumbar	√
R16	√	√	no thoracic

14.3 Table indicating sEMG results from participants

Biering-Sørensen Test	Participant No.					
Test No.	**1**	**2**	**3**	**4**	**5**	**6**
1			√		√	√
2	√	√				
3	√		√			√
Ito test						
Test No.	**1**	**2**	**3**	**4**	**5**	**6**
1						
McIntosh Test						
Test No.	**1**	**2**	**3**	**4**	**5**	**6**
1						
2						

Key to table above…

No experiment undertaken	
No sEMG collected	
sEMG collected – not/partially analysed due to noise or rogue channels.	
sEMG collected and analysed as part of protocol development	√

15. List of accompanying materials

16. Declaration of authorship
17. Acknowledgements
18. Papers and proceedings
19. Permission to reproduce images and text from journals

16. Declaration of authorship

I, Richard Collier declare that this thesis, entitled…

An anatomical and surface electromyography study of the fatigue characteristics of Longissimus Thoracis pars Thoracis, Iliocostalis Lumborum pars Thoracis and Lumbar Multifidus. …and the work presented in the thesis is both my own and has been generated by me as the result of my own original research. I confirm that:

- this work was done wholly or mainly while in candidature for a research degree at this University;
- where any part of this thesis has previously been submitted for a degree or any other qualification at this University or any other institution, this has been clearly stated;
- where I have consulted the published work of others, this is always clearly attributed;
- where I have quoted from the work of others, the source is always given. With the exception of such quotations, this thesis is entirely my own work;
- I have acknowledged all main sources of help;
- where the thesis is based on work done by myself jointly with others, I have made clear exactly what was done by others and what I have contributed myself;
- all post-mortem images have been taken and stored and presented in accordance with the Human Tissue Act (2004), the Human Tissue Authority Code of Practice and CLAS Standard Operating Procedures for recording and using photographic images for publishing purposes.

- parts of this work have been published or presented : [Section 18]

Signed: ……..

Date:……

17. Acknowledgements

Professor Robert Allen: For supervision and support throughout the study.

Dr Alexandra Webb: For supervising the anatomical study component.

Dr Dragana Nikolic: For the signal processing, programming the GUIs and for statistical support.

Professors Joy Conway and Dan Bader: For acting as advisors

Dr Angela Darekar and colleagues of Medical Physics Department, University Hospital, Southampton: For providing access to the PACS database, for obtaining and pre-screening MRI images and for providing training in the analysis of MRI series.

Dr Tamsyn Markham & Melanie Orchard: For assistance in muscle angle data collection as part of the anatomical study.

Royal National Lifeboat Institute: For providing participants for a component of the multi-channel sEMG study

EPSRC: For funding the RIB trials and providing funding for the multi-channel sEMG equipment.

Ship Science Colleagues: For providing the resources for the RIB trials and for collecting and providing the boat data in this study.

Professor Roberto Merletti: For running the winter school on multi-channel surface electromyography and for providing advice and support for the multi-channel component of the study.

Dr David Simpson: For help with the programming of the biofeedback device and help with statistics.

Dr Peter White & Dr Sean Ewing: For help with the statistical analysis.

Dr Lesley Collier: For constant support and modelling for many of the pictures.

Dr David Allen: For initial help with the study design and signal processing.

Study participants: Participants were recruited to the initial design phase of the study and who gave their time while the experimental methodology was being developed and during sEMG data collection.

A particular acknowledgement is made to those individuals who donated their bodies to the University of Southampton Centre for Learning Anatomical Studies.

18. Papers and proceedings

The following list papers and conferences at which elements of this thesis have been presented;

Fast Rescue Boats, Ride Quality and Crew Safety. Human Elements Advisory Group (HEAG16). University of Southampton, November 2012, **Collier, R.**

Muscle Fibre Orientation of the Iliocostalis Lumborum pars Thoracis. Paper presented at British Association of Clinical Anatomists, St Georges Hospital. December 2011. Orchard, M., Markham, T., **Collier, R.,** Webb, A.

Low Back Pain – the problem, methods of diagnosis and functional assessment: condition monitoring of the spine? CM 2011 and MFPT 2011. The Eighth International Conference on Condition Monitoring and Machinery Failure Prevention, Cardiff, June 2011. **Collier, R.**

TUTORIAL SESSION: Low Back Pain: the problem and methods of assessment. The Eighth IASTED International Conference on Biomedical Engineering. Innsbruck. February 2011. **Collier, R.**

Monitoring and assessing crew performance in high-speed marine craft – methodological considerations. Presented at the Institute for Computer Sciences, Social Informatics and Telecommunications Engineering Proceedings of MobiHealth 2010 International ICST Conference on Wireless Mobile Communication and Healthcare, Ayia Napa, Cyprus, 18-20 October 2010, 55, 219-226. Nikolić, D., R. **Collier, R.,** Allen, R.

Methodological considerations: The assessment of spinal muscle fatigue using multi-channel surface EMG. Bath Biomechanics Symposium; Biomechanics of the Spine: Engineering and Clinical Advances; University of Bath September 2010. **Collier, R.**

Fusion of biomedical and physical data for assessment of human performance in high speed marine craft. Proceedings of the 22nd Mediterranean Conference on Medical and Biological Engineering and Computing, MEDICON, Chalkidiki, Greece, 27-30 May 2010. Nikolić, D., R. **Collier, R.,** Allen, R.

Human factors in the design of high-speed marine craft. Maritime Event for Industry and the Public, National Oceanography Centre, Southampton, UK, 15 September 2009, Nikolić, D., Allen, R., **Collier, R.,** Taunton, D., Hudson, D. and Shenoi, R.A. (2009).

An evaluation of three clinical procedures measuring muscle fatigue within the lumbar spine using multi-channel surface EMG and electronic goniometry. Poster presentation at the IPEM Annual Scientific Meeting, York, UK, 2-4 September 2008, 48-49. **Collier, R.**

Papers in preparation:

Methodological considerations: The assessment of spinal muscle fatigue using multi-channel surface EMG. Journal of Occupational and Environmental Medicine. Nikolić, D., **Collier, R.,** Collier, L., Allen, R.,

Reappraisal of the DeFoa and Biedermann Paper. Journal of Anatomy. **Collier, R**., Webb, A.

An evaluation of three clinical procedures measuring muscle fatigue within the lumbar spine using multi-channel surface EMG and electronic goniometry.

R. Collier MSc, Y. Zheng PhD, L. Collier PhD, D. Simpson PhD, R. Allen PhD;
ISVR University of Southampton

UNIVERSITY OF Southampton
Institute of Sound and Vibration Research

Background and purpose
Measurement of muscle fatigue within the lumbar spine is used in clinical practice as a predictor of low back pain. People with short holding times are more likely to have low-back problems than those with long holding times. A number of different procedures have been used in clinical practice; however, there is lack of clarity of which procedure is most effective in accurately measuring muscle fatigue and most appropriate for field testing.

This pilot study compared three procedures using multi-channel surface electromyography (sEMG) and electronic goniometry to inform a future study of lumbar spine muscle fatigue.

Method
Standard lumbar extensor spinal muscle fatiguing protocols were compared using the methodology of method comparison studies as described by Bland & Altman [1]. The procedures compared were the Biering-Sorensen test, Fig 1 [2], the Ito modification, Fig 2 [3] and the Prone straight leg raise, Fig 3 [4].

Figure 1 Figure 2 Figure 3

Participants were recruited from healthy adults without acute low back pain and were tested using three procedures through simple randomisation. Surface EMG recordings were taken from lumbar spine muscles of each participant using standardised recording protocols in order to evaluate sensitivity and specificity of each procedure. Changes in position were determined by electronic goniometry.

Measures
EMG
During sustained isometric contraction the firing rate of motor units is influenced by muscle fatigue. Surface EMG signals were detected bilaterally using four 16 electrode sEMG adhesive linear arrays, (LISiN-SPES Medica) with 10mm inter-electrode distance (IED) placed over the fibres of longissimus thoracic pars thoracic, iliocostalis lumborum pars thoracic and a 64 electrode sEMG adhesive matrix with 10mm IED over the lumbar multifidus at the lumbo-sacral junction in monopolar configuration, Figs 5, 6 & 7. The arrays and matrix were connected to a 128 channel surface EMG amplifiers (LISiN-SEMA Elettronica, Torino, Italy). The EMG signals were amplified, band-pass filtered (3 dB bandwidth: 10-500 Hz), sampled at 2048 Hz, and converted in digital form by 12 bit A/D converters.

Figure 5 Figure 6 Figure 7

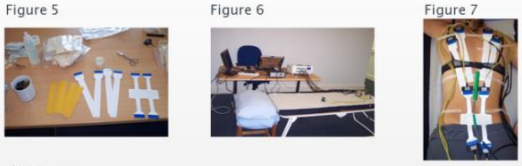

Anatomy
Anatomical landmarks of muscles were defined by a concurrent anatomy study of the longissimus dorsi, Fig 8 and the lumbo-sacral multifidus, Figs 9 & 10.

Figure 8 Figure 9 Figure 10

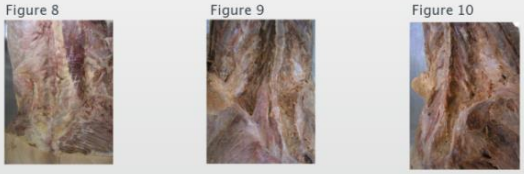

Electronic goniometer & tracking device
As participants fatigue their position during each procedure changes. In order to provide consistent feedback on position, test end and to record motion, a tracking device has been developed. An electronic goniometer attached to the skin overlying the lumbar spine provides a digital input to a Matlab programme which in turn provides a visual display of position in real time, Fig 11.

Figure 11

Borg Rating of Perceived Exertion (Borg RPE)
Subjective fatigue was recorded using the Borg RPE. [5] This scale gives expressions of effort, for example, 'No exertion at all' through to 'maximum exertion'. Participants were asked to rate their perceived exertion on completion of each procedure.

Data Analysis
Raw data can be viewed, filtered and channels rejected, using GUI developed for this purpose.

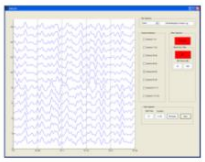

Results
Each of the three test procedures result in tracking angle changes;

Biering-Sørensen test Ito test Prone leg raise

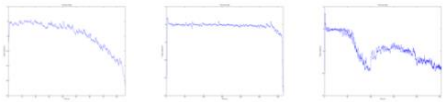

Examples of fatigue during test procedures - Biering-Sørensen x 2

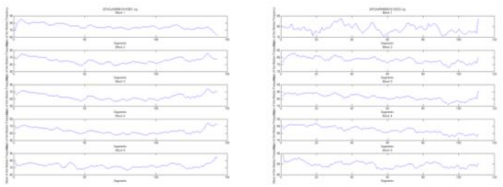

Ito Prone leg raise

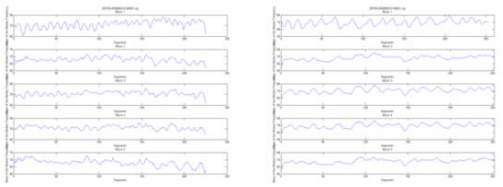

Examples of spatial changes in EMG amplitude

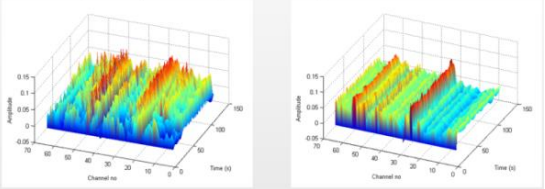

Conclusions
Interim analysis of pilot data indicates that fatigue testing using the procedures described produces valid data which can be used to undertake further signal analysis. The Biering-Sørensen test consistently produces fatigue of the longissimus dorsi and multifidus muscle groups and is the test that participants most regularly rate as 'hard' to 'very hard' on the Borg scale and which they associate with lumbar spine muscle fatigue. However, the Biering-Sørensen test may not be the most suitable for field testing.

There is some evidence that there is a shift from local stabilisers to global stabilisers as one of the strategies that is used to maintain position during the fatiguing task.

References

1. Bland, Altman. Statistical methods for assessing agreement between two methods of clinical measurement, Lancet, 1986: 8(1): 307-310.
2. Biering-Sorensen. Physical measurements as risk indicators for low back trouble over a one year period, Spine, 1984: 9:106-119.
3. Ito et al. Lumbar trunk endurance testing: an inexpensive alternative to a machine for evaluation, Arch Phys Med Rehabil, 1996: 77(1): 75-79.
4. Mc Kintosh. Trunk and lower extremity muscle endurance: normative data for adults, J Rehabil outcome Meas, 1998: 2: 20-39.
5. Borg G. Borg's Perceived Exertion and Pain Scales. 1 ed. Human Kinetics; 1998.

19. Permissions to reproduce images and text from journals:

Home | Create Account | Help

Title: Spinal and Supraspinal Factors in Human Muscle Fatigue
Author: S. C. Gandevia
Publication: Physiological Reviews
Publisher: The American Physiological Society
Date: Jan 10, 2001

User ID

Password

Enable Auto Login

LOGIN

Forgot Password/User ID?

If you're a copyright.com user, you can login to Rightslink using your copyright.com credentials.

Already **a Rightslink user** or want to learn more?

Permission Not Required

Permission is not required for this type of use.

BACK CLOSE WINDOW

RightsLink | Copyright Clearance Center

Thank You For Your Order!

Dear Mr. Richard Collier,

Thank you for placing your order through Copyright Clearance Center's RightsLink service. Elsevier has partnered with RightsLink to license its content. This notice is a confirmation that your order was successful.

Your order details and publisher terms and conditions are available by clicking the link below:

http://s100.copyright.com/CustomerAdmin/PLF.jsp?lID=2011110_1320764366658

Order Details
Licensee: Richard Collier
License Date: Nov 8, 2011
License Number: 2784260254658
Publication: Journal of Electromyography and Kinesiology
Title: Analysis of motor units with multi-channel surface electromyography
Type Of Use: reuse in a thesis/dissertation
Total: 0.00 GBP

To access your account, please visit https://myaccount.copyright.com.

Please note: Online payments are charged immediately after order confirmation; invoices are issued daily and are payable immediately upon receipt.

To ensure we are continuously improving our services, please take a moment to complete our customer satisfaction survey.

B.1:v4.2

Appendices

This is to confirm that Richard Collier is granted to use Primal Pictures images in his thesis entitled:

'An anatomical and elecromyographic study of Longissimus Thoracis pars Thoracis, Iliocostalis Lumborum pars Thoracis and Lumbar Multifidus'.

He must leave the Primal Logo and copyright on each image and credit Primal Pictures thus:

Anatomy images provided courtesy and copyright of www.primalpictures.com.

This is a permission to use the images for non-commercial use only.

Many thanks,

Dan McGarry

Primal Pictures Ltd. 4th Floor Tennyson House, 159-165 Great Portland Street, London W1W 5PA United Kingdom

T: +44 (0) 20 7637 1010 **F:** +44 (0) 20 7636 7776 **E:** dan@primalpictures.com
W: www.primalpictures.com